The Development of Sustainable Internal Curing Agents Using Natural Hollow Fibres

By

Amirmohammad Sabziparvar

Thesis submitted to the University of Ottawa
In Partial Fulfillment of the Requirements for degree of
Doctor of Philosophy in Civil Engineering

Department of Civil Engineering
Faculty of Engineering
University of Ottawa

This thesis is dedicated to the pillars of my life:

my parents, my loving wife, and my sisters.

Declaration

I hereby declare that, except where explicitly referenced, the content of this thesis is original and has not been submitted, either in whole or in part, for any other degree or qualification at this or any other university. This thesis is my own work and includes no collaborative contributions, except as indicated in the text and acknowledgements.

Amirmohammad Sabziparvar

May 2024

Acknowledgements

First and foremost, I want to express my profound gratitude to God for granting me the strength to complete my Ph.D. in Civil Engineering at the University of Ottawa, despite the challenges posed by the COVID-19 pandemic.

I am deeply thankful to my supervisor, Dr. Reza Foruzanmehr, for his invaluable guidance and unwavering support throughout my doctoral journey. I appreciate the opportunity to work in a collaborative environment in several labs at both the University of Ottawa and the University of Sherbrooke. I would like to thank Professors Majid Sartaj, Marc A. Dubé, and Mathieu Robert for their generosity in providing me the opportunity to conduct part of my research in their laboratories. I would like to extend my sincere gratitude to my defence committee, Professors Beatriz Martin-Perez, Leandro Sanchez, Mamadou Fall, and Ousmane Hisseine for their invaluable insights and feedback. Their contributions significantly enhanced the quality of this work. I would also like to thank the lab technical officers Dr. Gamal Elnabelsy and Dr. Muslim Majeed for their continuous support in the lab. Additionally, I want to express my heartfelt thanks to my colleagues at the University of Ottawa and the University of Sherbrooke for their assistance and friendship.

I owe a special debt of gratitude to my family, especially my dear parents, Ali and Zahra, for their unconditional support and sacrifices from thousands of kilometers away throughout these years. I can never fully repay you for all that you have done for me. A special thanks to my wife, Solmaz, for her unwavering belief in my abilities from the very beginning of this journey. It is an honor to have you in my life. Lastly, I want to acknowledge Prof. Asghar Habibnejad Korayem, my undergraduate supervisor, whose mentorship ignited my passion for research and teaching.

Abstract

The incorporation of superabsorbent materials as internal curing agents has demonstrated effectiveness in mitigating self-desiccation and early-age cracking in cement mixes characterized by low water-to-binder ratios (w/b). However, concerns related to sustainability, availability, and cost have emerged, primarily due to the petroleum-based nature of common superabsorbent polymers (SAP). This PhD research aims to investigate the use of locally available milkweed (MW) fibres, which possess a unique hollow structure, as internal curing agents for low-w/b Portland cement mixes. The study focused on examining the impact of different pre-treatment methods on the morphology, chemical composition, and hygroscopic characteristics of MW fibres in the initial phase. Two pre-treatment methods, namely hydrothermal treatment (HT), and hybrid treatment (HY), a combination of hydrothermal treatment with alkaline treatment, were explored. Findings from the first phase indicated that both HT and HY treatments effectively enhanced the water absorption capacity of MW fibres. However, water retention was influenced by the morphology of the fibres. The HT treatment preserved the hollow structure of the fibres, leading to improved water retention, whereas the HY treatment caused significant morphological changes, resulting in a noticeable reduction in water retention. In the second phase of the study, the impact of pre-treated MW fibres on the effective w/b of cement mixes was assessed through rheological measurements. In addition, the influence of MW fibres on the heat of hydration and hydration products was investigated. The introduction of MW fibres to Portland cement paste induced a shift in their effective w/b to lower values, attributed to the absorption action of MW fibres during the pre-saturation process. Furthermore, using 0.1% wt. pre-treated MW fibres resulted in a 17% improvement in the degree of hydration compared to the reference sample. This was accomplished by ensuring an adequate amount of free water for the initial reaction of cement hydration and

entrained water in the lumen for subsequent internal curing. In the third phase, the study investigated the kinetics of water transport from MW fibres to cementitious paste systems, using Nuclear Magnetic Resonance (NMR) and Differential Scanning Calorimetry (DSC). The observations revealed that both the morphological features and the release of extractives such as lignin impact the desorption kinetics of MW fibres' entrained water within cementitious matrices. The HT-MW fibres, with their preserved hollow morphology and enhanced hydrophilicity, exhibited the most effective performance, showing the highest amount of available internal curing water in the transverse relaxation time (T_2) measurements. In contrast, the absence of lignin in the HY-MW fibres allowed hydration products to migrate into their lumen. This led to the early consumption of the entrained water, a process further exacerbated by the holes and defects in the fibre walls. The shrinkage, mechanical strength, and microstructural development of cementitious mixes after incorporating pre-treated MW fibres were examined in the final phase. The internal curing role of the pre-treated MW fibres proved effective in reducing autogenous shrinkage, with significant reductions of up to 28% for 7 days compared to the plain samples. In addition, hydration products were observed to penetrate the lumen of the HY-MW fibres to a depth of up to 150 micrometres. This penetration exacerbated drying shrinkage by facilitating moisture transport to the unsaturated environment. Consequently, this phenomenon led to higher chance of cracking and also lower flexural strength in HY-MW fibres compared to HT- and N-MW fibres. The comprehensive analysis and findings of this PhD research supported the feasibility of using MW fibres as a sustainable internal curing agents to effectively reduce autogenous shrinkage after applying straightforward, cost-effective, and low-carbon footprint pre-treatment methods.

Keywords: Milkweed Fibres; Internal Curing; Superabsorbent; Hygroscopic Properties; Autogenous Shrinkage; Cement Hydration; Nuclear Magnetic Resonance (NMR) relaxometry.

TABLE OF CONTENTS

List of Figures

List of Tables

List of Acronyms/Abbreviations

^{1}H NMR	Proton Nuclear Magnetic Resonance
AC	Absorption Capacity
Am	Monosulfoaluminate
Aft	Ettringite
BET	Brunauer–Emmett–Teller
BSE	Backscattered Electron
CBW	Chemically Bound Water
CS	Chemical Shrinkage
C-S-H	Calcium Silicate Hydrate
C_2S	Dicalcium Silicate
C_3S	Tricalcium Silicate
C_3A	Tricalcium Aluminate
$CaCO_3$	Calcite
CH	Portlandite
CI	Crystallinity Index
CMF	Cellulose Microfibrils
CNC	Cellulose Nanocrystals
CNF	Cellulose Nanofibrils
CPMG	Carr-Purcell-Meiboom-Gill Pulse Sequence
DSC	Differential Scanning Calorimetry
EDS	Energy Dispersive X-ray Spectroscopy
FTIR	Fourier Transform Infrared
FW	Freezable water
GAA	Galacturonic Acid
GHG	Greenhouse Gas
GLA	Glucuronic Acid
GU	General-Use
H.B.	Herschel Bulkley Model
HPC	High-Performance Concrete
HT	Hydrothermally Treated

HY	Hybrid Treated
ITZ	Interfacial Transition Zone
LD	Laser Diffraction
LWA	Lightweight Aggregate
MC	Moisture Content
MW	Milkweed Floss Fibres
N	Non-Treated
PC	Portland Cement
RH	Relative Humidity
S1	External Secondary Wall
S2	Middle Secondary Wall
S3	Internal Secondary Wall
SAP	Superabsorbent Polymer
SCM	Supplementary Cementitious Material
SE	Secondary Electron
SEM	Scanning Electron Microscopy
SP	Superplasticizer
SRA	Shrinkage Reducing Admixture
T_2	Spin-spin (Transverse) Relaxation Time
TGA	Thermogravimetric Analysis
w/b	Water-to-Binder Ratio
WRR	Water Release Rate
XRD	X-ray Powder Diffraction
XRF	X-ray Fluorescence

Chapter 1 Introduction

1.1 Background

Although self-desiccation may exhibit advantageous characteristics in specific applications such as cemented paste backfill [1,2], it poses a significant challenge that can compromise the performance of cement mixes with low water-to-binder ratios (w/b), typically below 0.40 [3]. The phenomenon of self-desiccation refers to the reduction in internal relative humidity due to the partial desaturation of capillary pores within a hydrating cement paste. This process leads to the formation of water menisci within the capillary pores [4]. Consequently, due to surface tension, negative pressure (capillary pressure) builds up within the interconnected capillary pores. As capillary pressure increases over time, tensile forces exerted on the solid particles result in a reduction in the volume of the cementitious material [5]. This susceptibility to shrinkage makes cementitious materials with a low w/b prone to early-age cracking. Therefore, addressing the issue of self-desiccation is imperative for optimizing the potential properties of low w/b cementitious materials, such as their high mechanical performance and durability [6].

Internal curing has emerged as a prominent and efficient strategy in addressing self-desiccation in low w/b mixes. It stands out as one of the most effective methods for mitigating early-age cracking, leading to improved performance of low w/b cementitious materials [7–10]. The technique involves the application of internal curing agents such as superabsorbent polymers (SAP) to maintain the internal humidity beyond the self-desiccation threshold of the cementitious pastes [11–13]. SAP have a hydrophilic nature that allows them to absorb and retain water up to several hundred times of their dry weight [14,15]. Indeed, SAP can act as small water reservoirs that are spatially dispersed throughout the cementitious matrix, allowing them to cure anhydrous cement particles internally. In other words, once the moisture content

within the cement mixes falls below a specific threshold, SAP initiate the release of their entrained water to promote the hydration of cement particles. As a result, they have the potential to mitigate the self-desiccation shrinkage in low w/b cementitious matrices including high-performance concrete (HPC) mixes [16,17]. However, because SAP are petroleum-based compounds made from non-renewable materials (e.g., polyacrylate) they increase the matrices' carbon footprint [18]. It is crucial to emphasize, as illustrated by Bentz *et al.*, that internal curing agents have exhibited efficacy beyond HPC applications. They have proven effective in various scenarios within cement-based materials, including their application in repair materials essential for the restoration of concrete structures [19]. Hence, researchers have been investigating the development of more sustainable alternatives for SAP.

Over the past decade, there has been a surge in interest regarding the use of lignocellulosic materials, especially natural fibres, for internal curing applications. These materials, which include bast fibres [20], leaf fibres [21], and wood fibres [22,23], are being increasingly investigated as sustainable alternatives for SAP. One example of using lignocellulosic materials as internal curing agents is demonstrated by Lee *et al.*, who showed that by incorporating 2% weight of abaca fibres in plain cementitious mixes with a w/b of 0.30, the autogenous shrinkage was reduced by approximately 93% after 192 hours [21]. The adoption of lignocellulosic materials for internal curing relies on their excellent hygroscopic properties and strong affinity for water. This is attributed to components like cellulose and hemicellulose within the structure of lignocellulosic materials, which are inherently hydrophilic and serve as absorption sites for water molecules. Unlike synthetic counterparts like SAP, natural fibres are globally abundant, often at low or no cost. Consequently, this renewable resource offers a sustainable solution for construction materials, helping mitigate the construction industry's environmental impact.

Compared to other natural fibres, seed fibres, particularly those extracted from the Milkweed (MW) plant, have received less attention in research. MW fibres, characterized by their white, silky texture, are extracted from the seeds of the MW plant, primarily indigenous to North America. However, the presence of MW plants extends beyond North America; they are also found in countries such as China and Iran, where they are known as Akund and Estabragh, respectively. This plant thrives in a wide range of soil conditions and commonly inhabits roadside areas, fields, meadows, and wastelands [24]. MW floss fibres stand out due to their unique hollow structure, which distinguishes them from other types of natural fibres [25]. This structure comprises an exceptionally wide lumen and a thin wall, with the lumen accounting for up to 77% of the fibre volume and the wall measuring approximately 1.3µm in thickness [26,27]. Such architecture promises a notable water absorption capacity, primarily driven by capillary action. MW fibres consist of cellulose, hemicellulose, and lignin, along with trace amounts of waxes, pectin, and sugars. While cellulose and hemicellulose exhibit hydrophilic characteristics, serving as absorption sites for water molecules, other components like lignin and waxes are hydrophobic. Consequently, MW fibres can be categorized as amphiphilic materials capable of displaying both hydrophilic and hydrophobic properties. This dual nature may explain why previous studies have observed only moderate water absorption in as-received MW fibres due to the presence of certain hydrophobic components within the fibre structure [26,28]. Therefore, this study aims to enhance the hygroscopic properties of MW fibres through two distinct methods that exhibit cost-effectiveness and environmental friendliness. By leveraging the unique morphology of these fibres, the primary goal is to transform MW fibres into sustainable water reservoirs for internal curing of low w/b cementitious mixes to address their self-desiccation issue.

Despite their good hygroscopic behaviour, the compatibility of natural fibres with cementitious matrices may limit their potential as internal curing agents. The alkaline environment of cementitious matrices can lead to the degradation of lignocellulosic materials, resulting in the release of leachates. Consequently, these leachates may impact the fresh and hardened properties of cementitious mixes. Several approaches have been explored to enhance the compatibility of lignocellulosic materials with cementitious matrices. The primary and most widespread method involves extracting leachates from natural fibres through chemical or hydrothermal pre-treatment. Another strategy involves reducing the pH of the cement pore solution by incorporating pozzolanic materials to alleviate the degradation of natural fibres [29–31]. Among the pre-treatment methods, alkaline and hydrothermal pre-treatments can be named as the most common methods to improve the compatibility of lignocellulosic fibres with cementitious matrices due to their straightforward implementation at relatively low cost. Despite extensive research on using alkali-treated lignocellulosic fibres within cementitious matrices, there remains a knowledge gap regarding the impacts of other types of pre-treatments such as hydrothermal treatment and the hybrid treatment, which combines both hydrothermal and alkaline treatments. This knowledge gap highlights the need for further investigation to fully comprehend the implications of these treatments, particularly with the main goal of using these fibres as internal curing agents in low w/b cementitious mixes.

1.2 Knowledge Gaps

This section presents a brief overview of the knowledge gaps that motivated this study. These gaps were identified through an extensive review of the existing literature, as presented in Chapter 2.

1. There has been a notable lack of research on the hygroscopic properties of hollow floss fibres including MW fibres, and the potential to enhance these properties through pre-treatment techniques.
2. Understanding the internal curing impact of bio-based hollow floss fibres on the fresh and hardened properties of cementitious mixes remains incomplete.
3. A limited number of studies have systematically examined how pre-treatment techniques control the optimal removal of extractives (such as lignin, hemicellulose, waxes, and pectin) from hollow floss fibres and influence their internal curing efficiency.
4. There is a lack of research on examining the effective percentage of the hollow floss fibres (e.g., MW fibres) to mitigate autogenous shrinkage in low w/b cementitious mixes.
5. There have been very few studies investigating the kinetics of water transport between natural lignocellulosic fibres and cementitious matrices and notably no previous study has specifically studied the behaviour of MW fibres within this context.

1.3 Research Objectives

This doctoral research aimed to develop environmentally sustainable internal curing agents for Portland cement (PC) mixtures with low w/b, using MW fibres. To fulfill this primary objective, the following secondary objectives were pursued:

1. The first objective was to investigate the impact of different pre-treatment techniques on the hygroscopic characteristics, morphology, and chemical composition of MW fibres. This objective served as a crucial foundation for subsequent steps of the study for two key reasons. Firstly, comprehending the absorption and desorption characteristics

of pre-treated MW fibres is pivotal as it directly influences the w/b, subsequently impacting the fresh and hardened properties of cement mixes in the later stages of this study. Secondly, certain chemical components of fibres are removed during pre-treatments which may potentially lead to changes in fibre morphology. Therefore, understanding these morphological and chemical changes after the treatment of MW fibres is crucial for interpreting their contributions to internal curing within cement matrices.

2. The second objective aimed to study the effect of different dosages of pre-treated MW fibres on the effective w/b and hydration properties of cementitious mixes. The former is of great importance as it enables accurate comparisons of samples with identical effective water-to-binder ratios. In addition, since the literature suggests that lignocellulosic fibres may release leachates when incorporated into cementitious matrices, this study aimed to examine the influence of different MW fibre dosages on the early-age hydration characteristics of cementitious mixes. The goal was to clarify both the potential negative effects of leachates and the positive effects of enhanced hydration due to internal curing.
3. In the third objective of this research, the kinetics of water transport between MW fibres and the cementitious paste system was studied. This objective was essential for monitoring the actual desorption behaviour of MW fibres within the cementitious system. Moreover, it facilitated the study of the evolution of various types of water within the porous structure of cementitious paste as a consequence of internal curing by MW fibres. This objective complements our understanding of how MW fibres can potentially reduce autogenous shrinkage in low w/b cementitious mixes.

4. The final (i.e., fourth) objective of the study focused on investigating the microstructural evolution and shrinkage control in internally cured mortars using pre-treated MW fibres. The primary objective was to determine the most effective pre-treatment on the MW fibres aimed at reducing autogenous shrinkage in cementitious mixes. Furthermore, within this objective, the study investigated how different pre-treated MW fibres influence microstructural development and key mechanical properties of cementitious mixes.

1.4 Hypothesis

The formulation of the research hypothesis was guided by the insight obtained from the comprehensive literature review presented in Chapter 2. Based on this review, the following hypotheses were made:

1. Previous studies have demonstrated that MW fibres possess an extremely wide lumen and contain hydrophilic groups, such as hydroxyls, within their structure. These inherent characteristics would make MW fibres highly suitable for sustainable applications as superabsorbent, particularly when employed as internal curing agents in mixes with low w/b mixes [26,27].
2. MW fibres, like other lignocellulosic fibres, are composed of cellulose, hemicellulose, and lignin. However, other components such as waxes, pectin, and sugars are also present in small amounts (<5%) in MW fibres [25]. While some of these components are hydrophilic and can act as absorption sites for water molecules (mainly cellulose and hemicellulose), others, like waxes and lignin, are hydrophobic. As a result, MW fibres are classified as an amphiphilic material that exhibit both hydrophilic and hydrophobic

properties. It would be expected that applying certain pre-treatments could remove hydrophobic components from MW fibres, boosting their hygroscopic properties.

3. The presence of some components present in MW fibres would negatively impact the hydration of cementitious environment. Hence, applying simple and low-cost pre-treatments could improve the compatibility of MW fibres by removing those inhibitory substances to be used as internal curing agents in low w/b mixes.
4. It would be expected that MW fibres would have a significant impact on improving the degree of hydration by gradually delivering their adsorbed water to the anhydrous cement particles when the internal humidity of cement mixes dropped below the desiccation threshold. As a result, the risk of autogenous shrinkage in low w/b mixes would be expected to decrease by using pre-treated MW fibres.
5. Both the physical structure and chemical composition of MW fibres could impact the kinetics of water transport between the fibres and the cementitious system, as well as the development of microstructure.

1.5 Research Novelty and Contribution

There are several points of novelty in this research, which can be classified into fundamental novelty, novelty in application and novelty in characterization.

a) **Fundamental novelty:** Firstly, the hygroscopic properties of hollow MW floss fibres and the potential for enhancing these properties through pre-treatment techniques have not been thoroughly studied. This research investigated the effect of different pre-treatment methods on the morphology, chemical composition, and hygroscopic characteristics of MW fibres. It aimed to develop a comprehensive understanding of how pre-treatment can augment the water absorption capacity and water release rate of

MW fibres, thereby enhancing their suitability as internal curing agents. Secondly, the underlying mechanisms by which each component of bio-based internal curing agents influences fresh and hardened properties of cementitious mixes remain inadequately understood. This study aimed to investigate how each of these components, such as hemicellulose, lignin, and waxes, could impact the internal curing and properties of cementitious mixes.

b) **Novelty in application:** No previous studies have investigated the potential for improved performance of low w/b Portland cement mixes using MW fibres as internal curing agents. This research explored the use of MW fibres as internal curing agents, intending to mitigate autogenous shrinkage and enhance the hydration of Portland cement mixes. Furthermore, this research investigated the impact of different pre-treated MW fibres on the rheology, hydration, shrinkage, and mechanical strength of cementitious mixes.

c) **Novelty in characterization:** In addition to the novel research objectives, the proposed study also employed innovative characterization techniques, introducing a new method for measuring the hygroscopic properties of MW fibres. Furthermore, the research proposed a novel indirect approach for determining the effective w/b through rheological measurements.

By addressing these knowledge gaps, this research contributed to the development of environmentally sustainable internal curing agents for Portland cement mixtures with low w/b, using MW fibres.

1.6 Thesis Outline

As shown in Figure 1.1, the thesis manuscript is structured into eight chapters, with Chapters 3 to 6 presented in the format of technical papers. The content of these chapters is in the following manner:

Chapter One, Introduction, provides an overview of background of this study, knowledge gaps, research objectives, and research novelty and contribution. **Chapter Two** presents an extensive literature review about the importance of internal curing in low w/b mixes, conventional curing agents in cementitious mixes, natural fibres as internal curing agents, compatibility of natural lignocellulosic fibres with cementitious environment, and their effect on the properties of cementitious mixes. **Chapter Three (Technical Paper 1),** Effect of Fibre Length and Treatments on the Hygroscopic Properties of Milkweed Fibres for Superabsorbent Applications. The primary objective of this chapter is to investigate the key factors influencing the hygroscopic properties of MW fibres, with a specific focus on quantifying their water absorption capacity and water retention. These measurements were crucial for advancing to the subsequent phases of the study. **Chapter Four (Technical Paper 2),** Enhancing Hydration and Internal Curing in Cementitious Mixes: The Impact of Pre-Treated Milkweed Fibres. The primary emphasis of this chapter is to comprehend the influence of MW fibres on both the effective w/b and hydration kinetics of cementitious mixes. The investigation extended to examine the effect of different pre-treatment types and varying dosage of MW fibres within cementitious mixes. **Chapter Five (Technical Paper 3),** Investigation on the Kinetics of Water Transport by Milkweed Fibres During Internal Curing of Cementitious Paste. This chapter concentrates on assessing internal curing efficacy of different pre-treated MW fibre concerning their ability to supply water to the cementitious system during the cement hydration process. **Chapter Six**

(Technical Paper 4), Investigation on the Microstructural Evolution and Shrinkage Control in Internally Cured Mortars with Milkweed Fibres. The primary focus of this chapter is on assessing the effectiveness of MW fibres in mitigating autogenous shrinkage in mortar mixes. The chapter conducts a thorough examination of how MW fibres influence the microstructure of cementitious mixes in which they are incorporated. Additionally, it evaluates the impact of MW fibres on the mechanical properties of mortar mixes. In **Chapter Seven**, Synthesis, Integration and General Discussion of Results, a general discussion of the findings is presented. **Chapter Eight,** Conclusions and Future Works, summarizes the main conclusions and offers potential recommendations for future research endeavors.

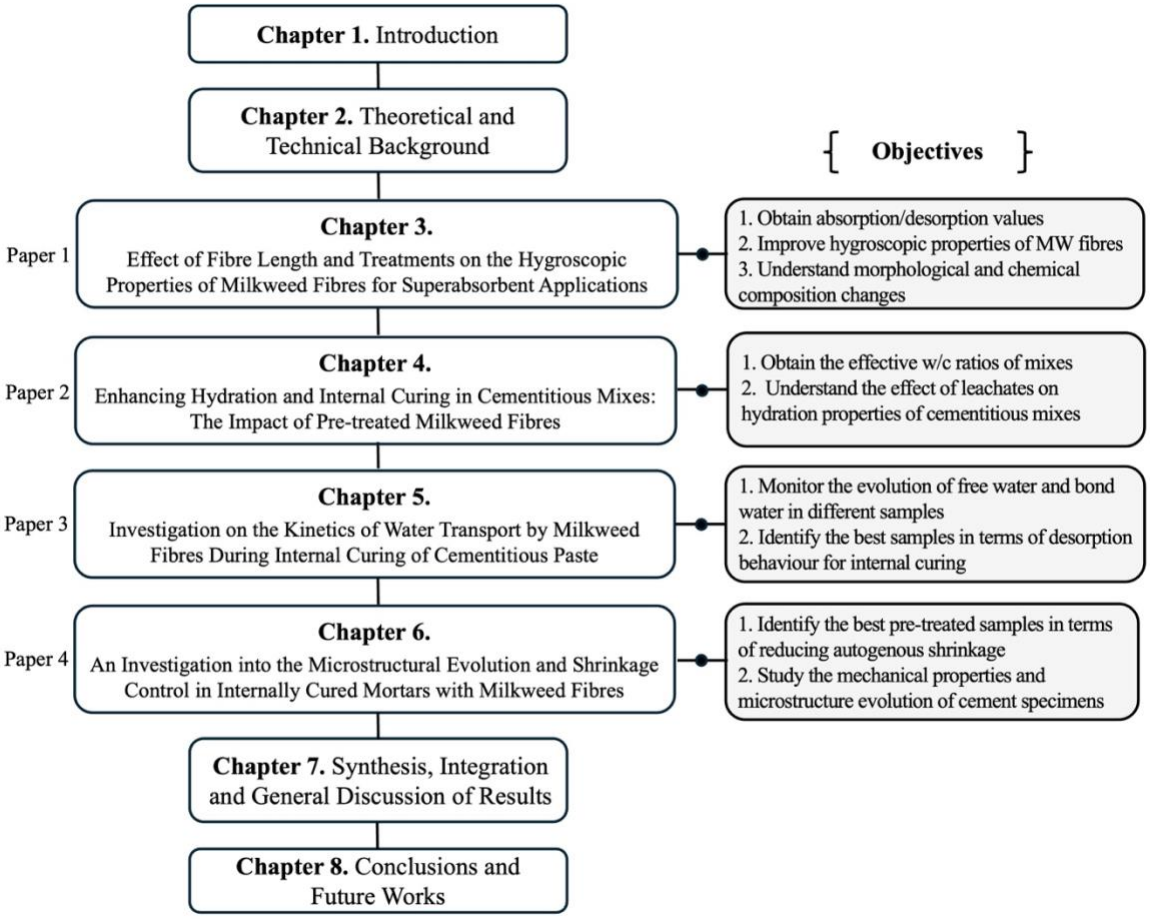

Figure 1.1. Thesis Organization

Chapter 2 Theoretical and Technical Background

The literature review commences by providing an overview of conventional internal curing agents, such as pre-wetted lightweight aggregate (LWA) and superabsorbent polymer (SAP), along with a comprehensive analysis of the factors that influence their efficiency in this role. Subsequently, the literature review investigates into the crucial characteristics of lignocellulosic fibres and their compatibility with cementitious environments, offering insight into their potential as internal curing agents. Furthermore, the literature review aims to provide a comprehensive overview of MW fibres, establishing a solid foundation for understanding their hygroscopic properties. The primary focus of this survey is to assess the potential of MW fibres in providing an internal curing effect in cementitious mixes.

2.1 Low w/b Mixes

The use of low w/b cementitious mixes has increased to enhance durability and mechanical performance of structural concrete elements, particularly in high-rise buildings, bridge decks, and offshore structures [32]. The increased strength and durability in low w/b mixes can be attributed to the reduced porosity present in these cementitious materials as opposed to the conventional ones. However, they have been shown to be more susceptible to early-age cracking in comparison with conventional concretes [33]. Self-desiccation caused by the inadequacy of traditional curing methods is one factor that causes early-age cracking in low w/b mixes [34]. Conventional curing methods may not always effectively provide the amount of water required for complete hydration of cement. First, as stated by Powers *et al.*, depercolation of capillary pores by hydration products significantly limits the accessibility of external curing water to the anhydrous cement particles, resulting in incomplete hydration of some zones in the concrete for mixes with a w/b of 0.42 or less [35]. Secondly, when there is a lack of additional water supply

during the hydration process, the cementitious material undergoes an internal drying mechanism. This self-desiccation process causes the capillary pores to empty, leading to the creation of water menisci within the capillary pores. These water menisci generate tension within the pore water and the surface of the cementitious material [36,37]. As a result, the cement matrix experiences shrinkage, rendering it susceptible to early-age cracking. Consequently, cementitious mixes with low w/b are prone to the development of shrinkage cracking. Figure 2.1 shows a hardened cement paste with a w/b of 0.2 which has more anhydrous cement grains in the cement paste along with less CSH and CH products, compared to a w/b of 0.4.

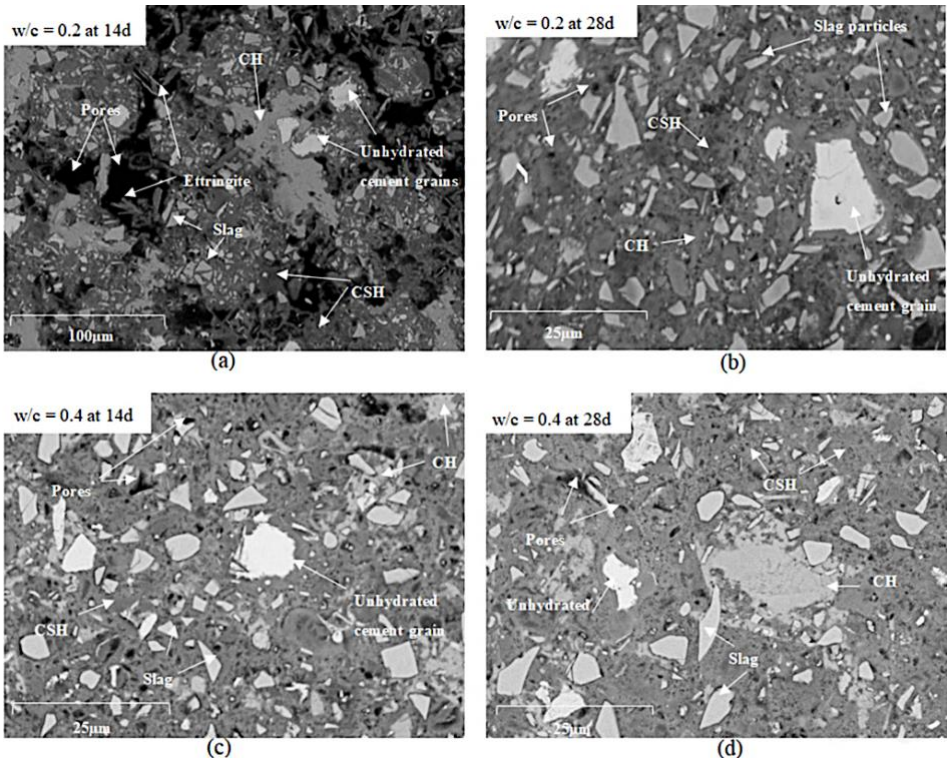

Figure 2.1. SEM images of a cement paste with different w/b: w/b of 0.2 after a) 14 days and b) 28days; comparing to a cement paste sample with w/b of 0.4 after c) 14 days and d) 28days [38]

First, in comparison to 50 years ago, PC particles are much finer and have a higher tricalcium silicate (C_3S) and alkali content [39]. As a result, cement particles are expected to hydrate faster

and gain much of its strength in the early days [40]. According to ACI 308-213, these cementitious mixes are also more prone to early-age cracking due to higher heat of hydration and higher autogenous strains and stresses. Bentz *et al.* reported that 0.07 kg of additional curing water is required per kg of cement to overcome this issue and maintain saturated conditions [13]. The higher water demand associated with the chemical shrinkage of supplementary cementitious materials (SCMs) makes internal curing essential in cementitious mixes that incorporate SCMs. SCMs like silica fume, slag, and fly ash exhibit significantly higher chemical shrinkage than ordinary Portland cement (OPC). For example, silica fume, slag, and fly ash have chemical shrinkage rates of 0.22, 0.18, and 0.10-0.16 kg water per kg cement, respectively, compared to OPC's rate of only 0.07 kg water per kg cement. Although this shrinkage occurs slightly later, it can lead to prolonged stress development and increased cracking potential. Internal curing effectively mitigates this risk by reducing residual stress and the likelihood of cracking [39,41,42].

Overall, the inadequacy of water for hydration of cementitious mixes with low w/b has two negative consequences. Firstly, it decelerates the rate of hydration, leading to inadequate strength development and increased porosity. Secondly, the loss of moisture in concrete results in drying shrinkage, which, if the system is restrained, can result in the development of stresses in the pore structure and eventually cracking [43]. Therefore, implementing an effective curing approach that enhances water availability to cementitious materials offers multiple benefits in extending the service life of concrete elements. These benefits include facilitating continuous hydration of cement paste, reducing permeability, and preventing early-age shrinkage cracking.

2.2 Internal Curing in Low w/b Mixes

To address the shortcomings associated with traditional external curing methods, a new method of curing, namely internal curing, has recently been introduced and implemented in cementitious mixes with low w/b. Internal curing, according to the ACI-308, is "the process by which the hydration of cement occurs due to the availability of additional internal water that is not part of the mixing water" [40]. This inside-out method can be used with a variety of absorbent materials, including pre-wetted LWA [44–49], SAP [9,50–61], pre-wetted wood fibres [23], and natural fibres [21,22,34,62–64]. These internal curing agents are distributed spatially in cementitious mixes and act as internal water reservoirs, gradually releasing water as needed during hydration. They are primarily pre-saturated materials with a high capacity for water absorption in aqueous solutions and a high desorption rate under pressure [65]. Internal curing methods offer a number of advantages. First and most importantly, internal curing is primarily introduced to overcome the high early-age shrinkage of cementitious mixes with low w/b that lack accessing water during their hydration period. In addition, even in high w/b mixes, internal curing can complement traditional curing practices for improved hydration, lower permeability, and higher compressive strength [66].

As shown in Figure 2.2, traditional curing's effectiveness in providing additional moisture is limited to the surface zone, whereas internal curing can provide extra moisture throughout the entire body of the cementitious system. This is because, after a few days, the effective zone of external curing at the surface is limited to the outer 4-8 mm (0.2-0.3 in) [13]. Overall, internal curing agents can be used to promote hydration of cement paste and to replenish water lost due to self-desiccation or evaporation due to adverse environmental conditions. By using internal curing methods to mitigate early-age cracking caused by autogenous shrinkage, cementitious

elements are expected to have a longer life cycle, contributing to greater sustainability. Furthermore, where external curing methods are difficult to apply on some concrete surfaces, internal curing can be advantageous.

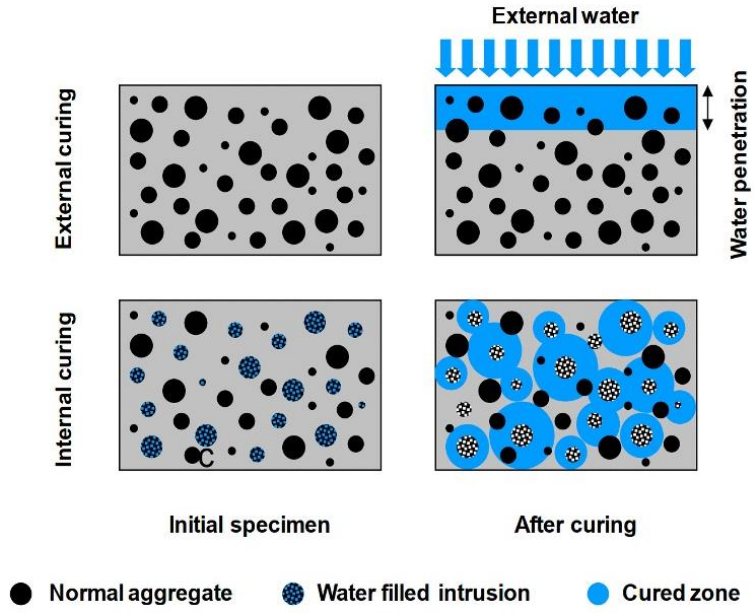

Figure 2.2. Comparison of the effective zone of traditional curing (external curing) and internal curing method [48]

2.3 Conventional Internal Curing Agents

Internal curing can be accomplished using a variety of agents such as pre-wetted LWA [44–49], SAP [9,50–61], pre-wetted wood fibres [23], and natural fibres [21,22,34,62–64]. These internal curing agents replenish the lack of water within the pores when the relative humidity (RH) drops, and thus can mitigate autogenous shrinkage caused by self-desiccation. However, the most common approaches in the internal curing of concrete, which will be thoroughly discussed in the following sections, are the use of pre-wetted LWA and SAP.

2.3.1 Lightweight Aggregate (LWA)

Lightweight aggregate (LWA) is a porous material that can be in the form of coarse aggregate with a bulk density of 1200 kg/m^3 or fine aggregate with a bulk density of 1100 kg/m^3 [44].

Although LWA was used for the first time for internal curing of concrete in 1991 by Philleo [67], it has long been used in concrete to produce lightweight concretes and improve thermal insulation.

2.3.1.1 Mechanisms of Internal Curing by LWA

Trtik *et al.* explained that there are three key aspects which need to be understood prior to mix proportioning of internally cured mixes. First, the distance the internal curing water can travel in a hardening cement paste, secondly, the amount of water which is released by the internal curing agent , and thirdly, the release time of internal curing water [47]. As a result, the best internal curing agent is one that can deliver a sufficient amount of water at the appropriate time and location to the cement grains. When pre-soaked LWA is added to a cementitious matrix prior to setting, there is no water exchange between them. However, after the setting process, vapour-filled pores arise when chemical shrinkage surpasses autogenous shrinkage, resulting in the movement of water from the pre-saturated LWA to the vapour-filled spaces in the cementitious matrix [13,55]. The direction of water transfer during the dormant phase can change depending on the saturation of LWA. In other words, when LWA is unsaturated, water is transferred from the fresh cement paste to the aggregate, whereas water is transferred from the aggregate to the cement paste when LWA is saturated [68]. Water may transfer from some pores of LWA with specific size ranges during each hydration stage. Even at the very early stages of hydration, the pore size of LWA is generally larger than that of cement paste [46]. As a result, the water absorbed in the largest pores of LWA is released into the cement paste, replenishing the capillary water consumed by the hydration process [69]. Capillary pressure rises as hydration progresses and the size of pores within the cement paste decreases, resulting in the release of the water absorbed in the smaller pores of LWA. It was found that when the

internal relative humidity (RH) of concrete reaches 96%, the majority of the water absorbed in LWA is released, and when RH=92%, all of the water is released to the concrete [46]. Hence, the internal RH of concrete plays a significant role when studying the effectiveness of an internal curing agent. Zhang *et al.* found that the changes in the internal RH of high-strength concrete made of LWA consist of two main stages [70]. The relative humidity is 100% in the first stage and gradually decreases in the second. As illustrated in Figure 2.3, LWA's role as internal curing agents is to prolong the first stage and reduce the decreasing rate at the second stage. As a result, LWA, as internal curing agents, can significantly reduce the drop in concrete's internal RH [71].

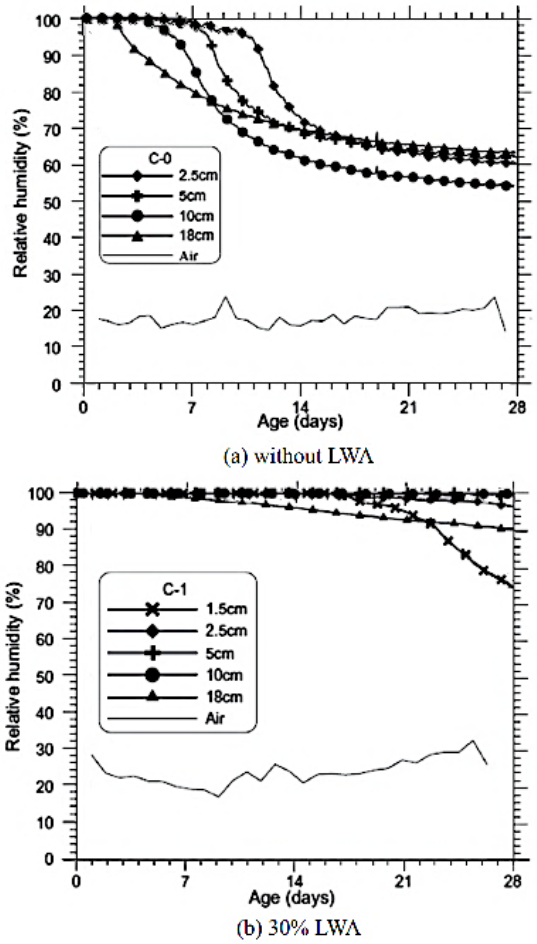

Figure 2.3. Changes in the internal relative humidity of concrete slab over time at different locations, a) without LWA, b) with 30% LWA [70]

As mentioned earlier, the migration distance of water released by LWA is one of the key factors in evaluating LWA's effectiveness as internal curing agents. Image analysis, 3D microstructural models, neutron and X-ray tomography are the methods which can be used to calculate migration distance. Based on the studies done using the above-mentioned characterization methods, the migration distance for LWA was determined to be in range of 1-3 mm [13,47,72]. To comprehend the ways in which LWA impact autogenous shrinkage and concrete hydration, it is necessary to examine pore structure and capillary pressure. In cementitious mixes with low w/b, liquid-vapour menisci develop within the pores. The shrinkage of pores occurs due to capillary pressure that is greater than air pressure. The correlation between capillary pressure and pore radius (or meniscus curvature) can be explained using the Young-Laplace equation (Equation 2.1)

$$\sigma_{cap} = \frac{2\gamma cos\theta}{r} \qquad \text{Equation 2.1}$$

Where:

$\sigma_{cap}(Pa)$: capillary pressure,

$\gamma(\frac{N}{m})$: surface tension of pore fluid,

$\theta(radians)$: liquid-solid contact angle (assumed to be zero radians), and

$r(m)$: radius of curvature of the meniscus or the pore size.

On the other hand, capillary pressure can be related to the internal humidity of concrete by using Kelvin's equation (Equation 2.2).

$$\sigma_{cap} = \frac{RT\ln(RH)}{V_m} \qquad \text{Equation 2.2}$$

Where:

R=8.3144 J/mol: universal gas constant,

$T(K)$: thermodynamic temperature,

$RH(\%)$: internal relative humidity, and

$V_m(\frac{m3}{mol})$: molar volume of pore solution.

As a result, by substituting the capillary pressure equation, shrinkage strain (ε_p) can be expressed based on pore saturation degree (S), and internal relative humidity (RH) as shown in Equation 2.3 and Equation 2.4, respectively.

$$\varepsilon_p = -\frac{S}{3}\sigma_{cap}(\frac{1}{K} - \frac{1}{K_S}) \qquad \text{Equation 2.3}$$

$$\varepsilon_p = -\frac{2}{3}\frac{RT\ln(RH)}{V_m}(\frac{1}{K} - \frac{1}{K_S}) \qquad \text{Equation 2.4}$$

Where K (Pa) is the mortar's bulk modulus, and K_S(Pa) is the bulk modulus of the solid skeleton of mortar. As a result of the internal curing agent releasing its water into the matrix, internal relative humidity rises, as does the degree of saturation of pores (S). Consequently, the capillary pressure within the pores decreases, resulting in less autogenous shrinkage.

2.3.1.2 Optimal Dosage of LWA as Internal Curing Agent

To achieve optimal internal curing goals without negatively impacting the strength, it is essential to control the percentage of LWA used in cementitious mixes. Although a higher proportion of LWA can potentially result in greater water absorption and increased water release for internal curing, it may also lead to decreased strength due to the introduction of more porous materials into the cementitious matrix. Therefore, it is important to strike a balance between the

two factors. Generally, a thorough investigation of the impact of different percentages of LWA on strength and internal curing properties is necessary to determine the optimal proportion for each specific application. The amount of LWA recommended for internal curing of cementitious materials is determined in ASTM C1761/ C1761M-17 based solely on the amount required to mitigate chemical shrinkage [73,74]. Based on the amount of water released by LWA at RH=94%, the mass of oven dried LWA required per unit volume of concrete is calculated as follows.

$$M_{LWA} = \frac{C_f \times CS \times a_{max}}{S \times \Phi_{LWA}} \qquad \text{Equation 2.5}$$

Where the values explained as follows:

M_{LWA} $(\frac{kg}{m3})$: mass of oven dried LWA needed per unit volume of concrete,

C_f $(\frac{kg}{m3})$: cement factor which is the total mass of cementitious materials used in concrete,

CS $(\frac{kg\ of\ water}{kg\ of\ cement})$: chemical shrinkage of cementitious materials at complete hydration,

a_{max} $(0 - 1.0)$: maximum potential degree of hydration of cementitious materials,

S $(0 - 1.0)$: degree of saturation of pre-wetted aggregate relative to the wetted surface-dry condition, and

Φ_{LWA} : absorption of LWA

The test method for obtaining W_{LWA} is provided in ASTM C1761/ C1761M-17 and can be calculated as follows:

$$W_{LWA} = \frac{M_{SD} - M_{94}}{M_{OD}} \times 100\% \qquad \text{Equation 2.6}$$

Where:

$M_{SD}(g)$: mass of LWA in wetted surface-dry condition,

M_{94} (g): the equilibrium mass of aggregate originally in wetted surface-dry condition and subsequently stored at 94% RH,

and M_{OD} (g): mass of LWA in oven-dry condition.

2.3.1.3 Effect of Pore Size Distribution of LWA as Internal Curing Agent

The pore size of LWA is a significant factor in determining their water absorption and desorption properties. Larger pores, with diameters exceeding 1 μm, have a higher absorption rate, but poor water retention capabilities. This leads to rapid release of the absorbed water, rendering them unsuitable for internal curing purposes that require water to be gradually released during hydration. Conversely, decreasing the size of the pores in LWA can considerably reduce the rate of absorption, resulting in a much longer time required for saturation. Furthermore, even though the very small pores of LWA can absorb water under vacuum, they may have poor water release properties. The optimal pore size for internal curing with LWA was found to be approximately 100 nm [75]. Water desorption is highly dependent on the pore size of LWA and the internal relative humidity of cementitious matrix. When the relative humidity remains constant, water in pores larger than the critical size is released, while water in pores smaller than the critical size remains saturated [46].

2.3.1.4 Effect of LWA on Properties of Cementitious Mixes

Fresh Properties

The impact of LWA on concrete flowability has received little attention. This could be because pre-saturated LWA neither absorbs nor releases water to the cement paste prior to concrete setting, leaving flowability almost unaffected [44]. However, due to the slow absorption rate of

LWA, if it is added to the mix in dry form along with the required internal curing water, it may cause bleeding and segregation.

Microstructure

The microstructure of the interfacial transition zone (ITZ) between the cement paste matrix and the aggregate has a significant impact on the properties of concrete and can be used to determine the effectiveness of incorporated internal curing agent. The internal curing water released by LWA aided in the hydration of ITZ, consequently lowering the porosity of concrete. When comparing the ITZ of concretes made with normal aggregate and those made with LWA, several significant differences can be recognized. First and foremost, as shown in Figure 2.4, a thin and denser ITZ forms around LWA [49,76,77], whereas when normal aggregate is used, the ITZ zone has high porosity with more portlandite and AFt [77]. Secondly, when LWA is used in concrete, the density of C-S-H is found to be increased [78]. Overall, using LWA is expected to improve the overall degree of hydration [72] and reduce the porosity [79], resulting in lower permeability of the concrete sample [44].

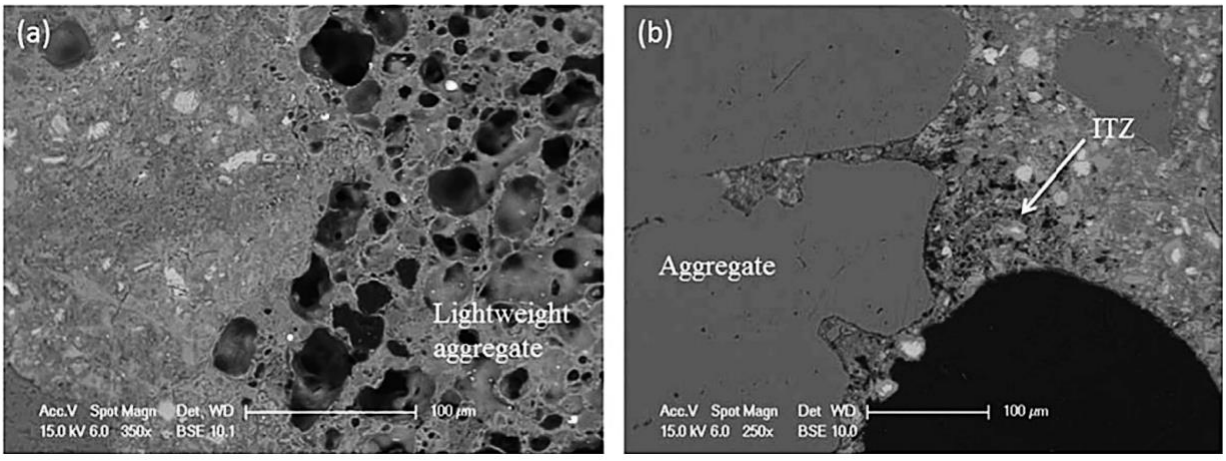

Figure 2.4. Difference between the microstructure of ITZ in cement mortar a) with LWA and b) with normal aggregate [10]

Autogenous shrinkage and drying shrinkage

As an internal curing agent, LWA can significantly reduce autogenous shrinkage and subsequently microcracking development [49,80,81]. The type of LWA and its saturation state influence its ability to reduce autogenous shrinkage. For example, vacuum-saturated LWA outperforms oven-dried LWA in terms of preventing autogenous shrinkage [50,82]. LWA that have been pre-wetted for 24 hours can typically reduce, if not completely eliminate, autogenous shrinkage [72]. Overall, different types of LWA with varying strengths, absorption capacity, and desorption can have different efficacy in reducing autogenous shrinkage. However, for dry LWA, lower absorption rate and higher strength LWA perform better in reducing autogenous shrinkage, whereas higher absorption rate and lower strength LWA are preferred for pre-wetted LWA [81].

Despite the effectiveness of LWA in reducing the autogenous shrinkage and total shrinkage at 28 days [46], it has been demonstrated that using LWA increases drying shrinkage. Using pumice aggregate, for example, resulted in a 34% increase in drying shrinkage when compared to the reference sample with normal aggregate [80]. However, a higher LWA dosage was shown to prolong the time of cracking. The lower modulus of elasticity of LWA could explain the increase in drying shrinkage of concrete [50,83]. Using shrinkage-reducing agents is one way to mitigate the negative effect of LWA on drying shrinkage [8]. Shrinkage reducing admixtures (SRA) can also extend the cracking time and reduce autogenous shrinkage by lowering the surface tension of the pore solution, hence reducing capillary pressure based on Equation 2.1 [8,84,85].

Mechanical Strength

It has been observed that incorporating LWA as internal curing agents leads to a reduction in the strength of concrete due to the relatively low strength of LWA itself [80,83]. However, this decrease in concrete strength appears to be more prominent during the early stages [86]. As the concrete ages, the strength either remains unchanged [87] or can even be improved by incorporating a significant amount of Class C fly ash [88]. Alternatively, to mitigate the negative impact of LWA on concrete strength, researchers have suggested reducing the size of LWA and enhancing its distribution within the cement mixture [70,89,90]. Agostini *et al.* conducted a study to investigate the effects of LWA on hydration products. Their findings indicated that the incorporation of LWA reduces the amount of CH and increases the density of CSH at the interface between the cement paste and aggregate [78].

2.3.2 Superabsorbent Polymers (SAP)

Superabsorbent polymers (SAP), also known as hydrogels, are polymeric materials capable of absorbing water and aqueous solutions to several hundred times their dry mass, leading to the formation of insoluble gels. Typically, available in the form of white granules or powders, SAP exhibit a particle size distribution ranging from micrometers to millimeters. Figure 2.5 illustrates the appearance of SAP in their dry state and after water absorption. The development of SAP originated in the 1970s, with Japan and the United States being the pioneering countries. The exceptional water absorption capacity and the ability to retain moisture under pressure have positioned SAP as remarkable absorbents in the market [91].

Besides the application of SAP in construction industry, they have diverse applications across other industries. In the personal hygiene sector, SAP are widely used in products such as diapers [92]. In the biomedical field, they are used in the production of wound dressings, surgical sponges, tissue engineering scaffolds, and more [93]. Other applications include meat

packaging, waste treatment [92], water conservation in agriculture [94], and water purification [95]. Extensive research has explored the use of SAP in the construction industry. These applications include the use of SAP as waterproof backfilling materials, extruded polymeric joint sealants, and as a means to mitigate shrinkage cracking [91]. The application of SAP in the construction sector has experienced significant growth, particularly in their role as internal curing agents to address autogenous shrinkage in low w/b cementitious mixes [96]. This approach has gained substantial attention and recognition, prompting the establishment of a RILEM technical committee in 2012. The committee published a comprehensive report assessing the effectiveness of SAP as internal curing agents specifically in low w/b concretes [75].

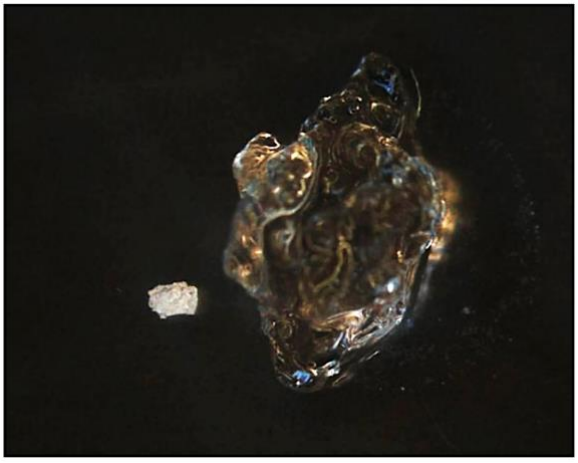

Figure 2.5. State of SAP before absorption (dry SAP; left) and after absorption (Swollen SAP; right) [75]

2.3.2.1 Effect of Particle Size of SAP as Internal Curing Agent

The particle size of SAP plays a crucial role in their water absorption and absorption rate. SAP with a smaller particle size distribution tend to reach swelling equilibrium more rapidly. However, compared to SAP with larger particles of the same chemical composition and synthesis method, they exhibit a lower absorption capacity [74,97]. Additionally, SAP can be

classified into two types based on their fluid retention behaviour: retentive and non-retentive (also known as self-releasing) [54,98].

2.3.2.2 Mechanisms of Internal Curing by SAP

There are notable differences between LWA and SAP. Firstly, SAP exhibit a significantly higher rate of water absorption compared to LWA. Moreover, SAP are typically incorporated into cementitious mixes in their dry form, whereas LWA are employed in a pre-saturated state. Another significant disparity lies in the aftermath of water release within the matrix. Desorbed SAP create empty pores within the matrix, which can be partially filled with hydration products [74]. On the contrary, LWA do not introduce any new pores, apart from their inherent porosity, upon water release.

SAP are primarily characterized by their absorption capacity and absorption rate, also referred to as swelling ratio and swelling rate, respectively. Factors such as the concrete mixing and compaction processes can influence the movement of water within SAP. The presence of aggregate can impose physical confinement and diminish the absorption capacity of SAP. However, the properties of the polymer itself and the fluid properties are the most critical parameters that can impact the absorption capacity and absorption rate of SAP. These aspects will be further discussed in the upcoming sections.

In addition to the intrinsic properties of the polymer itself, the characteristics of the fluid in which SAP are employed as internal curing agents can profoundly influence their effectiveness. Fluid properties, including chemical composition, pH, ionic concentration, temperature, and pressure, can all impact the performance of SAP. For example , while a typical SAP may exhibit a high absorption capacity of 1000 g/g in distilled water, this capacity can decrease by up to 90% to approximately 10-20 g/g when exposed to concrete pore solution due to alterations in

fluid composition [91]. Increasing the ionic concentration of the fluid diminishes both the water absorption capacity and absorption rate of SAP due to reduced osmotic pressure. Moreover, the type of ions present in the solution influences SAP absorbency, with multivalent cations such as Ca^{2+}, Mg^{2+}, and Al^{3+} causing a more pronounced reduction in absorption compared to monovalent cations like Na^{+} and K^{+} [74]. This is attributed to the formation of complexes between multivalent ions and the carboxylate groups of acrylate chains in SAP, impeding the mobility of polymer chains and impeding expansion. For instance, Ca^{2+} decrease the swelling capacity through creating a bidentate complex with acrylates of SAP [52,99–101]. The impact of multivalent divalent ions on the swelling behaviour of SAP can be observed in Figure 2.6, which demonstrates a lower absorption capacity of SAP in the presence of divalent calcium ions compared to a sodium chloride solution.

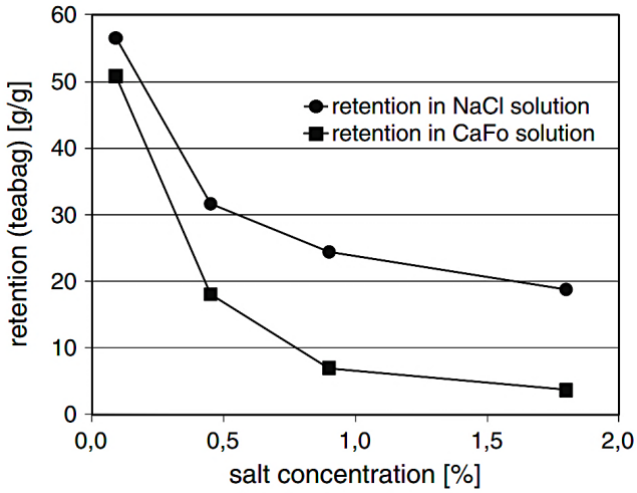

Figure 2.6. Absorption capacity of SAP in the solution of sodium chloride (NaCl) and calcium formate (CaFo) [75]

SAP have found extensive use in cementitious mixes, particularly for internal curing and prevent cracking due to shrinkage. Figure 2.7 shows the swelling and shrinking process of SAP in a cementitious system [91,102]. At the time of fabricating the cementitious mixes, dry granules of SAP are added to the mix and hence absorb part of the mix design water and swell

(Figure 2.7.A). When the relative humidity drops, either due to adverse external environmental conditions or self-desiccation during the hydration process, the swollen SAP release their absorbed water to replenish the shortage of water in the cementitious system. This results in the shrinkage of SAP and the formation of air-filled macropores known as "SAP voids" as illustrated in Figure 2.7.B. By re-wetting the concrete surface or ingress of water into the concrete, the empty SAP can be refilled with water and swell again.

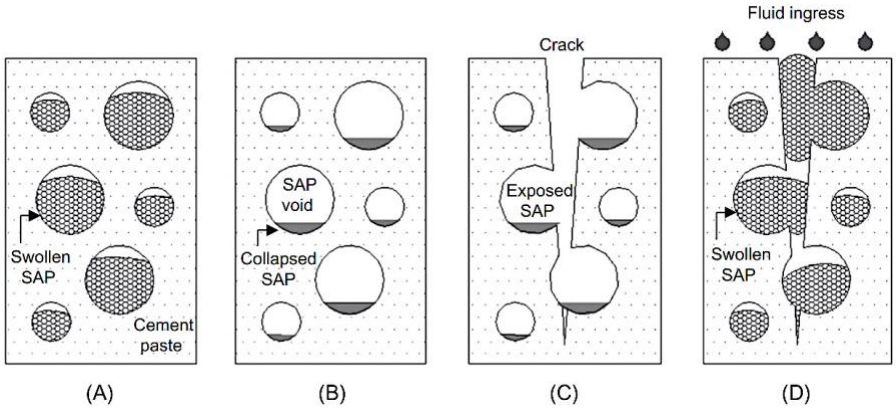

Figure 2.7. Schematic illustration of the process of releasing water by SAP to the cement paste A) initial water-filled swollen SAP, B) release of water by SAP for internal curing and leaving behind SAP voids C, D) re-swelling of SAP as a result of exposing to external wetting [91,102]

Understanding the adsorption-desorption behaviour of SAP in the alkaline environment of cement pore solution helps tackle challenges in their application in cementitious mixes. The cement pore solution is characterized by a diverse range of ions, and its chemical composition undergoes changes over time, which in turn affect the osmotic pressure and absorption-desorption behaviour of SAP. Upon introduction to the cementitious environment, the water absorption capacity of SAP is rapidly diminished within minutes. Consequently, the water absorption capacity of SAP decreases from several hundred grams per gram in deionized water to only 10-20 g/g in the cementitious environment [96,103]. Their water absorption rate is influenced by particle diameter; with larger particles exhibiting faster absorption rates [104].

On the other hand, water desorption of SAP is dependent on the internal relative humidity of the cement paste. The desorption occurs when the relative humidity decreases due to external drying or self-desiccation. In cementitious mixes with a low w/b, water desorption typically commences during the third stage of hydration, following the setting process. The duration of desorption varies depending on the particle size and can extend for several days until all the absorbed water is released [105,106]. Proper timing is crucial when using SAP as internal curing agents. If desorption occurs during the dormant period, excess water may lead to more porous concrete with reduced strength [50]. The most effective incorporation of SAP is achieved when desorption commences during the acceleration period and continues into the deceleration period of cement hydration [107].

2.3.2.3 Dosage and Dispersion of SAP in Cementitious Mixes

SAP have a variety of applications in cementitious materials, including serving as internal curing agents to reduce autogenous shrinkage and promote cement hydration plus enhancing freeze-thaw resistance. However, the dosage of SAP required in cement mixes depends on the specific application. For example, to achieve internal curing and improve freeze-thaw resistance, 0.3%-0.6% wt. of SAP are generally suggested, whereas for crack sealing, a minimum of 1% wt. is necessary [91].

In addition, the dispersion of SAP is a crucial factor that can impact their effectiveness as an internal curing agent in cementitious mixes. Two methods for dispersion are commonly used: dry mixing and pre-soaking. Dry mixing involves blending SAP with cement and aggregate before adding water, and this method is more commonly used because pre-soaked SAP have a tendency to clump together, creating a poor dispersion that can negatively impact the properties of the concrete [91].

2.3.2.4 Measuring techniques for absorption capacity of SAP

As previously mentioned, SAP are typically used in their dry form to ensure good dispersion when mixed with cement, aggregate, and water. However, this can result in the absorption of mix water by SAP, which can impact both the fresh and hardened properties of cementitious mixes. To compensate for this, an extra amount of "entrained water" must be added to the mix. However, determining the exact amount of absorption by the SAP in hardened paste, mortar, or concrete is not a simple task, due to the possibility of the chemical composition of the solution affecting the SAP' absorption capacity. Additionally, the effect of aggregate and the mixing process cannot be ignored. Therefore, it is crucial to determine the absorption capacity of SAP before designing the appropriate mix for each application. Various direct and indirect measurement methods have been proposed and implemented to measure the absorption capacity of SAP in hardened cementitious systems.

To measure the absorption capacity of SAP, there exist direct and indirect measurement methods. The direct methods involve the use of gravimetric methods, microscopy, and laser diffraction particle size analysis. The most commonly used direct method is the gravimetric tea-bag method, which is followed by conducting centrifugation and vacuum filtration [108]. However, despite its simplicity, the gravimetric method may overestimate the absorption capacity of SAP since it may not remove all physically held water before the measurement. The other methods, i.e., optical microscopy, and laser diffraction particle size analysis, however, can be implemented to avoid the error derived from the gravimetric method and measure the liquids which only absorbed by SAP [109]. Alternatively, the indirect methods involve measuring consistency and heat of hydration of cementitious mixes after incorporating SAP. In consistency methods, the absorption capacity of SAP is estimated by comparing the total w/b with the

effective w/b. The effective w/b can be estimated by comparing the slump flow of SAP mixes with a set of reference mixes with known w/b or by adjusting the batch water of SAP mixes until the same slump flow is achieved as reference mixes with known w/b [105,110,111]. The slump method suffers from a fundamental error in assuming that SAP have no influence on the rheological properties of cementitious mixes. Alternative approaches, such as using isothermal calorimetry to compare the heat of hydration between SAP mixes and reference mixes with a known w/b, have been proposed as an indirect means of measuring the absorption capacity of SAP [112]. Nonetheless, a significant drawback of employing this method to determine the effective w/b is that the use of SAP accelerates the hydration rate, leading to discrepancies in the comparison [91]. Overall, the primary challenge faced by indirect methods lies in producing a reference sample with the same effective w/b, hydration level, and air content, which may prove difficult to achieve [91].

2.3.2.5 Effect of SAP on Properties of Cementitious Mixes

Fresh Properties

The effect of SAP on the fresh properties of cementitious mixes largely relies on accurately estimating the absorption capacity of SAP in hardened state, which as discussed in the previous section is a complicated process. As a result, when discussing the influence of SAP on the rheological properties of cementitious mixes, two factors must be determined clearly: firstly, whether additional water is included in the cement mix to compensate for SAP absorption, and secondly, the technique employed to assess the amount of extra water needed. It has been noted that the addition of SAP leads to an increase in the yield stress and plastic viscosity of concrete, while the consistency and slump decrease [50,113,114]. As discussed in the previous sections, it is important to note that altering the type and size of SAP can impact their absorption capacity

and consequently influence the fresh properties of cement mixes. For instance, using smaller SAP particles can increase the yield stress and plastic viscosity of cement mortars, mainly because they have a larger surface area available for absorption [115].

Hydration and Microstructure

The impact of SAP on the early hydration of cement mixes has been observed to result in both delayed [50,53], and accelerated effects [116]. However, most studies have shown that hydration is promoted, particularly at later ages, due to the release of necessary water for anhydrous cement particles [117,118]. The increased hydration in SAP cement mixes can result in the refinement of pores and a decrease in porosity of hardened samples. However, this conclusion is complicated by the fact that the pore structure can be influenced by the dosage of SAP, absorption capacity, and amount of entrained water. Essentially, three mechanisms counteract each other to achieve low porosity in hardened samples: decreasing the effective w/b due to SAP absorption, leaving macro-voids of dried SAP, and improved hydration due to internal curing [91]. First, the initial absorption of SAP alters the effective w/b. Second, the release of absorbed water from SAP into the matrix promotes hydration and improves the microstructure at later stages. Finally, the presence of macro-voids due to the dried collapsed SAP influences the porosity.

In a study by Lura *et al.* that used X-ray tomography, reduced autogenous microcracking and lower small capillary pores were observed due to the internal curing effect of SAP [119]. Depending on the initial size of dry SAP and their swelling capacity, the size of macro-voids created by desorbed SAP may vary from 10 µm to over 500 µm [102,103,120]. These macro-voids may be filled with hydration products in the microstructure of the hardened cementitious sample [91].

When analyzing the microstructure of cement mixes incorporating SAP, special attention must be paid to the development of a new interface between the SAP and the cement paste matrix. This interface has been identified as highly porous, exhibiting lower cement content compared to the bulk paste located farther from the interface, primarily due to disrupted particle packing [91]. Additionally, this interface tends to be remarkably porous and may occasionally contain substantial deposits of calcium hydroxide. Moreover, the contraction of SAP during the drying process (release of internal curing water) can result in microcracking within the adjacent cement paste. However, it is anticipated that the release of internal curing water by SAP facilitates improved hydration and contribute to the ongoing development of the microstructure in the surrounding paste [102,103,121].

Autogenous shrinkage and drying shrinkage

It is widely accepted that the incorporation of SAP in cementitious mixes reduces autogenous shrinkage [96,122–124]. This effect is particularly significant in mixes with low w/b, which exhibits the efficacy of SAP as an internal curing agent. The decrease in autogenous shrinkage is most prominent during the early stages, as observed in a comprehensive inter-laboratory study involving 13 international research groups [50]. However, the impact of SAP on drying shrinkage is still a matter of debate. Some studies have reported a decrease in drying shrinkage when using SAP [125], while others have found an increase in drying shrinkage. For instance, it has been observed that although SAP may increase drying shrinkage, the overall shrinkage of cementitious mixes remains unchanged [96,110].

Mechanical Strength

The influence of SAP on the mechanical properties of cementitious mixes depends on multiple factors, including SAP dosage, effective w/b, and entrained water volume. However, as is often

the case with interpreting fresh properties in SAP cementitious mixes, the effect of SAP on mechanical properties is determined by opposing factors. On one hand, SAP can positively impact mechanical properties by enhancing hydration, promoting microstructure densification, and reducing autogenous microcracking. This, in turn, decreases micro porosity [117,119] and potentially leads to localized enhancements in mechanical properties. Recent nano-indentation studies have verified this effect, detecting the formation of high-density hydration products (C-S-H) within the vicinity of SAP particles, in the range of 60 to 120 μm [11]. On the other hand, as discussed earlier, the desorption of SAP may leave behind macro voids, potentially counteracting these benefits and affecting the mechanical properties of SAP cementitious mixes. All in all, the addition of SAP generally results in lower compressive strength at early ages [96,126,127], but the strength at later ages is typically similar to that of reference mixes [125,128]. In other words, the initial inclusion of SAP may temporarily reduce compressive strength due to the formation of macro voids. However, this negative effect will be compensated over time by the internal curing effect by promoting the cement hydration. As a result, the strength difference between reference mixes and SAP mixes will reduce as internal curing becomes more pronounced at later stages. The benefits of using SAP to enhance cement hydration are particularly apparent in two scenarios: when the w/b is below 0.42, owing to the significant internal curing effect over time, and when supplementary cementitious materials are employed, as water availability is crucial for their pozzolanic reaction at later stages [60,129]. A summary of the discussed effect of SAP on different properties of cementitious mixes is presented in Table 2.1.

Table 2.1. Summary of the literature review on the effect of SAP on different properties of cementitious mixes

Properties	Internal Curing Considerations	w/b	SAP (wt. %)	Summary of Findings	References
Flowability	Dry SAP: 0.05 extra water added.	0.24	0.4	Increase in the slump flow and a decrease in the V-funnel flow time values.	[130]
Flowability and air content	Dry SAP: 0.04-0.07 of extra water added.	0.22	0.3-0.4	* Extra water has to be added to preserve the slump. *Increase in air content.	[131]
Degree of Hydration	Dry SAP: No extra water added.	0.25	0.35-0.70	Hydration degree increased after 14 days	[117]
Degree of Hydration	Dry SAP: Extra water calculated based on absorption capacity of SAP.	0.3	0.2-0.6	Hydration degree increased after 28 days	[132]
Total Porosity	Dry SAP: 0.08 of extra water added.	0.22	0.6	Total porosity at all ages is about 6% higher than that in plain concrete.	[133]
Autogenous Shrinkage	Dry SAP: 0.05 of extra water added.	0.3	0.3-0.6	Completely countering autogenous shrinkage	[96]
Autogenous Shrinkage	Dry SAP: Extra water calculated based on absorption capacity of SAP.	0.25	0.11-0.33	Completely prevent autogenous shrinkage of early-age concrete.	[124]
Mechanical Strength	Dry SAP: No extra water added	0.45	0.2-0.6	No significant change observed in compressive strength.	[134]

2.3.3 Natural Fibres

The concept of sustainable development has become increasingly significant in recent years as the world grapples with the pressing issues of climate change and resource depletion. Sustainable development refers to the idea of meeting the current needs of society while ensuring that future generations can meet their own needs without any trade-offs [135]. This concept is particularly crucial in the construction industry, which is responsible for emitting approximately 5% of total human-made CO_2 emissions and depleting natural resources during

the production of concrete [136]. To tackle this issue, it is necessary to take steps towards the production of more sustainable cementitious materials using renewable substitutes like lignocellulosic wastes, specifically natural fibres. The benefits of using natural fibres as substitutes include a reduced environmental impact, lower costs, and conservation of resources and energy.

As previously discussed, SAP have emerged as a promising alternative for LWA for internal curing agent in cement-based materials due to their high absorption capacity. However, SAP are made of polyacrylate, a non-renewable and petroleum-based material, which can increase the carbon footprint of cement-based materials [18]. In contrast, natural fibres are mostly hygroscopic materials and can offer a cost-effective and sustainable option as internal curing agents. Using natural fibres can offer additional benefits as well. Unlike synthetic materials like SAP, natural fibres are widely available in many regions around the world at little to no cost. Thus, using natural fibres as renewable resources presents a sustainable solution that can provide cost-effective construction materials in any region worldwide while mitigating the environmental impact of the construction industry. Additionally, natural fibres are frequently derived from agricultural wastes and by-products, which can create a supplementary source of income for farmers if their benefits are fully explored and understood. Nevertheless, the mechanisms of natural fibres as internal curing agents in cementitious mixes have been less extensively studied in comparison to LWA and SAP, for which there is a reasonable understanding. Table 2.2 provides an overview of the pros and cons of each internal curing agent in comparison to natural fibres.

Table 2.2. A comparison of advantages and disadvantages of different internal curing agents

Internal Curing Agent	Pros	Cons
Lightweight Aggregate (LWA)	✓ Relatively low unit weight ✓ Absorption takes longer time	× Lower water absorption capacity and poorer water retention × Cause higher drop in strength and elastic modulus of concrete when compared to SAP × Can only store the water physically inside of their capillary pores
Superabsorbent Polymer (SAP)	✓ Very high absorption capacity ✓ Can absorb water due to chemical and physical bonds	× Non-renewable material × High production cost × Not locally available × Increase the embodied energy and carbon
Natural Fibres	✓ Excellent hygroscopic properties ✓ Can absorb water due to chemical and physical bonds due to presence of lumens ✓ Presence of hydrophilic components in their structure such as cellulose and hemicellulose ✓ Lightweight characteristic especially hollow fibres ✓ Abundantly available ✓ Little to no cost ✓ Renewable	× Leach out of some harmful extractives upon contact with alkaline environment × Require pre-treatment prior to use (compatibility issue with cementitious environment)

Natural fibres encompass a wide range of materials, including plant fibres, mineral fibres, and animal fibres as illustrated in Figure 2.8. Mineral fibres like asbestos and animal fibres such as silk are examples in their respective categories. However, the focus of this study is on plant fibres and their potential as internal curing agents in cementitious mixes. Natural lignocellulosic plant fibres, referred to as natural fibres henceforth, can be further classified into three categories based on their extraction location within the plant to: bast fibres, seed fibres, and leaf fibres. Bast fibres, also referred to as phloem fibres, are acquired from the fibre bundles tightly encircle the stem of plants [137]. Some examples of bast fibres include jute, flax, ramie, hemp, and kenaf [138,139]. Due to their higher cellulose content, bast fibres typically have greater tensile strength than other plant fibres [140]. Coconut fibres and sisal fibres are examples of

fruit and leaf fibres, respectively. Finally, wood fibres can be classified as softwood and hardwood fibres and are derived from a variety of trees. Seed fibres, such as cotton, MW fibres, and kapok are another type of natural fibres. Certain seed fibres, such as kapok and MW possess a unique hollow structure characterized by an exceptionally wide lumen and thin walls. This feature facilitates grain dispersal, aiding in germination. More importantly, the distinctive hollow morphology of these fibres imparts a lightweight property, making them ideal for the development of low-density and insulation applications [25].

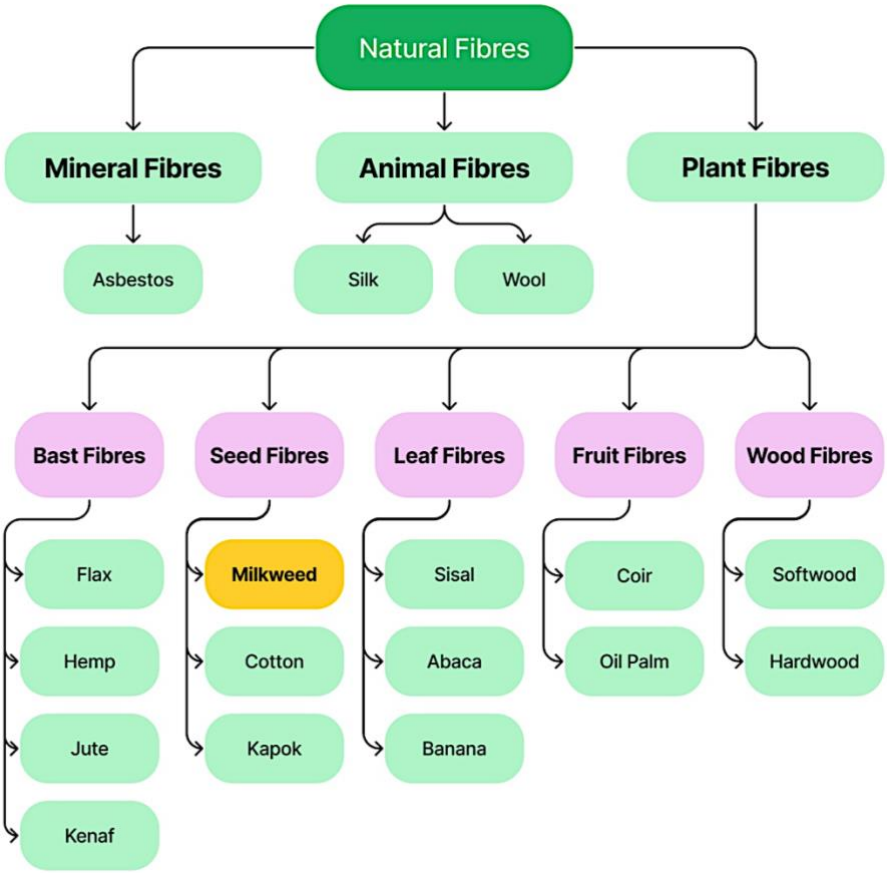

Figure 2.8. Summary of classification of different types of natural fibres

2.3.3.1 Characteristics of Lignocellulosic Fibres

The differences in the properties exhibited by various natural fibres can be attributed to their distinctive chemical compositions and physical structures. Natural fibres are considered natural

composites with a cellular structure which is intricately constructed. As depicted in Figure 2.9, the structure of natural fibres comprises a central channel known as the lumen, responsible for transporting water and nutrients, surrounded by the cell wall. The cell wall consists of multiple layers, including the middle lamella, the thin primary wall, and the secondary wall, further subdivided into the external secondary wall (S1), middle secondary wall (S2), and internal secondary wall (S3) [141]. Each of these layers contains microfibrils oriented in specific angles, unique to their respective layers. The primary wall is characterized by a disordered arrangement of cellulose fibrils embedded within a matrix of pectin, hemicellulose, lignin, and protein. In contrast, the secondary walls are composed of crystalline cellulose microfibrils arranged in a spiral configuration, where the middle layer (S2) plays a vital role in determining the mechanical properties of the fibres [142]. These microfibrils, are situated within an amorphous region formed by lignin and hemicellulose. The outermost layer of the cell, known as the middle lamella, primarily consists of pectin, which acts as a cementing material between adjacent fibres. Other components such as wax and impurities may also be present on the surface of natural fibres albeit in lower percentages. Consequently, as the variation in the content of each of the aforementioned components in fibre their properties may also differ. Secondly, the structural characteristics and morphology of natural fibres such as microfibril angle, crystallinity, surface defects and their hollow structure can result in different properties [143]. Additionally, it is noteworthy that the properties of a particular plant may vary significantly from one batch to another due to multiple factors such as variations in growing conditions and climates, plant age, and processing techniques. These variations can impact the chemical and physical structure of the natural fibres within the plant, leading to differences in their properties

[144–146]. This could pose a significant challenge, as it may result in unpredictable properties of the composite materials that incorporate these fibres [147,148].

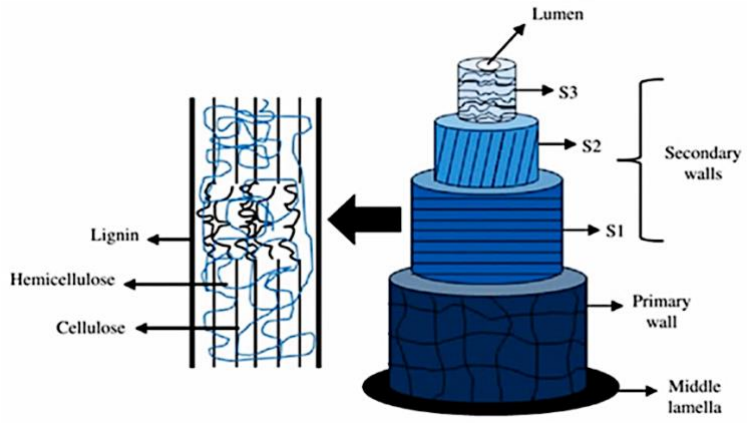

Figure 2.9. Schematic illustration of plant fibres structure: middle lamella, primary wall, S1 - external secondary wall, S2 - middle secondary wall and S3 -internal secondary wall and lumen, adapted from [142]

As mentioned above, natural fibres primarily consist of cellulose, hemicellulose, and lignin. Cellulose is a polymer composed of glucose units. Hemicellulose is another type of polymer made up of several polysaccharides while lignin is an amorphous and heterogeneous mixture of aromatic polymers and phenyl propane monomers. The composition of various fibres may differ, as demonstrated in Table 2.3.

Table 2.3. Composition of some natural plant fibres [149]

Fibre	Cellulose (%)	Hemicellulose (%)	Lignin (%)	Extractives (%)	Ash (%)
Eucalyptus	41.57	32.56	25.4	8.20	0.22
Coir	21.46	12.36	46.48	8.77	1.05
Bagasse	41.7	28.00	21.8	4.00	3.50
Sisal	73.11	13.33	11.00	1.33	0.33
Banana Leaf	25.65	17.04	24.84	9.84	7.02

Figure 2.10 depicts the structure of a cellulose microfibril. Cellulose is a sugar-based polymer consists of long chains of D-glucose units joined by β (1 → 4) glycosidic linkages which is shaded in Figure 2.10 [150]. Hence, cellulose is classified as a (1→4) β-glucan with a repeat unit of cellobiose which forms linear chains [150]. The cellulose microfibril, which is the fundamental structural component of plant cell walls, is formed by intrachain and interchain hydrogen bonding between cellulose chains (Figure 2.11). The hydroxyl groups are able to create hydrogen bonds with water molecules which is one of the primary reasons for excellent hygroscopic properties of natural fibres. Interestingly, cellulose microfibril has a semi-crystalline structure, consisting of both highly crystalline and some amorphous regions [151]. Due to their high tensile strength, the cellulose content of a natural fibre can serve as an indicator of its mechanical properties, with lower microfibril angles relative to the fibre axis generally resulting in superior mechanical performance [143]. Microfibril angle can be measured through the methods based on X-ray diffraction developed by Cave in 1997 [152].

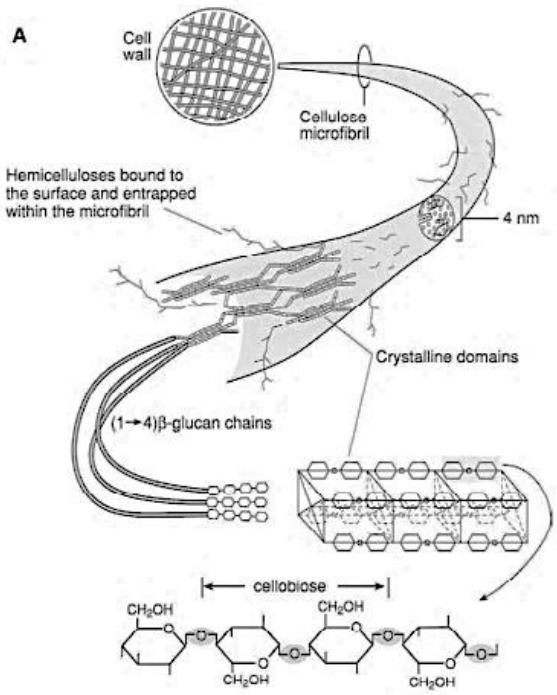

Figure 2.10. An illustration of Cellulose Structure [153]

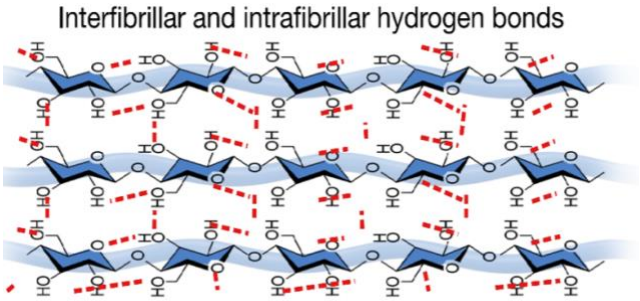

Figure 2.11. A schematic of the molecular structure of cellulose with lots of intrafibrillar and possible interfibrillar interactions [154]

Regarding the mechanical properties of natural fibres, it's important to note that due to the unidirectional reinforcement of cellulose, these fibres exhibit anisotropic behaviour. For example, in the longitudinal direction, the Young's modulus of cellulose microfibrils is around 137 GPa [155]. While natural fibres demonstrate remarkable mechanical properties in the longitudinal direction, they exhibit weakness in the radial direction due to their amorphous blend properties [151]. In general, the mechanical properties of natural fibres are highly

dependent on their chemical composition, with higher cellulose contents and lower microfibril angles being the most effective parameters [156]. Other factors such as fibre diameter, size of lumen, surface defects, and moisture content can also influence the mechanical properties of natural fibres [157].

2.3.3.2 Hygroscopic Properties of Lignocellulosic Fibres

Most natural fibres show strong affinity for water and hydrophilic behaviour and hence are considered to be hygroscopic materials. Generally, hygroscopic materials refer to the materials which interact with water molecules to achieve an equilibrium with the surrounding humidity of environment. The high tendency of natural fibres towards moisture adsorption has a considerable impact on their individual properties as well as the properties of the material they are integrated in. Consequently, it is crucial to thoroughly understand the hygroscopic characteristics of natural fibres before their integration into a matrix. According to the earlier explanation, the behaviour of natural fibres in adsorbing water depends on both their chemical composition and morphology. Given the physical makeup of natural fibres, some fibres with lumens and porous surfaces can increase the amount of liquid that enters their capillary spaces due to capillary pressure, which enhances their hygroscopic properties [151]. This distinct characteristic is particularly prominent in fibres possessing wide lumens, notably observed in hollow seed fibres, as shown in Figure 2.12

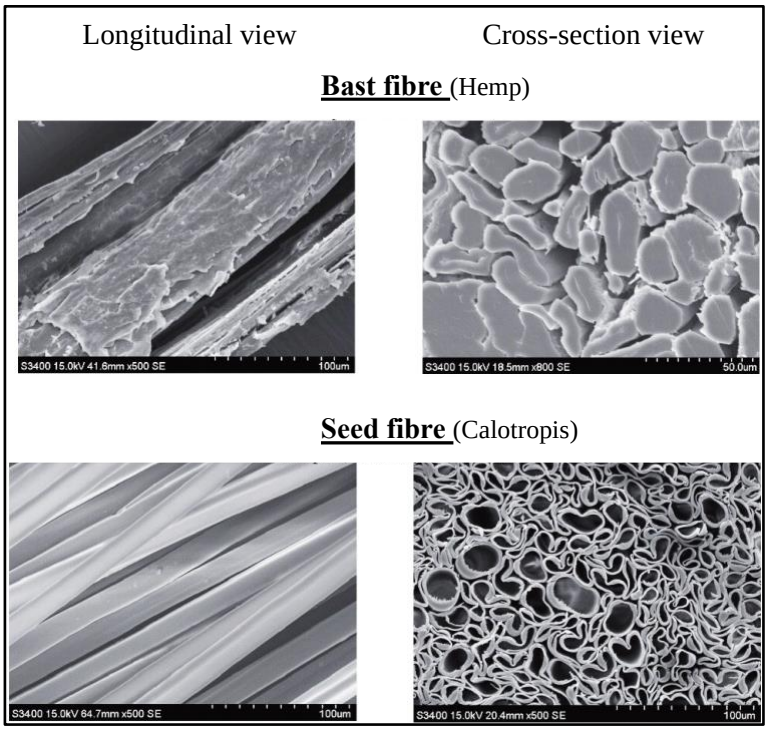

Figure 2.12. Comparison of the morphology of bast fibre (Hemp) vs seed fibre (Calotropis) [158]

Moreover, the hydrophilicity of natural fibres is significantly influenced by their chemical composition. In fact, polar polymeric structures found in natural fibres enable them form hydrogen bonds with water molecules. Therefore, polymers such as cellulose, hemicellulose, and pectin play a significant role in determining the hydrophilicity of natural fibres [159,160]. Célino *et al.* employed Fourier transform infrared (FTIR) spectroscopy to conduct qualitative and quantitative analyses, and investigated the influence of moisture content on infrared spectra of natural fibres [160]. Their findings suggest that amorphous cellulose and hemicellulose hydroxyl groups, as well as pectin's carboxylic groups, are viable water absorption sites. To initiate bonding between water molecules and these hydrophilic groups, the first water molecule must form a direct bond with the fibre's hydrophilic groups. Subsequently, subsequent water molecules may form either direct or indirect bonds with the fibre (Figure 2.13). The direct

bonding of the water molecules with the hydrophilic groups lead to more firm bonds comparing to the water molecules that are attached to the existing absorbed water molecules [161].

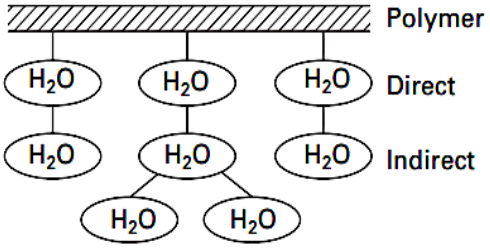

Figure 2.13. Direct and indirect absorption of water molecules by a polymer molecule [161]

To illustrate, cellulose molecules contain three hydroxyl groups for each glucose residue. When water molecules interact with the hydroxyl groups of the fibre, hydrogen bonds are formed and water is absorbed, as shown in Figure 2.14. It should be noted that during the absorption process, multiple water molecules may attach to each hydroxyl group [161].

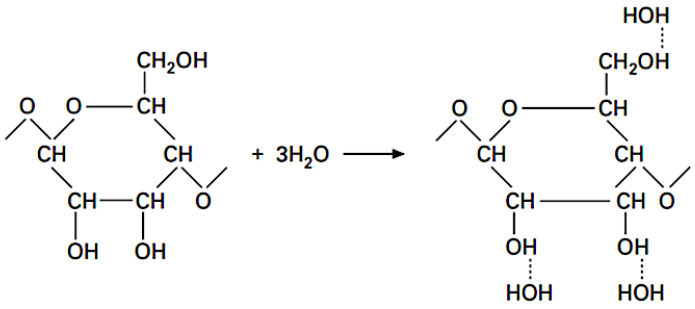

Figure 2.14. Absorption of water molecules to the hydroxyl group of a cellulose molecule by hydrogen bonding [161]

2.3.3.3 Application of Lignocellulosic Fibres as Internal Curing in Cementitious Mixes

The application of natural fibre in cement-based materials can be found in various products including extruded non-pressure pipes and non-structural building materials such as siding, cladding, and soffit panels [162]. However, in recent years, there has been growing interest in using cellulose-based natural fibres, such as pulp fibre, kenaf fibre, Lechugilla fibre, and cellulose filaments, as substitutes for conventional petroleum-based SAP for internal curing

applications. The reason for this is their remarkable hydrophilic nature, which has been documented in several studies [20,23,34,64,163]. A particularly noteworthy finding comes from Hisseine *et al.*, who reported that cellulose filaments can effectively mitigate autogenous shrinkage and reduce early-age deformation due to their outstanding hygroscopic behaviour. These filaments showed a water retention capacity exceeding 100% after just 6 hours of immersion and released up to 97% of that water after 48 hours, according to their research [64]. Jongvisuttisun *et al.* conducted another study using advanced techniques, such as NMR and MRI, to investigate the effect of hardwood eucalyptus pulps on the internal curing of cement paste samples during the early stages [22]. Their research revealed that water can move through the lumen and micropores in the cell wall via capillary flow, and through the cell wall through diffusion. Additionally, osmotic pressure can also impact the fluid transport in wood pulps. The cell walls of wood pulp act as semi-impermeable layers, and the gradient of counter-ion concentration across the cell wall creates an osmotic pressure that affects the fluid transport of wood pulps. These mechanisms of internal curing can be activated during different stages of cement hydration. The researchers made several observations, including that like LWA and SAP, the use of wood pulps resulted in a more pronounced increase in the heat of hydration at later ages rather than early ages. Furthermore, they noticed that after the addition of wood pulp to cement, pore solution ions would be absorbed into the cell walls of the pulps during the first stage of the process. The absorbed ions on the cell walls of wood pulps and their concentration are highly dependent on the chemical composition and pH of the cement pore solution. Eventually, during the self-desiccation stage, the internal curing effect of wood pulp becomes apparent through various mechanisms, such as capillary forces, water vapour diffusion, and osmotic pressure [22]. The internal curing effect of wood pulp on cement paste was categorized

into two time periods. In the first 25 hours of cement hydration, capillary forces drew the free water of the lumen and released it to the surrounding cement paste. Additionally, water vapour diffusion occurred due to the humidity gradient between the wood pulp and self-desiccating capillary pores. However, after 25 hours of hydration, only two sources of water molecules were available for hydration: the free water in small wall pores and the bound water of the wood pulps. Furthermore, considering the cell wall of wood pulp as a semi-impermeable layer, an osmotic pressure can be created by the gradient of counter-ion concentration across the cell wall, allowing for the transport of water through the cell walls of the pulps. Using NMR measurements and analyzing the T_2 relaxation times of wood pulps at varying moisture contents, the sequence of moisture migration from the fibre to the surrounding self-desiccating paste was determined. This sequence includes the removal of free water from the lumen, followed by the removal of free water from cell wall micropores, and finally the removal of bound water absorbed into the cell wall [22]. The study also employed SEM and AFM images to observe the precipitation of small, discrete particles on the surface of the wood pulps. XPS analysis determined that these particles were calcium-rich phases, which can act as nucleation sites and contribute to better interfacial bonding with cement, resulting in a higher rate of hydration [22].

2.3.3.4 Compatibility of Lignocellulosic Fibres in Cementitious Mixes

The incorporation of lignocellulosic fibres into cementitious mixes can have a significant impact on the hydration reactions of PC. The alkaline environment of cementitious matrices can lead to the degradation of lignocellulosic materials, resulting in the release of leachates. For instance, hemicellulose and lignin may dissolve in the alkaline cement pore solution, leading to the decomposition of extractives and the generation of polysaccharide hydrolysis by-products. Consequently, the hydration behaviour of aluminates, silicates, and aluminosilicates in the

presence of natural fibres is not solely determined by water content but is significantly influenced by the saccharides released by these fibres [164]. The saccharides can affect the hydration reactions with different mechanisms. Previous studies have proposed two main mechanisms that account for the interaction of plant fibre molecules with the hydration reactions of ordinary PC paste [164]. The first mechanism involves the capture and retention of calcium ions by alkaline-induced chelating agents, while the second mechanism entails the reversible physisorption of monosaccharides on anhydrous cement grains. The polysaccharides constituting the natural fibres possess potent Ca-chelating groups that have a high calcium binding capacity, which can reduce the concentration of calcium ions in the cement pore solution and inhibit the formation of hydration products such as C-S-H, portlandite and ettringite and hence cause a delay in the hydration process [165,166]. Furthermore, due to the alkali hydrolysis of the organic compounds present in natural fibres, some sugar moieties that are insoluble can form and create a protective layer around the partially hydrated cement particles. It is also worth noting that the difference in the molecular architecture of saccharides leads to their distinct alkaline stability, selective adsorption on and binding strength with anhydrous cement components [164]. As an example, glucose, a monosaccharide, undergoes degradation in the cementitious alkaline environment, producing by-products that contain carboxylic acids. These by-products exhibit non-selective adsorption on both hydrated silicates and aluminates. However, sucrose, a disaccharide, exhibits selective adsorption in their intact form at hydrated silicate sites and anhydrous aluminate moieties, but not at hydrated aluminate sites [164]. Hence, to prevent any adverse impact on the properties of cementitious materials and natural fibres themselves, it is critical to control alkali hydrolysis of natural fibres prior to their addition cementitious matrices.

Various strategies and treatments have been implemented to improve the compatibility of lignocellulosic materials with cementitious matrices, including but not limited to: alkali pre-treatment of fibres, using pozzolanic materials to reduce pH of cement pore solution, zirconium dioxide sol-gel fibre treatment, biopolymeric surface treatment of fibres, and carbonation of cementitious matrix in a CO_2-rich environment [29–31].

2.3.3.5 Effect of Lignocellulosic Fibres on the Properties of Cementitious Mixes

Flowability

Most research studies have shown that the incorporation of natural fibres can diminish the flowability of cementitious mixes. Mansur and Aziz, for instance, noted a reduction in workability when jute fibres were added to cement paste and mortar [167]. The extent of this impact depends on the quantity and aspect ratio of the natural fibres used in the mix. This is primarily due to the hydrophilic nature of natural fibres, which can absorb some of the mix water and reduce its consistency. However, several strategies can be employed to mitigate the negative impact of natural fibres on the fresh properties of cement mixes. First, the mix design water can be readjusted to account for the absorption of natural fibres. Alternatively, fibres can be pre-soaked to minimize their water absorption, or pre-treatment can be applied to the fibres to lessen their hydrophilic behaviour [63].

Shrinkage

Numerous studies have demonstrated the effectiveness of natural fibres in reducing plastic shrinkage in cementitious mixes. For example, Bighossian and Wegner found that increasing the amount of flax fibres in a mix led to a 99% decrease in maximum crack width and total crack area compared to reference samples [168]. The success of flax fibres in reducing plastic shrinkage can be attributed to their hydrophilic nature, which promotes good interfacial bonding

between the fibre and matrix. Similarly, the addition of MW fibres (Estbragh, Asclepias Procerais) at a concentration of 0.25-0.75% resulted in a significant reduction in crack number and width due to a crack-bridging effect [169]. In another study, the inclusion of a low volume fraction of short sisal and coconut fibres led to a decrease in the free plastic shrinkage of mortar samples [170]. This improvement may be attributed to the crack-bridging effect of these fibres and their higher modulus of elasticity compared to the cementitious matrix [170,171].

Hydration

Natural fibres have been found to delay the setting time and retard the cement hydration process [172–174]. This retardation is primarily attributed to the soluble sugars within the structure of some compounds. Among the various sugar components, sucrose and glucose were found to have a particularly detrimental effect on cement hydration [165,175]. The sugar components in natural fibres influence the hydration process through multiple mechanisms. Firstly, saccharides adsorb onto the surface of cement grains, forming a semipermeable layer that impedes water accessibility for hydration [165]. Secondly, the calcium binding capacity of the fibres, in the form of Ca-chelating group, hinders the formation of CSH, which is crucial for cement strength and stability [174–176]. In addition, acidic components such as galacturonic acid (GAA) and glucuronic acid (GLA) found in natural fibres leachates can reduce the pH level of the highly alkaline cement pore solution [177]. Furthermore, other fibre components like pectin may also adversely affect cement hydration [172]. To mitigate the delay in hydration of natural fibre-cement mixes, techniques similar to those mentioned earlier can be employed, such as pre-treatment of fibres and/or incorporating pozzolanic materials and supplementary cementitious materials (SCMs). The latter two approaches are particularly effective in reducing the alkalinity

of the cementitious environment, thereby assisting in alleviating alkali hydrolysis of natural fibres.

Mechanical Properties

Certain natural fibres, depending on their characteristics, volume fraction, and modulus of elasticity have the potential to enhance the mechanical properties of cementitious materials. A notable example is hemp fibres, which have been demonstrated to increase compressive strength by 4% and flexural strength by 9% in cementitious composites [178]. Moreover, the incorporation of hemp fibres can significantly improve flexural toughness and flexural toughness index by 144% and 214%, respectively [178]. Another fibre, coir fibre, exhibited exceptional impact resistance compared to fibres like Hibiscus Cannabinus, sisal, and jute fibres, with an increase in impact resistance of up to 253.5 J [179]. However, it is crucial to consider the moisture absorption characteristics when using natural fibres to improve mechanical properties. For instance, the moisture content of pulp fibre has been found to influence the mechanical strength and failure mechanism of mortar samples [180]. Over-drying of pulp samples has been shown to yield higher flexural strength, but lower toughness compared to samples subjected to air or wet curing conditions. This variation can be attributed to improved bond strength between the pulp fibre and matrix in dried samples, resulting in a shift in the failure mode from pull-out to a mixed mode of pull-out and fracture [180]. A summary of the discussed effects of natural fibres on different properties of cementitious mixes is also presented in Table 2.4.

Table 2.4. Summary of the literature review on the effect of natural fibres on different properties of cementitious mixes

Properties	Fibre Type	Pre-treatment	w/b	Amount (wt. %)	Summary of Findings	References
Flowability	Jute	Soaked in NaOH for 24 hours	0.45	0.25-0.75 vol. %	Increase in slump flow	[181]
Hydration	Bagasse	Thermal treatment at 175-250 °C	0.4-0.6	0.5-2	* Delayed the setting time * Decrease the maximum hydration temperature. * Better compatibility by thermal treatment.	[173]
Hydration and flexural strength	Hemp	Alkaline treatment with 6 wt.% NaOH solution for 48 hours and a slight acid treatment with 1 wt.% AlCl3 solution	0.5	2 vol. %	*Non-treated fibres resulted delayed setting times. * Alkaline treatment resulted in the highest flexural strength	[172]
Plastic shrinkage	Sisal	-	0.45-0.5	0.2	*Mitigating free plastic shrinkage, delaying the onset of the first crack, and managing crack progression.	[171]
Crack width and number, compressive and bending strength	Estabragh	-	0.52	0.25-0.75	*Reduction in both the number and width of cracks. *Slight improvement in compressive and bending strength	[169]
Plastic and drying shrinkage	Sisal and coconut	-	0.4-0.52	0.1-0.2	*Postponing the onset of initial cracking during restrained plastic shrinkage. *Increased the drying shrinkage.	[170]
Impact strength (projectile test on slabs)	Coir, sisal, jute, and hemp	-	0.47	0.5-2	Improved impact resistance	[179]

2.4 Kinetics of water transport in internally cured cementitious samples

Studying the kinetics of water transport from internal curing agents to the cementitious matrix is of great importance. One of the most powerful techniques for dynamically characterizing different types of water and pore structures in cementitious materials is ^{1}H Nuclear Magnetic Resonance (NMR) relaxometry. This method allows for the non-invasive and non-destructive measurement of free water, capillary water, and bound water over time. Unlike traditional methods like Mercury Intrusion Porosimetry (MIP), which require breaking hardened samples and halting hydration, NMR allows for non-destructive, dynamic, in-situ analysis of porous materials [182–184]. These advantages enable continuous observation without altering the samples. Consequently, NMR relaxometry has found wide applications in characterizing cementitious matrices in recent years.

The pore structure of cementitious materials is characterized by the different physical states of water in pores of varying sizes. When a magnetic field is applied, the hydrogen nuclei in the water within these pores act like subatomic magnets [185]. Upon excitation, these nuclei gradually lose their alignment through a process known as relaxation. The relaxation of hydrogen nuclei occurs more quickly in smaller pores due to their higher surface-to-volume ratio. This is explained by the fast exchange model as shown in Equation 2.7 where the spin-spin relaxation time (T_2) is inversely proportional to the surface-to-volume ratio of the pores is in contact with the fluid [51,186]. Assuming the presence of spherical pores with a diameter of d, the T_2 correlates with the distribution of pore sizes (i.e., $T_2 \sim \frac{d}{6}$) [187,188]. Consequently, as cement hydration progresses, the pore structure evolves and the T_2 distribution also changes. Therefore, the reduction in T_2 values observed during the evolution of hydration in the cement paste is attributed to the densification of the cement paste and the formation of hydration

products within water-filled pores and on the surface of cement grains [189]. This leads to a reduction in inter-particle spacing and consequently more confinement and shorter relaxation times (i.e. smaller T_2.)

$$T_2 = \frac{V}{S \times \rho_2} \qquad \text{Equation 2.7}$$

where V and S represent the volume and the surface, respectively, and ρ_2 is surface relaxivity. For a comprehensive review of the application of ^{1}H NMR relaxometry in cementitious materials, refer to the study by Valori *et al.* [190] and Monteiro *et al.* [185].

While extensive studies have investigated the kinetics of water transport between in SAP [51,188,191–194] and LWA [49,195–197] in cement paste using NMR, research on lignocellulosic materials remains limited and requires further exploration. The variability in the physical and chemical properties among different natural fibres suggests that their water transport kinetics could exhibit diverse behaviours, necessitating additional investigations.

2.5 Milkweed Fibres

Milkweed plant belongs to the weed family, which is generally defined as any plant not intentionally cultivated. Weeds are highly adaptable and can thrive in harsh soil and climate conditions where other plants struggle to survive. They can be classified as annuals, biennials, or perennials based on their growth cycle. Asclepias Syriaca, a perennial plant native to North America, is the most common species in the milkweed family (Asclepiadaceae). However, milkweed plants are also found in other countries, such as China and Iran, where they are known as Akund and Estabragh, respectively. Milkweed plant produces silky white fibres extracted from its seeds. Asclepias Syriaca can grow in a wide range of soil conditions and is commonly found along roadsides, fields, meadows, and waste areas [24]. In Canada, there are several other

milkweed species present, including common milkweed, white milkweed, green milkweed, purple milkweed, prairie milkweed, four-leaved milkweed, wooly milkweed, poke milkweed, oval-leafed milkweed, whorled milkweed, showy milkweed, butterfly milkweed, and swamp milkweed, according to the Canadian Wildlife Federation website. The factors that distinguish these species from each other are the growth range, habitats preferences, and their appearance.

The name "Asclepias Syriaca" also known as common milkweed, has two parts. The first part, "Asclepias" is derived from the Greek god of medicine, Asklepios, as some species of milkweed were historically used for medicinal purposes. The second part, "Syriaca" means originated in Syria. This name was mistakenly given by Carl Linnaeus, who is credited with the creation of the binomial nomenclature system, after the plant was first introduced to Europe [198].

An illustration of the different parts of the common milkweed plant can be seen in Figure 2.15. Milkweed plant is characterized by its stout and tall stem, which typically measures between 0.9 to 1.2 meters and is covered in fine, soft hairs. Its leaves are oblong to oval-shaped, with a length of 7.5 to 15 centimeters [25]. Upon being broken, the stem and leaves release a milky sap, which is why the plant is known as "milkweed". This sap is toxic to most animals due to the presence of cardiac glycoside, a dangerous compound that interferes with heart function. However, monarch butterfly caterpillars can ingest the toxin and use it to deter predators. Once milkweed seed pods ripen and harden, they split open gradually, releasing brown seeds attached to bunches of white, silky fibres called floss fibres. These fibres help to disperse the seeds and transport them over long distances through the wind for germination in new locations.

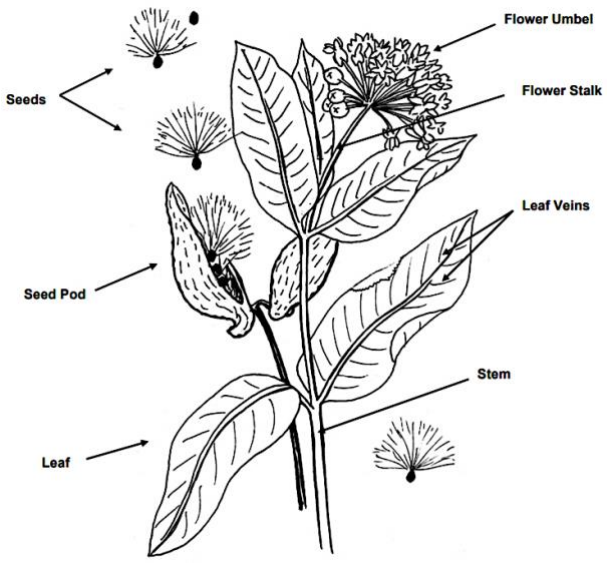

Figure 2.15. An illustration of the common milkweed (Asclepias Syriaca) (Environmental Education in Wisconsin website)

As shown in Figure 2.16, among natural fibres, MW floss fibres show a hollow structure which makes it unique compared to other natural fibres [25]. The extremely wide lumen of MW fibres, which takes up to 77% of the fibre volume and its thin cellulosic wall (approximately 1.3µm), can potentially promote its absorption capacity [26,27]. However, this hollow lumen also gives MW fibres a fluffily nature with a density of approximately 300 kg/m^3 comparing to conventional SAP with a dry density of around 1500 kg/m^3 [55,199]. This is an important characteristic which can be advantageous for the application of MW fibres in lightweight materials. MW fibres are classified as microfibres because they typically possess a length of less than 1 mm and a diameter within the range of 10 µm. As presented in Table 2.5, MW fibres are composed of cellulose (40-45%), hemicellulose (35-40%), and lignin (15%). However, other components such as waxes, pectin, and sugars are also present in small amounts (<5%) in MW fibres [25]. As discussed earlier, some of these components are hydrophilic and can act as absorption sites for water molecules (mainly cellulose and hemicellulose), whereas others, like waxes, are hydrophobic. As a result, MW fibres can be classified as an amphiphilic material

that can exhibit both hydrophilic and hydrophobic properties. For instance, Panahi *et al.* (2020) observed a superhydrophobic surface with a contact angle of around 140˚ and up to 100 g/g of oil absorption capacity in MW fibres [200]. Choi *et al* (1992) also reported a crude oil sorption capacity of 40 g/g previously [201]. On the other hand, some studies have shown the high potential of MW fibres for water absorption. For example, higher moisture regain has been reported for MW fibres in comparison to cotton (11% vs 8%, respectively) [26,28,202]. In addition, it was observed that the unique hollow channel in MW fibres can result in fast moisture absorption [199,203,204]. To the best of the authors' knowledge, there is only one study which has been done on the application of MW fibres as an absorbent material. Kumar *et al.* (2020) assessed the moisture behaviour properties of MW and MW/cotton blended sanitary napkins. They found out that the higher the blend percentage of MW fibres, the greater the amount of liquid absorption, liquid retention capacity, and liquid holding capacity under pressure of sanitary napkins [205]. Furthermore, the use of MW fibres in cementitious environments has been explored in limited studies [169,206], with a primary focus on mechanical performance. The first study revealed that although the strength of MW fibres may deteriorate in the alkaline cement environment, these fibres exhibited the ability to bridge micro cracks within the concrete matrix, resulting in a reduction in the width of surface cracks [169]. Conversely, another study reported lower compressive and flexural strength after incorporating MW fibres into the cementitious matrix [206]. These contrasting outcomes highlight the incomplete understanding of the influence of MW fibres on cementitious matrices, calling for further in-depth investigations.

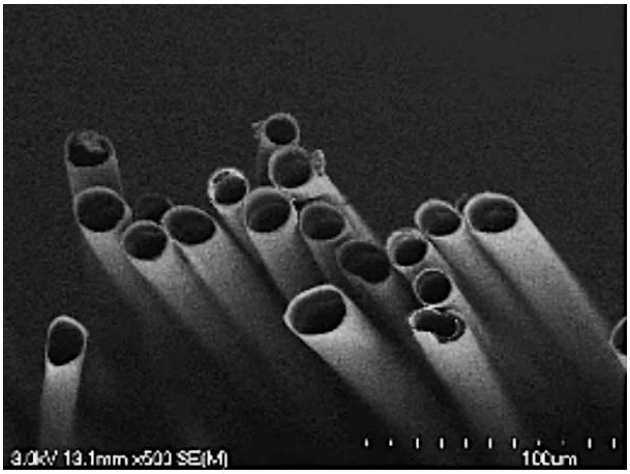

Figure 2.16. The hollow structure of common milkweed fibres [25]

Table 2.5. Chemical composition of common milkweed fibres

Cellulose (%)	Hemicellulose (%)	Lignin (%)	Wax (%)	Pectin (%)	Free sugars (%)	References
55	24	18	-	-	-	[207]
54.9	19.3	19.3	-	-	-	[208]
52	-	21.3	-	-	-	[209]
40-45	35-40	15	2-3	0.3	3	[25]

2.6 Conclusion of Literature Review

This chapter presents a comprehensive review consolidating the outcomes of various studies examining the effectiveness of internal curing agents commonly employed in low w/b cementitious mixtures. Additionally, the review explores the primary factors that significantly influence the performance of these internal curing agents. Drawing upon an extensive survey of the literature, the key findings can be summarized as follows:

1. Internal curing agents promote the hydration of cement paste, replenish lost water, and mitigate early-age cracking, especially due to autogenous shrinkage. By reducing early-

age cracking, their use can result in longer-lasting cementitious elements and enhanced sustainability.

2. The three most important factors in assessing the efficacy of an internal curing agents are: the timing of water release in the cement paste, the quantity of water released, and the distance it can travel to reach anhydrous cement particles.
3. In order to achieve the desired internal curing objectives without compromising strength, it is crucial to carefully manage the proportion of internal curing agents used in the cementitious mixtures. While a higher percentage of internal curing agents can enhance water absorption (i.e., higher entrained water) and release for internal curing, it can also diminish strength by increasing porosity and the risk of agglomeration. Therefore, finding the right balance between these factors is paramount.
4. The particle size of internal curing agents plays a vital role in their water absorption and desorption characteristics. Larger internal curing agents exhibit a higher absorption capacity but have limited water retention capabilities, leading to rapid water release that is unsuitable for gradual hydration in internal curing of cementitious mixtures. On the other hand, reducing the size of internal curing agents with smaller particles leads to reaching saturation faster but having a lower overall absorption capacity compared to larger particles of the same chemical composition.
5. The efficacy of internal curing agents is influenced not only by their intrinsic properties but also by the characteristics of the cement pore solution. The chemical composition, pH, ionic concentration, temperature, and fluid pressure play significant roles in determining the performance of internal curing agents. With its diverse range of ions, the cement pore solution changes over time, affecting the osmotic pressure and absorption-desorption

behaviour of internal curing agents. Therefore, understanding the dynamic nature of the cement pore solution is essential for optimizing the effectiveness of internal curing agents.

6. The desorption of entrained water from internal curing agents is closely linked to the internal relative humidity of the cement paste. Desorption takes place when the relative humidity of the cement paste decreases, which can occur due to external drying or self-desiccation. In cementitious mixes with a low w/b, desorption typically begins after the setting process, during the third stage of hydration. The duration of desorption depends on particle size and can last for several days until all absorbed water is released. Proper timing is crucial when using internal curing agents to avoid excess water during the dormant period, which can result in a more porous paste with reduced strength. The most effective use of internal curing agents occurs when desorption starts during the acceleration period and continues into the deceleration period of cement hydration.
7. While SAP have shown promise as internal curing agents in cement-based materials due to their high absorption capacity, their non-renewable and petroleum-based nature increases the carbon footprint of the construction industry. In contrast, natural fibres offer a sustainable and cost-effective alternative. Natural fibres are widely available in various regions, often at little to no cost, and their use in cement-based materials brings multiple benefits. They can serve as renewable resources, contributing to sustainable construction practices and reducing environmental impact. Moreover, natural fibres are frequently derived from agricultural wastes, creating additional income opportunities for farmers. However, further research is needed to fully understand the mechanisms of natural fibres as internal curing agents in cementitious mixes, as they have been less extensively studied compared to LWA and SAP.

8. Hollow natural fibres, such as MW fibres, can be promising options as internal curing agents due to their unique morphology, particularly their extremely wide lumen, which can act as reservoirs for internal curing water in cementitious mixes with low water-to-binder ratios. However, existing literature suggests that MW fibres have an amphiphilic nature, and their potential for improved hygroscopic properties needs further investigation. Additionally, the synergistic effects of morphology and chemical composition variations of MW fibres on various properties of cementitious mixes require further study.

Chapter 3 Effect of Fibre Length and Treatments on the Hygroscopic Properties of Milkweed Fibres for Superabsorbent Applications[1]

Amirmohammad Sabziparvar [a], Lina Boulos [a], M. Reza Foruzanmehr [a]

[a] Dept. of Civil Engineering, University of Ottawa, 161 Louis Pasteur St., Ottawa, Ontario K1N 6N5, Canada.

Abstract

This study investigated the influence of pre-treatment methods and size distribution on the hygroscopic properties of milkweed fibres (MW). Pre-treatment methods included hydrothermal treatment and hybrid treatment, which involves the hydrothermal treatment followed by the alkaline treatment. Scanning electron microscope (SEM), Fourier transform infrared (FTIR), and X-ray diffraction (XRD) were used to investigate the effect of pre-treatments on morphology, chemical composition, and crystallinity of milkweed fibres, respectively. Brunauer–Emmett–Teller (BET) surface area analysis was also used to measure the surface area of milkweed fibres after each pre-treatment. The results revealed that only after 5 minutes of stirring, hydrothermal treatment and hybrid treatment enhanced the water absorption capacity of non-treated MW fibres from 18 ±4 g/g to 54±4 g/g and 50±1 g/g, respectively. The SEM and FTIR confirmed the removal of waxes from the surface of milkweed fibres after applying hydrothermal treatment without causing any changes to the hollow structure of fibres. Hydrothermal treatment improved hydrophilicity and hence better hygroscopic characteristics of MW fibres, as evidenced by increased absorption capacity and

[1] A version of this chapter is published in Journal of Environmental Technology & Innovation (https://doi.org/10.1016/j.eti.2022.102930)
The paper is the own work of the candidate; author Lina Boulos contributed to the review and editing of the manuscript.

better water retention property. The hybrid treatment, on the other hand, caused the hollow structure of MW fibres to collapse completely, and left holes on the surface. As confirmed by FTIR and XRD, this occurred because of the dissolution of lignin and hemicellulose. As a result of these severe morphological alterations, the hybrid treated MW fibres showed inferior water retention properties compared to the hydrothermally treated sample. Furthermore, it was observed that MW fibres with larger size distribution exhibited higher water absorption capacity and better water retention properties compared to the smaller fibres. Therefore, it can be concluded that hydrothermal treatment can improve the hydrophilicity of MW fibres and pave the way for their application as superabsorbent materials in a simple and cost-effective manner.

Keywords: Milkweed fibres; Hygroscopic properties; Natural fibres; Superabsorbent

Graphical Abstract

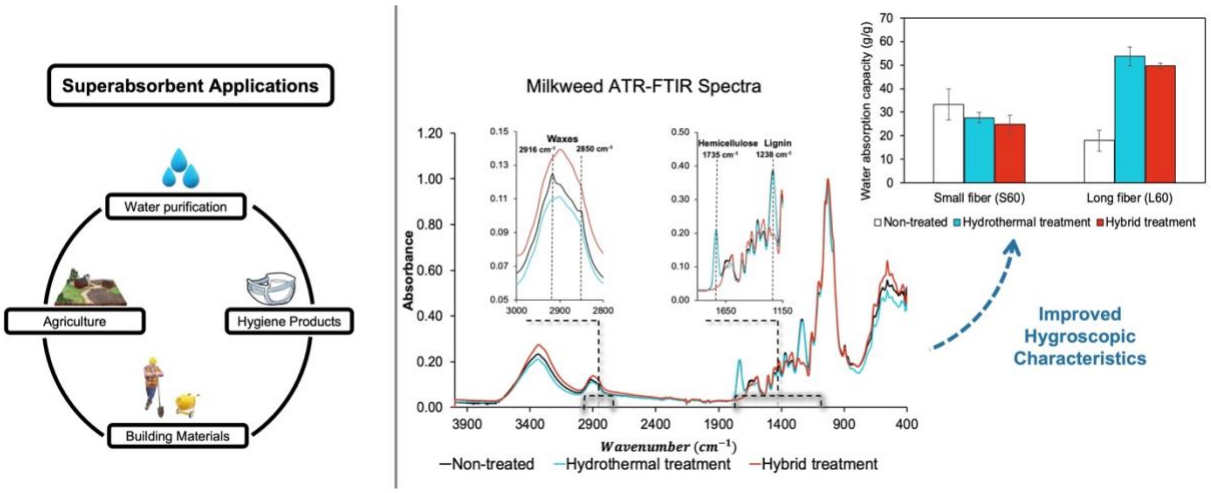

Figure 3.1. Graphical Abstract: Effect of Fibre Length and Treatments on the Hygroscopic Properties of Milkweed Fibres for Superabsorbent Applications

3.1 Introduction

Superabsorbent materials, also called *superabsorbents*, are materials that can absorb and retain water up to several hundred times their dry weight within their hydrophilic structure [14,15]. There is a growing interest in superabsorbent materials due to their high potential for various applications in the market, such as personal hygiene (e.g., diapers, etc.), biomedical (e.g., bondages, surgical sponges, etc.), meat packaging, waste treatment, water conservation in agriculture, water purification, and construction materials [13,92–95]. The majority of superabsorbent materials are synthetic and petroleum-based products, mainly made of polyacrylates, which are non-renewable [18]. Depending on their types, water absorption capacity of these petroleum-based SAP can be as high as 500-1000 g/g with absorption rate ranging from less than a minute to several hours [92,210]. However, SAP have significant manufacturing costs, high embodied carbon, and are environmentally harmful, making their usage incongruous with the principles of sustainability. Therefore, scientists have been working on using more environmentally friendly materials such as natural fibres in the aforementioned applications. Natural fibres are obtained from renewable resources and offer a number of benefits including availability, abundance, and low cost. In addition, one of the most important characteristics of natural fibres is their hydrophilic nature which allows them to become fairly high absorbent materials. The application of natural fibres as absorbents goes back to the days of the Egyptian civilization when they used cotton cellulose [211].

The hygroscopic behaviour of natural fibres is dependent on their chemical composition and physical structure. Chemical composition has a significant role in the hydrophilicity of natural fibres. Generally, natural fibres are composite materials made of a matrix consisting of lignin and hemicellulose, with cellulose fibrils, which act as reinforcements. Other components, such

as waxes are also present in lower percentages as well. The presence of waxes and other impurities provides a protective layer surrounding these natural fibres, preventing access to the reactive functional groups of the primary components. In general, those polymeric compounds in natural fibres that contain polar groups can establish hydrogen bonds with water molecules [151]. Célino *et al.* (2014) conducted qualitative and quantitative tests through FTIR spectroscopy and observed the effect of moisture content on natural fibres infrared spectra [160]. They found that hydroxyl groups of amorphous cellulose and hemicellulose, and carboxylic groups of pectin, are the potential sites for water absorption. In addition, the presence of a lumen and surface cavities can increase the hygroscopic properties of natural fibres due to capillary action [63].

Milkweed is a perennial plant native to North America, with *Asclepias syriaca* being the most common species. MW fibres are silky white fibres extracted from the seeds of the milkweed plant. Among natural fibres, MW floss fibre has a hollow structure which makes it unique compared to other natural fibres [25]. The extremely wide lumen of MW fibres, which takes up to 77% of the fibre volume and its thin cellulosic wall (approximately 1.3µm), can potentially, promote its absorption capacity [26,27]. However, this hollow lumen also gives MW fibres a fluffy nature with a density of approximately 300 kg/m^3 comparing to conventional SAP with a dry density of around 1500 kg/m^3 [55,199]. This is an important factor which need to be taken into consideration for the application of MW fibres as a lightweight material. MW fibres, like other lignocellulosic fibres, are composed of cellulose (39%), hemicellulose (36%), and lignin (18%). However, other components such as waxes, pectin, and sugars are also present in small amounts (<5%) in MW fibres [25]. As discussed in the previous paragraph, some of these components are hydrophilic and can act as absorption sites for water molecules (mainly

cellulose and hemicellulose), whereas others, like waxes, are hydrophobic. As a result, MW fibres can be classified as an amphiphilic material that can exhibit both hydrophilic and hydrophobic properties. For instance, Panahi *et al*. (2020) observed a superhydrophobic surface with a contact angle of around 140° and up to 100 g/g of oil absorption capacity in MW fibres [200]. Choi *et al.* (1992) also reported a crude oil sorption capacity of 40 g/g previously [201]. On the other hand, some studies have shown the high potential of MW fibres for water absorption. For example, higher moisture regain has been reported for MW fibres in comparison to cotton (11% vs 8%, respectively) [26,28,202]. In addition, it was observed that the unique hollow channel in MW fibres can result in fast moisture absorption [199,203,204]. To the best of the authors' knowledge, there is only one study which has been done on the application of MW fibres as an absorbent material. Kumar *et al.* (2020) assessed the moisture behaviour properties of MW and MW/cotton blended sanitary napkins. They found out that the higher the blend percentage of MW fibres, the greater the amount of liquid absorption, liquid retention capacity, and liquid holding capacity under pressure of sanitary napkins [205].

Depending on the intended use of natural fibres, different pre-treatment processes may be used. Alkaline treatment (also known as mercerization) is a popular treatment procedure for natural lignocellulosic fibres [212,213]. Alkali treatment can remove and/or reduce lignin and hemicellulose by changing the concentration and duration, which makes fibres increase their surface roughness [214,215]. Hydrothermal treatment is also a simple way to reduce or remove polysaccharides and impurities (such as waxes, pectin, and volatile compounds), from the natural fibres and thus enhance their affinity to aqueous media [215–217]. This is done by implementing hot water of 80 °C to 125 °C since most gums, tannins, starches, and sugars dissolve in water within this temperature range [215].

Size is another important factor in superabsorbents and can remarkably impact their hygroscopic properties. Smaller absorbent particles reach their swelling equilibrium sooner, while their absorption capacity is lower than the identical absorbent with larger dimensions [74]. Furthermore, the size of superabsorbents influences their water retention and release behaviour [218,219]. Water retention of superabsorbents is projected to decrease with finer particle sizes, resulting in a higher release rate. [220].

This study aims to study the hygroscopic properties of MW fibres for their use in superabsorbent applications. The influences of fibre length and pre-treatment methods on hygroscopic properties of MW fibres are investigated. Pre-treatments involve the hydrothermal (HT) and hybrid treatments (HY, i.e., the combination of the hydrothermal and alkaline treatments). The effect of each pre-treatment on the morphological change and chemical composition of MW fibres is thoroughly studied using SEM, BET, FTIR, and XRD.

3.2 Material and Methods

3.2.1 Materials

Milkweed fibre (MW) batches were provided by Protecstyle, Quebec, Canada. All chemical products were purchased from Sigma-Aldrich. Whatman Grade 4 filter paper also purchased from Cytiva.

3.2.2 Fibres Size Gradation:

To investigate the effect of size on hygroscopic properties of MW fibres, size reduction of the fibres was conducted through both grinding and sieving. Size reduction is beneficial in preventing the entanglement of long fibres and studying the behaviour of individual fibres rather than entangled bundles. Size reduction was made through intermittent grinding and sieving cycles. The grinding was done with a blade grinder for 10 seconds. After grinding, sieves No.

25 and No. 60 (with a mesh size of 710 µm and 250 µm, respectively) were used to grade the fibres. The sieving process was done with an electrical sieving apparatus for 5 minutes. Therefore, two grades of fibre length were obtained, including fibres retained on sieve No. 60 and fibres passed through sieve No. 60, designated as L60, and S60, respectively. Particle size analysis was implemented using SEM images in low magnification mode. ImageJ software was used to analyze SEM images, which involved measuring the length of at least 500 unique fibres for each size range.

3.2.3 Fibre Pre-treatments

Two types of pre-treatments were conducted to study their ability to remove hydrophobic components from MW fibres and subsequently improve their hydrophilicity. The hydrothermal treatment was done by soaking and stirring MW fibres in boiling water for 2 hours. The water temperature was monitored to be at least 90±2°C during the treatment. The HY treatment, which involves the hydrothermal treatment followed by the alkaline treatment, was also studied. The alkaline treatment was conducted by soaking and stirring MW fibres in 5 wt.% NaOH solution at room temperature for 15 min. Afterwards, in all pre-treatments, samples were removed, washed thoroughly with distilled water and oven-dried at 85 ±2°C for 24 hours.

3.2.4 Fibre Hygroscopic Properties

The moisture content of the as-received MW fibres was determined through weighing, oven-drying, and re-weighing procedures similar to ASTM D2495-07. Five samples of 0.5 gr MW fibres were placed in the oven at 85°C±2°C and regularly weighed until the mass became constant. The moisture content (MC) of the as-received MW fibres were determined to be approximately 8%. The required time for complete removal of the MW fibres' moisture was

recorded and used for drying the specimens before characterizing hygroscopic properties of the fibres.

Water Absorption Capacity

Figure 3.2 depicts the overall procedure for determining the hygroscopic characteristics of MW fibres. Water absorption capacity was measured by immersing the MW fibres in distilled water using a magnetic stirrer set at 700 rpm. Milkweed fibres were immersed and stirred for various durations, i.e., 5 min, 30 min, and 1 hr and their absorption capacity were measured through a filtration method using the Whatman 4 filter. The filter was saturated prior to the filtration to ensure it didn't influence the water absorption measurements. The filtration process continued until the interval between the successive drops became at least 1 min. The water absorption capacity (AC) was calculated as follows (Equation 3.1):

$$AC\ (g/g) = \frac{(m_2 - m_3)}{m_1} \qquad \text{Equation 3.1}$$

Where m_1 is the initial oven-dried fibres mass, m_2 is the initial mass of water, and m_3 is the filtered water. All the measurements were performed for five replicates.

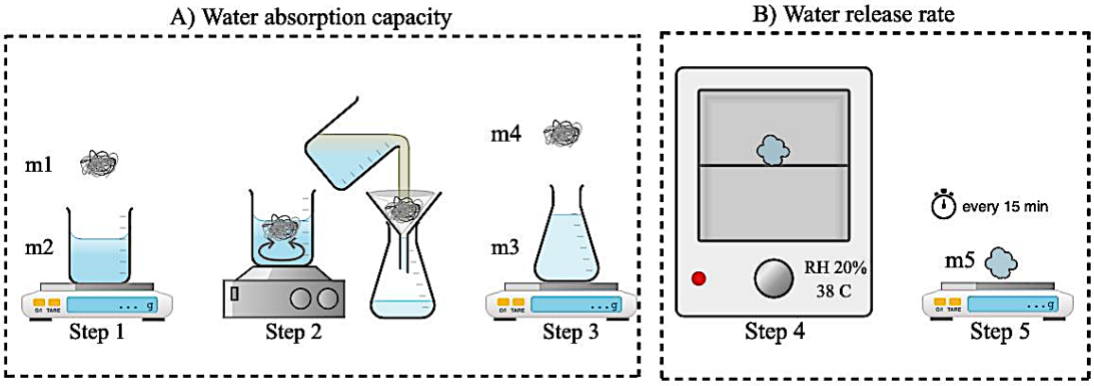

Figure 3.2. Schematic view of the main steps in the measurement of the hygroscopic properties of MW fibres

Applying an external force to establish immersion state is necessary due to the entrapped air inside the lumen. For example, the conventional teabag method [221] was not successful when the authors attempted to measure the behaviour of MW fibres' absorption during the preliminary trials. In fact, the reason the entrapped air stays inside the lumen is the morphology and the size of the lumen. Although improving the hydrophilicity of fibres may increase the capillary pressure, this increase is not high enough to expel the entrapped air and thus fibres will not be submerged in water. Therefore, an extra centrifugal force is needed to replace air with water.

Water Release Rate

Water release rate (WRR) of treated and non-treated (N) fibres were determined directly following the absorption capacity tests. Following the filtration process, the filter paper, together with the fibres that remained on the filter, were weighed and recorded as m_4. In the next step, they were placed in a humidity chamber and exposed to a dry environment of 38±1°C and RH of 20±1%, and the weight of the filter containing the fibres was recorded as m_5 every 15 min. However, to avoid counting in the amount of water absorbed on the filter papers during this test, the weight of ten individual saturated filter papers (without any fibres) was recorded each 15 min while exposed to the dry environment in the humidity chamber (i.e., 38±1°C and RH of 20±1%). The obtained data was then used to be subtracted from the recorded values of the primary test. WRR was then calculated with Equation 3.2.

$$WRR(\%) = \frac{m_4 - m_5}{m_4 - m_1} \times 100 \qquad \text{Equation 3.2}$$

Where m_4 is the mass of saturated fibre obtained just after water absorption capacity test, m_5 is the mass of fibre after each time exposed to the humidity chamber environment, and m_1 is the initial oven-dried fibre mass.

3.3 Characterizations

3.3.1 Morphology and Specific Surface Area

A scanning electron microscopy (SEM) JEOL JSM-7500F was used to study the size classification of MW fibres. The SEM images were taken using a lower secondary electron (LEI) detector with a 3 kV acceleration voltage. In addition, the effect of different treatment methods on the morphology of MW fibres was also observed by SEM. The Brunauer–Emmett–Teller (BET) surface area analysis of MW fibres was performed with a Micromeritics Gemini VII - 2390t using ultra-high purity liquid nitrogen. Fifteen samples were used for SEM analysis, and three samples were used for BET analysis for each specimen.

3.3.2 Chemical Composition

FT-IR Spectrometer in attenuated total reflectance mode (Thermo Fischer, Nicolet 6700) was used for FTIR analyses of MW fibres after each treatment method. The spectra were acquired between 400 and 4000 cm^{-1} with a resolution of 2 cm^{-1} at room temperature. The average spectrum was then calculated from five samples tested for each specimen.

The crystallinity modifications of MW fibres (after treatments) were studied using X-ray diffraction (XRD). A Rigaku Ultima IV X-ray diffractometer with a sealed tube Cu K source was used for the XRD experiment. For each sample, the crystallinity index was computed using the Segal technique [222] and the Area method [223]. The Segal technique uses Equation 3.3 to compute the crystallinity index (CI) of a material based on the intensity of peaks in the crystalline and amorphous regions. The area method also calculates the crystallinity index from the integral area of the (002) reflection over the total area.

$$CI(\%) = \frac{I_{002} - I_{am}}{I_{002}} \times 100 \qquad \text{Equation 3.3}$$

In this equation, I_{002} is defined as the maximum intensity of the crystalline (002), which appears at $2\theta = 22°$ while I_{am} is the minimum intensity of the amorphous region occurs at $2\theta = 18°$. The deconvolution of XRD spectra for MW fibres was acquired using Gaussian function [224].

3.3.3 Statistical Analysis

Statistical analyses were performed to confirm the influence of each treatment method on the hygroscopic properties of MW fibres. Since the population of samples was less than 30 samples, p-values were calculated in Microsoft Excel using a one-tailed hypothesis from T score results. T-scores were calculated using the formula below (Equation 3.4):

$$T_{score} = \frac{\mu_A - \mu_B}{\sqrt{\frac{\sigma_A^2}{n_A} + \frac{\sigma_B^2}{n_B}}} \qquad \text{Equation 3.4}$$

Where μ_A and μ_B are the mean values of samples A and B, σ_A and σ_B are the standard deviations of the samples and n_A and n_B represents the number of tests specimens in each condition. If the calculated p-value for a test was less than 0.05, the result was considered statistically significant. The results of statistical analysis of hygroscopic property measurements are presented in Appendices.

3.4 Results and Discussion

3.4.1 Particle Size Distribution

Microscopy-based technique such the SEM image analysis is a powerful tool for particle size characterization because it enables direct size measurement and morphology analysis [225]. The

size distribution of each grade of the ground and sieved MW fibres is measured by SEM image analyses and presented in Table 3.1. The as-received MW fibres exhibited a vast range of fibre lengths between 60 µm and 1000 µm. The high variation in the fibre length of as-received MW fibres was noticeable in their elevated standard deviation which is equal to 224 µm. The d (0.9) of the as-received sample was revealed to be approximately 484 µm. The d (0.9) value represents the size in which 90% of the sample is lower than this size. The reduction in the size of the fibres through the grinding and sieving processes resulted in a narrower range of fibre size for L60 and S60, with d (0.9) value of 331 µm and 236 µm, respectively. Furthermore, the L60 and S60 samples with standard deviation values of 153 µm and 96 µm, respectively, showed that the graded samples had a more uniform size distribution than the as-received fibres.

Table 3.1. Size classification of MW fibres by SEM image analyses

Sample	d (0.9)	SD
As received	484 µm	± 224 µm
L60	331 µm	± 153 µm
S60	236 µm	± 96 µm

3.4.2 Effect of Treatments on Morphology and Surface Area of Milkweed Fibres

In Figure 3.3, SEM micrographs depict the morphological changes in MW fibres after the HT and HY treatments. Figure 3.3 (a, b) demonstrate the N-MW fibres with a hollow structure and smooth surface. The presence of smooth protrusions on the surface of the N-MW fibres could be the trace of wax debris. The debris was removed after the hydrothermal treatment, resulting in a smoother surface with fewer protrusions (Figure 3.3 (d)). The hydrothermal treatment had no significant impact on the morphology of MW fibres, and the fibres were able to maintain their hollow structure, revealed in the SEM micrograph (Figure 3.3 (c)). However, drastic morphological changes were observed in MW fibres followed by the HY treatment (Figure 3.3 (e, f)). The SEM micrographs revealed prominent morphological changes in the HY samples.

The samples no longer exhibited, a hollow structure and exhibited some defects on their surface. This finding is related to the dissolution of lignin and hemicellulose (i.e., the matrix for cellulose microfibrils in lignocellulosic fibres) that decrease the fibre strength against the radial recoil [226].

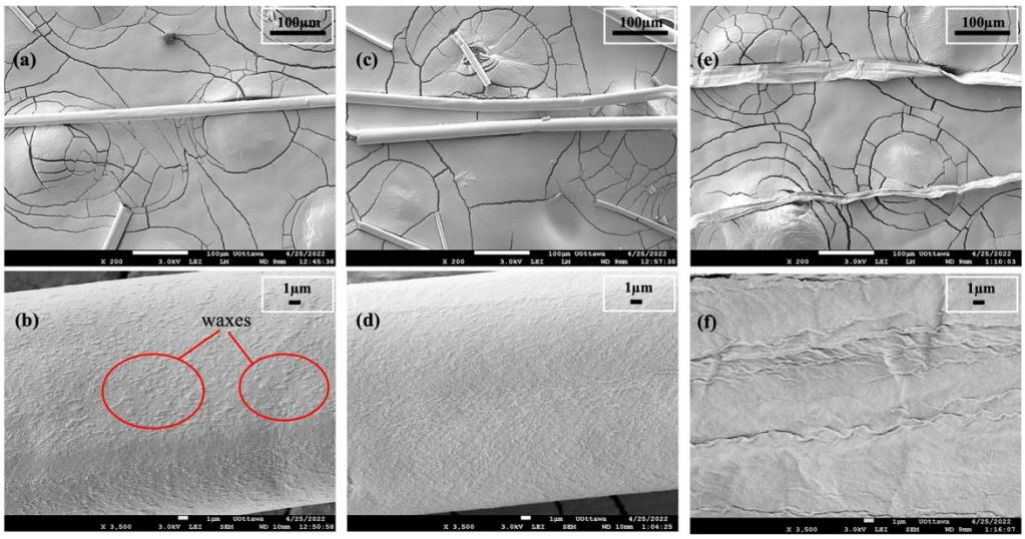

Figure 3.3. SEM images of as-received milkweed fibres (a, b), after hydrothermal treatment (c, d), and after hybrid treatment (e, f)

The specific surface area was measured and compared with the N-MW fibres (Table 3.2). The BET surface area of the N-MW fibres was computed as 2.3 m^2/g. However, the HT-MW fibres showed a smaller value of 2.1 m^2/g. As observed in SEM images, hydrothermal treatment only affects the surface of MW fibres and removes protrusions from the surface of MW fibres, which is reflected in their slightly lower BET surface area. On the contrary, for the HY-MW fibres, the removal of lignin and hemicellulose during alkaline treatment resulted in a remarkably greater BET surface area of 3.3 m^2/g.

Table 3.2. BET surface area of the non-treated and treated MW fibres

Sample	**Non-treated (N)**	**Hydrothermal (HT)**	**Hybrid (HY)**
BET surfaces area (m^2/g)	2.3±0.5	2.1±0.4	3.3±0.3

3.4.3 Effect of Treatments on Chemical Composition of Milkweed Fibres

In this section, first, FTIR and XRD analyses of the N-MW fibres will be discussed in detail. Following sections discuss the effect of each pre-treatment method on the composition and crystallinity of MW fibres.

Non-treated Milkweed Fibres

Figure 3.4 shows the FTIR spectra of the N-MW fibres. The FTIR spectra were normalized to the 1035 cm^{-1} peak. According to the literature, the absorption peaks between 3400 and 3200 cm^{-1} in the functional region, and 1035 cm^{-1} in the fingerprint region are characteristic peaks of general cellulose, attributing to O-H stretching and C-O stretching, respectively [227,228]. The absorption peak at 1735 cm^{-1} is mainly due to the C=O stretching vibration of the carboxylic acid in hemicellulose of MW fibres [227]. The main peaks associated with lignin also can be found in several wavebands such as 1595, 1505, and 1238 cm^{-1} [25]. Although the identification of the three main components of lignocellulosic fibres (i.e., cellulose, hemicellulose, and lignin) using FTIR has been well-documented in the literature, the characterization of waxes and pectin has still remained challenging. However, Richard *et al.* (2019) were able to extract waxes from MW fibres and characterize its FTIR spectra [25]. One of the characteristic peaks of the extracted wax from MW fibres is located near 2916 cm^{-1}, which corresponds to the asymmetric and symmetric aliphatic CH_2 and CH_3 stretching [229,230]. In addition, this wax is characterized by another peak at 2850 $cm^{-1,}$ corresponding to C-H stretching mode [25]. The same absorption peaks at 2850 cm^{-1} and 2920 cm^{-1} also reported for greases and polysaccharides in flax fibres, respectively [231]. The following sections (i.e., 3.3.2 and 3.3.3), discuss the influence of each treatment method on the removal of the aforementioned components.

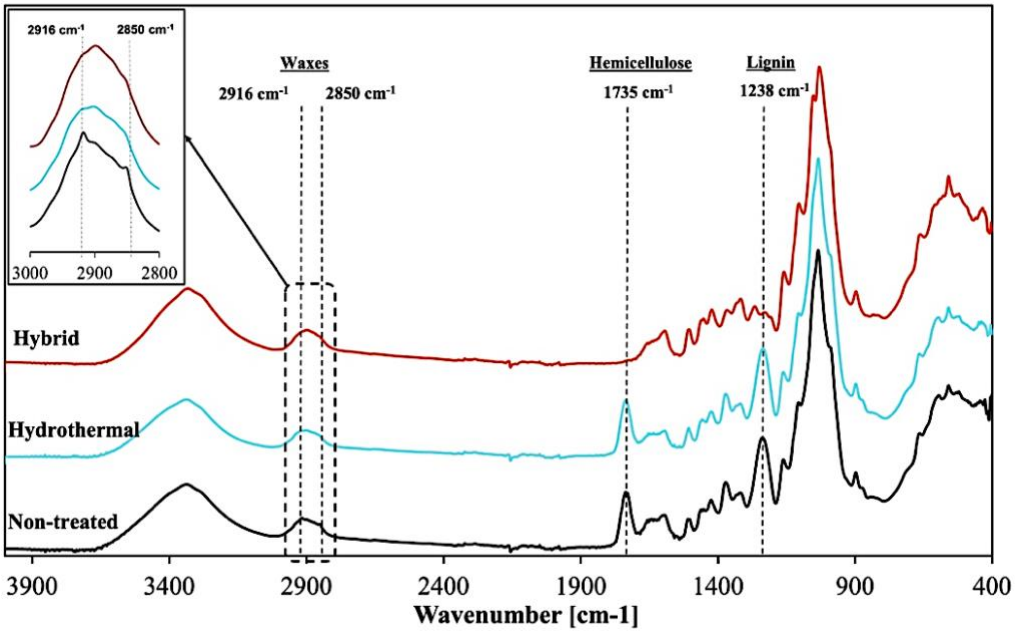

Figure 3.4. FTIR analysis of milkweed fibres with different treatments

X-ray diffraction (XRD) is a technique implemented to assess the crystallinity degree of material. Among the main components of a lignocellulosic fibre, cellulose is semicrystalline, whereas lignin and hemicellulose are non-crystalline [232,233]. Figure 3.5 shows the X-ray diffractograms of non-treated and treated MW fibres. The diffractograms indicate that the main crystalline peak that appeared at approximately $2\theta = 22.1°$ corresponds to the cellulose crystallographic plane (002) (Figure 3.5, (a)). The other peak appeared as a single broad peak between 15° and 16°, which can be recognized using peak deconvolution and separated into two independent peaks at 14.8° and 16.9°, representing (110) and $(1\bar{1}0)$, respectively. These two peaks are cellulose type I peaks that have been smeared due to the presence of (012) peak at 20.9° (Figure 3.5, (b)). In fact, when the amorphous content of the fibre (hemicellulose, lignin, pectin, and amorphous cellulose) is substantial, these two peaks (i.e., $14.8° \; and \; 16.9°$) combine to form a single broad peak [234]. Crystallinity indices (CI) were calculated based on the Segal

method as well as area method (i.e., the integral area of the (002) reflection over the total area) and presented in Table 3.3 [235].

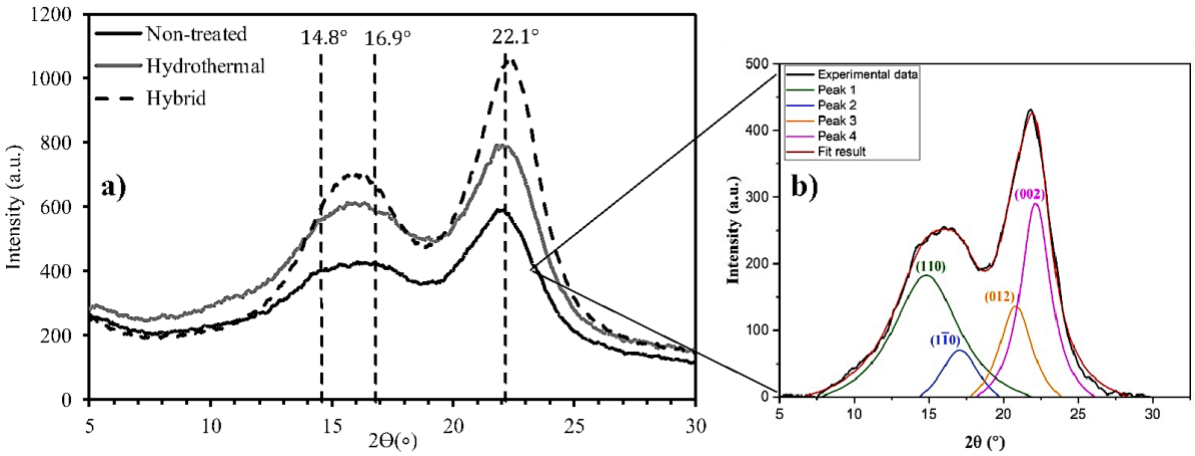

Figure 3.5. X-ray diffraction curves of non-treated and treated milkweed fibres (a), and peak deconvolution of non-treated milkweed fibre

Table 3.3. CI (%) of milkweed fibres with different treatment methods

Sample	Non-treated	Hydrothermal	Hybrid
Segal	45	47	63
Area	53	54	64

Hydrothermally Treated Milkweed Fibres

Treatment of natural fibres with hot water is a non-aggressive approach for removing non-cellulosic components from the fibre [236]. In addition, hydrothermal treatment is an easy and low-cost method that produces no toxic by-products and is thus an environmentally friendly approach. The most prominent change after hydrothermal treatment is the removal of wax, which was congruent with the disappearance of two FTIR peaks at two peaks at 2850 cm^{-1} and 2916 cm^{-1} (magnified in the top left of Figure 3.4). As discussed earlier, these two peaks are the main characteristic peaks of waxes in MW fibres which is attributed to the asymmetric and symmetric stretching of the CH_2-group mainly due to the presence of the aliphatic hydrocarbon

in waxes [25,230,237]. Therefore, the FTIR results revealed that the hydrothermal treatment of MW fibres removed a significant amount of wax from the surface of MW fibres.

X-ray diffractograms demonstrated that the Segal crystallinity index (CI) for MW fibres slightly improved to 47% after hydrothermal treatment, compared to 45% for the N-MW fibres. The same increase was seen using the Area technique, with a N-MW fibre having a crystallinity index of 53% compared to 54% for a HT-MW fibre. The removal or reduction of amorphous matters such as waxes and pectin can be linked to the greater crystallinity of MW fibres after hydrothermal treatment [238]. In other words, the hydrothermal treatment could gently remove waxes and pectin but not the major components, preserving the MW fibres' primary hollow structure. The FTIR spectra also confirmed that there were no significant changes in the bands of cellulose, hemicellulose, and lignin.

Hybrid Treated Milkweed Fibres

The HY treatment is the hydrothermal treatment followed by 15 minutes of alkaline treatment. Alkaline treatment is one of the most widely used methods for the treatment of natural fibres [239,240]. Basically, an alkaline treatment is able to remove all non-cellulose components except waxes [241,242]. In addition to the removal of waxes, which was observed in the HT-MW fibres, the main changes in the FTIR spectra of the HY-MW fibres are the removal of peaks at 1735 cm^{-1} and 1238 cm^{-1} corresponding to hemicellulose and lignin, respectively. These alterations are attributed to the alkaline treatment. The absence of a peak near 1735 cm^{-1} corresponding to carbonyl group (C=O) stretching was mainly due to extracting hemicellulose and lignin. When compared to the non-tread fibres, the partial removal of lignin was likewise consistent with a considerable drop in the intensity of the peak at 1238 cm^{-1}. The band at 1238 cm^{-1} appeared to be the C–O stretching vibration in the lignin of MW fibres [243]. Furthermore,

the elimination of the shoulder peak at 970 cm^{-1} (=C-H- deformation) was another indication of the removal of hemicellulose [25].

The removal or reduction of lignin and hemicellulose followed by the HY treatment was confirmed the XRD analyses, revealing the higher CI. Figure 3.5 shows that the HY sample had the most substantial rise in the intensity of the (002) plane, which is primarily attributable to alkali treatment. The CI of the HY sample increased to 64% compared to the N sample (CI:53%), according to the area technique. This finding is congruous with the previous literatures that reported increased crystallinity of natural fibres after exposure to alkaline solution [244]. The alkaline treatment decreases non-crystalline elements (lignin and hemicellulose) and allows more cellulose to be exposed, resulting in a higher crystallinity index value.

3.4.4 Hygroscopic Properties of Milkweed Fibres

Water Absorption Capacity (AC)

The influence of different stirring times on the water absorption capacity of MW fibres of each treatment method and size gradation was investigated and shown in Figure 3.6.

Effect of size

Fibre length can have a huge impact on water absorption capacity. For an extremely hollow fibre like MW, the effect of length is even more pronounced. MW fibres with longer lengths can contain more entrapped air than those with shorter lengths when they are plunged into water. The water absorption capacity of S60 MW fibres did not vary considerably when the stirring time increased or when the treatments were applied (See Appendices, which shows insignificant difference between the groups of S60 MW fibres). This indicated that after the first 5 minutes, S60 MW fibres had almost reached their maximum absorption capacity, and that continued immersion in water would not enhance the amount of water absorbed. In other words, due to

less entrapped air in their hollow structure, shorter MW fibres, i.e., S60, reached their full absorption capacity sooner. It has been reported that cotton can absorb water up to 24-27 times its own weight. For the S60 MW fibres which are not prone to interlocking and establishing 3D-scaffolding, the absorption capacity of treated fibres is between 25±4 g/g and 41±2 g/g [245]. Furthermore, the L60 sample had a higher water absorption capacity than the S60 sample, with the exception of a 5-minute stirred N sample. The same phenomenon was observed for SAP as well, where smaller particle sizes exhibited lower absorption capacity because they reached swelling equilibrium faster than the identical SAP type with larger particles [73,74]. The higher water absorption capacity of L60 samples compared to S60 samples could be due to the entanglement of long L60 fibres. In other words, since the L60 sample has longer fibres, they may become entangled and form a 3D scaffold. This system provided an additional space to store extra water between the individual fibres and increased the water absorption capacity. Besides, for non-treated L60 MW fibres, the results showed that the prolonged stirring helped the release of entrapped air in the long lumen and enhanced their water absorption capacity.

Effect of treatments

As the graphs demonstrate, the absorption capacity for the N-MW fibres is approximately 59 ±8 g/g, which is obtained after 60 minutes. The HT-MW and HY-MW increased the maximum absorption capacity to 66±3 g/g and 76±5 g/g, respectively. The results revealed that only after 5 minutes of stirring, hydrothermal treatment and hybrid treatment enhanced the water absorption capacity of the N-MW fibres from 18 ±4 g/g to 54±4 g/g and 50±1 g/g, respectively. Regardless of stirring duration, the pre-treatments were able to enhance the water absorption rate of the fibres by removing the hydrophobic components like wax and lignin. In addition to enhanced hydrophilicity, this could be due to a larger induced capillary pressure (P_{cap}) in the lumen of the HT-MW fibres, as stated in the previous section. In other words, the pre-treatments

made the fibres' interior walls more hydrophilic and thus decreased the water contact angle inside the lumen. Young's equation (Equation 3.5) explains how a decrease in contact angle leads to a higher P_{cap}. In fact, the more hydrophilic fibres are, the higher positive capillary pressure is that will add up to the centrifugal forces and help fill in the lumens with water.

$$P_{cap} = \frac{2\gamma_{lv}\, cos\, cos\, \theta}{r} \qquad \text{Equation 3.5}$$

Where γ_{lv} is liquid surface free energy, θ is the water contact angle, and r is the radius of capillary.

As shown in Figure 3.6, the impact of centrifugal force on treated fibres is significantly lower when compared with the N-MW fibres. In other words, the treatment made the MW fibre more hydrophilic, resulting in higher absorption rates and thus they absorbed a major portion of water within only 5 minutes. For instance, the increase in the absorption capacity when the stirring duration is increased from 5 to 60 minutes is 227% for the N samples compared to 52% for the HY-MW fibres. This value is 24% for the HT-MW fibres. However, longer duration of centrifugal forces helped to increase the absorption capacity of MW fibres primarily in two ways. First, expulsion of the air entrapped from the lumens, which facilitated the water ingress into the lumen of MW fibres. The storage of water within the 3D-sacffolding network of long fibres is the second mechanism that causes an increase in water absorption capacity by increasing the stirring duration. While the first mechanism is especially true for the N-MW and HT-MW fibres with intact lumens, the latter is the primary mechanism for HY samples.

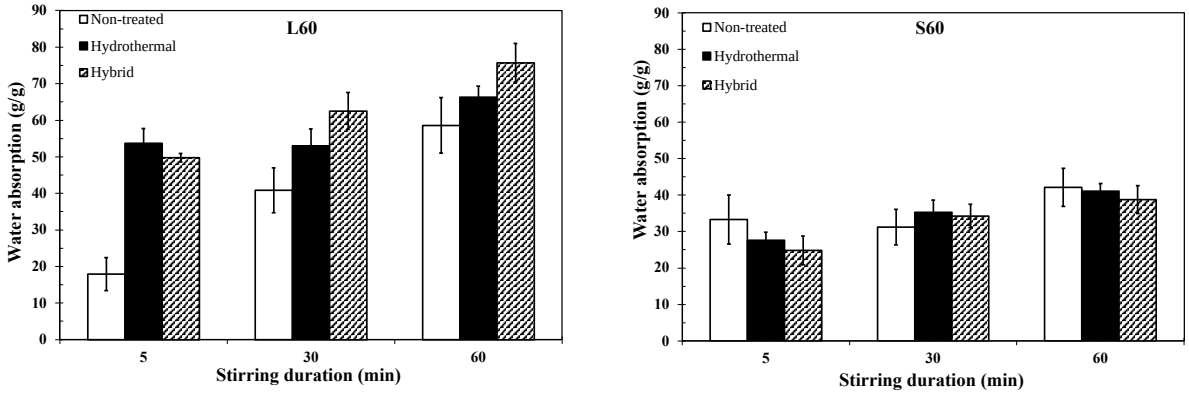

Figure 3.6. Water absorption capacity of milkweed fibres with different treatment methods after different stirring durations, for size classifications of L60 (left) and S60 (right)

Water Release Rate (WRR)

Water release rate is an essential factor in evaluating the efficacy of superabsorbent materials. The fibres were immersed in water and stirred for 5 minutes before measuring the WRR. The effect of each pre-treatment method on the water release rate of MW fibres is shown in Figure 3.7 for the L60 and S60 samples. It is worth mentioning that MW fibres samples with the stirring durations of 30 min and 60 min exhibited almost the same desorption behaviour as 5 min stirring and were so excluded from the graph. However, the complete results for all durations of stirring are also presented in Appendix, Figure AP.1.

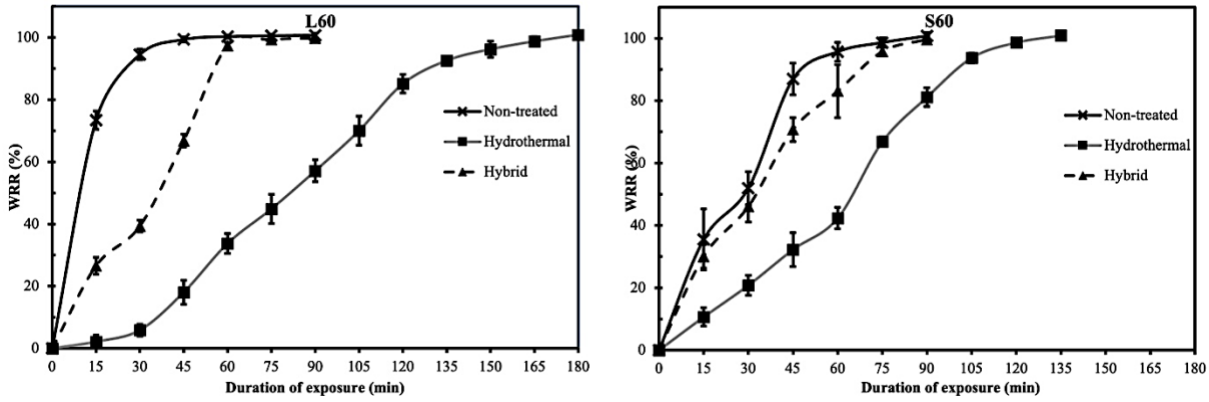

Figure 3.7. Effect of pre-treatments on the water release rate of milkweed fibre after 5 minutes of stirring, for size gradation of L60 (left) and S60 (right)

The result showed that the HT-MW fibres released their water content over a longer period than the N- and HY-MW fibres. The HT-MW fibres gradually released their absorbed water content over 180 minutes for L60 size and 135 minutes for S60 size. Furthermore, for the HT-MW fibres, when L60 fibres were compared to S60 fibres, it was observed that the longer fibres were able to hold their absorbed water content for a longer period of time. However, for the N-MW fibres and HY-MW, the water release rate of L60 fibres was faster than S60 fibre. For instance, L60 hybrid treated fibres release 90% of their water in 55min while this value for S60 fibres with the same treatment was 68min.

The statistically significant difference in the water release behaviour of the HT-MW fibres relative to the N-MW fibres can be justified by their enhanced hydrophilicity due to the removal of wax from the surface of MW fibres. The enhanced hydrophilicity of the HT-MW fibres can help to improve water retention property through two mechanisms. First, the fibres become more hydrophilic and since the fibre morphology remains intact, water absorption can take place by entering the lumen due to high capillary pressure. Secondly, the removal of waxes from the surface, led to greater water storage while fibres are entangled. However, the dramatic morphological changes results in a dramatic decrease in the water retention capacity of the HY-MW fibres (see Figure 3.8 that shows the formation of holes and defects). In other words, the alkaline treatment part of the HY pre-treatment caused permanent morphological changes that diminished their water release behaviour by allowing water to ooze out from the holes and defects. This indicates that the damaged lumen in the HY samples is no longer able to hold water inside the lumen. Consequently, a high percent of absorbed water is kept between the entangled fibres, as confirmed by the higher water release rate of L60 fibres comparing to S60 fibres.

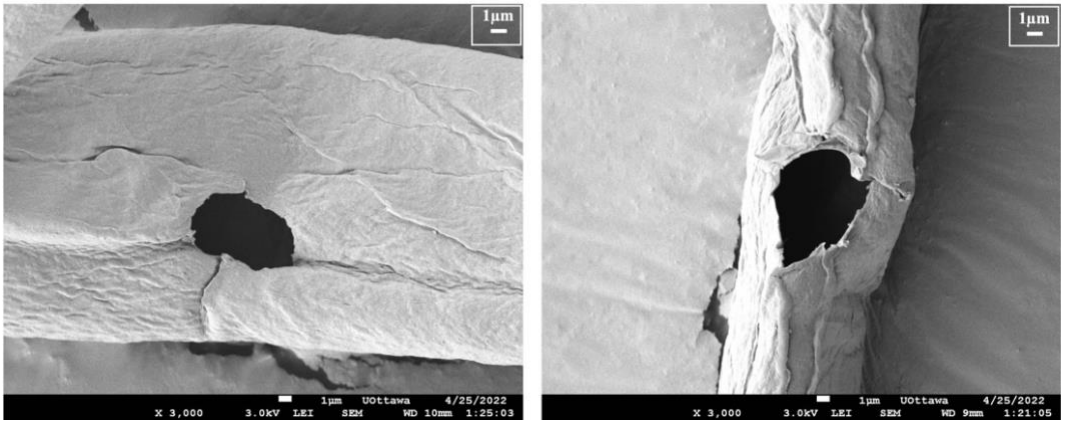

Figure 3.8. SEM micrographs showing the holes and defects in the hybrid-treated MW fibres

3.5 Conclusions

This study focused on the influence of pre-treatments and size distribution on the hygroscopic properties of MW fibres. In addition, the effect of pre-treatments, including hydrothermal treatment and hybrid treatment, on the morphology, chemical composition, crystallinity, and thermal stability of MW fibres was investigated.

The study revealed that the hydrothermal treatment could be a simple and low-cost method to remove the waxes from MW fibres while maintaining the hollow structure of the fibre. As a result of the removal of waxes, the hygroscopic properties of MW fibres improved significantly compared to the N-MW fibres. In addition, SEM micrographs also confirmed that the hydrothermal treatment could gently remove waxes and other impurities from the surface of MW fibres without causing any damage to its unique hollow structure.

Conversely, the HY pre-treatment led to a drastic morphological change of MW fibres due to the removal of lignin and hemicellulose. Although HY treatment resulted in enhanced water absorption capacity comparable to the HT-MW fibres, they demonstrated an inferior water retention behaviour compared to the HT samples. In other words, the defects and holes in the

MW fibre surface and the removal of hemicellulose after the HY treatment resulted in a significant reduction in their water retention property.

Besides, the results showed that MW fibres with larger lengths (i.e., L60) exhibited higher water absorption capacity and better water retention property. The smaller MW fibres (i.e., S60) provided a limited absorption capacity and released the absorbed water faster comparing to larger MW fibres.

The comprehensive analysis and findings of this study support the feasibility of using MW fibres as a superabsorbent after removing hydrophobic substances using proper pre-treatment methods, especially hydrothermal treatment. As a result, the next step of the study will look into the application of MW fibres as superabsorbent materials, specifically for use as an internal curing agent in cement-based materials.

Chapter 4 Enhancing Hydration and Internal Curing in Cementitious Mixes: The Impact of Pre-Treated Milkweed Fibres[2]

Amirmohammad Sabziparvar [a], Donato Taleponga [b], M. Reza Foruzanmehr [a]

[a] Dept. of Civil Engineering, University of Ottawa, 161 Louis Pasteur St., Ottawa, Ontario K1N 6N5, Canada.

[b] Center of Innovative Technology and Ecodesign (CITÉ), University of Sherbrooke, Sherbrooke, Quebec J1K 2R1, Canada.

Abstract

This study investigates the internal curing effects of milkweed fibres (MW) in Portland cement mixes, exploring different dosage levels and pre-treatment methods. The study first assessed the impact of MW fibres on the effective w/b through rheological measurements, enabling accurate comparisons of samples with identical effective w/b. Both MW fibre pre-treatments and dosages were found to impact the effective w/b in the mixes, leading to the categorization of MW fibre-incorporated samples into three groups based on their effective w/b. In the subsequent phase, the internal curing effect and hydration characteristics of cementitious mixes were evaluated with varying dosages of MW fibres. Optimal internal curing performance was achieved with 0.1% pre-treated MW fibres compared to 0.2%, resulting in up to a 17% improvement in the degree of hydration compared to the reference sample with the same effective w/b. This showed the adverse effect of higher MW dosage due to the reduction in the free water availability and higher leaching of extractives, which further intensified the hindrance of the hydration process. Furthermore, microstructure analyses, including TGA/DTG, XRD,

[2] A version of this chapter is published in Journal of Case Studies in Construction Materials (https://doi.org/10.1016/j.cscm.2024.e03079)
The paper is the own work of the candidate; author Donato Taleponga contributed to the preparation of samples for SEM and isothermal calorimetry.

and SEM-EDS, of cementitious mixes incorporating MW fibres confirmed that the inclusion of 0.1% hybrid and hydrothermally-treated MW fibres resulted in a higher formation of hydration products. This is achieved by providing an adequate amount of free water for the initial reaction of cement hydration and entrained water in the lumen for the subsequent internal curing. These findings show the effectiveness and suitability of using pre-treated MW fibres for internal curing applications, as validated by the comprehensive analyses conducted in this study.

Keywords: Milkweed fibres; Internal Curing; Hydration; Rheology; Superabsorbent

4.1 Introduction

Cementitious composites with low water-to-binder ratio (w/b < 0.4) exhibit a significant susceptibility to early-age cracking, primarily attributed to autogenous shrinkage and self-desiccation of the paste. Conventional curing techniques are insufficient for mitigating early-age cracking in low w/b mixes. This is due to the lower porosity (i.e., limited permeability) of PC pastes with low w/b [246]. Among the proposed methods for minimizing the self-desiccation of the pastes, internal curing has been effective in preventing early-age cracking [7–10]. In this method, internal curing agents such as SAP are used to maintain the internal humidity beyond the self-desiccation threshold of the pastes [11–13]. They can internally cure cementitious materials and serve as small water reservoirs spatially dispersed throughout the fresh cement pastes with low w/b. In other words, when the internal humidity of cement mixes drops below the desiccation threshold SAP begin gradually delivering their adsorbed water to the anhydrous cement particles. This elevates internal humidity, improves hydration, and effectively mitigates self-desiccation in the cement matrix, thereby reducing the risk of early-age cracking caused by autogenous shrinkage [16,17]. However, because SAP are petroleum-based compounds made from the non-renewable material polyacrylate, they increase the HPC's carbon footprint [18]. Hence, researchers and industries have been investigating the development of more sustainable alternatives.

In recent years, lignocellulosic materials such as abaca fibres, pulp fibres, Kenaf fibres, Lechuguilla fibres, and cellulose filaments have been the subject of numerous studies as sustainable internal curing alternatives to SAP [20,21,23,34,63,64,163]. For instance, the incorporation of 2% wt. of abaca fibres has demonstrated a substantial reduction of approximately 93% at age of 192 h in the autogenous shrinkage of cementitious mixes with a

w/b of 0.30 [21]. Compared to cellulose nanocrystals (CNC), cellulose nanofibrils (CNF), and cellulose microfibrils (CMF), hollow natural fibres are readily available across various regions worldwide, often at minimal or no cost, and possess carbon sequestration capabilities. Recent studies have highlighted that the carbon dioxide emissions associated with producing CNC, CNF, and CMF can exceed those of PC. Despite earlier assertions that CNC and CNF are environmentally friendly or carbon-neutral, further research has indicated significant greenhouse gas (GHG) emissions during their production, largely due to the prevalent use of acid hydrolysis in both commercial and research settings [247]. In contrast, hollow natural fibres demonstrate comparable hygroscopic properties, which can be further improved through cost-effective and low-carbon footprint pre-treatments, such as hydrothermal and alkali treatments.

Natural fibres are typically categorized into three main groups based on the part of the plant from which they are harvested: bast fibres, seed fibres, and leaf fibres. Milkweed (MW) fibres, which fall into the second category, are white silky fibres extracted from the seeds of the milkweed plant which is native to North America. However, milkweed plants are also found in other countries, such as China and Iran, where they are known as Akund and Estabragh, respectively. They can grow in a wide range of soil conditions and are commonly found along roadsides, fields, meadows, and waste areas [24]. MW fibres have a hollow structure with an extremely wide lumen taking up to 77% of the fibre volume and thin wall, which makes it unique compared to other natural fibres [25–27]. The chemical composition and morphology of MW fibres may vary greatly depending on their origin, type, and size. The authors have recently demonstrated that pre-treatments can also alter the chemical composition and morphology of MW fibres in favour of developing sustainable superabsorbent materials [248].

Despite their good hygroscopic behaviour, it's essential to acknowledge that natural fibres may present compatibility challenges when incorporated into cementitious matrices, and these should be carefully addressed before using them as internal curing agents. Initially, the hydrophilic nature of natural fibres can cause them to absorb part of the mix design water, which can compromise the rheological properties of cementitious mixes [63,249]. Secondly, the alkaline environment within cementitious matrices can induce the degradation of lignocellulosic materials, resulting in the release of leachates that may impede cement hydration, causing delays in the process [165,172–176,250].

In the initial phase of this study, we examined the impact of non-treated and treated MW fibres on the w/b in the resulting cement mixtures by implementing rheological measurements using a rheometer. Key rheological parameters, including yield stress, viscosity, and thixotropic behaviour were examined for precise measurements. The outcomes allowed us to determine the effective w/b, a vital parameter for more accurate subsequent assessment and comparison of samples with identical effective w/b in the subsequent section of the study—specifically, isothermal calorimetry. Moreover, the second objective of this study is to identify the appropriate pre-treatment conditions and content, ensuring the most effective internal curing while minimizing adverse effects on the rheological properties and hydration kinetics of General-use (GU) Portland cement paste. The pre-treatments of MW fibres include a hydrothermal treatment and a hybrid treatment. The later included an additional alkaline process in comparison with the former. Two different dosages of MW fibres, specifically 0.1% and 0.2% by weight of cement, were employed. Furthermore, a comprehensive analysis of how MW fibres affect the evolution of the hydration products was conducted using thermogravimetric

analysis (TGA/DTG), X-ray Powder Diffraction (XRD), and Scanning Electron Microscopy (SEM).

4.2 Materials and Methods

4.2.1 Materials

GU cement obtained from Colacem Canada with a specific gravity of 3.17 and Blaine fineness of 383 m^2/kg was used in this study. The chemical and mineral compositions of the cement determined by X-ray fluorescence (XRF) and X-ray diffraction/Rietveld analysis, respectively, are outlined in Table 4.1 The MasterGlenium 7500 superplasticizer (SP), supplied from Master Builders Solutions, was used to modify the consistency of the cementitious mixes. The full-range water-reducing admixture MasterGlenium 7500 is based on polycarboxylates and complies with ASTM C 494/C 494M for Type A water-reducing admixtures and Type F high-range water-reducing admixtures. Sodium hydroxide used for the alkaline treatment of MW fibres was also purchased from Sigma-Aldrich.

Table 4.1. Chemical and mineral Composition of cement (wt.%)

Chemical Composition (%)							
CaO	SiO_2	Al_2O_3	Fe_2O_3	MgO	K_2O	Na_2O	Loss on ignition
62.85	19.78	4.92	2.24	2.33	1.08	0.26	2.84
Mineral Composition (%)							
C_3S		C_2S		C_3A		C_4AF	
53.0		14.3		7.4		6	

Protecstyle, Quebec, Canada supplied this research with MW Floss fibres. In this study, MW fibres were ground and sieved to meet S60 gradation criterion. S60 stands for 90% of the fibres passing through sieve #60 and having a length less than 236 µm ± 96 µm. Three different

conditions of MW fibres were studied: N-MW fibres, HT-MW fibres, and HY-MW fibres. The HT-MW fibres were obtained after soaking them in boiling water for 2 hours. And the HY-MW fibres were subjected to a hydrothermal treatment followed by an alkaline treatment. The authors' previous study contains a detailed description of the pre-treatment process for MW fibres [248]. The water absorption capacity of the N-MW, HT-MW, and HY-MW fibres were reported to be 41±5, 41±2, and 39±4 g/g, respectively [248].

4.2.2 Mix Proportions

Figure 4.1 depicts the correlation between the quantity of MW fibres needed for the internal curing of cementitious mixes at different w/b. This graph was derived from Equation 2.5 developed by Bentz *et al.* for calculating the amount of LWA required for internal curing of a cementitious mixes [251]. The average absorption capacity of different pre-treated S60 MW fibres, assumed to be 40 g/g, was used to generate this graph, with dashed lines indicating standard deviations from the authors' previous study [248]. The saturation level of the internal curing agent (i.e., MW fibres) was assumed to be 1 as it is pre-soaked before mixing with cement. Additionally, based on the Power's model the chemical shrinkage (CS) was set at 0.07 g water/g cement, considering the use of only type I PC in this study [252]. The graph demonstrates a linear increase up to a w/b of 0.36, as higher w/b correlate with heightened degrees of hydration and chemical shrinkage. Consequently, α_{max} is estimated as (w/b)/0.36 for w/b < 0.36. However, Bentz *et al.* proposed that a mixture with a w/b of 0.36 or higher can achieve complete hydration under saturated conditions. Therefore, α_{max} is set to $\alpha_{max}=1$ for $0.36 \leqslant w/b \leqslant 0.42$, resulting in a constant amount of a required amount of internal curing agent for mixes within this range. All in all, the recommended dosage for using MW fibres as internal curing agents, based on the Bentz *et al.* model, falls within the range of 0.1% to 0.2% by weight

of cement. Consequently, two distinct dosages of MW fibres, specifically 0.1% and 0.2% wt. cement, were selected for use in this study to achieve a targeted w/b of 0.30. This specific w/b ratio was selected for two reasons. First, as previously mentioned, it falls below the critical threshold of 0.36, which is the minimum required w/b for complete hydration of cement. Second, a w/b ratio of 0.30 is particularly suitable for observing the impact of MW fibres as internal curing agent, as the autogenous shrinkage is significantly high in such low w/b. This methodology aligns with a similar approach employed previously by Kawashima *et al.* [163] for estimating the dosage of cellulose fibres.

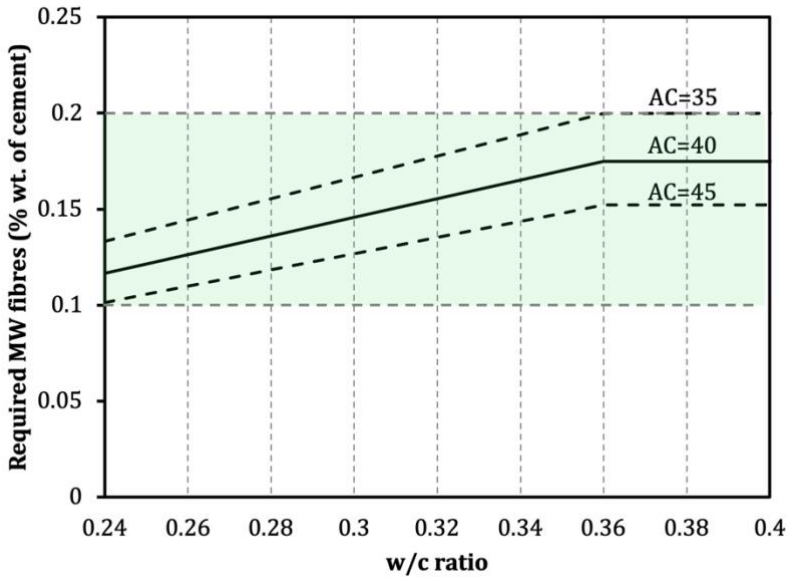

Figure 4.1. Required dosage of MW fibre (% wt. of cement) for internal curing of cementitious mixes based on Equation 2.5

In addition, as a result of preliminary tests, the choice of a maximum of 0.2% for MW fibres served as a threshold, allowing for effective dispersion during the pre-soaking process. Beyond this point, the dispersion of MW fibres was compromised, leading to the formation of fibre clumps and subsequent failure of the pre-soaking procedure.

The mix proportions for the cement paste samples are listed in Table 4.2. For all MW fibre-containing samples, the total w/b was set at 0.30. In addition to the reference sample which had the same total w/b of 0.30 (i.e., REF30), another reference sample with a w/b of 0.28 was prepared. The second reference sample (REFE28) was specifically employed to investigate into the effective w/b of cementitious mixtures containing internal curing agents (MW fibres). The MW fibres content was 0.1% and 0.2% by weight of GU cement. Using a magnetic stirrer set at 500 rpm, natural fibres were pre-soaked in a mixture of total mixing water (distilled water) and SP for one hour. According to our previous study, 1 hour is the approximate time required to achieve the water uptake at saturation of the MW fibres [248]. In order to prepare the rheological test samples, the suspension consisting of mixing water, MW fibres, and SP was mixed with cement in accordance with the ASTM C305-14 [253].

For improved clarity in referencing samples both in the text and graphs, a specific designation assigned to each sample. The sample designation consists of three sections; the first letter denotes the type of fibres added to the cement paste, the first two numbers display two decimal places for w/b, and the dashed number represents the first decimal place for the MW fibre weight percentage. For instance, HT30_2 denotes a cement paste sample containing 0.2% of MW fibres that have undergone hydrothermal treatment and has a total w/b of 0.30.

Table 4.2. Mix proportions of the control and MW-fibre cementitious pastes

	Control cement pastes		**MW Fibre-cement pastes**	
	REF28 w/b=0.28	REF30 w/b=0.30	N30_1, HT30_1, HY30_1 0.1% MW	N30_2, HT30_2, HY30_2 0.2% MW
Cement (g)	100	100	100	100
Water (g)	28	30	30	30
MW fibre (g)	-	-	0.1	0.2
Total w/b	0.28	0.30	0.30	0.30
Superplasticizer (mL)	1	1	1	1

4.2.3 Testing Procedure

Flow Rheology

Using an Anton Paar MCR 301 rotational rheometer, flow curve tests were obtained to examine the time-dependent rheological behaviour of the cement paste samples as a result of MW fibres' interaction with the matrix. A concentric cylinder geometry (28.9 mm inner diameter, 26.6 mm outer dimension) was employed. Measurements were taken 10 minutes after mixing at a constant temperature of 23 ± 1 °C. The cement paste samples were pre-conditioned by shearing them at 300 s^{-1} for 1 minute and then resting for 2 minutes. The hysteresis flow curves are obtained then by speeding up from 0 to 100 s^{-1} and subsequently stepping down from 100 to 0 s^{-1}. The Herschel Bulkley (H.B.) rheological model was chosen for analysis since it offered the greatest R^2 values (R^2>0.99) of data fitting to the experimental results compared to other models like Bingham and Casson, demonstrating its suitability for representing shear rate-dependent viscosity changes in cement paste mixes. In order to assess the statistical significance, five samples were tested for rheological measurements.

Isothermal Calorimetry

An isothermal calorimetry test was performed to evaluate the effect of MW fibres on the heat of hydration of cement paste following ASTM C1679-22. Isothermal calorimetry is a useful tool for continuous measurement of the early stages of hydration when the heat release rate is relatively high. The heat flow was measured by an 8-channel standard volume isothermal calorimeter (TAM Air 8-channel instrument). The cement was mixed with the suspension containing MW fibres, superplasticizer, and water for approximately 1 min in 20 mL plastic (HDPE) closed ampoules and immediately placed in the calorimeter. The experiment was

conducted over an 80-hour period at a constant temperature of 23°C. The induction period and acceleration period were also determined based on the method suggested by Bai *et al.* [254].

X-ray Powder Diffraction (XRD)

The XRD tests were carried out using a Rigaku Ultima IV X-ray diffractometer that used a sealed tube Cu Kα source. The data were collected by scanning the 2θ range from 5° to 65° with a 0.02° step size. To prepare the cement paste samples for testing, they were first ground with a mortar and pestle, and then sieved through a #200 mesh to obtain a fine, uniform powder. The hydration was then arrested by solvent exchange method and the solvent was subsequently removed by evaporation using a vacuum desiccator. The same procedure was followed to prepare the TGA test samples.

Thermogravimetric Analysis (TGA)

A Perkin Elmer TGA 4000 thermogravimetric analyzer was employed to obtain the weight loss of cement paste samples. The samples were subjected to temperatures ranging from 30 °C to 995 °C, with a heating rate of 10°/min, and under a nitrogen environment. To ensure that the effects of C-S-H dehydration were not present, the mass loss curve of CH was identified by drawing extended lines from the onset to the end at the temperature of the inflection point. This helped to accurately pinpoint the mass loss curve of CH without any interference from C-S-H dehydration [255].

Scanning Electron Microscopy (SEM)

The microstructure analysis of cement paste samples incorporating MW fibres was conducted using a Thermo Scientific Phenom XL scanning electron microscope (SEM) equipped with a backscattered electron (BSE) detector. A 20 nm thick carbon coating was applied on each sample prior to the test. This analysis was carried out at an accelerating voltage of 10 kV.

Furthermore, polished samples were prepared for examining the elemental composition in the interface of MW fibres and cement matrix using energy dispersive X-ray spectroscopy (EDS) operating at accelerating voltage of 15 kV. Before evaluation, the hydration process of all samples was halted by solvent exchange method using isopropanol.

4.2.4 Statistical Analysis

Statistical analyses were conducted to assess the effect of each type of fibres on the rheological properties of cement paste samples. The statistical analysis was performed using Equation 4.1 to determine P-values from T-score results, which were based on a one-tailed hypothesis.

$$T_{score} = \frac{\mu_A - \mu_B}{\sqrt{\frac{\sigma_A^2}{n_A} + \frac{\sigma_B^2}{n_B}}} \qquad \text{Equation 4.1}$$

The mean values of samples A and B are represented by μ_A and μ_B, respectively. The standard deviations of the samples are denoted by σ_A and σ_B, while the number of tested specimens in each condition is represented by n_A and n_B. A p-value less than 0.05 indicated a statistically significant result. The supplementary material contains the results of the statistical analysis of rheological behaviour measurements.

4.3 Results and Discussion

4.3.1 Effect of MW Fibres on the Effective w/b of Cement Paste Samples

The concepts of effective and total w/b are pivotal when evaluating samples with incorporated internal curing agents. The effective w/b accounts for the total w/b minus the water absorbed by internal curing agents (i.e., entrained w/b), ensuring the initial cementitious matrix resembles one without the agents. Determining the precise effective w/b, or the actual water absorbed by the internal curing agent in cement mixes, is challenging due to the complex nature of cement

pore solution. However, in previous studies, the slump test served as a qualitative tool to assess the slump loss resulting from the inclusion of internal curing agents [256–259]. Comparing these results with plain cement mixes enabled the estimation of the approximate effective w/b in mixes containing internal curing agents.

The yield stress and plastic viscosity values of the cement paste samples containing MW fibres are presented in Table 4.3. Yield stress and plastic viscosity are key indicators, representing the shear stress required to initiate flow and the material's resistance to flow once movement has begun, respectively [260,261]. In this study, we refined the method of estimating the effective w/b by measuring yield stress values using a rheometer. This approach was further validated through viscosity values, ensuring a more precise and quantitative analysis. This method has also been recently implemented by Ma *et al.* to establish a relation between effective w/b and yield stress values [56]. In this method, the effective w/b in the cement paste samples incorporating the MW fibres was determined by a two-step technique. First, yield stress values of reference samples were obtained by a rheometer and then correlated against their w/b. Given the narrow range of w/b (0.28 to 0.30), a linear relationship between w/b and yield stress was deemed an accurate model, as shown in Figure 4.2. Then the effective w/b of the MW samples were calculated and obtained by the first-order Newton interpolation method. To validate these calculations, plastic viscosity values were measured, ensuring that MW-incorporated samples share the same effective w/b and belong to the same group. This enhanced and quantitative method provides a more realistic assessment of the internal curing effect of the MW fibres on the cement paste. This becomes key when investigating the cement pastes' degree of hydration through the isothermal calorimetric analysis.

Table 4.3. Yield stress and plastic viscosity values of cement paste samples

Mixture	REF28	REF30	N30_1	HT30_1	HY30_1	N30_2	HT30_2	HY30_2
Yield stress (Pa)	19.91 ± 0.85	3.84 ± 0.36	11.11 ± 1.80	11.35 ± 2.01	15.84 ± 1.21	16.03 ± 2.12	15.93 ± 1.62	18.70 ± 1.75
Plastic viscosity (Pa.S)	1.21 ± 0.08	0.65 ± 0.06	0.94 ± 0.11	1.16 ± 0.11	1.03 ± 0.10	1.10 ± 0.11	1.11 ± 0.07	1.32 ± 0.02

As depicted in Figure 4.2, the inclusion of MW fibres led to an elevation in yield stress values compared to the REF30 sample. This increase can be attributed to the absorption action of MW fibres during the pre-soaking process, resulting in a clear reduction in the effective w/b of cement mixes. As noted by Banfill, a lower w/b corresponds to higher yield stress values [262]. Based on the results obtained, the samples with MW fibres were categorized into three groups based on their effective w/b: Gp1: HY30_2 with an effective w/b of 0.28, Gp2: HY30_1, N30_2, and HT30_2 with an effective w/b of 0.285, and finally Gp3: N30_1 and HT30_1 with an effective w/b of 0.29.

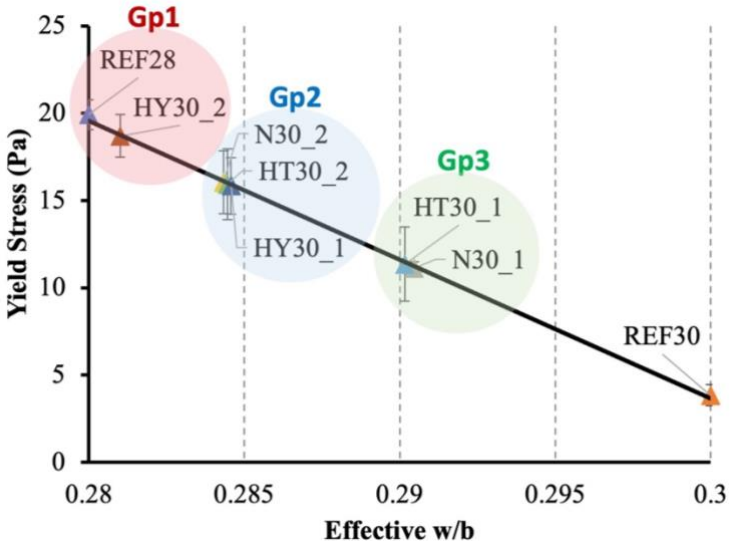

Figure 4.2. Effect of MW fibres on the effective w/b of their corresponding cement paste mixes. Error bars exhibit the standard deviations

After determining the effective w/b of cementitious mixes containing MW fibres by interpolating yield stress values in Figure 4.2, plastic viscosity values were compared for each group with the same effective w/b, as depicted in Figure 4.3. This was done to verify that the MW-incorporated samples share the same effective w/b and belong to the same group. Given the shear rate dependence in the Herschel–Bulkley model, a constant viscosity value cannot be assumed. However, at high shear rates, viscosity tends to stabilize. Thus, the apparent viscosity at the maximum shear rate in this study (i.e., $\dot{\gamma} = 100\ s^{-1}$) is considered the plastic viscosity of cement paste mixes [263]. In Figure 4.3, it is evident that all MW fibre-containing samples have higher viscosity values than the REF30 sample with the same total w/b. When comparing samples with the same effective w/b, the statistical analysis showed no significant differences. This reaffirms the equality in effective w/b among the groups determined in the Figure 4.2.

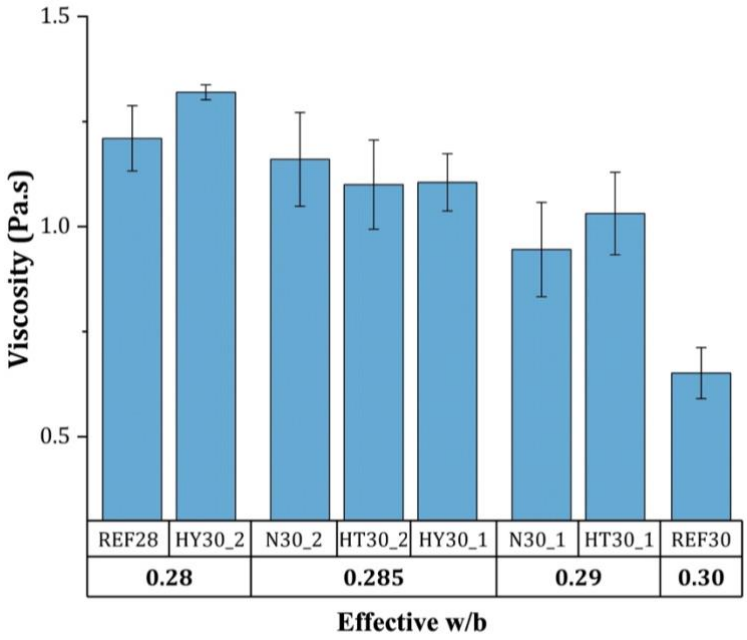

Figure 4.3. Viscosity changes of cement paste samples at different effective w/b

Figure 4.4 depicts the hysteresis flow curves of cement paste samples with and without the HY-MW fibres. Since the other MW fibre-containing cement paste samples exhibited comparable curves, only the comparison between the reference samples (REF28 and REF30) and the hybrid-

treated samples (HY30_1 and HY30_2) are shown in Figure 4.4, and the hysteresis areas of all samples (calculated by the Rheocompass software) are presented in Figure 4.5. The flow characteristics of the cement paste samples with MW fibres shifted toward those of the reference samples with a lower w/b (i.e., 0.28), confirming a decrease in the effective w/b of the cement paste.

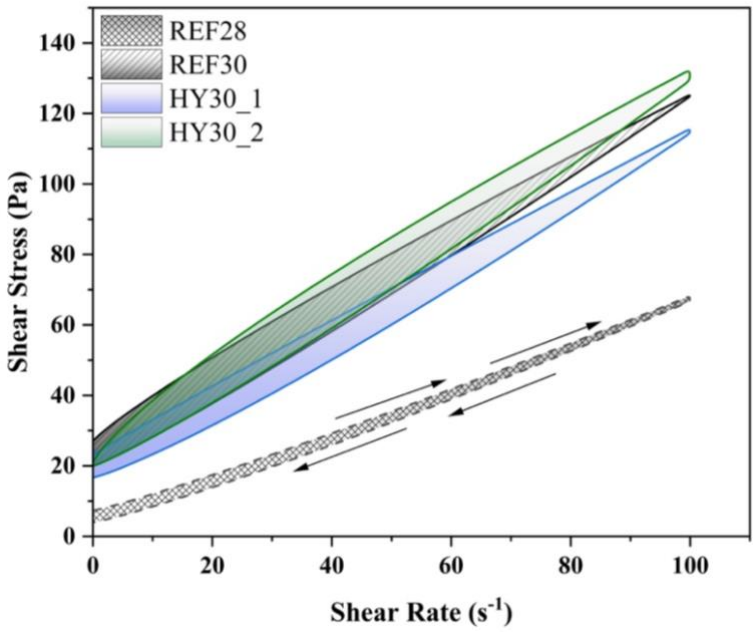

Figure 4.4. Effect of MW fibres on flow curve behaviour of cement paste

The hysteresis area, which is the area between the ascending and descending curves, provides a valuable measure of the thixotropic behaviour and shows the structural breakdown and buildup of mixtures as the shear rate varies. The reference mix with w/b=0.30 (REF30) showed the smallest hysteresis area value since the additional water acts as a lubricant between the cement particles, bringing the ascending and descending curves of each loop closer together [263]. Among samples with the same effective w/b, the only statistically significant difference was observed in the HT30_2 sample (compared to N30_2 and HY30_1). This indicates that the removal of the protective layer of waxes during hydrothermal treatment led to greater exposure of lignin and hemicellulose to alkaline hydrolysis, resulting in higher leaching into the cement

paste samples. Specifically, lignin is recognized as a plasticizing agent, playing a substantial role in reducing hysteresis areas [264]. The amplified leaching of this plasticizing agent in the HT30_2 sample resulted in a decrease in thixotropic structural build-up, evident through a smaller hysteresis area [265].

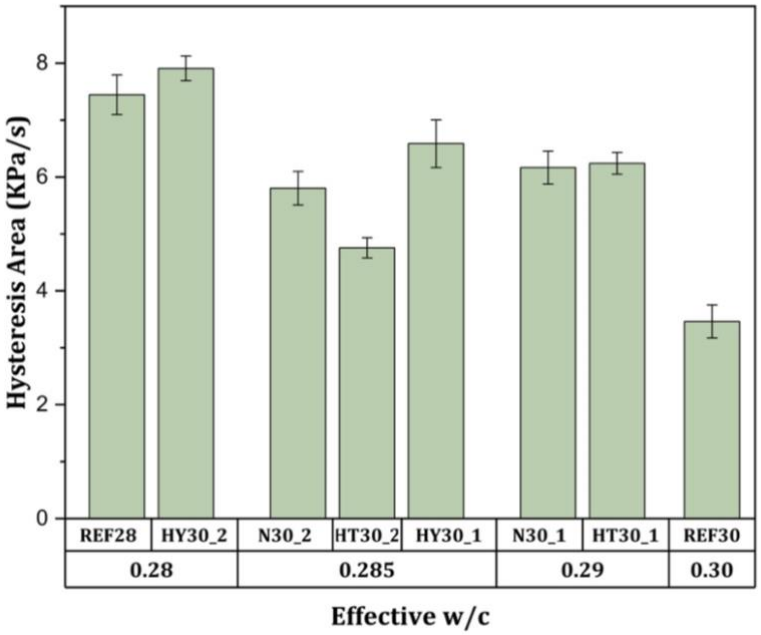

Figure 4.5. The hysteresis loop area of cement paste mixtures

In conclusion, despite maintaining a consistent total w/b of 0.30 across all specimens, the introduction of MW fibres to PC paste resulted in a shift in their effective w/b, leading to three distinct categories based on this ratio: Gp1 (HY30_2) with an effective w/b of 0.28, Gp2 (HY30_1, N30_2, and HT30_2) with an effective w/b of 0.285, and finally Gp3 (N30_1 and HT30_1) with an effective w/b of 0.29. Subsequently, for the following study sections, comparisons will be conducted among samples with identical effective w/b. This approach ensures a more realistic assessment of the internal curing efficiency of MW fibres.

4.3.2 Effect of MW Fibres on the Hydration of the Cement Paste Samples

Internal Curing Effect by MW Fibres

Figure 4.6 illustrates the variations in cumulative heat for plain cement pastes and those with 0.1% and 0.2% MW fibres. Upon examining the cumulative heat curves of cement paste samples containing 0.1% MW fibres, it became evident that all three conditions of MW fibres (non-treated, hydrothermally-treated, and hybrid-treated) outperformed the reference sample with identical w/b at the end of the testing time which is 80 hours (Figure 4.6, b and c). Notably, this improved cumulative heat was observed even when compared with the REF30 sample, with the same total w/b. This significant enhanced degree of hydration observed after incorporation of MW fibres can be attributed to the release of previously stored water within the lumens of fibres, thereby improving the availability of water for additional hydration of cement particles. The age at which the MW-added cement paste samples surpassed REF30 were as follows: 24 hours for the N30_1, 31 hours for the HT30_1, and 22 hours for the HY30_1. Similar internal curing behaviour were observed for other internal curing agents, such as SAP and wood pulp, which exceeded the cumulative heat of the reference sample with the same total w/b after approximately 24 hours [22,53]. The comparatively more gradual improvement in hydration observed in the HT30_1 sample, when compared to the other samples, can also be ascribed to the varying rates at which different MW fibres release water. Previous research findings have shown that both the HY-MW and N-MW fibres exhibit quicker water release behaviour. However, the improved hydrophilicity and intact morphology of the HT-MW fibres leads to a more gradual water release rate, attributed to the strong absorption of water within the lumens (Figure 4.7) [248].

Overall, after 3 days, the cumulative heat increased by 13%, 17%, and 14% in N30_1, HT30_1, and HY30_1, respectively, compared to the reference sample with the identical w/b. This finding suggests that the addition of 0.1% MW fibres provide an internal curing effect that

involves the gradual release of entrained water at later ages, ultimately resulting in enhanced hydration. While a minor variation of 0.02 in the w/b may seem insignificant, such subtle changes in the mix composition, especially in mixes with a low w/b, can profoundly impact the internal curing performance and enhance the degree of hydration. For example, studies conducted by Shen *et al.* and Justs *et al.* have reported analogous effects when using SAP as internal curing agents. These investigations have shown that alterations in the w/b ranging from 0.01 to 0.05 lead to a marked and consistent improvement in the degree of hydration at specific ages [9,266].

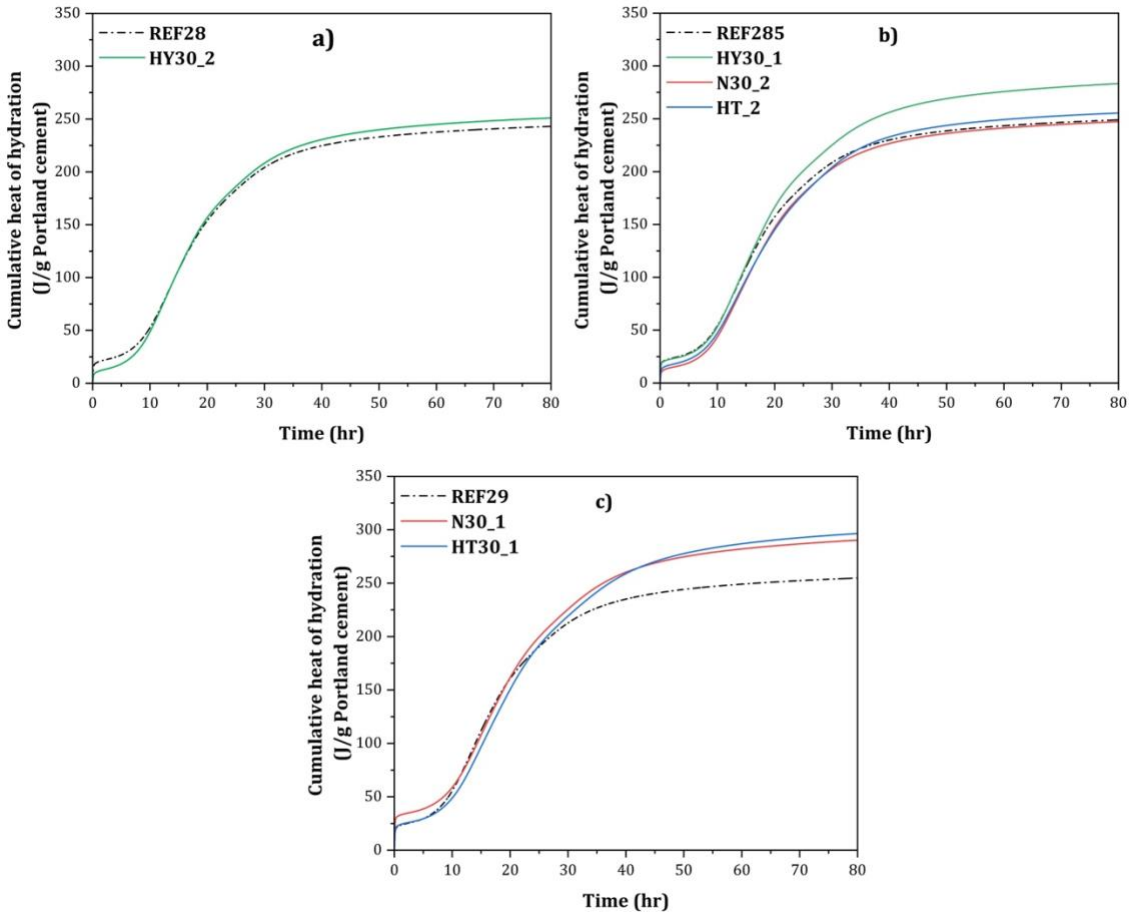

Figure 4.6. Cumulative heat of hydration of cement paste specimens with MW fibres with effective w/b of a) 0.28, b) 0.285, and c) 0.29

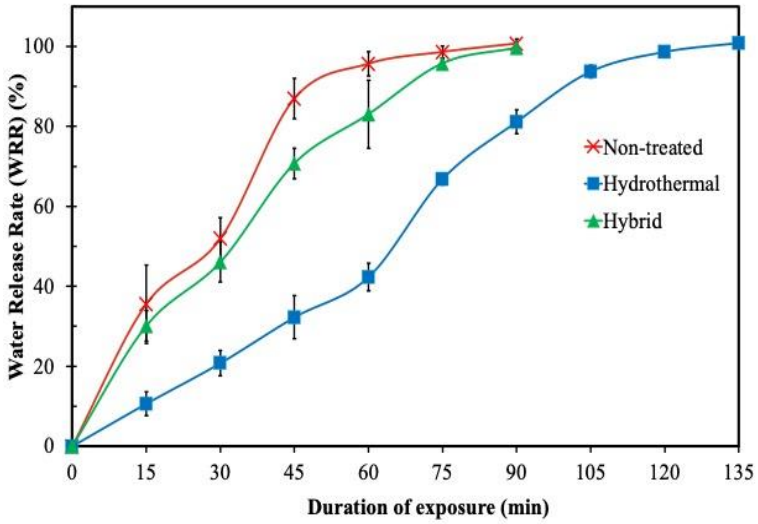

Figure 4.7. The water release rate of different pre-soaked MW fibres [248]

As the amount of MW fibres was further increased to 0.2%, the cumulative heat of the samples remains almost constant when comparing them to their identical effective w/b reference mixes (Figure 4.6, a and b). In general, adding more MW fibres shifted the cumulative heat curves to lower values. As a result, the heat of hydration is reduced. Previous studies have shown that a similar effect occurred with SAP, where excessive dosages significantly reduced the heat of hydration [58]. The reduced water availability observed in the samples containing 0.2% MW fibres is further supported by the shorter period of pre-induction when compared to the samples with 0.1% fibres (Figure 4.11).

Effect of MW Fibres Extractives on Early Hydration of Cement Paste

Non-treated MW fibres are made up primarily of cellulose (39%), hemicellulose (36%), and lignin (18%), with trace amounts of waxes, pectin, and sugars (5%) [25]. As demonstrated in the previous study by the authors, hydrothermal treatment effectively removes waxes from MW fibres. This is supported by the disappearance of two FTIR peaks at 2850 cm^{-1} and 2916 cm^{-1} [248]. It is also well established that pectin is removed during the hydrothermal treatment [217]. Therefore, it can be inferred that the main distinction between the chemical composition of the

N-MW fibres versus the HT-MW fibres lies in the absence of waxes and pectin in the latter. Therefore, the influence of waxes/pectin on the hydration of PC, can be distinguished by comparing the N30_1 and HT30_1. In addition, during the hybrid treatment lignin and hemicellulose are also removed from MW fibres (in addition to pectin and waxes), resulting in a composition that was predominantly cellulose. Similarly, the impact of hemicellulose/lignin can be identified by comparing the HT30_1 and HY30_1.

Effect of Waxes/Pectin

The addition of 0.1% N-MW fibres resulted in a rapid and intense reaction during the first few minutes of cement hydration, as evidenced by a sharp peak in the first few minutes (Figure 4.10-b). This could explain the higher cumulative heat observed during the initial 10 hours for the non-treated sample (N30_1) compared to the reference sample. Conversely, the HT30_1 exhibited a less pronounced initial peak than N30_1. The initial fast reaction period is contributed by the dissolution of particles resulting mainly in the formation of ettringite as a result of the reaction of C_3A and sulfates [267]. After that, the adsorption of the sulfate and/or calcium ions on the surface of C_3A blocks active dissolution sites and decelerates the hydration of C_3A to enter the dormant period [268,269]. In the case of samples incorporating the N-MW fibres, it was observed that during the initial few minutes of hydration, the sugars and/or their degradation by-products resulting from the alkali hydrolysis of waxes and pectin reacted with C_3A. This reaction increases the concentrations of ions in the pore solution and promotes an accelerated dissolution rate of C_3A [270].

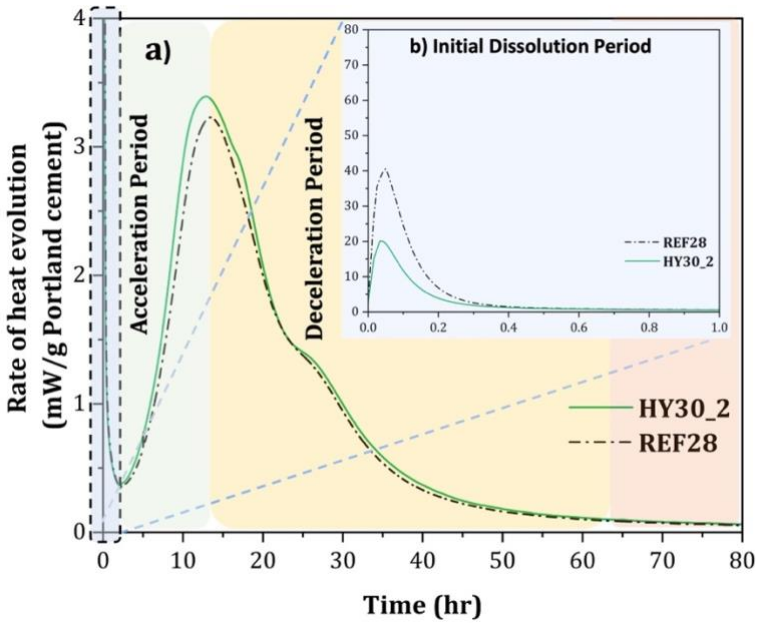

Figure 4.8. a) Hydration heat evolution rate, and b) initial dissolution period, of cement paste specimens with effective w/b=0.28

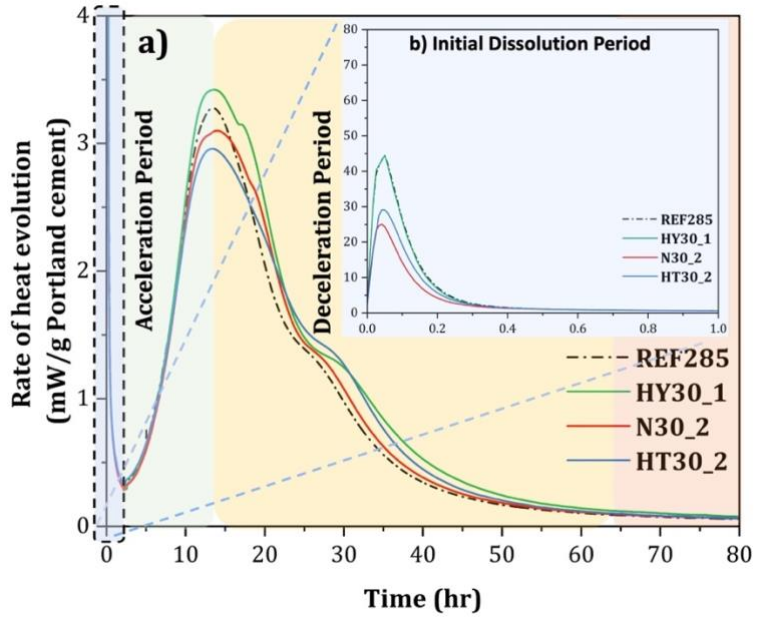

Figure 4.9. a) Hydration heat evolution rate, and b) initial dissolution period, of cement paste specimens with effective w/b=0.285

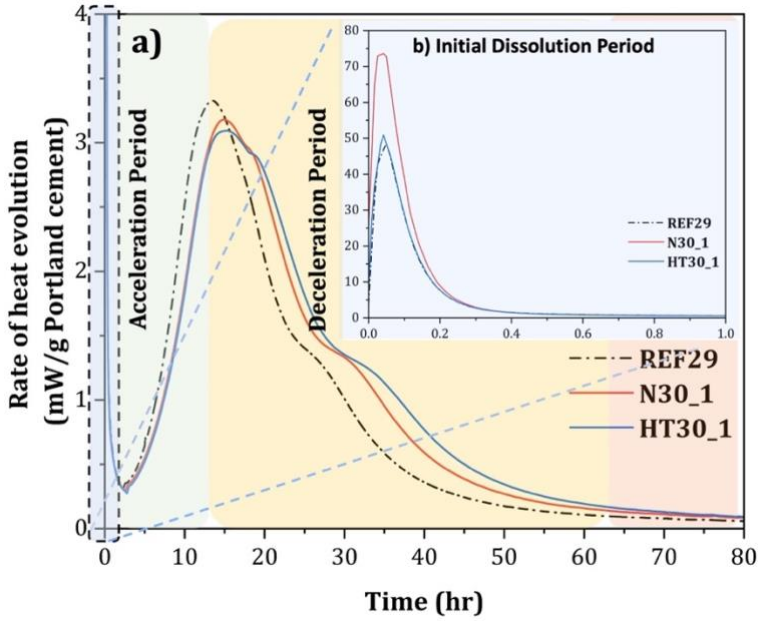

Figure 4.10. a) Hydration heat evolution rate, and b) initial dissolution period, of cement paste specimens with effective w/b=0.29

Effect of Lignin/Hemicellulose

As demonstrated in Figure 4.8, Figure 4.9, and Figure 4.12, adding 0.1% HY-MW fibres to the paste had a negligible impact on the time of main C_3S hydration peak, with a released heat rate higher than the reference sample with the identical effective w/b. However, the incorporation of 0.1% of both the N- and HT-MW fibres caused a delay in the appearance of the C_3S hydration peak, with a significantly reduced magnitude compared to REF29 sample. Furthermore, as depicted in Figure 4.11, both the N30_1 and HT30_1 samples exhibit a prolonged acceleration period. The unregulated hydration of C_3S seen in the N30_1 and HT30_1 is evidenced as the C_3S hydration peak emerged at 15 and 15.2 hours, respectively. This indicates a retardation of 1.6 and 1.8 hours compared to the plain cement paste samples without fibres. It appears that both the N-MW and HT-MW fibres underwent significant saccharide leaching when exposed to highly alkaline pore solution, resulting in hydration delays. In other words, the presence of lignin and hemicellulose in the N30_1 and HT30_1 plays a crucial role in influencing the

hydration of C_3S. Specifically, hemicellulose has conventionally been considered the primary source of monomeric sugars, which are believed to have the most significant delaying effect on cement hydration [165,271]. The hydration of cement particles is delayed due to the formation of a semipermeable organic layer around the cement grains or nucleation poisoning, which causes a decrease in the rate of water osmosis to the cement grains. This effect was obvious in the N30_1 and HT30_1 samples, where the presence of this semipermeable organic layer contributed to the slower hydration kinetics compared to other samples. As shown in Figure 4.11, there was approximately 15% longer acceleration period for the N30_1 and HT30_1, whereas the hybrid-treated sample (HY30_1) exhibited almost the same duration when compared to the reference sample. As shown by Garrault *et al*., the nucleation and growth of C-S-H on the surface of C_3S is shown to be a rate-controlling factor during the acceleration period [272,273]. Therefore, the nucleation poisoning of cement particles by lignin and hemicellulose leached in the N30_1 and HT30_1 appeared to be a valid hypothesis. In addition, The polysaccharides constituting the MW fibres possess potent Ca-chelating groups that have a high calcium binding capacity, which can reduce the concentration of calcium ions in the cement pore solution and inhibit the formation of hydration products such as C-S-H, portlandite and ettringite and hence cause a delay in the hydration process [165,166].

Moreover, upon comparing the hydration evolution curves of cement paste samples containing 0.2% MW fibres, it became obvious that only HY30_2 demonstrated a significantly higher rate of hydration heat during the acceleration period, compared to the reference samples with identical w/b (Figure 4.8). Both the N30_2 and HT30_2 samples exhibited maximum peaks at a magnitude lower than the reference samples with identical w/b (i.e., REF28) (Figure 4.9 and Figure 4.12). The C_3S hydration peak values seen in Figure 4.9-a are smaller, likely due to the

negative impact of the leachates on the hydration reactions, leading to less heat being released during the hydration process caused by the N-MW and HT-MW fibres.

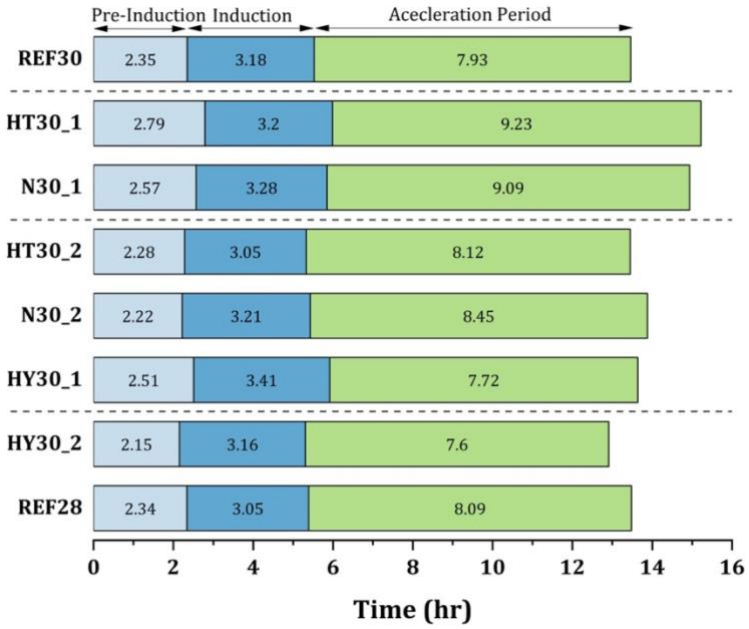

Figure 4.11. Duration of pre-induction, induction and acceleration period for different cement paste samples containing MW fibres

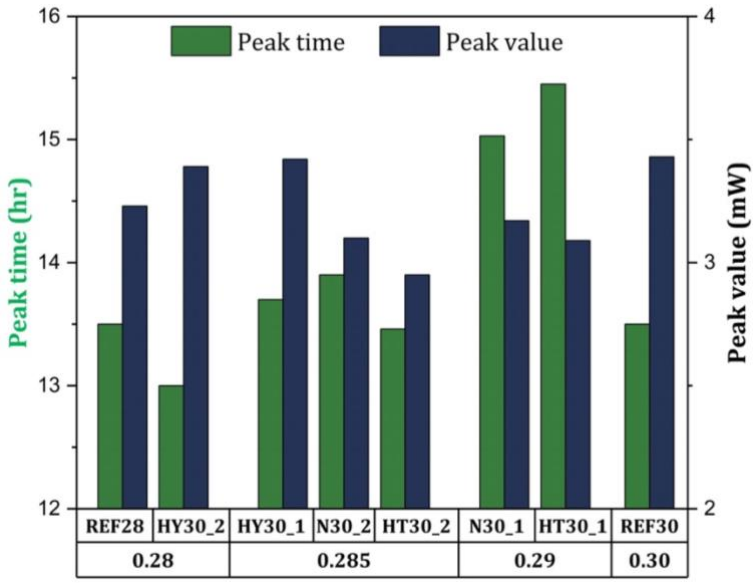

Figure 4.12. Peak time and peak values of the maximum rate of the heat of hydration for different samples

In conclusion, these findings suggest that the hydration process is influenced by the dosage of MW fibres, and an excessive quantity of fibres can negatively affect the hydration reactions. The results indicated that the use of 0.1% MW fibres resulted in a higher degree of hydration as shown in cumulative heat results, providing an adequate amount of free water for the initial reaction of cement hydration and entrained water in the lumen for the subsequent internal curing. With the understanding that MW fibres were pre-soaked in the entire mix water before being mixed with cement, the addition of 0.2% pre-soaked MW fibres led to increased water absorption by the fibres during the pre-soaking process. This resulted in a higher volume of entrained water, evident from their lower effective w/b in Figure 4.2. Consequently, there was an insufficient amount of effective free water available for reaction with cement during the early hydration stage, as a significant portion of the water was retained in the lumen of the fibres. Furthermore, an increased quantity of MW fibres may result in higher levels of extractives and saccharides leaching into the cement pore solution, thereby exacerbating the hindrance of the hydration in early ages.

Therefore, to attain an efficient degree of hydration, which is vital for internal curing, the optimal dosage of MW fibres in the rest of the study was set to 0.1%. It's important to note that comprehending the enhanced hydration achieved with 0.1% MW fibres requires an examination of their impact on hydration products. Consequently, this dosage was selected to investigate the influence of MW fibres on the formation of hydration products in the following sections through TGA and XRD analyses, along with microstructural examination using SEM. These results are pivotal in understanding the promotion of hydration by MW fibres.

4.3.3 Effect of MW Fibres on the Formation of Hydration Products

The DTG curves of cement paste samples hydrated for 1 and 2 days, with the addition of 0.1% MW fibres, are shown in Figure 4.13. These curves provide additional insights into the impact of MW fibres on hydration products. Based on DTG curves three main temperature ranges can be identified. Between 50 and 200 ºC, the first peak is associated mainly with the thermal decomposition of C-S-H and AFt phases, while the second one is attributed to AFm. Furthermore, within the second range of weight loss a major peak between 400 and 500 ºC indicates the dehydration of portlandite (CH). Additionally, the decarbonation of the three polymorphs of calcium carbonate takes place within the temperature range of 550 to 900 °C [274]. Vaterite, the least stable polymorph in ambient conditions, undergoes decarbonation first, contributing to the initial peak observed between 550 and 675 °C, followed by aragonite between 675 and 720 °C [275,276]. On the other hand, calcite, the most thermodynamically stable polymorph of calcium carbonate, exhibits the highest decarbonation temperature, occurring between 720 and 875 °C.

The inclusion of MW fibres in cement paste samples presents challenges in accurately determining the quantity of chemically bound water due to the varying decomposition rates of individual fibres, influenced by their different pre-treatment types. Using conventional calculation methods may lead to erroneous conclusions and an imprecise understanding of the actual amount of chemically bound water. Therefore, the current study focused on evaluating the amount of portlandite produced as a more reliable approach to assess the impact of MW fibres on the evolution of hydration products.

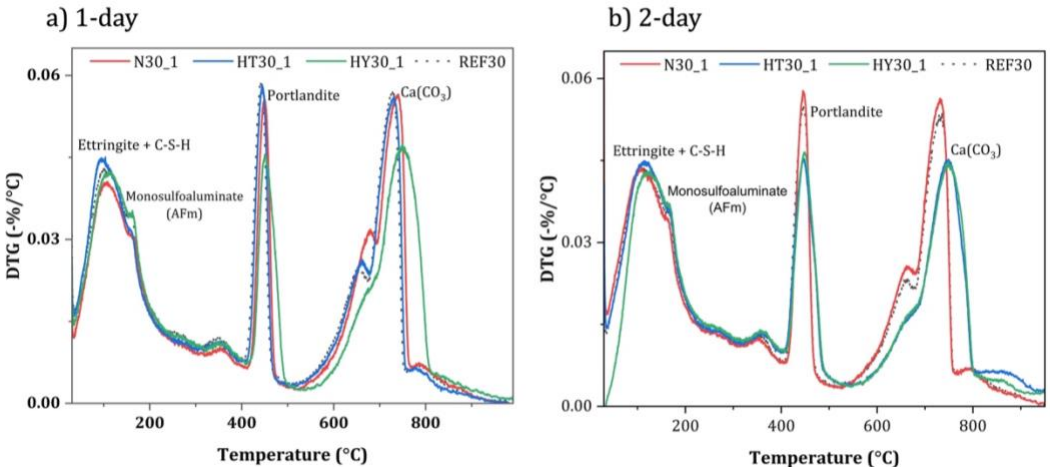

Figure 4.13. DTG curves of cement paste samples with MW fibres hydrated for 1 and 2 days

Figure 4.13 presents the DTG curves of cement paste samples containing MW fibres, compared to the reference sample with the same total w/b. The DTG curves for reference samples with identical effective w/b ratios are not shown to keep the graphs clear and avoid clutter. Instead, Figure 4.14 provides a focused comparison by illustrating the weight loss associated with portlandite dehydration. This weight loss is calculated and compared across each sample, including those with identical effective w/b ratios, providing a clearer understanding of the influence of MW fibres on cement hydration. The TGA/DTG analyses revealed that the HT30_1 and N30_1 exhibited a lower portlandite content compared to reference sample with the same effective w/b, within the first 24 hours. However, the hybrid-treated cement paste sample showed a slight increase in its portlandite content. This is consistent with the isothermal calorimetry results, where the N30_1 and HT30_1 samples had lower cumulative heat compared to the reference sample before 24 hours, while HY30_1 exceeded the reference sample around 22 hours. After 2 days of hydration, the amount of portlandite in the HT30_1 and HY30_1 samples surpassed that of corresponding references. This is attributed to the enhanced cement hydration facilitated by internal curing and the subsequent release of entrained water stored within the MW fibres. In other words, the improved availability of water enables a more

extensive hydration reaction of C_3S and C_2S, resulting in the formation of calcium silicate hydrates (C-S-H) and portlandite (CH). The XRD analyses discussed in the next section also further supported this by confirming a decrease in the peak associated to silicates (i.e., C_3S and C_2S). This interesting finding suggested that despite the unregulated hydration kinetics caused by the HT-MW fibres during the first hours, specifically delaying in the emergence of the C_3S hydration peak (as evidenced by isothermal calorimetry results), their enhanced hydrophilicity due to the removal of waxes led to superior performance in terms of internal curing. Consequently, this superior internal curing performance translated into improved hydration outcomes after 2 days, characterized by a higher production of portlandite. However, for N30_1, the negative effects of leachates seemed to dominate, compromising the internal curing effect, and consequently negatively impeding the hydration process. As a result, N30_1 showed a decreased amount of portlandite compared to the reference sample.

Moreover, the peak associated with AFm was observed for HY30_1 at day 1, whereas the N30_1 and HT30_1 only displayed the AFm peak after two days. The reason for the absence of monosulfoaluminate formation in both the N and HT samples during the 1-day TGA analysis can be attributed to the inhibitory influence of leached saccharides on monosulfoaluminate formation [164]. Besides, DTG profiles indicated a reduction in the intensity of the shoulder peak at approximately 650 ºC in the HT and HY samples following a two-day hydration period. This suggests a lower presence of less thermally stable polymorphs, such as vaterite and aragonite. On the other hand, the slight shift towards higher temperature in the peak associated with the decomposition of calcium carbonates at approximately 750 ºC in these samples confirms the formation of thermally more stable polymorphs of calcium carbonates i.e., calcite [275].

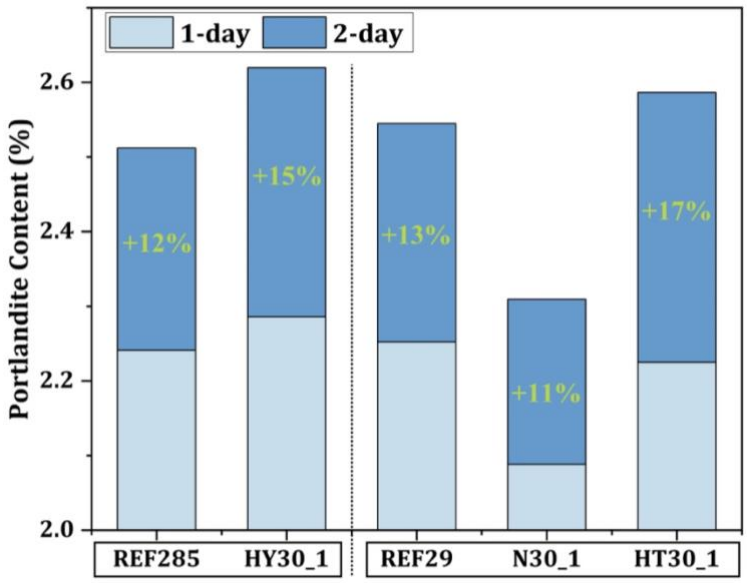

Figure 4.14. Portlandite content (%) of the cement paste mixes with MW fibres addition measured by TGA (numbers in green showing the increase in portlandite content compared to 1-day content)

Figure 4.15 illustrates the XRD patterns of cement pastes incorporating 0.1% MW fibres, hydrated for 1 day and 2 days. To monitor hydration progress and facilitate inter-sample comparisons, the silicates' peak (i.e., C_3S and C_2S) at ($2\theta \approx 32°$) was analyzed. The N30_1 sample exhibited no reduction in the silicates peak, while the HT30_1 sample demonstrated the most significant decrease, followed by the HY30_1. This trend aligns with findings from TGA/DTG analyses, suggesting that the improved hydration reaction facilitated by internal curing effect of MW fibres within the cementitious matrix promoted the formation of a greater quantity of hydration products [277]. In contrast, no consistent trend was recognized in the (0 0 1) CH peak ($2\theta \approx 18.1°$) across samples. This inconsistency may be attributed to the substantial influence of preferred mineral grain orientation on the (0 0 1) CH peak, as previously noted by Pang *et al.* [278].

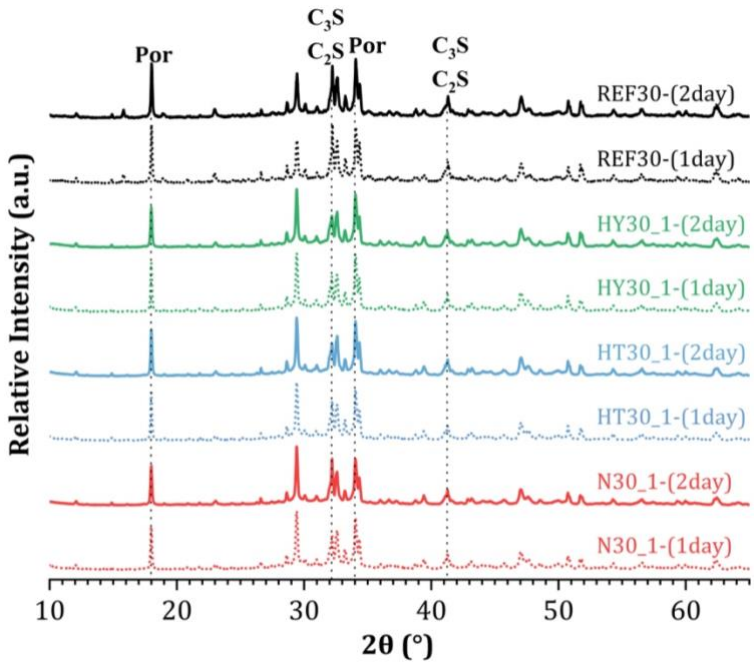

Figure 4.15. XRD patterns of 1- and 2-day cement paste samples with different conditions of 0.1% MW fibres. (Por: Portlandite)

4.3.4 Effect of MW Fibres on the microstructure of cement paste

Figure 4.16 visually represents backscattered SEM images of cement samples incorporating MW fibres, revealing the presence of small, discrete crystalline products observed on the surface of MW fibres. MW fibres increased the available surface area, potentially serving as nucleation sites for the precipitation of hydration products. The acceleration of cement hydration attributed to increased surface area has been documented in previous research [279] even with materials that are chemically inert. This nucleation effect of MW fibres is further evidenced by our isothermal calorimetry findings, which showed a respective increase of 13%, 17%, and 14% in cumulative heat generation for samples N30_1, HT30_1, and HY30_1, when compared to the reference sample with identical effective w/b.

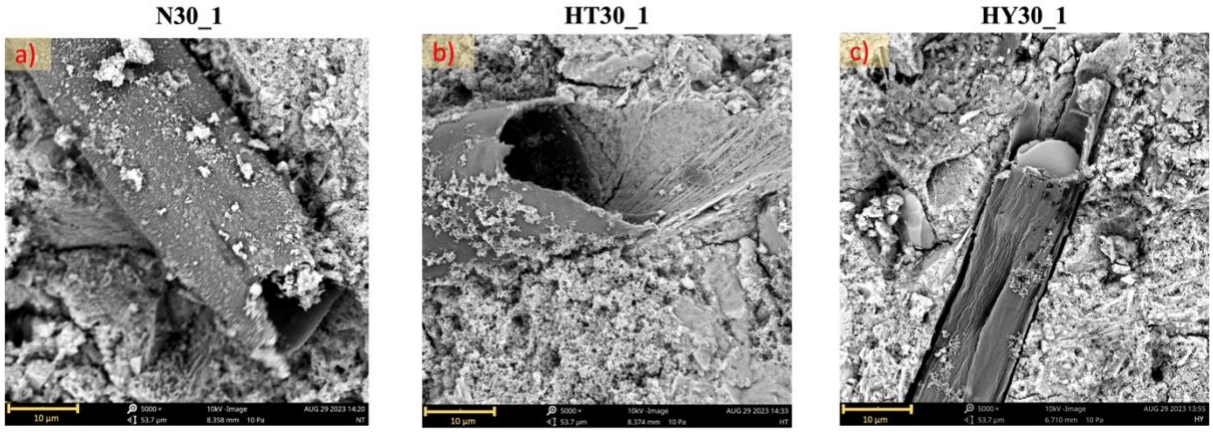

Figure 4.16. Backscattered scanning electron (BS-SEM) micrographs of cementitious samples containing MW fibres after 3 days of hydration: a) Non-treated MW fibres (N30_1), b) Hydrothermally treated MW fibres (HT30_1), c) Hybrid treated MW fibres (HY30_1)

Furthermore, the analysis of elemental mapping in the vicinity of MW fibres within the 3-day hydrated cement paste samples was conducted using Energy Dispersive X-ray Spectroscopy (EDS) and is presented in Figure 4.17. The atomic concentrations of each element are also detailed in Table 4.4. Notably, the N30_1 sample exhibited the lowest Si concentration and Si/Ca ratio. This observation highlighted the significant retarding effect caused by the leaching of saccharides from the N-MW fibres, which retarded cement hydration and led to a reduced release of Si^{4+} into the cement solution. In contrast, the HT30_1 and HY30_1 sample exhibited elevated Si and Si/Ca concentrations, in consistent with the TGA and XRD findings, signifying more promoted hydration. Significantly, these outcomes highlighted the beneficial internal curing function of the HT-MW fibres, offsetting their initial adverse influence on hydration and promoting enhanced hydration in later stages.

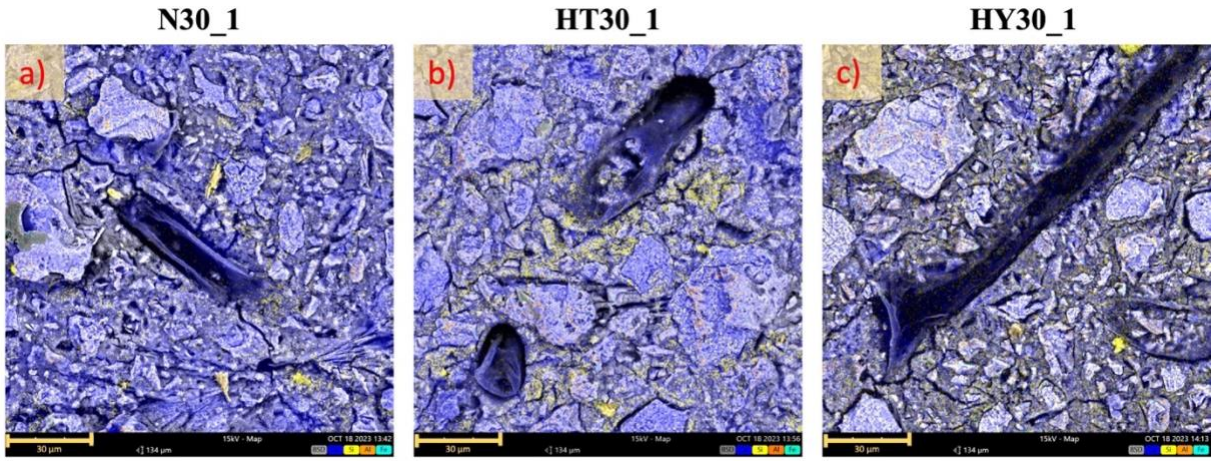

Figure 4.17. Energy dispersive X-ray spectroscopy (EDS) dot maps of polished cement paste samples containing MW fibres after 3 days of hydration (Yellow: Si, Blue: Ca, Orange: Al, Cyan: Fe): a) Non-treated MW fibres (N30_1), b) Hydrothermally treated MW fibres (HT30_1), c) Hybrid treated MW fibres (HY30_1)

Table 4.4. Elemental compositions analysis (atomic concentration) acquired based on Energy dispersive X-ray spectroscopy (EDS) from polished cement paste sample containing MW fibres after 3 days of hydration

Mixture	Al	Fe	Si	Ca	Al/Ca	Si/Ca
N30_1	10.75	2.99	22.94	63.32	0.17	0.36
HT30_1	11.81	3.29	24.51	60.38	0.20	0.41
HY30_1	10.69	2.47	25.76	61.09	0.17	0.42

4.4 Conclusions

In the initial phase of the study, the impact of MW fibres on the effective w/b was assessed through rheological measurements. This analysis facilitated a more precise comparison of samples with identical effective w/b in subsequent study sections. The introduction of MW fibres modified the effective w/b in cementitious mixes due to water absorption by these fibres. Nevertheless, our findings revealed that different pre-treatments and dosages resulted in varying levels of absorption, consequently influencing the effective w/b. Based on the results, samples

with MW fibres can be classified into three groups based on their effective w/b: HY30_2 with an effective w/b of 0.28, HY30_1, N30_2, and HT30_2 with an effective w/b of 0.285, and finally, N30_1 and HT30_1 with an effective w/b of 0.29.

Furthermore, certain components within MW fibres, notably lignin, showed to have the capacity to leach into the surrounding cement paste, resulting in a plasticizing effect that subsequently alters the rheological characteristics of the cement paste. This was specifically observed in the N-MW and HT-MW fibres, as evidenced by their lower hysteresis area, yield stress, and viscosity values. However, in the HT samples, the plasticizing impact induced by fibres was more prominent. This can be attributed to the elimination of the protective wax layer around the fibres, resulting in greater exposure and leaching of lignin into the cement paste.

In the second stage of the investigation, the internal curing effect and hydration properties of cementitious mixes were assessed with different dosages of MW fibres. It was observed that superior internal curing performance was achieved when 0.1% MW fibres were used compared to the use of 0.2% MW fibres. The detrimental impact of an excessive quantity of MW fibres on hydration evolution was attributed to the significant reduction in the effective w/b and the agglomeration of fibres, hindering access to entrained water and reducing the availability of free water. Furthermore, the presence of excess MW fibres led to increased leaching of extractives, exacerbating the hindrance of the hydration process.

The improved hydration was demonstrated through a higher cumulative heat of hydration in the isothermal calorimetry test for 0.1% MW fibre-incorporated samples compared to the reference sample. However, microstructure analyses of cementitious mixes incorporating MW fibres revealed that only the pre-treated MW fibres (i.e., HT-MW and HY-MW) samples demonstrated an improvement in the production of hydration products. This improvement was evidenced by

higher portlandite content, as indicated by TGA/DTG analyses, and further supported by XRD examination. Additionally, the findings were validated by increased Si concentration, as observed in the SEM-EDS analyses. Overall, the incorporation of 0.1% HY-MW and HT-MW fibres in cementitious mixes delivered an enhanced degree of hydration compared to the use of 0.2% MW fibres. This is achieved by providing an adequate amount of free water for the initial reaction of cement hydration and entrained water in the lumen for the subsequent internal curing. Nevertheless, a crucial distinction between the HT-MW and HY-MW fibres emerged in their impact on hydration kinetics. The former exhibited a gradual improvement in hydration owing to the gradual release of stored water in the lumen, while the latter resulted in a prompt hydration reaction without any retardation. These findings showed the effectiveness and suitability of using pre-treated MW fibres for internal curing applications, as validated by the comprehensive analyses conducted in this study.

Chapter 5 Investigation on the Kinetics of Water Transport by Milkweed Fibres During Internal Curing of Cementitious Paste [3]

Amirmohammad Sabziparvar [a], M. Reza Foruzanmehr [a]

[a] Dept. of Civil Engineering, University of Ottawa, 161 Louis Pasteur St., Ottawa, Ontario K1N 6N5, Canada.

Abstract

The use of lignocellulosic materials as internal curing agents, attributed to their remarkable hygroscopic properties and strong affinity towards water, is gaining attention as a cost-effective and sustainable solution. Hollow natural fibres such as Milkweed fibres, distinguished by their exceptionally wide lumen, exhibit excellent hygroscopic characteristics, positioning them as ideal candidates for serving as internal curing agents. This study investigated into the kinetics of water transport between MW fibres and the cementitious matrix, employing Nuclear Magnetic Resonance (NMR) relaxometry and Differential Scanning Calorimeter (DSC). NMR and DSC measurements revealed that the morphological features and the release of extractives, such as lignin, significantly influence the desorption kinetics of entrained water in MW fibres within cementitious matrices. Lignin played a key role in protecting the internal curing water from migration of hydration products into the lumen, as evidenced by the highest proton concentration in T_2 measurements of HT-MW fibres. Morphological features also notably affected the behaviour of MW fibres in the cementitious matrix. Holes and defects in HY-MW fibres increased water mobility and extended relaxation time, leading also to quicker water desorption. In contrast, HT-MW fibres with intact lumens showed shorter T_2 and a highest

[3] A version of this chapter is submitted in the Journal of Case Studies in Construction Materials

available internal curing water. Consequently, HT-MW fibres demonstrated superior internal curing capabilities compared to other types of MW fibres.

Keywords: Milkweed fibres; Internal Curing; Nuclear Magnetic Resonance (NMR); Water Transport Kinetics

5.1 Introduction

Internal curing, a concept first introduced by Philleo in 1991, marks a novel approach in mitigating early-age cracking in low w/b cementitious mixes [67]. Unlike traditional external curing methods, which prove insufficient for the highly dense microstructure of these mixes due to the limited penetration of curing water into the concrete, internal curing emerges as a promising alternative [280]. Internal curing is typically done by using well-dispersed absorptive particles as water-filled reservoirs within the cementitious matrix. This approach, established over the past decade, facilitates hydration reactions by supplying sufficient water to the cement paste, thus counteracting self-desiccation and reducing autogenous shrinkage [13]. Consequently, internal curing mitigates early-age cracking, which is a common phenomenon in the initial days in low w/b mixes.

Recent studies have shown the potential of lignocellulosic materials, such as natural fibres, for internal curing applications in low w/b cementitious mixes [20–22,34,62,64,162,163,281]. Their remarkable hygroscopic properties, coupled with their cost-effectiveness and availability, position them as sustainable alternatives to non-renewable SAP, aiding in the reduction of CO_2 emissions in the construction industry. While previous studies by the authors have shown that pre-treated MW fibres can improve the degree of hydration, there remains a lack of clear understanding of their adsorption/desorption behaviour within cementitious mixes [282]. For example, adding 0.1% wt. MW fibres resulted in a 17% increase in the cumulative heat of hydration of cementitious pastes compared to the reference cement paste after 3 days. This indicates a significant impact of MW fibres on early-age hydration, yet the mechanisms of water transport between the fibres and cementitious matrix need further investigation.

MW fibres are white, silky fibres extracted from the seeds of the milkweed plant, which is also found in China and Iran, where they are known as Akund and Estabragh, respectively. MW fibres

possess unique characteristics, including an exceptionally wide lumen that occupies nearly 90% of their volume and a thin wall with a thickness as low as 0.5 µm. These characteristics—the wide lumen and thin wall—can significantly alter the kinetics of water transport through the wall and along the lumen after pre-treatments. Despite moderate research into the use of lignocellulosic materials as internal curing agents, gaps persist in understanding the kinetics of water transport between the hollow natural fibres and the cement paste. Nuclear Magnetic Resonance (NMR) emerges as a powerful technique to study water transport kinetics between internal curing agents and the cement matrix. Unlike traditional methods like Mercury Intrusion Porosimetry (MIP), which requires breaking hardened samples and halting hydration, NMR allows for non-destructive, dynamic, in-situ analysis of porous materials [182–184]. These advantages enable continuous observation without altering the samples. While studies have investigated the kinetics of water transport between SAP and cement paste using NMR [51,188,191–194], research on lignocellulosic materials remains limited while no research has yet been conducted on the natural hollow fibres such as MW fibres. In one of the few studies available on lignocellulosic materials, Jongvisuttisun *et al.* used NMR to investigate the internal curing mechanism of hardwood pulp within cement composites. Their findings showed a sequential moisture migration process from eucalyptus fibre to the self-desiccating paste over a hydration period exceeding 13 hours. This migration involved the successive removal of free water from the lumen, small cell wall pores, and bound water in the cell wall [22]. This again emphasizes the importance of the morphological characteristics of fibres on the kinetics of water desorption from fibres within cementitious mixes. In another study by Zhang *et al.*, NMR was employed to monitor water distribution and pore size distribution over time and space in coir fibre-cement matrix composites. They found that coir fibres

improved moisture distribution and enhanced pore size distribution, contributing to internal curing, enhanced water transport, and crack control in the hydrating cement [184].

Morphological features such as porous cell walls, thickness, and lumen size are key parameters that can alter the adsorption/desorption kinetics of fibres within cementitious matrices [22]. Additionally, the presence of extractives such as lignin, hemicellulose, waxes, and pectin could also affect the mechanisms of water desorption from fibres within cementitious mixes, thereby influencing their internal curing behaviour. Therefore, in this study, three different types of MW fibres, each with distinct chemical compositions and morphologies, were examined to understand how these factors affect the kinetics of water transport between MW fibres and the cement matrix. We investigated the kinetics of water transport between MW fibres and the cement matrix, starting from the initial hours of hydration up to 7 days. To prevent any adverse impact on the fresh properties of cement mixes, MW fibres were used in a pre-saturated condition—a technique commonly applied with SAP and LWA [184,283–285]. In the subsequent phase, we employed a complementary technique, differential scanning calorimetry (DSC), to qualitatively measure freezable water in cement paste samples during the initial 24 hours of hydration. The findings obtained from these two methods contribute to a more comprehensive understanding of the kinetics of water transport between MW fibres and the cementitious matrix.

5.2 Materials

General-use Portland cement (GU) from Colacem Canada was used to make cement pastes, with its consistency adjusted using the MasterGlenium 7500 superplasticizer (SP) from Master Builders Solutions. Two types of pre-treated milkweed (MW) fibres were employed: hydrothermally treated (HT) and hybrid treated (HY), as detailed in the prior study by the authors [248]. The as-received

MW fibres consist of approximately 39% cellulose, 36% hemicellulose, and 18% lignin, with minor amounts of waxes, pectin, and sugars totaling less than 5% [25].

5.3 Mix Proportions

The mix proportions for the cement paste samples are listed in Table 5.1. The w/b was set at 0.30 for all cement paste samples containing MW fibres. The MW fibres content was 0.1% of the weight of PC. To use MW fibres in a saturated state, they were pre-soaked in the total mixing water (distilled water) and dispersed with the superplasticizer (1 wt.% of cement) for 1 hour using a magnetic stirrer at 500 rpm. According to the earlier study, 1 hour is roughly the time required to achieve MW fibres saturation [248].

Table 5.1. Mix proportions of the test specimens

Mix #	Total w/b	Entrained w/b	MW (%)	SP (%)	MW treatment
REF30	0.30	-	0	1	-
N	0.30	0.010	0.1	1	Non-treated
HT	0.30	0.010	0.1	1	Hydrothermal
HY	0.30	0.015	0.1	1	Hybrid

*wt.% by Portland cement (PC)

5.4 Testing Procedure

5.4.1 ^{1}H Nuclear Magnetic Resonance (NMR)

A Bruker Avance-III 200 MHz nuclear magnetic resonance (NMR) spectrometer was used to monitor the transverse magnetization relaxation of hydrogen atoms (^{1}H) in water molecules within the cement paste specimens. The Carr-Purcell-Meiboom-Gill (CPMG) pulse sequence with variable delays was implemented for determining the transverse NMR relaxation time (T_2) of the sample [286]. A total of 28 echoes were acquired, spanning echo times from 10 μs to 820 ms. The 90° pulse length (P1) was set at 5 μs; and the relaxation delay (D1) was fixed at 2.5 s. The spectra were then processed using Bruker TopSpin 4.3 software and the recorded transverse magnetization

decays subsequently underwent analysis with a regularized Inverse Laplace Transform (ILT) using Dynamics Centre software provide by Bruker to derive the T_2 distribution. Each cement paste sample was poured into small NMR tubes with dimensions of outer diameter (OD) of 7 mm and a length of 27 mm and then sealed with a plastic lid. All CPMG NMR measurements were conducted at 21 ± 2 °C at various hydration intervals of 1, 3, 6, 9, 12, 18, 24 hours, 3 days, and 7 days from the initial mixing of cement and water.

5.4.2 Differential Scanning Calorimeter (DSC)

A PerkinElmer DSC 4000 differential scanning calorimeter was employed to qualitatively measure freezable water in cement paste samples during the very early stages of hydration, specifically at 3 hours and 24 hours after mixing cement with water. Approximately 150 mg of fresh cement paste sample was poured into an aluminum crucible and hermetically sealed with a lid to prevent moisture loss. The DSC measurements comprised four steps: rapid cooling from room temperature to -30°C at a rate of −10 °C/min, equilibrating the sample at a temperature of -30 °C, heating from -30 °C to -12°C at 18°C/min, and heating from -12 °C to 25 °C at 4°C/min. The percentage of freezable water (FW) was calculated by determining the integral area of the endothermic peak, representing the percentage of frozen water present in the paste [287–290]:

$$FW(\%) = \left(\frac{Q}{H_f \times m}\right) \times 100 \qquad \text{Equation 5.1}$$

where Q denotes the enthalpy (J), H_f the heat of fusion of water (333.5 J/g), and m the sample mass (g).

5.5 Results and Discussion

5.5.1 NMR relaxation of hydrating plain cement paste

In the conventional classification of pores, there are two main categories [291]. Firstly, gel pores (<10 nm) are linked to the formation of hydration products and can be more precisely classified into small capillary pores (small mesopores), micropores, and interlayer spaces, ranging from the largest to the smallest. Secondly, capillary pores (10 nm~10,000 nm) can be further identified as large capillary pores (macropores) and medium capillary pores (large mesopores). The pore structure of cementitious materials is also characterized by the different physical states of water in pores of varying sizes. When a magnetic field is applied, the hydrogen nuclei in the water within these pores act like subatomic magnets [185]. Upon excitation, these nuclei gradually lose their alignment through a process known as relaxation. The relaxation of hydrogen nuclei occurs more quickly in smaller pores, where the surface-to-volume ratio is higher. This is explained by the fast exchange model as shown in Equation 5.2 where the spin-spin relaxation time (T_2) is inversely proportional to the surface-to-volume ratio of the pores in contact with the fluid [51,186]. Assuming the presence of spherical pores with a diameter of d, the T_2 correlates with the distribution of pore sizes (i.e., $T_2 \sim \frac{d}{6}$) [187,188]. Consequently, as cement hydration progresses, the pore structure evolves and the T_2 distribution also changes. Therefore, the reduction in T_2 values observed during the evolution of hydration in the cement paste is attributed to the densification of the cement paste and the formation of hydration products within water-filled pores and on the surface of cement grains [189]. This leads to a reduction in inter-particle spacing and consequently more confinement and shorter relaxation times (i.e. smaller T_2.)

$$T_2 = \frac{V}{S \times \rho_2}$$ Equation 5.2

where V and S represent the volume and the surface, respectively, and ρ_2 is surface relaxivity. Figure 5.1 illustrates the evolution of the T_2 distribution in the REF30, during the hydration period spanning from 1 hour to 7 days. The T_2 relaxation distribution of the plain cement paste sample revealed the presence of two peaks. The first primary T_2 peak of the REF30 sample, initially appeared at approximately 0.56 ms, and decreased to 0.18 ms after the 7-day hydration period. The secondary peak also emerged within the range of 3.16 ms to 5.62 ms. It is proposed that the first major T_2 peak, approximately around 0.5 ms, can be attributed to bound water on the surfaces of cement grains and free water which is between cement grains due to capillary tension. The second T_2 peak within the range of ~5-9 ms is also suggested to represent free water within pores of 56 nm to 100 nm [22,183,184].

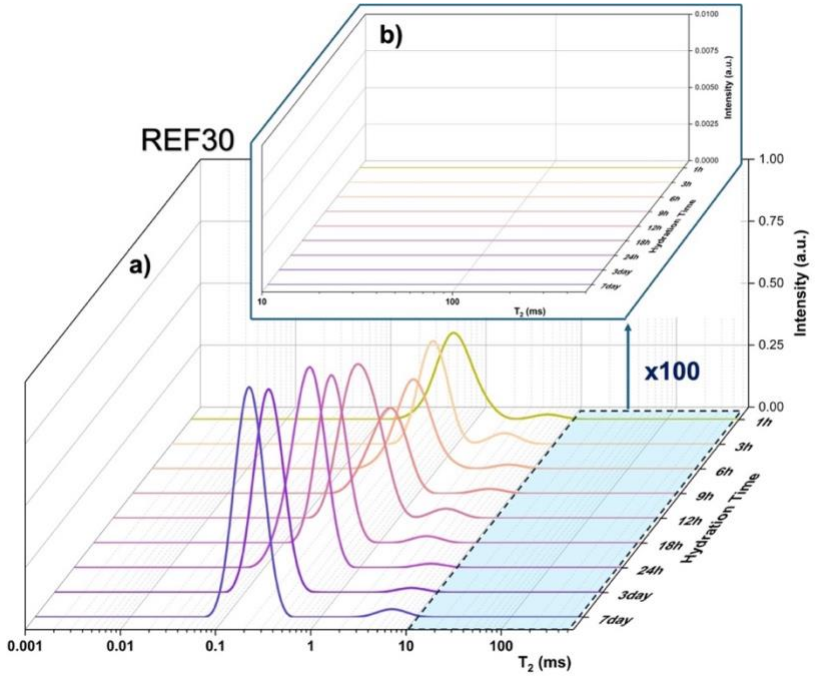

Figure 5.1. Distribution of the transverse relaxation time (T_2) of plain Portland cement paste (REF30) during different hydration time from 1 hour to 7 days (a), and magnified signal intensity in the range of 10 ms to 500 ms (b)

5.5.2 Kinetics of internal curing water of MW fibres in early hydration

NMR measurements offer valuable insights into the kinetics of entrained water (internal curing water) as it migrates from MW fibres to the hydrating cementitious paste. In Figure 5.2, Figure 5.3, and Figure 5.4, the T_2 distribution signals are presented for cement paste samples containing the N-MW, HT-MW, and HY-MW fibres, respectively. Notably, T_2 values shorter than 10 ms across all specimens revealed a dual-peak pattern similar to the reference sample's T_2 distribution. The first primary peak initially detected around 0.61 ms during the initiation of hydration, decreased to 0.14 ms for all N, HT, and HY samples after the 7 days. This consistent trend aligns with prior observations, highlighting the tendency of T_2 values to shift towards shorter relaxation times by hydration evolution. Additionally, the second peak emerged within the range of approximately 1.64 ms to 7.19 ms for all samples. A notable difference can be noticed when comparing the first 2 primary peaks of the MW-incorporated cement samples (Figure 5.2.a, Figure 5.3.a, Figure 5.4.a) with the reference sample (Figure 5.1.a) during the first hours of hydration. While in the plain cement paste, two distinct peaks are evident from the beginning of the hydration, in the MW-incorporated cement samples the peaks were initially combined. This combined peak split into two distinguishable peaks after approximately 9h for the cement paste samples containing the HT-MW and HY-MW fibres and after 12h for the N-MW cement paste sample. This indicates that in the reference sample, small pores were isolated from large ones starting from the first hour of hydration. In contrast, in cement paste samples with MW fibres, this isolation process took between 9 to 12 hours. The longer time for the isolation of gel pores from mesopores (in the range of 1.64 ms to 7.19 ms) in MW-incorporated samples could be linked to the presence of MW fibres themselves. These fibres could contribute to the connectivity of the pores up to 9 to 12 hours as

their hygroscopic characteristics facilitated the transport of water between gel pores and mesopores.

More importantly, for the T_2 values longer than 10 ms, MW-incorporated cement paste samples revealed the presence of at least one additional peak. As shown in Figure 5.2.b, in the case of cement paste samples incorporating the N-MW fibres, the 3rd peak appeared at 19.31 ms, persisting with high intensity for up to 9 hours of hydration. The cement paste samples with HT-MW fibres also exhibited a 3rd peak at the same T_2 of 19.31 ms; endured until 6 hours (Figure 5.3.b). Conversely, cement paste samples with the HY-MW fibres displayed a subtle 3rd peak at 51.79 ms after 6 hours of hydration (Figure 5.4.b). Given the exceptionally wide lumen of MW fibres, it is expected that the predominant volume of internal curing water (entrained water) is stored in these wide lumens. Consequently, the presence of a third peak in the cement paste specimens incorporating MW fibres serves as evidence for internal curing facilitated by these fibres. This range of relaxation also falls within the range of relaxation times previously documented as characteristic of free water within the lumen of lignocellulosic materials (i.e., T_2 within the range of 19.9–76.3 ms) [22,292,293].

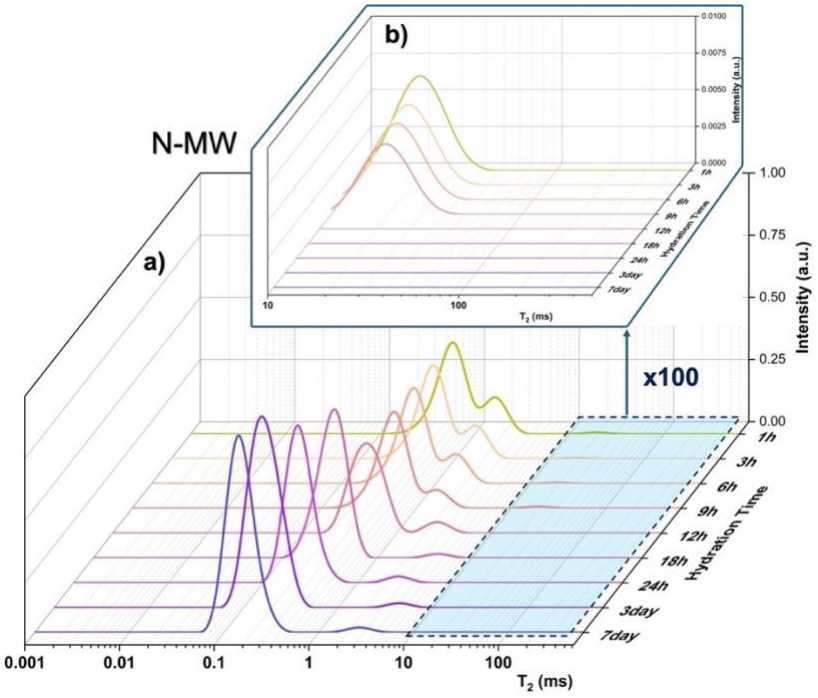

Figure 5.2. Distribution of the transverse relaxation time (T_2) of Portland cement paste with non-treated MW fibres (N-MW) during different hydration time from 1 hour to 7 days (a), and magnified signal intensity in the range of 10 ms to 500 ms (b)

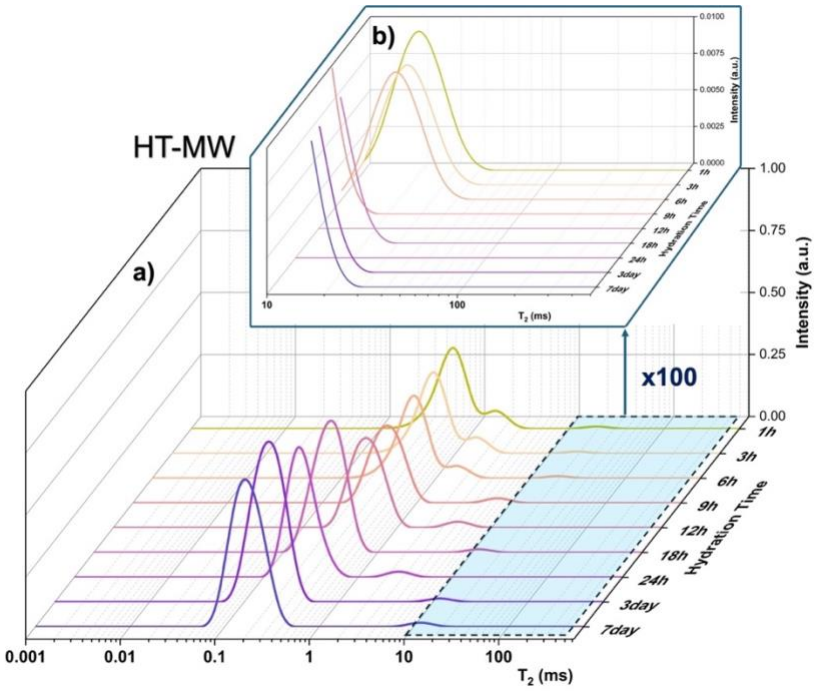

Figure 5.3. Distribution of the transverse relaxation time (T_2) of Portland cement paste with hydrothermally treated MW fibres (HT-MW) during different hydration time from 1 hour to 7 days (a), and magnified signal intensity in the range of 10 ms to 500 ms (b)

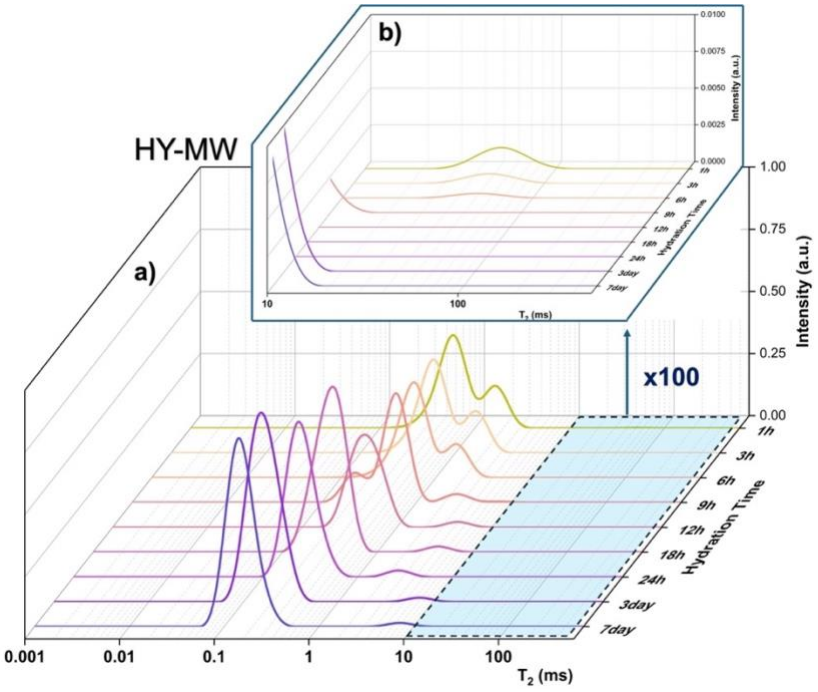

Figure 5.4. Distribution of the transverse relaxation time (T_2) of Portland cement paste with hybrid treated MW fibres (HY-MW) during different hydration time from 1 hour to 7 days (a), and magnified signal intensity in the range of 10 ms to 500 ms (b)

To understand the difference between the desorption kinetics of different pre-treated MW fibres the area under the 3rd peak was calculated and demonstrated in Figure 5.5. As mentioned earlier, the plain sample without fibres lacked a 3rd peak, and thus, no reference sample is depicted in Figure 5.5. In the MW-incorporated samples, however, the HT sample demonstrated the greatest area under the curve, followed by N, while the HY samples exhibited the lowest area under the curve. As the hydration reaction progresses, the area under the T_2 distribution decreases due to the consumption of entrained water for cement hydration.

Effect of morphology

By comparing the third peaks in the MW-incorporated samples, a noticeable shift in the relaxation time is evident when comparing the N/HT samples to the HY sample, changing from 19.31 ms to 51.79 ms. This indicates that the water is more mobile within the HY-MW fibres, resulting in a peak at a longer relaxation time. The increased mobility of the water in the HY-MW fibres is likely

due to the defects and holes that appeared in the fibre walls after the HY treatment, as observed in the authors' previous SEM images (Figure 3.8) [248]. Additionally, these holes led to quicker desorption of water when the HY-MW fibres were incorporated within the cementitious matrix, resulting in a significantly lower area under the curve, which implies lower proton concentration and less entrained water compared to the other samples (Figure 5.5). In contrast, the N-MW and HT-MW fibres, with their intact lumens, accommodated water in more confined spaces for longer time, appearing as shorter T_2 with higher area under the curve in the NMR analysis.

Effect of chemical composition

The observation of the largest area under the curve for the HT sample implies a greater amount of entrained water available in the lumen of the HT-MW fibres during the initial 6 hours of hydration compared to the other samples. This finding is consistent with previous findings by the authors, which showed the superior water retention property and more gradual water release of the HT-MW fibres compared to two other fibre types [248]. The improved hydrophilicity, resulting from the removal of hydrophobic components such as waxes is the main factor significantly contributing to the superior water retention property of the HT-MW fibres, resulted in higher proton concentration when compared to N samples (Figure 5.5). In contrast, the lack of lignin resulted in the penetration of hydration products inside the lumen of the HY-MW fibres, as shown in the next chapter in the Figure 6.13). This phenomenon led to the early consumption of entrained water, which should ideally be stored in the lumen of fibres, thereby losing its role as a water reservoir. However, in the case of the N-MW and HT-MW fibres, lignin acted as a barrier, preventing mineralization and thereby protecting the entrained water stored inside the lumen. Additionally, the completion of the desorption process can be identified at 6 hours for the HT and HY samples, while it extends to 9 hours for N samples. The prolonged retention of free water in the N samples

can be correlated with their hydration retarding impact, as evidenced by calorimetry results, leading to the delayed consumption of water.

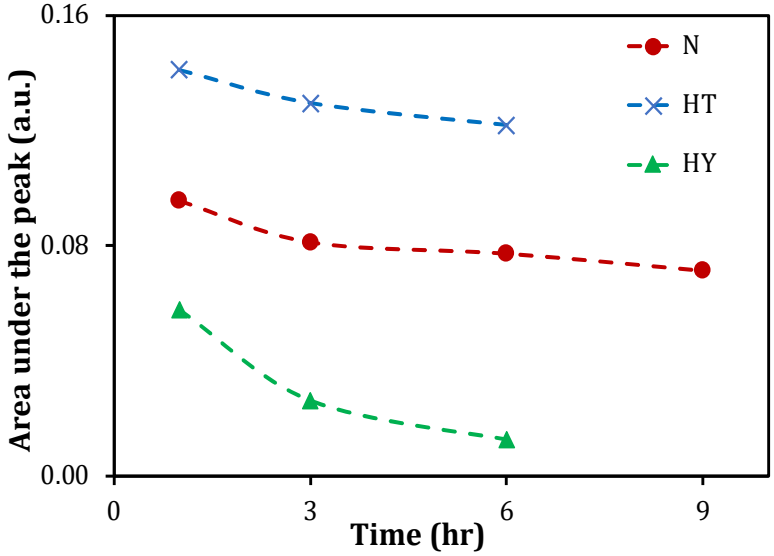

Figure 5.5. The area under the peak at T_2 within the range of 19.9–76.33 ms for different MW-incorporated samples

5.5.3 Freezable water (FW) evolution over time

Differential scanning calorimetry can provide information about the total amount of freezable water in cement paste samples, allowing for a qualitative comparison of the effect of various types of MW fibres on hydration evolution at early hours. This technique serves as a complementary analysis to NMR analysis. The impact of MW fibres with different pre-treatment techniques on the quantity of freezable water (i.e., melting heat) of cement paste samples is depicted in Figure 5.6 and the corresponding results summarized in Table 5.2. When compared to the reference sample (REF30), the cement paste samples containing the N-MW and HT-MW fibres showed the highest amount of freezable water (FW) in both the 3- and 24-hour. This indicates that more free water was available, resulting in more formed capillary pore ice, which required more heat to melt (indicated by the larger area under the curve) [290]. However, the amount of freezable water in the sample containing the HY-MW fibres is comparable to that of the reference sample (17.7% vs.

17.3%, for 3 hours and 1.2% vs 1.1% for 24 hours, respectively). These observations align well with the results obtained from the NMR analysis. In the NMR analysis, the N and HT samples showed a higher amount of capillary water for a longer duration compared to the HY sample. This correlates with the higher amount of freezable water (corresponding to the water in large capillary pores) in the N and HT samples.

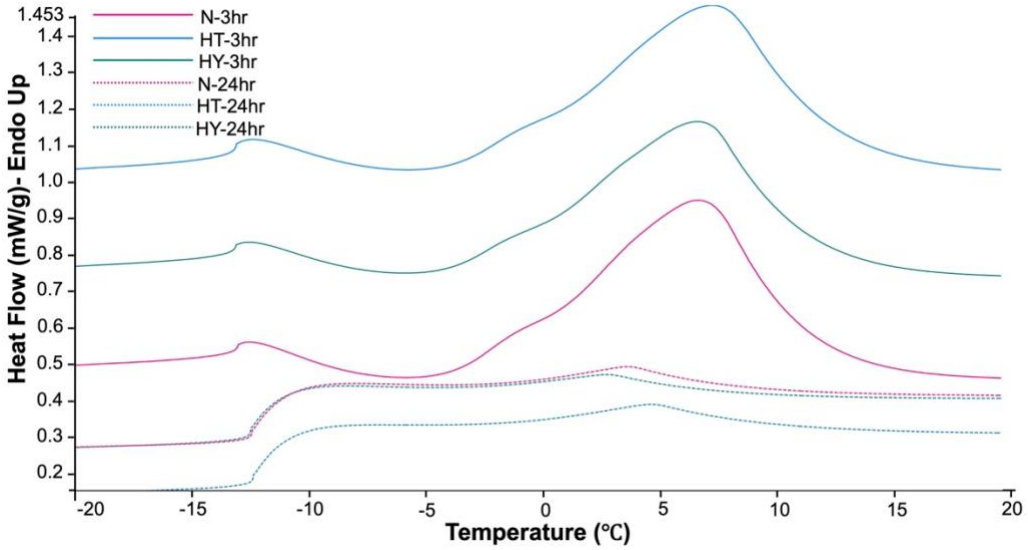

Figure 5.6. Low-temperature DSC heat flow curves of cement pastes after the addition of non-treated (N) and pre-treated (HT and HY) MW fibres at 3- and 24-hour

Table 5.2. Freezable water percentage of the cement paste samples with and without MW fibres addition, after 3 hours, and 24 hours

Mixture	3hr-FW (%)	24hr-FW (%)
REF30	17.35	1.07
N	19.09	1.60
HT	18.51	2.03
HY	17.68	1.17

Moreover, as revealed in the NMR analysis, the T_2 peaks of free water in the MW fibres' lumen persisted until 6 and 9 hours for the N and HT samples, respectively. This suggests that, while the

retarding effect of the N-MW and HT-MW fibres (observed as 1 to 2 hr in calorimetry results [282]) could partly explain the higher amount of free water observed compared to the HY-MW fibres, another factor is also at play. Scanning electron microscopy (SEM) results indicated that the lignin present in the N-MW and HT-MW fibres could act as a physical and chemical barrier. This barrier prevents hydration products from migrating into the lumen of these fibres, protecting the entrained water inside. Consequently, water remains stored in the lumen of the N-MW and HT-MW fibres for a longer duration compared to the HY-MW fibres. This explains the prolonged presence of the third peak in relaxation time and the higher amount of freezable water observed in DSC analyses.

5.6 Conclusions

This study investigated the desorption kinetics of internal curing water of MW fibres in low w/b paste mixes. The presence of a 3rd peak in MW-incorporated cement paste, particularly in the T_2 range of 19.9–76.33 ms, served as evidence for internal curing facilitated by MW fibres. It was observed that MW fibres can act as water reservoirs, supplying internal curing water for 6-9 hours during the early stages of cement hydration. Drawing conclusions from the results obtained through NMR and DSC measurements, it was observed that both the morphological features and the presence of extractives can impact the kinetics of water transport from MW fibres to cementitious matrix. It was found that lignin plays a key role in protecting the entrained water against the migration of hydration products within the lumen. In the HY-MW fibres, where lignin had been removed during the pre-treatment, there was a greater tendency for hydration products to migrate into the lumen, leading to early consumption of the internal curing water. This was demonstrated in the T_2 measurements and confirmed by DSC analysis. In contrast, the HT fibres showed the highest proton concentration in the T_2 measurements, indicating superior internal

curing water availability, followed by the N-MW fibres. Moreover, morphological features showed a significant impact on the behaviour of MW fibres within the cementitious matrix. The presence of holes and defects in the HY-MW fibres led to an increased mobility of water and longer relaxation time compared to other types of MW fibres. These defects also led to quicker water desorption in the cementitious matrix. In contrast, N-MW and HT-MW fibres, with intact lumens, retained water in more confined spaces, appearing as shorter T_2 with a higher area under the curve in NMR analysis. Therefore, the HT-MW fibres exhibited significant internal curing capabilities when compared to the other types of MW fibres.

Chapter 6 An Investigation into the Microstructural Evolution and Shrinkage Control in Internally Cured Mortars with Milkweed Fibres [4]

Amirmohammad Sabziparvar [a], M. Reza Foruzanmehr [a]

[a] Dept. of Civil Engineering, University of Ottawa, 161 Louis Pasteur St., Ottawa, Ontario K1N 6N5, Canada.

Abstract

This study investigated the impact of Milkweed (MW) fibres as internal curing agents on the shrinkage development and mechanical properties of low w/b cement-based materials. The focus of this research is on the pre-treatment methods applied to MW fibres and the influence of the pre-treated fibres, as internal curing agents, on the shrinkage of cement mortars. The hydration behaviour and microstructural development were revealed using a series of tests including setting time, compressive strength, flexural strength, scanning electron microscopy (SEM), and thermogravimetric analysis (TGA/DTG). Observations revealed that 0.1% wt. of hydrothermally treated (HT) and hybrid treated (HY) MW fibres played an effective role in internal curing, leading to significant reductions of up to 28% in autogenous shrinkage at 7 days compared to plain mortars. Furthermore, it was observed that the compressive strength gap between reference mixes and those with pre-treated MW fibres became smaller as internal curing enhanced in the later stages. Moreover, our analysis uncovered the pivotal role of lignin in mechanical properties, drying shrinkage and microstructural development of natural fibre-incorporated cementitious mixes. Specifically, lignin functions as a protective barrier within the fibres structure, shielding MW fibres from the infiltration of cement products into their lumina. Additionally, it acts as a

[4] A version of this chapter has been submitted to the Journal of Building Engineering

physical/chemical barrier, hindering moisture transport through the capillary network during drying conditions, thereby mitigating the adverse effects on drying shrinkage development.

Keywords: Milkweed fibres; Internal Curing; Shrinkage; Mechanical Properties

6.1 Introduction

The challenge of autogenous shrinkage-induced cracking is particularly pronounced in cement-based materials with a low w/b, typically below 0.42. In low w/b mixes, the main factors contributing to autogenous shrinkage are the insufficient supply of capillary water during cement hydration and the presence of a fine pore size distribution [59]. According to Powers' model, when the w/b falls below 0.42, there is not enough capillary water for the complete hydration of cement [252]. Hence, the decrease in relative humidity results in increased capillary pore tension, leading to autogenous shrinkage deformations in the solid skeleton of the hydration product. Due to the limited strength of the cementitious materials at early ages, the stress induced by autogenous shrinkage deformation surpasses the tensile strength. This leads to the formation of microcracks, which compromise mechanical properties and durability [281,294,295].

To counteract the adverse effects of autogenous shrinkage in cement-based materials with a low w/b, methods such as internal curing (IC) and the use of shrinkage-reducing admixtures (SRA) have been introduced. However, SRA come with notable drawbacks, including a significant retardation of early hydration, destabilization of air voids, and diminishing effectiveness over time [296]. Consequently, the adoption of internal curing techniques has become crucial, involving the incorporation of materials with high water absorption capacity, such as SAP [45,50,51,60,111]. In the internal curing process, internal curing agents release their water into the cementitious matrix during self-desiccation, maintaining high internal relative humidity [13,61,297]. This helps to reduce autogenous shrinkage, preventing early-age cracking.

However, SAP have their limitations, primarily due to their non-renewable polyacrylate composition, raising sustainability concerns [18]. The availability and production costs of SAP impose additional drawbacks. Moreover, there is a risk of particle agglomeration for SAP, leading

to the formation of large pores that can negatively impact the mechanical properties of cementitious materials [298]. To address these issues, recent research efforts have focused on developing renewable internal curing agents, with particular emphasis on lignocellulosic-based materials such as natural fibres, which exhibit promising hygroscopic properties [21,34,281,299]. Natural fibres offer advantages over synthetic counterparts like SAP, as they are abundant in many regions at minimal or no expense. Thus, their application as renewable resources provides an environmentally friendly solution, producing affordable construction materials that can be universally used while reducing the construction sector's environmental carbon footprint. Nevertheless, the mechanisms underlying the efficacy of natural fibres as internal curing agents in cementitious mixes have received less attention compared to SAP, where a more comprehensive understanding exists.

Prior studies have shown the effectiveness of natural fibres as internal curing agents [21,22,34,62,281,300,301]. However, the development of durable cement-based materials incorporating natural lignocellulosic fibres faces two interrelated challenges. Firstly, these fibres undergo degradation in the highly alkaline environment of cementitious matrices, primarily due to the alkali hydrolysis of amorphous components such as lignin and hemicellulose [174,302,303]. The readers can refer to the investigation undertaken by Wei and Meyer to understand the various degradation mechanisms of natural fibres [303]. The second challenge involves the retarding effect caused by soluble sugars and monosaccharides leaching from natural fibres during cement hydration [174,304]. Several proposed pre-treatment methods aim to enhance the durability of cementitious composites using natural fibres. These methods include fibre pre-treatment, the incorporation of pozzolanic materials and the carbonation of the cementitious matrix in a CO_2-rich environment to lower the pH of the cement pore solution [29–31].

As shown in Figure 6.1, besides wood fibres, plant fibres can be categorized into four groups based on their extraction location within the plant: bast fibres, seed fibres, leaf fibres, and fruit fibres. Certain seed fibres, such as MW floss fibres, exhibit a unique hollow structure characterized by an exceptionally wide lumen and thin walls (Figure 6.2.c). This hollow channel, referred to as the lumen, allows MW fibres to absorb water through capillary action, similar to a thin tube, storing the absorbed water within the lumen. As demonstrated in a prior study by the authors, the distinctive hollow morphology of MW fibres results in remarkable hygroscopic properties, particularly in terms of water absorption capacity and water retention [248].

Consequently, the authors investigated the hydration characteristics of PC when combined with pre-treated MW fibres serving as sustainable internal curing agents [282]. The findings indicated that optimal internal curing performance could be attained by introducing 0.1% wt. of either the HT-MW or the HY-MW fibres. Significantly, among the two pre-treatment methods, the HT-MW fibres displayed a more gradual internal curing effect, owing to their superior water retention.

Expanding on the findings of the previous research, this study aims to evaluate the impact of different pre-treated MW fibres on the shrinkage and mechanical properties of cement-based materials with low w/b. Mortars with a w/b of 0.30, both with and without pre-treated MW fibres as internal curing agents, were examined. The choice of such a low w/b was deliberate, creating conditions that intensify self-desiccation for the assessment of the internal curing efficacy of MW fibres in reducing autogenous shrinkage. Furthermore, this study broadened its scope to include a comprehensive microstructural analysis, seeking insights into how MW fibres influence the development of hydration products and interact with the cementitious matrix. We aimed to clarify the effects of lignocellulosic hollow MW fibres, acting as internal curing agents, on shrinkage

reduction and the mechanical properties of cementitious specimens. This involved analyzing and comparing different pre-treated MW fibres.

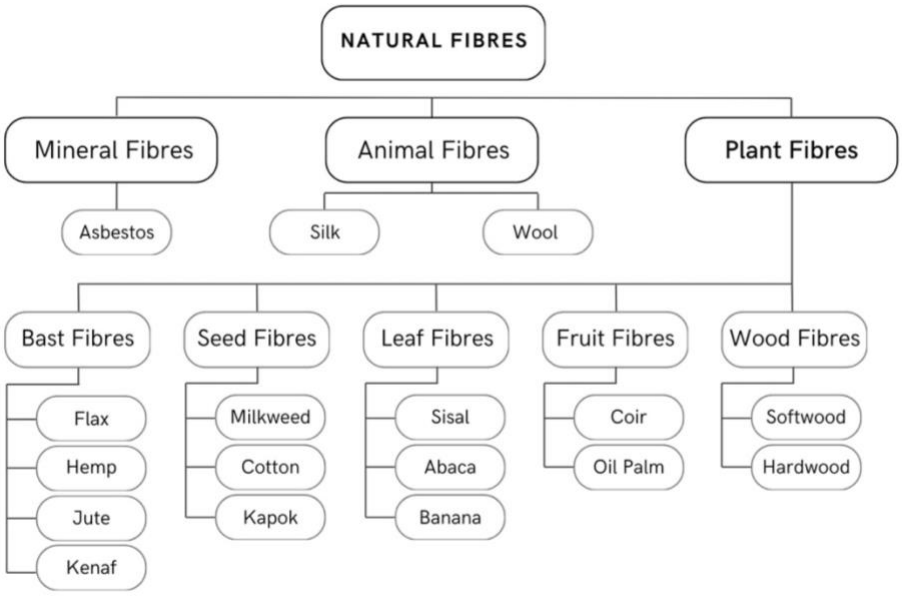

Figure 6.1. Summary of classification of different types of natural fibres

6.2 Materials

In this study, ordinary PC conforming to the Type 1 GU cement standard was employed. The chemical compositions of the cement are outlined in Table 6.1. A constant dosage of 1% polycarboxylate-based superplasticizer (MasterGlenium 7500, Master Builders Solutions) falling under the category of Type F high-range water-reducing admixtures was employed to enhance consistency. Mortar samples were manufactured using standard sand, which met the grading requirements specified in ASTM C788. Additionally, sodium hydroxide was obtained from Sigma-Aldrich for the alkaline pre-treatment of HY MW fibres.

Table 6.1. Chemical Composition of cement (wt.%)

Chemical Composition (%)							
CaO	SiO_2	Al_2O_3	Fe_2O_3	MgO	K_2O	Na_2O	Loss on ignition

62.85	19.78	4.92	2.24	2.33	1.08	0.26	2.84

Mineral Composition (%)			
C_3S	C_2S	C_3A	C_4AF
53.0	14.3	7.4	6

The MW Floss fibres were sourced from Protecstyle, located in Quebec, Canada. The appearance and microstructure of MW fibres are shown in Figure 6.2. SEM micrographs revealed the distinctive characteristics of the fibres, showing an exceptionally wide lumen and a thin wall. The measurements from these micrographs indicated an approximate lumen diameter of 9 μm and a wall thickness of about 0.5 μm. This suggests that the empty lumen constitutes a substantial portion, approximately 90%, of the fibre's total volume. The N-MW fibres are made up primarily of cellulose (39%), hemicellulose (36%), and lignin (18%), with trace amounts of waxes, pectin, and sugars (5%) [25]. To prepare the MW fibres for the study, the fibres were ground and sieved to pass through sieve #60, resulting in an approximate size of 236 ± 96 μm. Two distinct pre-treatments were applied to the fibres. The first pre-treatment involved hydrothermal treatment, immersing the fibres in boiling water for 2 hours. The second pre-treatment, known as the HY treatment, included both hydrothermal treatment and subsequent alkaline treatment. For a more comprehensive understanding of the pre-treatment process applied to the fibres, a detailed description is available in the authors' previous study [248].

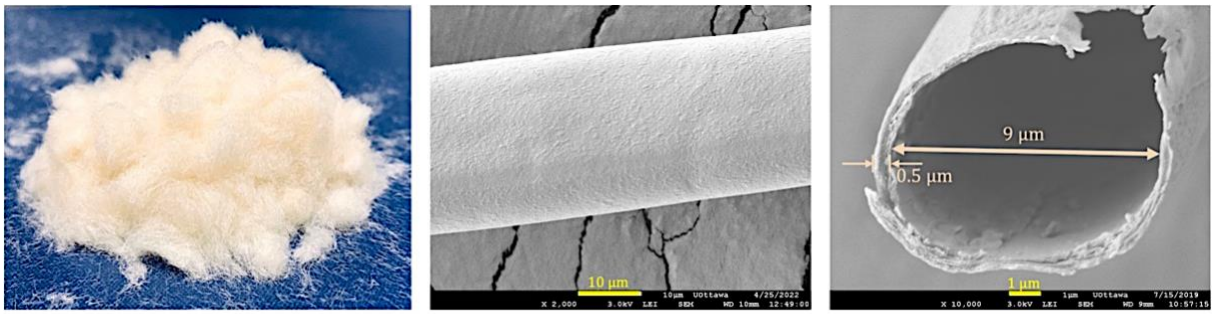

a) Milkweed fibres b) Lateral surface view c) Lumen view

Figure 6.2. Image of as-received milkweed fibres

6.3 Mix Proportions

The mortar mixtures used in this study consisted of GU cement, standard sand, and water in the respective proportions of 1:2.75:0.30. Detailed mix proportions for the mortar specimens can be found in Table 6.2. The fibres' content was set at 0.1% wt., identified as an optimum dosage in the previous study by the authors [282]. Assuming an average density of 0.296 g/cm^3 for MW fibres [199], their volume fraction is estimated to be around 0.34%.The variable parameter in the mixtures focused on the pre-treatment of MW fibres, including N, HT, and HY MW fibres. The water absorption capacity of the N, HT, and HY-MW fibres were determined to be 41±5, 41±2, and 39±4 g/g, respectively. According to the previous study by the authors, N and HY MW fibres released nearly 100% of their absorbed water within 90 minutes. However, the HT-MW fibres exhibited a better water retention, releasing only 80% of their absorbed water when subjected to a dry environment (38°C and 20% relative humidity)[248].

The total w/b remained constant at 0.30 for all MW fibre-incorporated mixes. However, due to water absorption by the fibres during the pre-soaking process, a portion of mix design water was stored in the fibres. This resulted in a modification of the effective w/b in MW incorporated samples. The effective w/b for cement paste samples containing MW were determined through rheological measurements, as depicted in Figure 4.2 [282]. The samples containing N and HT MW fibres exhibited an effective w/b of 0.29, while those with HY fibres had a slightly lower effective w/b of 0.285. Consequently, three reference samples were prepared to compare the samples incorporating MW fibres with their corresponding reference samples with identical w/b: one with the same total w/b of 0.30, and two others with effective w/b of 0.285 and 0.29. The rationale for incorporating an entrained w/b of 0.01 to 0.015 using 0.1% MW fibres is discussed in detail in section 4.2.2. In summary, this dosage was derived from the Equation 2.5 developed by Bentz *et*

al., which calculates the amount of internal curing agents needed to mitigate chemical shrinkage (CS) in cementitious mixes, targeting CS=0.07 g water/g cement for Type I GU-PC [251]. Additionally, the results obtained in Chapter 4, established 0.1% as the maximum effective dosage for MW fibres in terms of providing improved degree of hydration.

Table 6.2 Mix proportions of the control and MW-fibres mortars

	Control samples			**MW Fibre-added samples**	
	REF285 w/b=0.285	REF29 w/b=0.29	REF30 w/b=0.30	N, HT 0.1% MW	HY 0.1% MW
Cement (g)	500	500	500	500	500
Water (g)	142.5	145	150	150	150
Sand (g)	1375	1375	1375	1375	1375
MW fibre (g)	-	-	-	0.5	0.5
Total w/b	0.285	0.29	0.30	0.30	0.30
Superplasticizer (mL)	5	5	5	5	5
Entrained w/b	-	-	-	0.01	0.015

6.4 Testing Procedure

6.4.1 Setting Time

The determination of the initial and final setting times of the samples in this study was conducted by the Vicat needle test, through ASTM C191 guidelines. This test involves assessing the depth of penetration of the Vicat needle into the cement paste samples. A total of three samples were tested for each specimen.

6.4.2 Drying Shrinkage and Autogenous Shrinkage

To evaluate the unrestrained shrinkage of mortar samples, prisms measuring 25×25×285 mm^3 were made, following the guidelines outlined in ASTM C157-17. The prism moulds were filled with mortars in two layers, sealed, and allowed to be set for 24 hours. After demoulding, the specimens were stored in a controlled room at 50±5% relative humidity (RH) and a temperature of 20±2 °C.

The length change of specimens was measured at different time intervals. Autogenous deformation measurements were performed on prismatic samples using the same procedure as the drying shrinkage samples. However, after de-moulding, the autogenous shrinkage samples were sealed with aluminum tape and measured within a metallic frame equipped with a digital deformation transducer [184,305]. Additionally, the mass loss of each autogenous shrinkage prism was monitored, revealing a minimal value of less than 0.11% after 50 days. This demonstrates the negligible influence of evaporative losses and shows the efficacy of the sealing process employed in maintaining the integrity of the measurements. A total of seven samples were tested for each specimen.

6.4.3 Flexural and Compressive Tests

The compressive strength and flexural strength of the mortars were determined using 40×40×160 mm^3 prism specimens, following the procedures outlined in ASTM C348-21. Twelve samples per specimen were compacted using a tamper, applying twelve strokes each. Following compaction, the specimens were covered with plastic foil and placed in an environment with a temperature of 20 ± 2 °C for 24 hours. Subsequently, the specimens were de-moulded, wrapped in plastic foil, and stored under standard laboratory conditions (20 ± 2 °C) until the testing age was reached. The flexural strength was assessed through a three-point bending test machine. For the determination of compressive strength, portions of the mortar prisms initially tested in flexure were used, adhering to ASTM C349 standards.

6.4.4 Scanning Electron Microscopy (SEM)

To reveal the microstructure of cement paste samples after the incorporation of different types of MW fibres, a Thermo Scientific Phenom XL scanning electron microscope (SEM) was used in secondary electron (SE) and backscatter electron (BSE) modes, operating at accelerating voltages

of 10 kV and 15 kV, respectively. Two types of samples were prepared for microscopy including fractured parts and polished specimens. For the fractured parts, SE microscopy was employed, while polished samples were prepared to investigate the elemental composition in the interface of MW fibres and the cement matrix using BSE and energy-dispersive X-ray spectroscopy (EDS). To avoid the direct polishing treatment from modifying the microstructure at the interface and jeopardizing the authenticity of the test surface, the samples were initially subjected to resin impregnation. After polishing, all samples were coated with a carbon film to reduce charging and improve the contrast of SEM images. In addition, the hydration process of all samples was halted using the solvent exchange method with isopropanol before examinations.

6.4.5 Thermogravimetric analysis (TGA)

To gain a better understanding of how different pre-treated MW fibres affect the hydration characteristics of cementitious composites, a Perkin Elmer TGA 4000 thermogravimetric analyzer was used for thermogravimetric analysis of 7-day specimens. Before the test, cement samples were grounded using a mortar and pestle and passed through a #200 sieve. Subsequently, the samples underwent decomposition in a temperature range from 30 °C to 995 °C, with a heating rate of 10°/min, under a nitrogen environment. The amount of portlandite ($Ca(OH)_2$) were then estimated using Equation 6.1.

$$m\ (CH) = m_c \frac{M_{(Ca(OH_2))}}{M_{(H_2O)}} + m_d \frac{M_{(Ca(OH_2))}}{M_{(CO_2)}} \qquad \text{Equation 6.1}$$

Besides, the hydration degree of samples was studied based on the amount of chemical bound water ($m\ (CBW)$) using Equation 6.2 [306].

$$m\ (CBW) = m_b + m_c + m_d \frac{M_{(H_2O)}}{M_{(CO_2)}}$$ Equation 6.2

Where m_b is weight loss rate (%) between 70 to 400 °C (C-S-H gel, AFt, AFm and other hydration products), $m_c and\ m_d$ represents weight loss rate in 400–650 °C ($Ca(OH)_2$) and 650–750°C ($CaCO_3$), respectively. $M_{(H_2O)}$, $M_{(CO_2)}$, and $M_{(Ca(OH_2))}$ also represents the relative molecular weights which are equal to 18, 44, 74, respectively. Based on the derivative curve (DTG), the precise limits for the temperature interval of CH and CBW contents were established.

6.5 Results and Discussion

6.5.1 Effect of MW fibres on setting time of cement paste samples

The effect of pre-treated MW fibres on the initial and final setting times of cement paste is presented in Figure 6.3 It is evident that while the MW fibres had no significant impact on the initial setting time, they notably affected the final setting time. The most prominent delay in the final setting time was observed in the N and HT samples, with respective delays of 45±5 minutes and 40±6 minutes. The nearly identical final setting times of the N and HT samples indicated that the removal of waxes and pectin during the hydrothermal process for the HT sample had a relatively minor effect on the final setting time. Instead, other compounds, such as hemicellulose, predominantly influenced the delay in the final setting time of the cement paste samples.

The delay in the setting time of cement composites following the incorporation of lignocellulosic fibres has been previously reported [172–174,307]. For example, in the case of hemp fibres, their retarding effect was attributed to the trapping of OH^- ions. This trapping was proposed to be primarily carried out by the free carboxylate and alcohol functional groups present in pectin, which made up around 20% of the composition of hemp fibres [172]. However, it's important to highlight

that MW fibres possess approximately 0.4% pectin in their composition [25], making it improbable that pectin was the main factor responsible for the observed delaying effect in this study. Instead, the high concentration of hemicellulose in MW fibres, estimated at around 36%, is proposed to play a crucial role in the delayed setting time [282]. Hemicellulose contains free carboxylate functional groups in its structure, which become ionized in alkaline media. This leads to the surface fibre carrying a negative electrical charge that can adsorb and trap Ca^{2+} ions, acting as a retarder and growth inhibitor for CSH hydrates [172]. Another mechanism explaining the retarding effect of the N-MW and HT-MW fibres is the adsorption of monosaccharides, primarily originating from hemicellulose, onto anhydrous cement grains, inducing a setting delay by hindering water access to non-hydrated cement grains [175,176]. The notably reduced delay in setting time for samples containing HY fibres (i.e., 18±3 minutes) confirmed this conclusion that the removal of hemicellulose from MW fibres during the hybrid pre-treatment process resulted in decreased leaching of retarding extractives. This removal of hemicellulose from the HY-MW fibres was evidenced in the authors' previous studies by the disappearance of the FTIR absorption peak at 1735 cm^{-1} C=O stretching vibration of the carboxylate group followed by the pre-treatment [248]. Consequently, this resulted in a significantly weaker retarding effect when compared to the reference sample and demonstrated the relative efficacy of the hybrid pre-treatment method in minimizing the adverse impact of lignocellulosic fibres on the PC setting time.

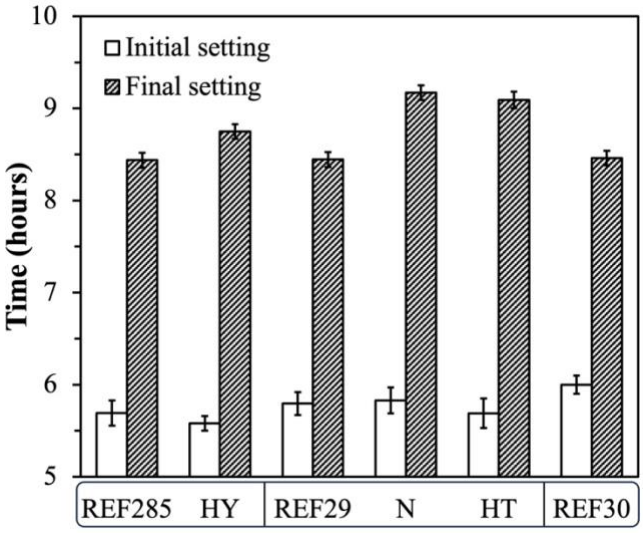

Figure 6.3. Variation of setting time of cement paste with non-treated and pre-treated MW fibres

6.5.2 Effect of MW fibres on the degree of hydration of cement paste samples

As illustrated in Figure 6.4, TGA was performed on 7-day specimens to examine the impact of MW fibres on the degree of hydration. The summary of the calculated portlandite content and chemically bound water, derived from TGA thermograms, is presented in Table 6.3. It is evident that the HT and HY samples displayed the highest portlandite content at 17.7% and 17.6%, respectively. In contrast, the N sample exhibited the lowest portlandite content at 16.7%, compared to REF30, which showed a portlandite content of 17.7%. This indicates that both pre-treated MW fibres, HT and HY, were successful in achieving a similar degree of hydration as the reference sample with the same total w/b. This is further confirmed by the percentage of chemically bound water (CBW), where the HT and HY samples demonstrated the highest percentages of CBW at 6.4% and 6.6%, respectively, compared to 6.4% in the REF30 sample.

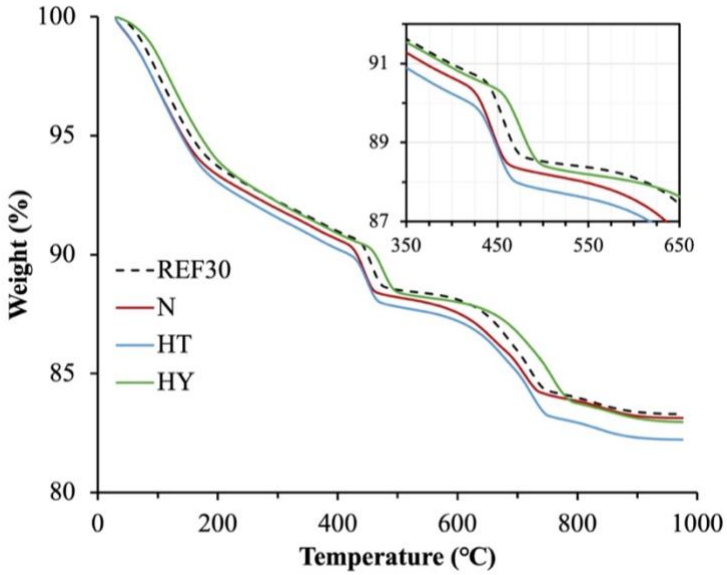

Figure 6.4. TGA results of the MW incorporated specimens

Table 6.3. Chemically bound water (m (CBW)) and Portlandite content (m (CH) of MW incorporated specimens based on TGA/DTG curves

Mixture	$m\,(FW)$ (%)	$m\,(CBW)$ (%)	L CH (%)	L Calcite (%)	$m\,(CH)$ (%)
REF30	2.6	6.4	2.5	4.5	17.7
N	3.3	6.0	2.4	4.0	16.7
HT	3.3	6.4	2.4	4.6	17.7
HY	2.7	6.6	2.4	4.6	17.6

6.5.3 Effect of MW fibres on autogenous shrinkage of mortar samples

During the hydration process of cement, water is gradually consumed, causing the initially water-filled pores to become partially unsaturated. This phenomenon triggers the formation of menisci within the pores. The drying capillary pores form menisci with a small curvature radius, resulting in significant capillary tension, and as a result, substantial autogenous shrinkage strains [308–310]. The magnitude of autogenous shrinkage is directly related to the w/b. Lower w/b facilitate the rapid formation of smaller pores, intensifying capillary tension and resulting in higher shrinkage

due to pore size refinement [311,312]. This relationship is evident in Figure 6.5, where mortar samples with lower w/b exhibit higher absolute shrinkage values. Autogenous shrinkage is particularly concerning in the early ages as it develops rapidly when the cement paste possesses weaker mechanical properties compared to long-term drying shrinkage [313]. In this study, the term 'early-age' refers to the period from the placement of the mixes up to 7 days.

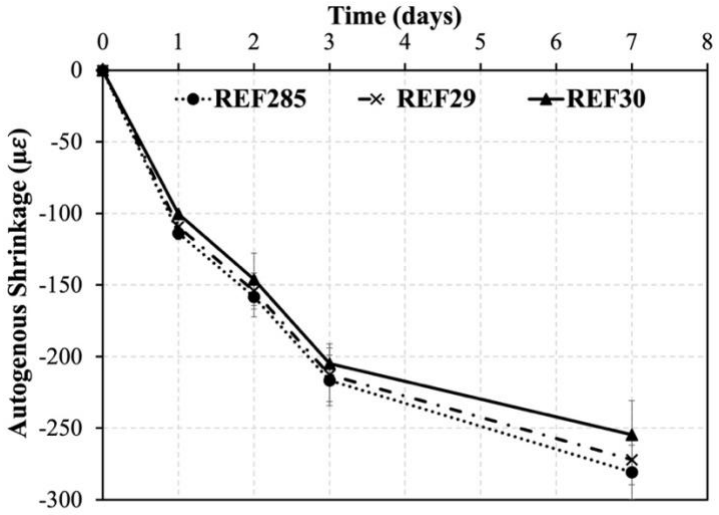

Figure 6.5. Autogenous shrinkage development of the reference mortar mixes with w/b=0.285, w/b=0.29, and w/b=30

Figure 6.6 and Figure 6.7 depict the autogenous shrinkage strains of cement mortar mixtures containing MW fibres at both early and long-term ages. Typically, the most significant autogenous shrinkage occurs within the initial days following mixing. During this period, the mixture lacks sufficient tensile strength to withstand the crack propagation triggered by shrinkage stresses. The 3-day autogenous shrinkage of all specimens reached approximately 80-85% of their autogenous shrinkage at 7-days, showing that the major portion of autogenous shrinkage appeared at the first 3 days. While autogenous shrinkage typically stabilizes within the initial days for cement mixes with a normal w/b (i.e., w/b> 0.42), the continual rise in shrinkage strains across all mixtures can be attributed to the low w/b and high cement dosage. Comparatively, the N sample showed negligible changes in autogenous shrinkage strains, whereas the HT and HY samples exhibited

meaningful reductions, demonstrating the efficacy of internal curing water released by the HT and HY pre-treated MW fibres. Specifically, the HT sample demonstrated a remarkable 27% reduction in autogenous shrinkage at 3 days, maintaining a consistent reduction of 23% and 28% at 4 and 7 days, respectively. Conversely, the HY sample showed a 12% reduction at 3 days, progressively enhancing its effectiveness with reductions of 17% and 26% at 4 and 7 days, respectively. These reductions showed the effective role of the pre-treated MW fibres in the internal curing of the mortar. This effect plays a crucial role in mitigating tension induced by drying capillary pores during cement hydration, consequently reducing autogenous shrinkage in the cementitious mixes. It is important to note that the comparisons are made against reference samples having the same w/b as those samples that incorporate fibres (i.e., HT vs. REF29 and HY vs. REF285). Notably, the HY samples faced a harsher condition in terms of self-desiccation due to their slightly lower effective w/b.

In summary, pre-treated MW fibres can effectively reduce autogenous shrinkage through two mechanisms. Firstly, both the HT-MW and HY-MW fibres contribute to internal curing, maintaining high humidity within the cementitious matrix for continued hydration. Secondly, after releasing their water, the bridging effect of the fibres helps mitigate autogenous deformations [314]. A comparison of autogenous shrinkage values between the HT-MW and HY-MW fibres suggested that the latter exhibited slightly a higher shrinkage strain (i.e., the absolute value) in the early stages of the experiment. This difference in behaviour can be attributed to the superior bridging effect of HT-MW fibres compared to HY MW fibres, owing to their lower susceptibility to mineralization and subsequent alkaline degradation (i.e., loss of integrity). This resulted in a less pronounced shrinkage in the HT sample compared to samples with HY MW fibres. This aspect was thoroughly discussed later in the section 6.5.6 In contrast, as received MW fibres i.e., N MW

fibres, displayed no reduction in the autogenous shrinkage of cementitious specimens. This lack of effectiveness in reducing autogenous shrinkage is attributed to their inadequate internal curing capability. In particular, the diminished internal curing performance of N MW fibres was evidenced by a lower formation of hydration products, as confirmed through TGA and EDS analyses.

In comparison to other lignocellulosic fibres, the pre-treated MW fibres (i.e., HT and HY) demonstrated a notably effective impact on reducing autogenous shrinkage. For instance, when compared to plain mortar, 0.25% weight of abaca fibres reduced autogenous shrinkage at 8 days by 21% [21]. Additionally, the addition of 1% cellulose fibres resulted in a 13% reduction in 7-day autogenous shrinkage in mortar [163]. However, 0.1% wt. pre-treated MW fibres exhibited autogenous shrinkage reduction ranging from 12% to 27% in within 3 days in mortar samples. This reduction further increased to 26% to 28% within 7 days. This demonstrated the critical role of the unique hollow structure in MW fibres for their effectiveness in internal curing and mitigating autogenous shrinkage, setting them apart from other lignocellulosic materials.

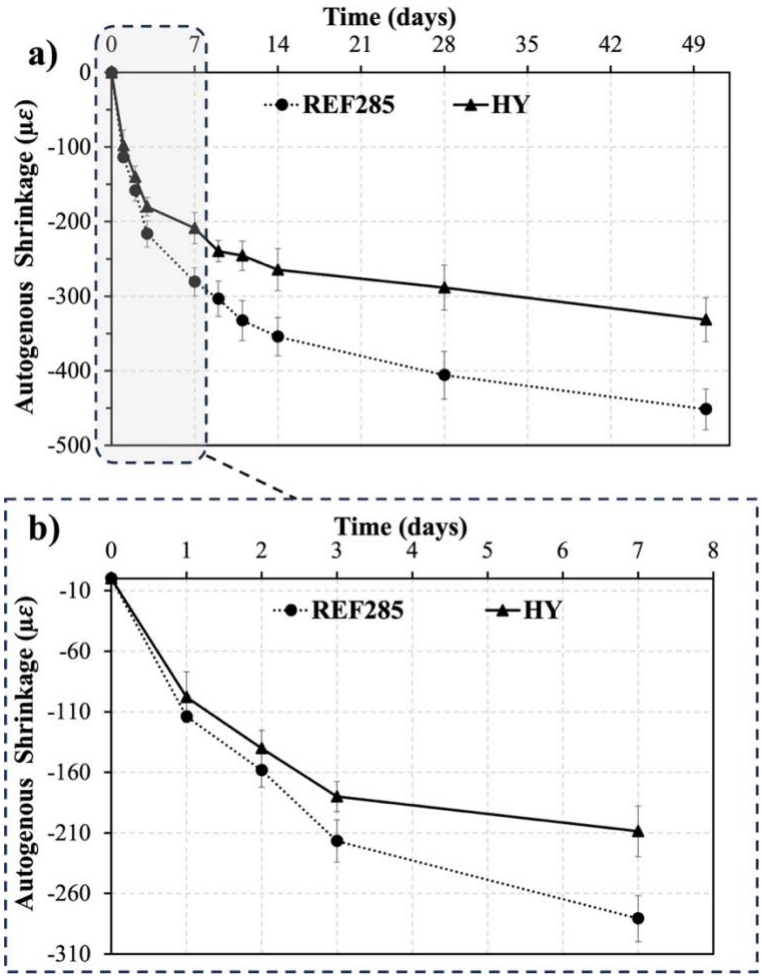

Figure 6.6. a) early age, and b) long-term autogenous shrinkage development of mortar mixes containing hybrid treated MW fibres, compared to the reference sample with the same effective w/b

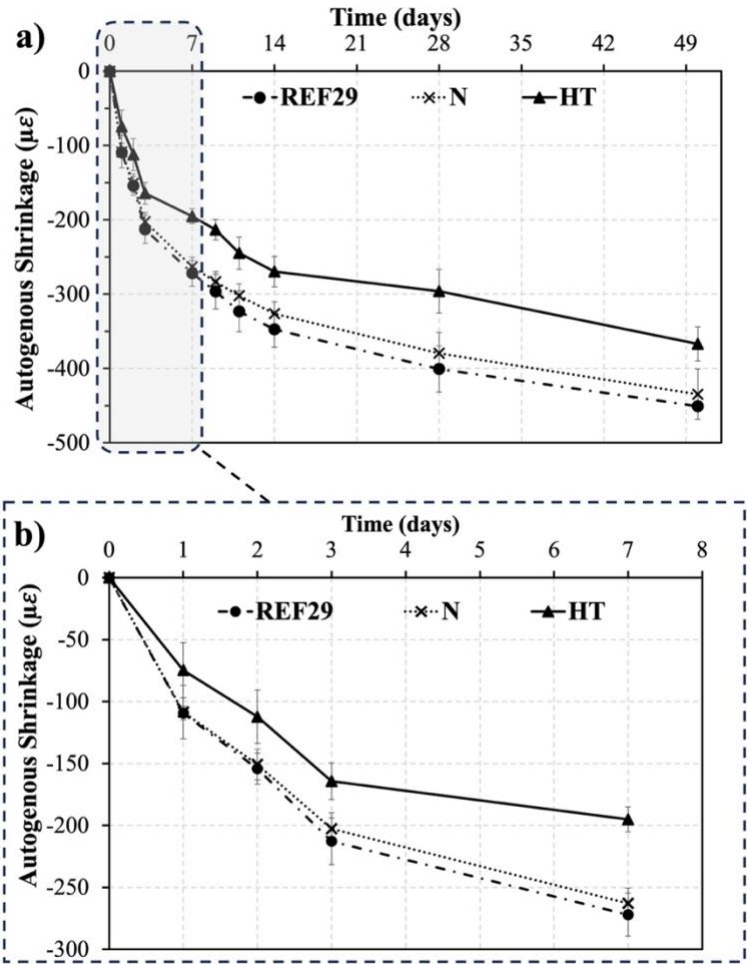

Figure 6.7. a) early age, and b) long-term autogenous shrinkage development of mortar mixes containing non-treated and hydrothermally treated MW fibres, compared to the reference sample with the same effective w/b

6.5.4 Effect of MW fibres on drying shrinkage of mortar samples

Figure 6.8 illustrates the drying shrinkage strain of cement mortar mixtures incorporating MW fibres. The drying shrinkage behaviour of mortar specimens with MW fibres showed two different patterns. Firstly, both the N and HT samples experienced significantly higher drying shrinkage, with increases of 30% and 29% respectively compared to their corresponding plain mortar samples, within the first 3 days. However, as the testing period progressed to 63 days, the drying shrinkage values for these MW fibre-containing samples gradually approached those of the plain mortar samples, with the difference becoming negligible (i.e., <±5%) and statistically

insignificant. In contrast, the HY sample demonstrated less severe drying shrinkage in the first 3 days, with a 20% increase compared to the plain mortar sample. However, after the initial three days, the drying shrinkage in the mortar samples containing HY increased compared to the plain mortar samples. This trend persisted throughout the remainder of the testing period. For instance, the increase in drying shrinkage from the 7^{th} day to the 28^{th} day ranged between 15% and 9%, respectively. The water loss measurements of samples incorporating MW fibres under drying conditions exhibited the same overall trends, as depicted in Figure 6.9.

The observed difference between the drying shrinkage behaviour of the HY sample in comparison to the N and HT sample in the later ages is an interesting finding, necessitating a deeper understanding of the underlying factors influencing drying shrinkage in cementitious matrices. The drying shrinkage of the cementitious matrices is closely related to the magnitude of its porosity and the size and connectivity (percolation) of the capillary system in the hydrated cement paste [170,315]. The higher the connectivity of capillary pores network, the higher the drying shrinkage. Thus, the different responses of various MW fibres in mitigating drying shrinkage can be explained by their role in connecting to the capillary network.

HY MW fibres, having undergone a pre-treatment process that removes lignin, exhibit greater hydrophilicity compared to the N and HT MW fibres. Consequently, HY MW fibres, reaching several hundred micrometers in size, establish new pathways for transporting moisture outward by connecting to the capillary pore network, microcracks (induced by shrinkage), and macro cracks (induced by fibre contraction after release of their entrained water). This connection to the pore network of the cementitious system was mainly facilitated by the migration of cement products into the lumen of HY MW fibres (as shown in Figure 6.13-a.1-2). These newly formed extensive pore networks created by HY MW fibres subsequently exacerbate drying shrinkage by facilitating

moisture transport to the unsaturated environment. Additionally, the distinct morphology of HY MW fibres could be an additional reason in facilitating moisture transport within these pore networks. Firstly, the removal of hemicellulose and lignin during the pre-treatment process results in accelerated moisture transport through thinner cell walls (i.e., removing a physical barrier). Moreover, the presence of defects and holes within the structure of HY MW fibres could also contribute to easier moisture transport. These drastic morphological changes were previously showed in the study by the authors [248].

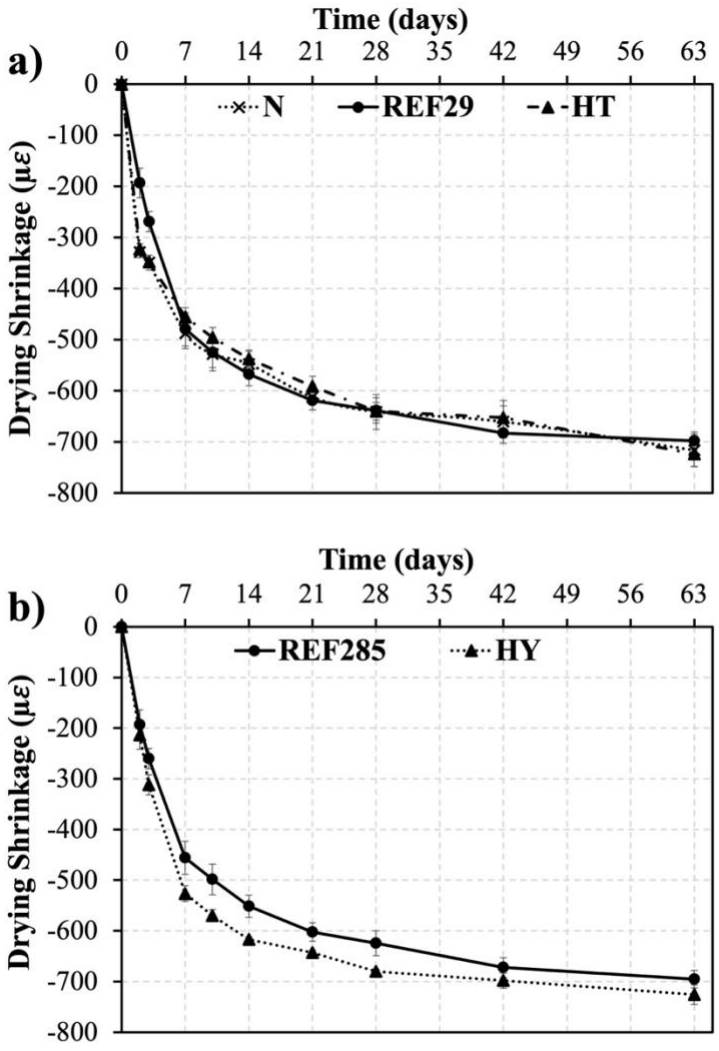

Figure 6.8. Drying shrinkage deformations of mortar mixes with; a) non-treated (N) and hydrothermally treated (HT), and b) hybrid-treated (HY) MW fibres comparing to reference mixes with the same effective w/b

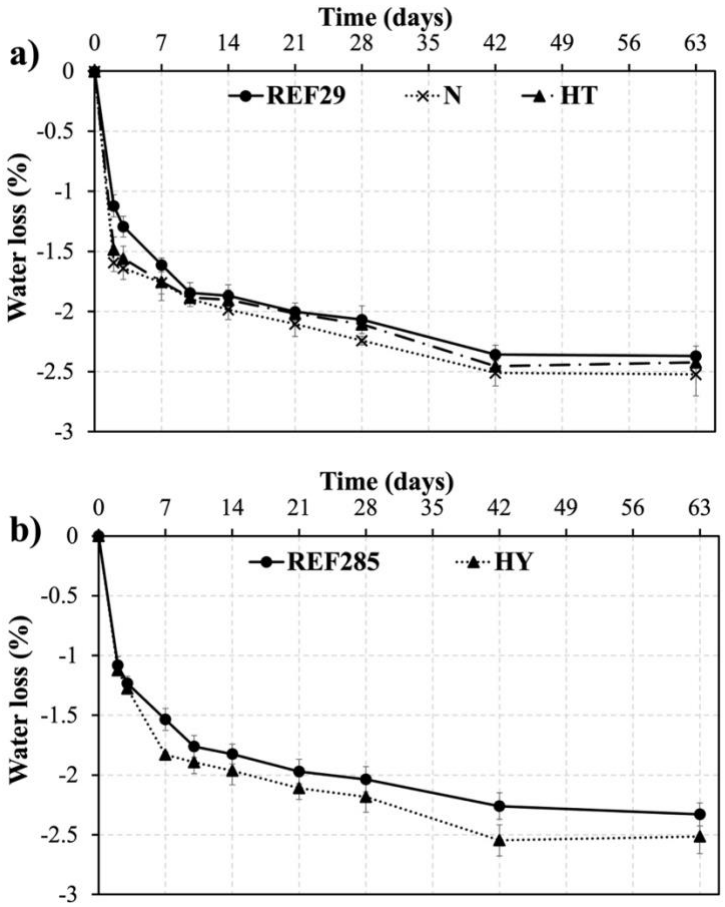

Figure 6.9. Water loss (%) of mortar mixes with; a) non-treated (N) and hydrothermally treated (HT), and b) hybrid-treated MW fibres (HY) comparing to reference mixes with the same effective w/b

6.5.5 Effect of MW Fibres on mechanical properties of mortar samples

The effects of adding MW fibres on both the compressive strength and the flexural strength of mortar mixes are depicted in Figure 6.10 and Figure 6.11, respectively. For the N samples, there was a notable reduction in compressive strength by 9.5% at 7 days and 8.4% at 28 days compared to the reference sample. The HT sample underwent a 4.7% decrease in compressive strength at 7 days, but by the 28th day, the HT and its corresponding reference exhibited almost identical strengths, both reaching around 71 MPa. In contrast, the HY samples maintained similar compressive strengths to those of their corresponding reference samples at both the 7- and 28-day curing ages, recording strengths of 64 MPa and 72 MPa, respectively.

Regardless of the incorporation of MW fibres, it can be seen that as the w/b decreases, the compressive strengths increase. This is due to the fact that the paste's strength is typically a function of number and size of capillary pores, which is primarily dependent of w/b [316]. An exception was observed in the N sample, which can be attributed to the significant poisoning effect of leachates and their role in interruption of hydration reaction [282]. The existing literature suggests that the inclusion of internal curing agents, such as SAP, and natural fibres such as sisal fibres, and Lechuguilla fibres, often leads to a decrease in early-age compressive strength. This reduction is attributed to the increased porosity of the cementitious composite due to the macro voids introduced by the internal curing agents following the release of their entrained water [34,62,127,281]. However, the reduction in compressive strength can be compensated at later ages, as the hydration proceeds at a higher rate since a higher internal RH is maintained in the internally cured specimens [128]. Consequently, the strength gap between reference mixes and those with internal curing agents becomes smaller as internal curing becomes more pronounced in the later stages. This holds true for both pre-treated MW fibres i.e., HT and HY, where their efficiency of internal curing has been shown previously. However, the HY samples, owing to their quicker release of internal curing water, exhibited superior performance even at early stages.

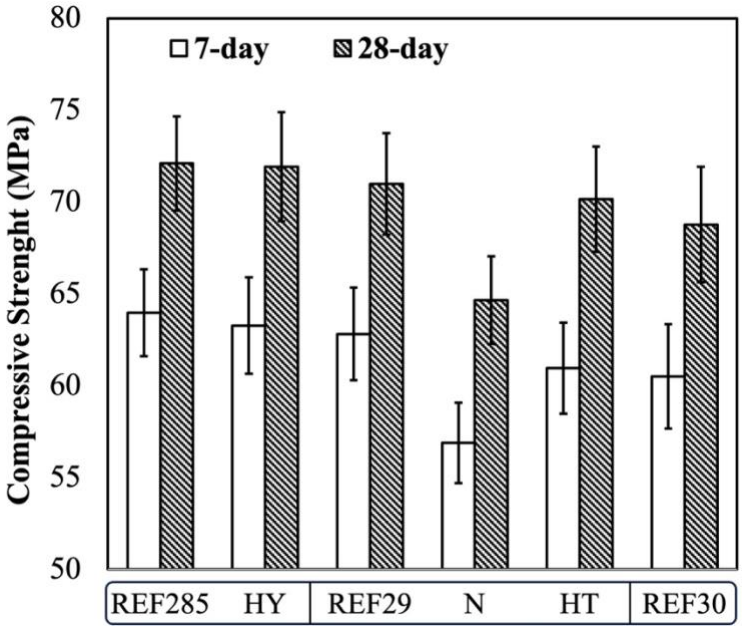

Figure 6.10. Compressive strength of mortar mixes after addition of MW fibres

Analyzing the flexural strengths of mixtures with MW fibres showed a different pattern than seen in the compressive strength results. Initially, at 7 days, pre-treated MW fibres (the HT and HY samples) showed a statistically significant increase in flexural strength (6.8 MPa and 6.6 MPa, respectively), whereas the N sample maintained almost the same flexural strength compared to their reference samples. However, by the 28-day age, the inclusion of MW fibres led to a notable decrease across all types compared to their corresponding reference, with the N samples showed the lowest strength at 6.9 MPa and the HT samples exhibited the highest flexural strength at 7.8 MPa. This decrease in flexural strength of all samples at 28 days compared to their references can be attributed to the alkali degradation of MW fibres due to prolonged exposure to the high alkali environment of the cementitious matrix.

Variations in the flexural strength of samples can be linked to the different drying shrinkage behaviours of MW-incorporated samples, as observed in Figure 6.8. Indeed, the primary mechanism impacting the flexural strength of specimens is the microcracks induced by drying shrinkage. These microcracks can serve as stress risers, significantly reducing the flexural strength

of the specimens. This effect was notably observed when comparing the HT sample to the HY sample. While the difference in flexural strength between the HT and the HY sample was relatively small at 7 days, the significant development of drying shrinkage-induced microcracks in the HY sample resulted in a notable drop in its flexural strength compared to the HT sample. For instance, the 28-day drying shrinkage of HY sample compared to the HT sample was recorded 681 με and 640 με, respectively. Additionally, the inferior flexural strength of the N samples can be attributed to their pronounced poisoning effect and poor internal curing performance compared to the pre-treated samples, leading to a weaker cement matrix with lower flexural strength at both ages.

It is of great importance to understand that the role of MW fibres here was not intended for reinforcing the cementitious matrix. This is because hollow fibres, such as those derived from Milkweed and Kapok, typically have low tensile strength (within the range of 100-300 MPa) [199,317,318] unlike bast fibres such as Flax, Jute, Hemp, and Kenaf, which exhibit higher tensile strength (ranging from 400-1000 MPa) [319]. Moreover, the interfacial adhesion between lignocellulosic fibres and the cementitious matrix is usually weak resulting in incomplete load transfer [302,319–322]. However, in addition to the mechanism explained in the previous paragraph, the bridging effect of MW fibres can be a secondary mechanism to explain lower flexural strength of the HY sample compared to the HT sample. Specifically, the strength of the HY-MW fibres was expected to be lower due to the more rigorous pre-treatment process compared to HT-MW fibres. This conclusion was supported by previous morphological observations, which revealed the presence of holes and defects within the structure of HY MW fibres, while the HT-MW fibres exhibited almost intact morphology [248]. Mineralization of lime within the lumen of the HY MW fibres is another phenomenon which increases fibre embrittlement and could diminish the flexural strength comparing to the HT sample, which is shown in Figure 6.13.a.1-2.

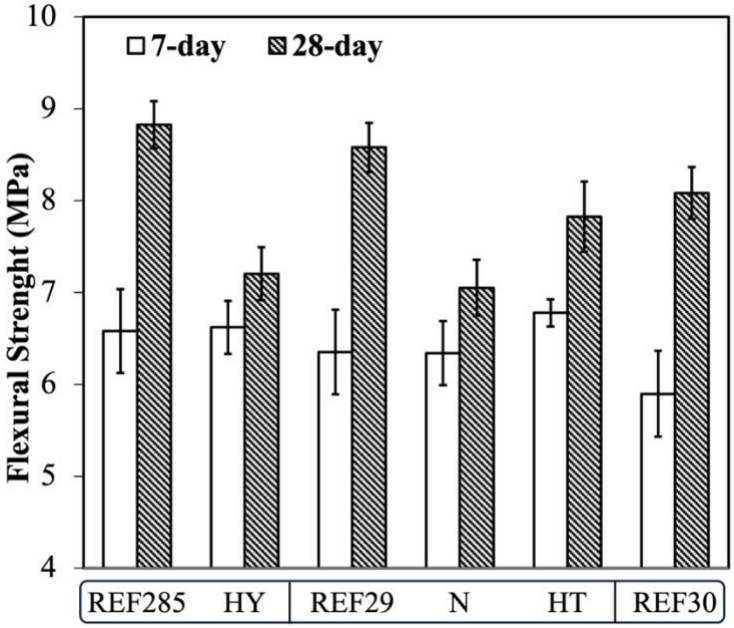

Figure 6.11. Flexural strength of mortar mixes after addition of MW fibres

6.5.6 Effect of MW Fibres on the microstructure of mortar Samples

Figure 6.12 shows the dispersion of 0.1% wt. MW fibres throughout the cement paste samples. As discussed earlier, these water reservoirs, while serving as internal curing agents, may act as macro voids after delivering their entrained water to the matrix, thereby affecting the compressive strength and drying shrinkage [170,323,324]. No evidence of agglomeration was detected during the assessment of dispersion for both non-treated and pre-treated MW fibres. The effective dispersion of internal curing agents (i.e., MW fibres) is a crucial factor which not only contributes to the mechanical properties of the final cementitious composite but also impact their internal curing capability in reducing autogenous shrinkage. For instance, recent studies on Eucalyptus fibres and cellulose fibres revealed that higher dosages can lead to poor dispersion, resulting in inadequate internal curing efficiency and diminished performance in reducing autogenous shrinkage of the cementitious composites [23,163].

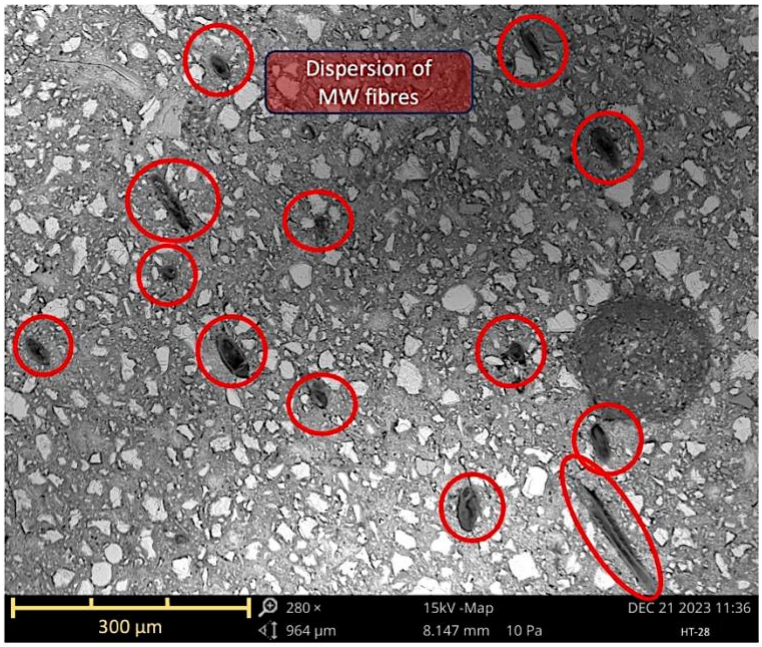

Figure 6.12. SEM image of dispersion of MW fibres across cement paste matrix

As previously mentioned, both the N- and HT-MW fibres primarily consist of cellulose, hemicellulose, and lignin. In Figure 6.13. b-1, it is evident that the HT-MW fibres exhibit an empty lumen cavity within the cementitious matrix, a characteristic also observed in N MW fibres. The main component of lignocellulosic fibres which acts as a physical and or chemical barrier to the migration and precipitation of cement into the fibre cavity is reported to be lignin [325,326], which is present in both the N- and HT-MW fibres. In fact, fibres with lignin have lower surface energy, resulting in higher contact angles with water (or other polar liquids) and reduced hydrophilicity compared to fibres from which lignin has been removed during pre-treatment (i.e., the HY sample) [327]. Consequently, the presence of lignin in the N- and HT-MW fibres renders them less susceptible to mineralization compared to the HY-MW fibres. It's worth mentioning, however, that in some HT and N fibres, minor mineral precipitation was observed at the fibre openings with no penetration into the lumen, as shown in as shown in Figure 6.13.b-2. This observation showed how the presence of lignin can disconnect the fibres from the pore network of cementitious system,

which resulted in a better drying shrinkage behaviour of the N and the HT sample compared to the HY sample as observed in Figure 6.8.

On the other hand, the elimination of lignin in HY MW fibres resulted in increased surface energy and hydrophilicity, thereby increasing their susceptibility to mineralization, as demonstrated in Figure 6.13.a-1. The mineralization of HY MW fibres occurs through the migration of calcium hydroxide (CH) and Ca^{2+} ions to the lumen cavity, where CH crystallizes [328]. The depth of penetration of these hydration products inside the fibre lumen reached up to 150 μm, as evidenced by SEM micrographs in Figure 6.13.a-2. Consequently, it is crucial to note that not all MW fibre-incorporated samples led to empty macro voids after delivering their entrained water, as mineralization can fill up the fibres in the absence of lignin. Furthermore, as discussed earlier, mineralization is one of the main reasons for the formation of an integrated pore network within the cementitious matrix after incorporating HY MW fibres, resulting in their poor drying shrinkage behaviour compared to the N and HT sample.

Elemental maps presented in Figure 6.14, Figure 6.15, and Figure 6.16 illustrate spatial distribution of major chemical elements at the interface between the N, HT, and HY MW fibres with cementitious matrix after 28 days, respectively. Micrographs and data summarized in Table 6.4 show that the HY samples exhibited the highest concentration of Si and Si/Ca values in the vicinity of the fibres, followed by the HT samples. This observation is attributed to the enhanced internal curing efficacy of HY MW fibres, improved hydration, and may also be related to mineralization occurring in their lumen, which was not possible for the N and HT MW fibres due to the presence of lignin within the structure of fibres.

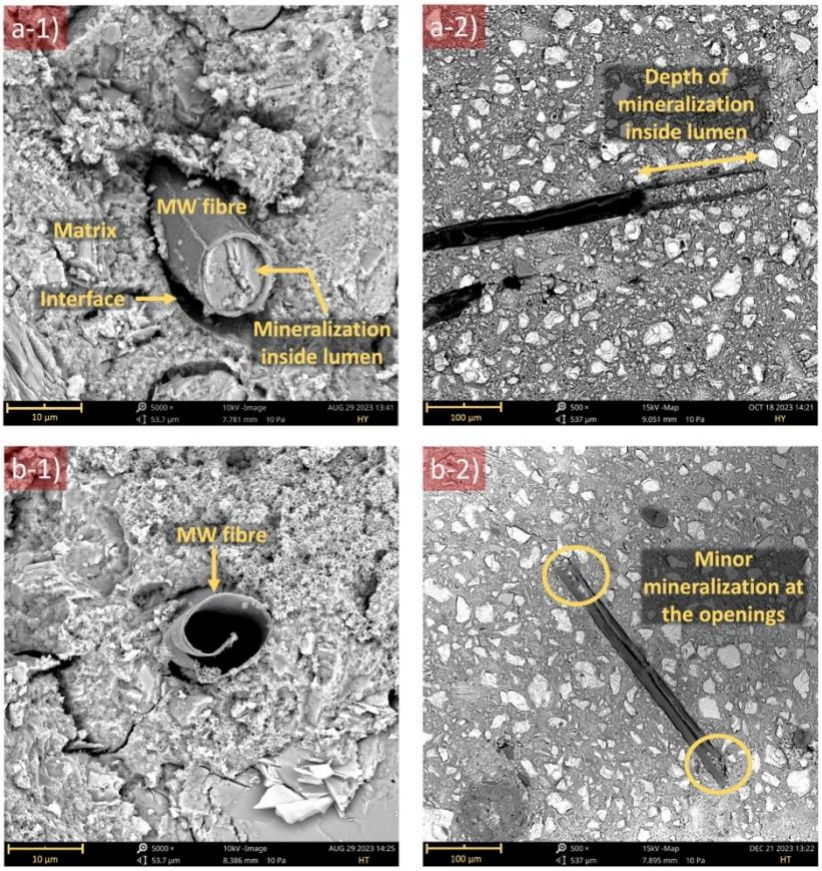

Figure 6.13. SEM micrographs of the effect of a) hybrid treated (HY), and b) hydrothermally treated (HT) on the microstructure of cement paste samples after 7 days

Another significant characteristic observed in the micrographs is the degradation of all fibres after exposure to the cementitious matrix for 28 days. This phenomenon explains the lower observed 28-day flexural strength of MW-incorporated samples compared to their corresponding references. For the N and HT MW fibres, the alkaline attack due to the severe alkaline environment of the matrix led to the destruction of fibre integrity through alkali hydrolysis of hemicellulose and lignin. In contrast, HY MW fibres exhibited a different mechanism of degradation, namely mineralization through the growth of hydration products inside the lumen.

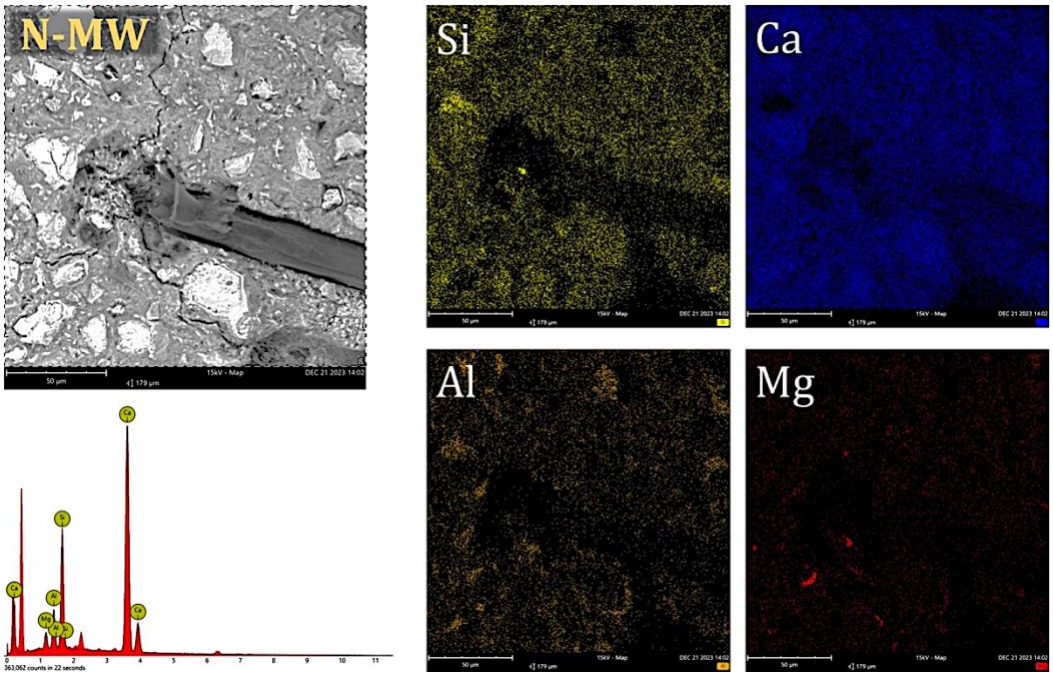

Figure 6.14. Elemental map by EDS of non-treated MW fibres in cement paste

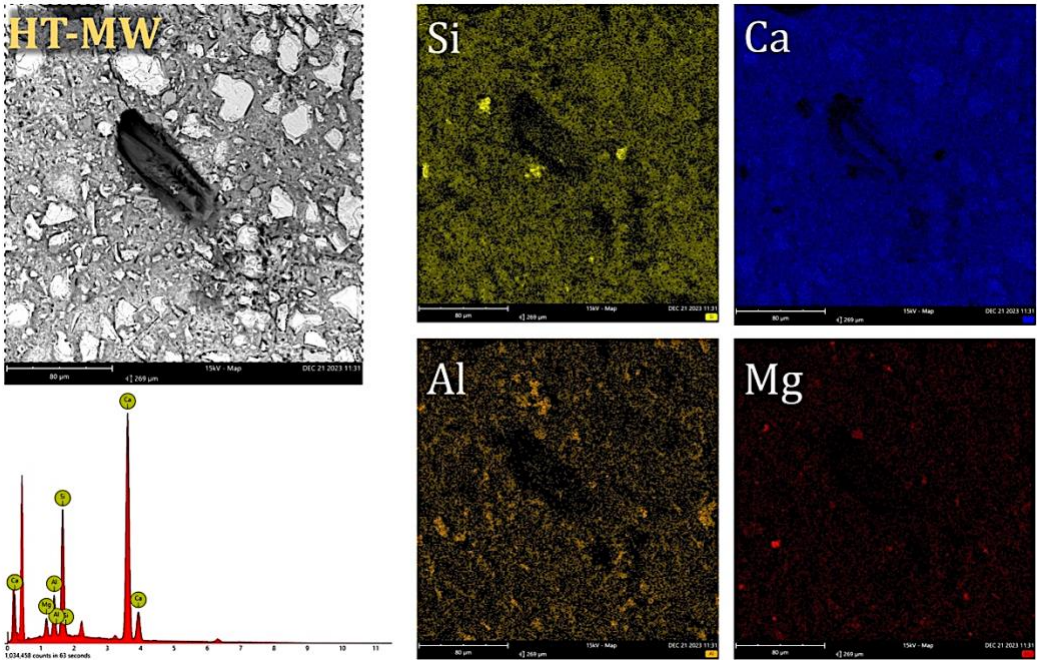

Figure 6.15. Elemental map by EDS of hydrothermally treated MW fibres in cement paste

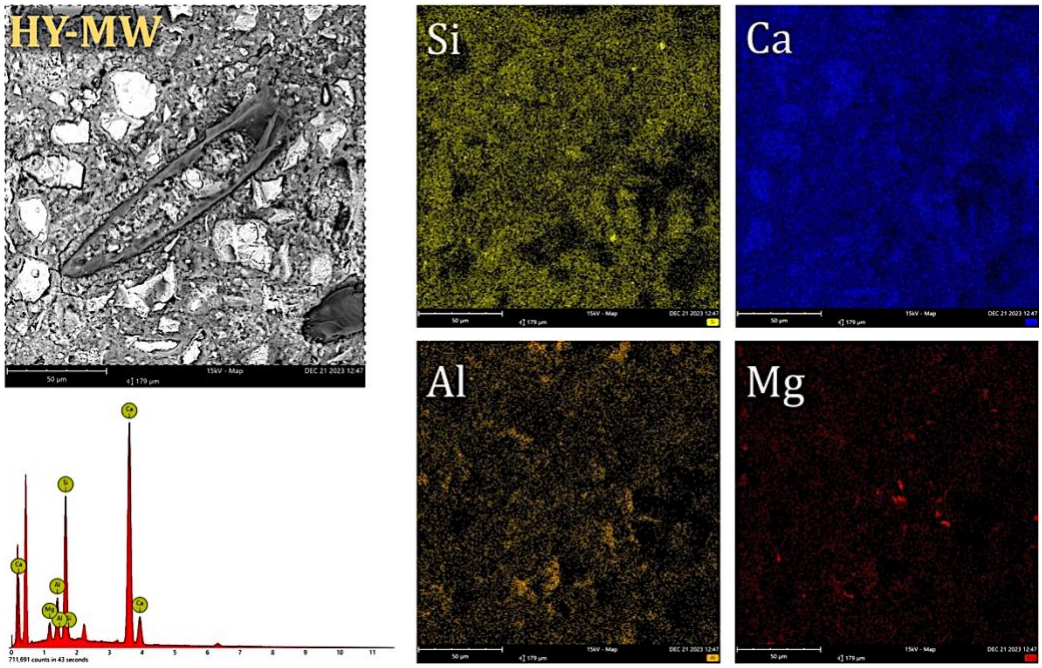

Figure 6.16. Elemental map by EDS of hybrid treated MW fibres in cement paste

Table 6.4. Elemental compositions analysis (atomic concentration) acquired based on Energy dispersive X-ray spectroscopy (EDS) from polished cement paste sample containing MW fibres after 28 days of hydration

Mixture	Al	Mg	Si	Ca	Al/Ca	Si/Ca
N	8.82	4.12	22.47	64.59	0.14	0.35
HT	8.91	4.45	23.32	63.33	0.14	0.37
HY	8.93	4.16	25.98	60.93	0.15	0.43

6.6 Conclusions

The incorporation of pre-treated MW fibres was shown to effectively reduce autogenous shrinkage in mortar samples. This reduction is primarily attributed to their role as water reservoirs, releasing entrained water during the self-desiccation process and maintaining high internal relative humidity in the cementitious matrix. The pre-treated MW fibres i.e., the HT and HY samples, exhibited superior performance, demonstrating reductions of 28% and 26% at 7 days compared to their

corresponding reference samples, respectively. These results are particularly promising when contrasted with other lignocellulosic materials used in higher dosages but showing less effectiveness in reducing autogenous shrinkage. This efficacy is mainly linked to the extremely wide cavity of MW fibres, which serves as a reservoir for internal curing water.

It was also observed that lignin within the structure of MW fibres plays a critical role in the development of drying shrinkage in natural fibre-incorporated cementitious samples. Indeed, the presence of lignin in the HT sample was shown to have a positive effect in controlling drying shrinkage while also exhibiting higher flexural strength. In contrast, it was shown that removing lignin resulted in greater hydrophilicity of HY MW fibres, leading to the migration of cement products into the fibre lumen. This mineralization formed an extensive integrated network for moisture transport by connecting to the capillary pores, microcracks, and macrocracks, ultimately exacerbating drying shrinkage behaviour. The higher occurrence of microcracks induced by severe drying shrinkage in turn diminished the flexural strength of the HY sample at later ages.

Moreover, incorporating MW fibres led to a slight reduction in the 7-day compressive strength of mortars incorporating the HT-MW fibres, whereas it did not significantly alter the strength for the HY samples. However, the internal curing role of both pre-treated MW fibres (i.e., HT and HY) resulted in almost identical compressive strength as the reference sample as internal curing enhanced in the later stages.

In conclusion, this study demonstrated the potential of using pre-treated MW fibres as internal curing agents to effectively reduce autogenous shrinkage, with minimal compromise in terms of the compressive strength of cementitious composites.

Chapter 7 Synthesis, Integration and General Discussion of Results

Finding economically viable and environmentally friendly superabsorbent materials for internal curing of low w/b cementitious mixes is gaining importance in the drive toward sustainability. The use of such materials extends beyond construction applications, encompassing diverse markets such as personal hygiene, biomedical products, meat packaging, waste treatment, agriculture water conservation, and water purification. Natural hollow fibres present a practical solution sourced from renewable resources, offering advantages like availability, abundance, and affordability. This study specifically focused on MW hollow fibres, found abundantly in roadside areas, fields, meadows, and waste zones. The distinctive morphology of these fibres enables them to store water within their extremely wide lumens, serving as efficient water reservoirs. This provides a sustainable option for internal curing of low w/b cementitious mixes, which are susceptible to self-desiccation. However, fibre pre-treatment is essential not only to enhance their hygroscopic behaviour but also to improve compatibility with the cementitious matrices they are incorporated into. Hydrothermal treatment and alkaline treatment are cost-effective and environmentally friendly methods capable of enhancing the hygroscopic properties and compatibility of lignocellulosic fibres. Therefore, this research investigated the internal curing efficacy of the HT-MW fibres and HY-MW fibres (undergoing additional alkaline treatment alongside hydrothermal treatment) in four phases.

To gain a comprehensive understanding of the behaviour of MW fibres and their overarching impact on the properties of cementitious mixes, this chapter consolidates and discusses the results obtained from all four technical papers. In the initial stage outlined in Chapter 3, a comprehensive investigation was conducted into the impact of fibre length and different pre-treatment methods on the hygroscopic properties. Furthermore, a detailed examination of the morphological changes

and the chemical composition of MW fibres after each pre-treatment was undertaken. The primary goals of this phase were twofold: (1) To understand whether a particular pre-treatment strategy demonstrate superior hygroscopic properties compared to others. (2) To investigate the influence of fibre size on the relative hygroscopic performance of these fibres. In the second phase (Chapter 4), the influence of different pre-treated MW fibres and their dosage on the effective w/b and the hydration process of cement paste was studied. The specific objectives of this phase included: (1) Determining the effective w/b of each cement mix after the incorporation of MW fibres. (2) Assessing whether specific pre-treated MW fibres enhance or hinder the degree of hydration in cementitious mixes. (3) Investigating the impact of fibre dosage on the hydration properties of cementitious mixes at early-ages. In the third phase (Chapter 5), the study investigated the kinetics of water transport between the pre-saturated MW fibres and the PC pastes. The primary objective was to determine how morphological features and chemical composition impact the internal curing, specifically focusing on the water desorption behaviour of fibres within the cementitious matrix. The fourth phase (Chapter 6), focused on evaluating the effectiveness of different pre-treated MW fibres in mitigating drying and autogenous shrinkage of low w/b mixes. Additionally, it involved an examination of compressive strength, flexural strength and microstructural development in internally cured cementitious composites.

A detailed examination of the morphological changes and chemical composition of MW fibres resulting from each pre-treatment was performed using SEM, BET, FTIR, and XRD techniques.

All tests were conducted on GU PC paste, with the exception of assessments related to mechanical properties and shrinkage, which were carried out on cement mortar using standard sand. Furthermore, a thorough analysis of the impact of MW fibres on the evolution of hydration products and microstructure of cement mixes was undertaken using TGA/DTG, XRD, and SEM.

The integration of ^{1}H NMR with DSC allowed for a comprehensive analysis of water transport kinetics during the early stages of hydration in cement pastes. The key findings of this research are synthesized and discussed in the following sections.

7.1 Study of characteristics of pre-treated MW fibres

The results revealed a hollow structure with a smooth surface for the N-MW fibres, featuring some protrusions indicative of wax debris. Following the hydrothermal treatment, these protrusions were eliminated, resulting in a smoother surface with reduced protrusions in the HT-MW fibres. This process effectively removed waxes, pectin, and impurities, demonstrating that hydrothermal treatment was a simple and non-aggressive approach that did not significantly impact the morphology of MW fibres, allowing them to retain their hollow structure. However, a drastic alteration in the morphological characteristics of MW fibres was observed after the HY treatment. This treatment led to the removal of lignin and hemicellulose, causing the collapse of the hollow structure and the formation of defects and holes on the fibre wall. Moreover, it was seen that both pre-treatments were able to enhance the water absorption rate of the fibres by removing the hydrophobic extractive components. Furthermore, the HT-MW fibres exhibited a superior water retention property when compared to the two other fibre types (i.e., NT and HY). This improvement was linked to their enhanced hydrophilicity and the preservation of their intact hollow structure. Additionally, it was noted that an increase in the length of the fibres correlated with a higher absorption capacity and improved water retention compared to the MW fibres with shorter lengths. However, the easier dispersion of shorter fibres in cementitious mixes presented a significant advantage over using the longer fibres. This facilitated more uniform distribution and integration within cement mixes, preventing any possible agglomeration and enhancing the overall performance of the final internally cured cementitious mixes.

7.2 Study of properties of cementitious mixes after incorporating MW fibres

7.2.1 Effective w/b

The introduction of MW fibres to PC paste resulted in a shift in their effective w/b to lower values. This occurred because of the absorption action of MW fibres during the pre-saturating of the fibres prior to adding them to the cement paste. The amount of entrained w/b ranged from 0.01 to 0.02, resulted from incorporation of 0.1% to 0.2% wt. of MW fibres.

7.2.2 Internal Curing Effect

The introduction of 0.1% HY- and HT-MW fibres into cementitious mixes yielded an improved degree of hydration of 14% and 17%, respectively. This was achieved by supplying of an adequate amount of free water for the initial cement hydration reaction and entrained water in the lumen of MW fibres for subsequent internal curing. A critical distinction between the HT-MW and HY-MW fibres emerged in their impact on hydration kinetics. The former displayed a gradual enhancement in hydration due to the steady release of stored water in the lumen, while the latter resulted in a prompt hydration reaction without any retardation. Despite the unregulated hydration kinetics caused by the HT-MW fibres during the first hours, their enhanced hydrophilicity and water retention property led to superior performance in terms of internal curing.

7.2.3 Effect of fibre dosage

It was observed that using 0.1% MW fibres resulted in superior internal curing performance compared to using 0.2% MW fibres. The incorporation of an excessive quantity of MW fibres (0.2% wt.) harmed the development of the hydration process. This was linked to a notable decrease in the effective w/b and the agglomeration of fibres, hindering the access to entrained water and reducing the availability of free water crucial for the hydration process. Additionally, the presence

of an excess of MW fibres led to an augmented leaching of extractives, adding further hindrance to the overall hydration process.

7.2.4 Compatibility

The HY treatment of MW fibres was observed to successfully enhance their compatibility with the cementitious environment while minimally affecting the progression of hydration. However, the addition of the N- and HT-MW fibres led to unregulated hydration. The leaching of hemicellulose in the alkaline environment of the cement matrix played a pivotal role in influencing the hydration of C_3S. Notably, hemicellulose as the primary source of monomeric sugars, exhibited the most significant retarding effect on cement hydration. The delay in the hydration of cement particles was attributed to the formation of a semi-permeable organic layer around the cement grains or nucleation poisoning, resulting in a reduced rate of water osmosis to the cement grains. Furthermore, in the initial minutes of hydration, it was observed that sugars and their degradation by-products, resulting from the alkali hydrolysis of waxes and pectin, reacted with C_3A. This reaction increased ion concentrations in the pore solution, which accelerated the dissolution rate of C_3A. Consequently, the rate of hydration significantly increased within the first few minutes in the N-MW fibres.

7.2.5 Microstructure development

The existence of lignin within the structure of MW fibres was found to exert a notable impact on the development of the microstructure. In both the NT- and HT-MW fibres, the presence of lignin along their walls served as a hindrance to the penetration and precipitation of calcium-rich minerals within the lumen of the fibres. However, in the HY-MW fibres, where a significant portion of hemicellulose and lignin had been removed, the ingress and formation of hydration products, primarily calcium hydroxide (CH), within the lumen of the fibres was observed.

7.2.6 Water transport between fibres and the cement matrix

The presence of a 3rd peak in the T_2 range of 19.9–76.33 ms in MW-incorporated cement pastes, served as evidence for internal curing water stored within the wide lumen of MW fibres. The lumens of MW fibres acted as water reservoirs, supplying internal curing water for 6-12 hours. Based on the NMR and DSC results, it was observed that both the morphological features and the presence of extractives such as lignin can impact the kinetics of entrained water transport from MW fibres to cementitious matrices. The presence of holes and defects on the wall of HY-MW fibres resulted in higher mobility of entrained water (i.e., longer T_2) compared to other types of MW fibres. In addition, these morphological defects led to quicker depletion of water and lower proton concentration in NMR analyses. Besides, lignin was shown to have a key role in the kinetics of water transport from MW fibres to the cement paste. Lignin acted as a barrier, preventing mineralization and thereby protecting the entrained water stored inside the lumen in N- and HT-MW fibres. However, the absence of lignin in HY-MW fibres led to the migration of hydration products into the lumen and early consumption of their entrained water. Overall, the HT-MW fibres, with their preserved hollow morphology and enhanced hydrophilicity, demonstrated effective performance, showing the highest amount of available internal curing water due to their superior water retention.

7.2.7 Autogenous shrinkage

The N-MW fibres exhibited minimal changes in autogenous shrinkage strains of cement mortars. In comparison to other lignocellulosic fibres, the pre-treated MW fibres (i.e., HT and HY) demonstrated a significantly effective impact on reducing autogenous shrinkage considering their low dosage. These reductions, measured at 28% and 26% at 7 days for the HT and HY samples, respectively, showed the role of internal curing by the MW fibres in mitigating capillary pore

emptying during the hydration of cement, thereby effectively reducing autogenous shrinkage in cement mortars. A comparison of autogenous shrinkage between HT-MW and HY-MW fibres exhibited the superior bridging effect of HT-MW fibres. Their lower susceptibility to mineralization and alkaline degradation (i.e., loss of integrity) resulted in less pronounced shrinkage compared to HY-MW fibres.

7.2.8 Drying shrinkage

It was observed that lignin within the structure of MW fibres played a critical role in the development of drying shrinkage in natural hollow fibre-incorporated cementitious samples. The presence of lignin in the N and HT samples had a positive effect on controlling drying shrinkage. In contrast, removing lignin resulted in greater hydrophilicity of the HY-MW fibres, leading to the migration of cement products into the fibre lumen. This mineralization formed an extensive integrated network for moisture transport to the surface by connecting to the capillary pores, microcracks, and macrocracks, ultimately worsening the drying shrinkage behaviour.

7.2.9 Compressive strength

It was observed that the NT-MW fibres led to a decrease in compressive strength at both 7-day and 28-day ages in comparison to its corresponding reference sample. For the HT MW fibres, the compressive strength exhibited a slight decrease at the 7-day age; however, by the 28-day age, it converged to its reference counterpart. On the contrary, the incorporation of the HY samples demonstrated almost identical compressive strengths to its reference sample at the 7- and 28-day ages. The initial addition of internal curing agents may cause a temporary reduction in compressive strength due to the formation of macro voids and the low densities of the added natural fibres, however, this drop was offset at later ages by the internal curing effect of the pre-treated MW fibres.

7.2.10 Flexural strength

The incorporation of both types of pre-treated MW fibres (i.e., the HT- and HY-MW fibres) yielded enhanced flexural strength compared to their respective reference samples, whereas the N sample maintained nearly identical flexural strength at the 7-day age. However, by the 28-day age, the inclusion of MW fibres led to a notable decrease across all types compared to their respective references. Among the pre-treated MW fibres, the HY-MW fibres exhibited slightly lower flexural strength. The higher occurrence of microcracks in the HY sample, induced by severe drying shrinkage at later ages, could act as stress risers and significantly diminish flexural strength. Moreover, the mineralization of lime within the lumen of HY-MW fibres led to increased fibre embrittlement, consequently reducing the flexural strength.

Chapter 8 Conclusions and Future Work

8.1 Conclusions

This PhD project investigated the potential of natural hollow fibres, specifically MW fibres, as superabsorbent materials for use as internal curing agents in low w/b mixes. The core idea was based on the extremely wide lumen of MW fibres, which was hypothesized to substantially improve their hygroscopic properties compared to other natural fibres, through capillary action.

The first phase of this study focused on understanding the hygroscopic behaviour of MW fibres after different treatment methods, forming the foundation for the project's next phase. Different pre-treatment techniques were tested, such as hydrothermal and hybrid treatments (which involved hydrothermal treatment followed by alkaline treatment). A challenge encountered in this phase was the fluffy nature and low density of MW fibres. These characteristics, linked to the hollowness and extremely thin walls of the fibres, posed difficulties in measuring hygroscopic properties. Thus, the common measurement standards used for superabsorbent materials were not applicable to MW fibres. Therefore, a new modified method was developed to overcome this obstacle, involving a stirring followed by a filtration method for measuring hygroscopic properties.

It was expected that the hybrid treatment would significantly improve hygroscopic properties due to the alkaline treatment—commonly reported in the literature as effective for enhancing hygroscopic properties. While the hybrid treatment enhanced water absorption, it compromised water retention due to morphological defects caused by the removal of lignin and hemicellulose. On the other hand, hydrothermal treatment showed outstanding water absorption and retention by removing waxes and pectin without compromising the hollow structure, as confirmed by FTIR and SEM examinations. It was also observed that the longer MW fibres had higher water absorption and retention properties. However, the main challenge with long MW fibres was their

difficulty in dispersing in water compared to the shorter fibres. Therefore, to avoid the consequences of fibres agglomeration within the cementitious matrix, it was decided to incorporate the MW fibres of shorter lengths.

Although absorption and desorption values in water provided insight into the relative hygroscopic properties of different pre-treated MW fibres, the key question remained about their behaviour in the cement matrix. The complexity of the cement pore solution, with its high alkalinity and changing ion composition, necessitated understanding the hygroscopic behaviour of MW fibres in a cementitious matrix. Due to the potential for MW fibres to agglomerate when mixed with dry cement powder, they were introduced in a pre-soak condition. Future studies could explore using dry fibres in mix designs after understanding their dispersion and hygroscopic behaviour in cementitious mixes. Comprehensive rheological measurements showed that the entrained w/b was reduced by 0.01 to 0.02, depending on the type and dosage of the pre-soaked fibres, closely matching the estimated absorption calculated in the initial step. The desorption kinetics of MW fibres within the cementitious mixes were also examined using ^{1}H-NMR relaxometry and DSC analyses. Relaxation time observations confirmed that the HT-MW fibres significantly improved water absorption and retention compared to other types of MW fibres. In contrast, HY-MW fibres with holes in their walls quickly deplete their entrained water due to the higher mobility of their stored water. The significant difference in desorption kinetics between the HT-MW and the HY-MW fibres was not solely due to morphological changes though. Comprehensive microstructural analyses revealed that the absence of lignin in the HY-MW fibres led to the migration of hydration products into the fibre cavity, diminishing its water retention behaviour in the cement matrix. On the other hand, the presence of lignin acted as a physical and chemical barrier, protecting the internal curing water stored within the cavity of the HT-MW fibres. The migration of hydration

products into the lumen of HY-MW fibres also had adverse effects on drying shrinkage and flexural strength. This mineralization formed a network for moisture transport to the surface, connecting to capillary pores, microcracks, and macrocracks, worsening drying shrinkage behaviour and negatively impacting the flexural strength of the HY-MW fibres incorporated samples.

The calorimetry results showed that introducing 0.1% wt. HY- and HT-MW fibres into cementitious mixes promoted a degree of hydration up to 17%. However, an excessive dosage of MW fibres (0.2% wt.) had an adverse impact on hydration. This was due to higher leaching of extractives from the fibres and/or lower availability of free water for the initial cement hydration. The retentive behaviour of the HT-MW fibres was also observed in the calorimetry results. The HT-MW fibres gradually improved hydration by slowly releasing the internal curing water, while the HY-MW fibres caused a prompt hydration reaction without retardation. Despite unregulated early hydration kinetics, the HT-MW fibres exhibited superior internal curing performance at later ages. This distinction was also seen in the compressive strength of mortar specimens. The HY samples had almost identical compressive strengths to their reference samples at 7 days. In contrast, the HT samples' compressive strength converged to their reference counterpart later, at 28 days. In the final step, it was observed that the pre-treated MW fibres (HT-MW and HY-MW) showed substantial reductions in autogenous shrinkage strains up to 28% at 7-day. This demonstrated the effectiveness of internal curing water released by pre-treated MW fibres.

The comprehensive analysis and findings of this study supported the feasibility of using MW fibres as sustainable internal curing agents to effectively reduce autogenous shrinkage, particularly after applying a straightforward, cost-effective, and low-carbon footprint hydrothermal pre-treatment method. Incorporating MW fibres into the production of internally cured cementitious mixes offers

several practical advantages. Firstly, they provide a sustainable and cost-effective alternative to SAP, helping reduce the construction industry's carbon footprint. By transforming non-usable waste—often burned or dumped—into valuable products, this process not only reduces waste but also provides farmers with additional income. The promising hygroscopic properties of MW fibres suggest potential applications as superabsorbents in other industries, such as personal hygiene (e.g., diapers), biomedical products (e.g., bandages, surgical sponges), meat packaging, waste treatment, and water conservation in agriculture. Furthermore, developing MW fibre-based products could help preserve monarch butterflies, declared endangered in Canada in 2023, by encouraging the growth of milkweed plants and ensuring sufficient habitat for these butterflies.

8.2 Recommendation for future work

- To Examine the hygroscopic properties of MW fibres in the cement pore solution, with a particular focus on different chemical compositions, variations in pH, as well as ionic concentration.
- To study the internal curing efficacy of MW fibres in low w/b mixes, involving the incorporation of pozzolanic materials and supplementary cementitious materials.
- To examine the potential for enhancing the dispersion of long MW fibres and the feasibility of using them as retentive internal curing agents in mitigating autogenous shrinkage of low w/b mixes.
- To study the internal curing efficacy of MW fibres in combination with external curing practices such as water ponding.
- To investigate the efficiency and behaviour of MW fibres as internal curing agents in mitigating autogenous shrinkage in blended cement mixtures and alkali-activated mixtures,

given their significantly higher chemical shrinkage compared to mixtures based on ordinary PC.

- To examine the migration distance of water released by MW fibres to cementitious matrix by 3D microstructural models, neutron and X-ray tomography.
- To assess the temporal distribution of the internal curing water stored within MW fibres inside cementitious matrix using magnetic resonance imaging (MRI).

Appendix

The table below shows the IR peak regions of different components of lignocellulosic fibres.

Table AP.1. Characteristic IR peaks of lignocellulosic fibres adopted from [25,329,330]

Peak zone (cm^{-1})	**Approx. peak in MW fibre (cm^{-1})***	**Assignment**	**Possible Components**	**Predominant bond**
3400-3200	3338	O-H stretching	Hydroxyl group of cellulose, hemicellulose and waxes Phenolic and aliphatic hydroxyl groups of lignin Ref. [331–333]	Cellulose [227]
2920-2800	2916 and 2850	C-H stretching	Aliphatic and alkyl compounds of cellulose Methyl groups of hemicellulose Methoxyl groups of lignin and methylene groups of waxes Ref. [331–333]	Wax [25]
1800-1720	1735	C = O stretching	Carbonyl ester and carboxyl of carboxylic acid of hemicellulose Carbonyl aldehyde or ketone, and carboxyl of carboxylic acid of lignin Carboxyl ester of pectin and carbonyl ester of waxes Ref. [334–336]	Hemicellulose [227]
1650-1630	-	OH (Water)	Water [25]	-
1600-1500	1595 and 1505	C = O aromatic	Lignin	Lignin [25]
1500-1300	1420, 1362 and 1313	CH_2	Lignin	Lignin [25]
		C-H bending	Cellulose, hemicellulose and lignin	-
1280-1150	1238 and 1155	C-O-C stretching	Hemicellulose, cellulose, and lignin, pectin, waxes [227,243,330,331,337]	Lignin [25]
		C-C stretching	Aromatic ring of lignin [338]	
1100-900	1035	C-O stretching and deformation	Alcohol groups of cellulose [227], Aliphatic alcohols and ethers of lignin [336], and Pectin [339]	Cellulose [227]
900-800	895	C-O-C	Amorphous cellulose [25]	Amorphous cellulose [25]
	-	C–H out-of-plane bending	Aromatic hydrogen of lignin [227,338]	Lignin [337]

* Found in this study

Table AP.2. and Table AP.3. show the statistical analyses of results found in water absorption capacity and water release rate tests, respectively.

Table AP.2. Statistical contrasts between each pair of groups in water absorption capacity (AC) measurements for different immersion durations

MW fibres Size	Group 1	Group 2	P-value		
			5 minutes	30 minutes	60 minutes
L60	Hydrothermal	Non-treated	0.000001 (S)	0.004225 (S)	0.043388 (S)
	Hybrid	Non-treated	0.000021 (S)	0.000164 (S)	0.006116 (S)
	Hydrothermal	Hybrid	0.046009 (S)	0.007406 (S)	0.002122 (S)
S60	Hydrothermal	Non-treated	0.067420 (NS)	0.082618 (NS)	0.000033 (S)
	Hybrid	Non-treated	0.023748 (S)	0.137134 (NS)	0.187433 (NS)
	Hydrothermal	Hybrid	0.104789 (NS)	0.322094 (NS)	0.140293 (NS)

S: Significant, NS: Not-significant

Table AP.3. Statistical contrasts between each pair of groups in water release rate (WRR) measurements for different immersion durations

MW fibres Size	Group 1	Group 2	P-value		
			5 minutes	30 minutes	60 minutes
L60	Hydrothermal	Non-treated	0.002184 (S)	0.008475 (S)	0.018302 (S)
	Hybrid	Non-treated	0.184782 (NS)	0.272413 (NS)	0.425001 (NS)
	Hydrothermal	Hybrid	0.026686 (S)	0.032164 (S)	0.026561 (S)
S60	Hydrothermal	Non-treated	0.084300 (NS)	0.136703 (NS)	0.052336 (NS)
	Hybrid	Non-treated	0.387131 (NS)	0.484063 (NS)	0.192927 (NS)
	Hydrothermal	Hybrid	0.131971 (NS)	0.113875 (NS)	0.246719 (NS)

S: Significant, NS: Not-significant

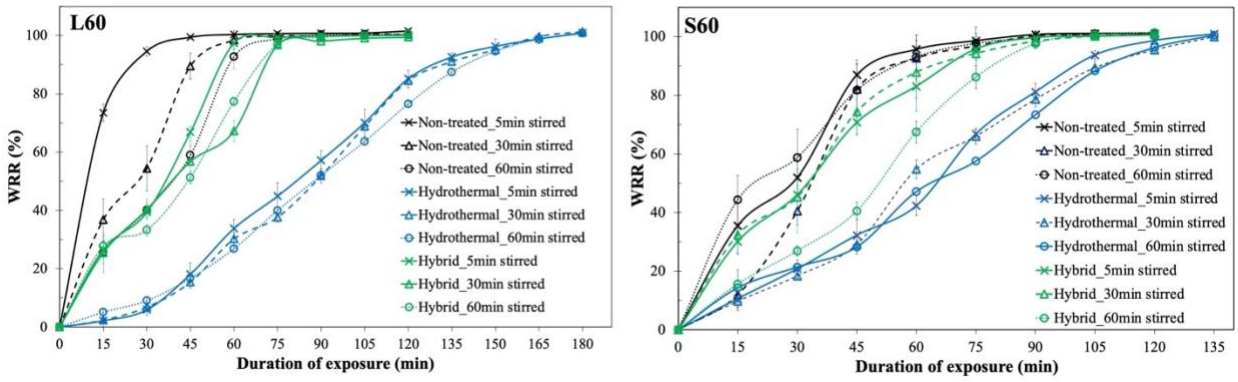

Figure AP.1. Effect of pre-treatments on the water release rate of milkweed fibre after various durations of stirring, for size gradation of L60 (left) and S60 (right)

References

[1] W. Li, M. Fall, Strength and self-desiccation of slag-cemented paste backfill at early ages: Link to initial sulphate concentration, Cem. Concr. Compos. 89 (2018) 160–168. https://doi.org/https://doi.org/10.1016/j.cemconcomp.2017.09.019.

[2] G. Fagerlund, Self-desiccation and its importance in concrete technology : proceedings of the Second International Research Seminar in Lund, June 18, 1999, Division of Building Materials, LTH, Lund University, 1999.

[3] Z. Jiang, Z. Sun, P. Wang, Internal relative humidity distribution in high-performance cement paste due to moisture diffusion and self-desiccation, Cem. Concr. Res. 36 (2006) 320–325. https://doi.org/10.1016/j.cemconres.2005.07.006.

[4] M. Pathirage, D.P. Bentz, G. Di Luzio, E. Masoero, G. Cusatis, The ONIX model: a parameter-free multiscale framework for the prediction of self-desiccation in concrete, Cem. Concr. Compos. 103 (2019) 36–48. https://doi.org/https://doi.org/10.1016/j.cemconcomp.2019.04.011.

[5] A. Jamali, J. Mendes, B. Nagaratnam, M. Lim, A new four stage model of capillary pressure in early age concrete: Insights from high capacity tensiometers, Cem. Concr. Res. 161 (2022) 106955. https://doi.org/10.1016/j.cemconres.2022.106955.

[6] P.C. Ai'tcin, Durable concrete-current practice and future trends, Am. Concr. Institute, ACI Spec. Publ. SP-144 (1994) 85–104. https://doi.org/10.14359/4488.

[7] L. Montanari, P. Suraneni, M.T. Chang, C. Villani, J. Weiss, Absorption and desorption of superabsorbent polymers for use in internally cured concrete, Adv. Civ. Eng. Mater. 7 (2018). https://doi.org/10.1520/ACEM20180008.

[8] J. Liu, C. Shi, X. Ma, K.H. Khayat, J. Zhang, D. Wang, An overview on the effect of internal curing on shrinkage of high performance cement-based materials, Constr. Build. Mater. 146 (2017) 702–712. https://doi.org/10.1016/j.conbuildmat.2017.04.154.

[9] J. Justs, M. Wyrzykowski, D. Bajare, P. Lura, Internal curing by superabsorbent polymers in ultra-high performance concrete, Cem. Concr. Res. 76 (2015) 82–90. https://doi.org/10.1016/j.cemconres.2015.05.005.

[10] J.T. Kevern, Q.C. Nowasell, Internal curing of pervious concrete using lightweight aggregates, Constr. Build. Mater. 161 (2018) 229–235. https://doi.org/10.1016/j.conbuildmat.2017.11.055.

[11] J. Liu, N. Farzadnia, C. Shi, Microstructural and micromechanical characteristics of ultra-high performance concrete with superabsorbent polymer (SAP), Cem. Concr. Res. 149 (2021) 106560. https://doi.org/10.1016/j.cemconres.2021.106560.

[12] Z. He, A. Shen, Y. Guo, Z. Lyu, D. Li, X. Qin, M. Zhao, Z. Wang, Cement-based materials modified with superabsorbent polymers: A review, Constr. Build. Mater. 225 (2019) 569–590. https://doi.org/10.1016/j.conbuildmat.2019.07.139.

[13] D.P. Bentz, W.J. Weiss, Internal Curing : A 2010 State-of-the- Art Review, Civ. Eng. (2011).

[14] F. Ai, X. Yin, R. Hu, H. Ma, W. Liu, Research into the super-absorbent polymers on agricultural water, Agric. Water Manag. 245 (2021) 106513. https://doi.org/10.1016/j.agwat.2020.106513.

[15] F. Esposito, M.A. Del Nobile, G. Mensitieri, L. Nicolais, Water sorption in cellulose-based hydrogels, J. Appl. Polym. Sci. 60 (1996) 2403–2408. https://doi.org/10.1002/(SICI)1097-4628(19960627)60:13<2403::AID-APP12>3.0.CO;2-5.

[16] H. Liu, Y. Bu, J.G. Sanjayan, A. Nazari, Z. Shen, Suitability of polyacrylamide superabsorbent polymers as the internal curing agent of well cement, Constr. Build. Mater. 112 (2016) 253–260. https://doi.org/10.1016/j.conbuildmat.2016.02.217.

[17] L. Senff, R.C.E. Modolo, G. Ascensão, D. Hotza, V.M. Ferreira, J.A. Labrincha, Development of mortars containing superabsorbent polymer, Constr. Build. Mater. 95 (2015) 575–584. https://doi.org/10.1016/j.conbuildmat.2015.07.173.

[18] F. Nnadi, C. Brave, Environmentally friendly superabsorbent polymers for water conservation in agricultural lands, J. Soil Environ. Manag. 2 (2011) 206–211.

[19] D.P. Bentz, S.Z. Jones, M.A. Peltz, P.E. Stutzman, Mitigation of autogenous shrinkage in repair mortars via internal curing, Concr. Aust. 41 (2015) 35–39.

[20] V. Zanjani Zadeh, C.P. Bobko, Nano-mechanical properties of internally cured kenaf fiber reinforced concrete using nanoindentation, Cem. Concr. Compos. 52 (2014) 9–17. https://doi.org/10.1016/j.cemconcomp.2014.04.002.

[21] G.W. Lee, Y.C. Choi, Effect of abaca natural fiber on the setting behavior and autogenous shrinkage of cement composite, J. Build. Eng. 56 (2022) 104719. https://doi.org/10.1016/j.jobe.2022.104719.

[22] P. Jongvisuttisun, J. Leisen, K.E. Kurtis, Key mechanisms controlling internal curing

performance of natural fibers, Cem. Concr. Res. 107 (2018) 206–220. https://doi.org/10.1016/j.cemconres.2018.02.007.

[23] P. Jongvisuttisun, C. Negrello, K.E. Kurtis, Effect of processing variables on efficiency of eucalyptus pulps for internal curing, Cem. Concr. Compos. 37 (2013) 126–135. https://doi.org/10.1016/j.cemconcomp.2012.11.006.

[24] T. Just., J.M. Fogg, Weeds of Lawn and Garden. A Handbook for Eastern Temperate North America., University of Pennsylvania Press, 1945. https://doi.org/10.2307/2421121.

[25] C. Richard, P. Cousin, Mr. Foruzanmehr, S. Elkoun, M. Robert, Characterization of components of milkweed floss fiber, Sep. Sci. Technol. 54 (2019) 3091–3099. https://doi.org/10.1080/01496395.2018.1556691.

[26] J.Y.F. Dréan, J.J. Patry, G.F. Lombard, M. Weltrowski, Mechanical Characterization and Behavior in Spinning Processing of Milkweed Fibers, Text. Res. J. 63 (1993) 443–450. https://doi.org/10.1177/004051759306300803.

[27] T.T. Lim, X. Huang, Evaluation of kapok (Ceiba pentandra (L.) Gaertn.) as a natural hollow hydrophobic-oleophilic fibrous sorbent for oil spill cleanup, Chemosphere. 66 (2007) 955–963. https://doi.org/10.1016/j.chemosphere.2006.05.062.

[28] J.C. Sakthivel, S. Mukhopadhyay, N.K. Palanisamy, Some studies on Mudar fibers, J. Ind. Text. 35 (2005) 63–76. https://doi.org/10.1177/1528083705053390.

[29] L. Boulos, M.R. Foruzanmehr, A. Tagnit-Hamou, M. Robert, The effect of a zirconium dioxide sol-gel treatment on the durability of flax reinforcements in cementitious composites, Cem. Concr. Res. 115 (2019) 105–115. https://doi.org/10.1016/j.cemconres.2018.10.004.

[30] F.D. Tolêdo Romildo D., K. Ghavami, G.L. England, K. Scrivener, Development of vegetable fibre-mortar composites of improved durability, Cem. Concr. Compos. 25 (2003) 185–196. https://doi.org/10.1016/S0958-9465(02)00018-5.

[31] P.R.L. Lima, H.M. Santos, G.P. Camilloto, R.S. Cruz, Effect of surface biopolymeric treatment on sisal fiber properties and fiber-cement bond, J. Eng. Fiber. Fabr. 12 (2017) 59–71. https://doi.org/10.1177/155892501701200207.

[32] O.E. Gjørv, High-strength concrete, in: S.B.T.-D. in the F. and R. of C. (Second E. Mindess (Ed.), Dev. Formul. Reinf. Concr., Woodhead Publishing, 2019: pp. 153–170. https://doi.org/10.1016/B978-0-08-102616-8.00007-1.

[33] T.C. RILEM, 181-EAS, Early Age Crack. Cem. Syst. RILEM Tech. Comm. TC. (2002).

[34] R. Dávila-Pompermayer, L.G. Lopez-Yepez, P. Valdez-Tamez, C.A. Juárez, A. Durán-Herrera, Lechugilla natural fiber as internal curing agent in self compacting concrete (SCC): Mechanical properties, shrinkage and durability, Cem. Concr. Compos. 112 (2020) 103686. https://doi.org/10.1016/j.cemconcomp.2020.103686.

[35] T.C. Powers, J.C. Copeland, H.M. Mann, Capillary Continuity or Discontinuity in Cement Pastes, 1959.

[36] E.E. Holt, Early age autogenous shrinkage of concrete, University of Washington, 2001.

[37] L. Barcelo, M. Moranville, B. Clavaud, Autogenous shrinkage of concrete: A balance between autogenous swelling and self-desiccation, Cem. Concr. Res. 35 (2005) 177–183. https://doi.org/10.1016/j.cemconres.2004.05.050.

[38] J. Kheir, B. Hilloulin, A. Loukili, N. De Belie, Chemical shrinkage of low water to cement (W/c) ratio cem i and cem iii cement pastes incorporating silica fume and filler, Materials (Basel). 14 (2021) 1–13. https://doi.org/10.3390/ma14051164.

[39] D.P. Bentz, Internal curing of high-performance blended cement mortars, ACI Mater. J. 104 (2007) 408–414. https://doi.org/10.14359/18831.

[40] ACI Committee, ACI (308-213) Report on Internally Cured Concrete Using Prewetted Absorptive Lightweight Aggregate, Am. Concr. Inst. 28 (2015) 0–15.

[41] O.M. Jensen, P.F. Hansen, Autogenous deformation and RH-change in perspective, Cem. Concr. Res. 31 (2001) 1859–1865. https://doi.org/10.1016/S0008-8846(01)00501-4.

[42] X. Feng, D.P. Bentz, P.E. Stutzman, Experimental studies of portland cement/slag hydration, in: Present. 102nd Annu. Meet. Am. Ceram. Soc. St. Louis, Mo, 2000.

[43] J. Weiss, D. Bentz, S. Anton, P. Lura, Constructing More Robust Concrete, Struct. Mag. Intern. Curing. (2012) 10.

[44] X. Ma, J. Liu, C. Shi, A review on the use of LWA as an internal curing agent of high performance cement-based materials, Constr. Build. Mater. 218 (2019) 385–393. https://doi.org/10.1016/j.conbuildmat.2019.05.126.

[45] G.R. de Sensale, A.F. Goncalves, Effects of Fine LWA and SAP as Internal Water Curing Agents, Int. J. Concr. Struct. Mater. 8 (2014) 229–238. https://doi.org/10.1007/s40069-014-0076-1.

[46] R. Henkensiefken, Internal curing in cementitious systems made using saturated lightweight

aggregate., PhD Diss. Univ. (2008).

[47] P. Trtik, B. Münch, W.J. Weiss, A. Kaestner, I. Jerjen, L. Josic, E. Lehmann, P. Lura, Release of internal curing water from lightweight aggregates in cement paste investigated by neutron and X-ray tomography, Nucl. Instruments Methods Phys. Res. Sect. A Accel. Spectrometers, Detect. Assoc. Equip. 651 (2011) 244–249. https://doi.org/10.1016/j.nima.2011.02.012.

[48] J. Castro, L. Keiser, M. Golias, J. Weiss, Absorption and desorption properties of fine lightweight aggregate for application to internally cured concrete mixtures, Cem. Concr. Compos. 33 (2011) 1001–1008. https://doi.org/10.1016/j.cemconcomp.2011.07.006.

[49] J. Liu, C. Shi, N. Farzadnia, X. Ma, Effects of pretreated fine lightweight aggregate on shrinkage and pore structure of ultra-high strength concrete, Constr. Build. Mater. 204 (2019) 276–287. https://doi.org/10.1016/j.conbuildmat.2019.01.205.

[50] V. Mechtcherine, M. Gorges, C. Schroefl, A. Assmann, W. Brameshuber, A.B. Ribeiro, D. Cusson, J. Custódio, E.F. Da Silva, K. Ichimiya, S.I. Igarashi, A. Klemm, K. Kovler, A.N. De Mendonça Lopes, P. Lura, V.T. Nguyen, H.W. Reinhardt, R.D.T. Filho, J. Weiss, M. Wyrzykowski, G. Ye, S. Zhutovsky, Effect of internal curing by using superabsorbent polymers (SAP) on autogenous shrinkage and other properties of a high-performance fine-grained concrete: Results of a RILEM round-robin test, Mater. Struct. Constr. 47 (2014) 541–562. https://doi.org/10.1617/s11527-013-0078-5.

[51] P. Zhong, Z. Hu, M. Griffa, M. Wyrzykowski, J. Liu, P. Lura, Mechanisms of internal curing water release from retentive and non-retentive superabsorbent polymers in cement paste, Cem. Concr. Res. 147 (2021) 106494. https://doi.org/10.1016/j.cemconres.2021.106494.

[52] H.X.D. Lee, H.S. Wong, N.R. Buenfeld, Effect of alkalinity and calcium concentration of pore solution on the swelling and ionic exchange of superabsorbent polymers in cement paste, Cem. Concr. Compos. 88 (2018) 150–164. https://doi.org/10.1016/j.cemconcomp.2018.02.005.

[53] J. Justs, M. Wyrzykowski, F. Winnefeld, D. Bajare, P. Lura, Influence of superabsorbent polymers on hydration of cement pastes with low water-to-binder ratio: A calorimetry study, J. Therm. Anal. Calorim. 115 (2014) 425–432. https://doi.org/10.1007/s10973-013-3359-x.

[54] C. Schröfl, V. Mechtcherine, M. Gorges, Relation between the molecular structure and the

efficiency of superabsorbent polymers (SAP) as concrete admixture to mitigate autogenous shrinkage, Cem. Concr. Res. 42 (2012) 865–873. https://doi.org/10.1016/j.cemconres.2012.03.011.

[55] V. Mechtcherine, H.W. Reinhardt, RILEM State of the Art Reports 2" Application of Super Absorbent Polymers (SAP) in Concrete Construction", 2008). ACI SP-256, Intern. Curing High-Performance Concr. Lab. F. Exp. CDROM. Am. Concr. Institute. Neville, AI, Aïtcin, PC (1998). High Perform. Concr. Overview. Mater. Struct. 31 (2012) 111–117.

[56] X. Ma, Q. Yuan, J. Liu, C. Shi, Effect of water absorption of SAP on the rheological properties of cement-based materials with ultra-low w/b ratio, Constr. Build. Mater. 195 (2019) 66–74. https://doi.org/https://doi.org/10.1016/j.conbuildmat.2018.11.050.

[57] J. Liu, N. Farzadnia, K.H. Khayat, C. Shi, Effects of SAP characteristics on internal curing of UHPC matrix, Constr. Build. Mater. 280 (2021) 122530. https://doi.org/10.1016/j.conbuildmat.2021.122530.

[58] S.E. Chidiac, S.N. Mihaljevic, S.A. Krachkovskiy, G.R. Goward, Characterizing the effect of superabsorbent polymer content on internal curing process of cement paste using calorimetry and nuclear magnetic resonance methods, J. Therm. Anal. Calorim. 145 (2021) 437–449. https://doi.org/10.1007/s10973-020-09754-0.

[59] X. Huang, X. Liu, H. Rong, X. Yang, Y. Duan, T. Ren, Effect of Super-Absorbent polymer (SAP) Incorporation method on mechanical and shrinkage properties of internally cured concrete, Materials (Basel). 15 (2022) 7854.

[60] M.T. Hasholt, O.M. Jensen, K. Kovler, S. Zhutovsky, Can superabsorent polymers mitigate autogenous shrinkage of internally cured concrete without compromising the strength?, Constr. Build. Mater. 31 (2012) 226–230. https://doi.org/10.1016/j.conbuildmat.2011.12.062.

[61] M. Wyrzykowski, S.I. Igarashi, P. Lura, V. Mechtcherine, Recommendation of RILEM TC 260-RSC: using superabsorbent polymers (SAP) to mitigate autogenous shrinkage, Mater. Struct. Constr. 51 (2018) 1–7. https://doi.org/10.1617/s11527-018-1241-9.

[62] Y.C. Choi, Hydration and internal curing properties of plant-based natural fiber-reinforced cement composites, Case Stud. Constr. Mater. 17 (2022) e01690. https://doi.org/10.1016/j.cscm.2022.e01690.

[63] O. Onuaguluchi, N. Banthia, Plant-based natural fibre reinforced cement composites: A

review, Cem. Concr. Compos. 68 (2016) 96–108. https://doi.org/10.1016/j.cemconcomp.2016.02.014.

[64] O.A. Hisseine, A.F. Omran, A. Tagnit-Hamou, Influence of Cellulose Filaments on Cement Paste and Concrete, J. Mater. Civ. Eng. 30 (2018) 4018109. https://doi.org/10.1061/(asce)mt.1943-5533.0002287.

[65] B. Han, L. Zhang, J. Ou, Smart and multifunctional concrete toward sustainable infrastructures, Springer, 2017. https://doi.org/10.1007/978-981-10-4349-9.

[66] G. Espinoza-Hijazin, M. Lopez, Extending internal curing to concrete mixtures with W/C higher than 0.42, Constr. Build. Mater. 25 (2011) 1236–1242. https://doi.org/10.1016/j.conbuildmat.2010.09.031.

[67] R. Philleo, Concrete science and reality, Mater. Sci. Concr. II. (1991) 1–8.

[68] L. Bello, E. Garcia-Diaz, P. Rougeau, An original test method to assess water absorption/desorption of lightweight aggregates in presence of cement paste, Constr. Build. Mater. 154 (2017) 752–762. https://doi.org/10.1016/j.conbuildmat.2017.07.236.

[69] T. Knudsen, M. Geiker, Chemical shrinkage as an indicator of the stage of hardening, Proc. Int. Conf. Concr. Early Ages, Vol. I. (1982) 163–165.

[70] J. Zhang, Q. Wang, J. Zhang, Shrinkage of internal cured high strength engineered cementitious composite with pre-wetted sand-like zeolite, Constr. Build. Mater. 134 (2017) 664–672. https://doi.org/10.1016/j.conbuildmat.2016.12.182.

[71] W. Meng, K. Khayat, Effects of saturated lightweight sand content on key characteristics of ultra-high-performance concrete, Cem. Concr. Res. 101 (2017) 46–54. https://doi.org/10.1016/j.cemconres.2017.08.018.

[72] B. Akcay, M.A. Tasdemir, Effects of distribution of lightweight aggregates on internal curing of concrete, Cem. Concr. Compos. 32 (2010) 611–616. https://doi.org/10.1016/j.cemconcomp.2010.07.003.

[73] ASTM Committee C09.21, ASTM C1761-15 Standard Specification for Lightweight Aggregate for Internal Curing of Concrete, Annu. B. ASTM Stand. Vol. 04.02. (2015) 1–8.

[74] O.M. Jensen, P.F. Hansen, Water-entrained cement-based materials - I. Principles and theoretical background, Cem. Concr. Res. 31 (2001) 647–654. https://doi.org/10.1016/S0008-8846(01)00463-X.

[75] V. Mechtcherine, H.-W. Reinhardt, Application of Super Absorbent Polymers (SAP) in

Concrete Construction, Springer Science & Business Media, 2012. https://doi.org/10.1007/978-94-007-2733-5.

[76] A. Elsharief, M.D. Cohen, J. Olek, Influence of lightweight aggregate on the microstructure and durability of mortar, Cem. Concr. Res. 35 (2005) 1368–1376. https://doi.org/10.1016/j.cemconres.2004.07.011.

[77] P.K. Mehta, P.J.M. Monteiro, Concrete: microstructure, properties, and materials, McGraw-Hill Education, 2014.

[78] F. Agostini, C.A. Davy, F. Skoczylas, T. Dubois, Effect of microstructure and curing conditions upon the performance of a mortar added with Treated Sediment Aggregates (TSA), Cem. Concr. Res. 40 (2010) 1609–1619. https://doi.org/10.1016/j.cemconres.2010.07.003.

[79] K.M.A. Hossain, S. Ahmed, M. Lachemi, Lightweight concrete incorporating pumice based blended cement and aggregate: Mechanical and durability characteristics, Constr. Build. Mater. 25 (2011) 1186–1195. https://doi.org/10.1016/j.conbuildmat.2010.09.036.

[80] H. Costa, E. Júlio, J. Loureno, New approach for shrinkage prediction of high-strength lightweight aggregate concrete, Constr. Build. Mater. 35 (2012) 84–91. https://doi.org/10.1016/j.conbuildmat.2012.02.052.

[81] Y.Z. Zhuang, D.D. Zheng, Z. Ng, T. Ji, X.F. Chen, Effect of lightweight aggregate type on early-age autogenous shrinkage of concrete, Constr. Build. Mater. 120 (2016) 373–381. https://doi.org/10.1016/j.conbuildmat.2016.05.105.

[82] A. Bentur, S.I. Igarashi, K. Kovler, Prevention of autogenous shrinkage in high-strength concrete by internal curing using wet lightweight aggregates, Cem. Concr. Res. 31 (2001) 1587–1591. https://doi.org/10.1016/S0008-8846(01)00608-1.

[83] P. Lura, J. Bisschop, On the origin of eigenstresses in lightweight aggregate concrete, Cem. Concr. Compos. 26 (2004) 445–452. https://doi.org/10.1016/S0958-9465(03)00072-6.

[84] T. Deboodt, T. Fu, J.H. Ideker, Evaluation of FLWA and SRAs on autogenous deformation and long-term drying shrinkage of high performance concrete, Constr. Build. Mater. 119 (2016) 53–60. https://doi.org/10.1016/j.conbuildmat.2016.05.068.

[85] T. Deboodt, T. Fu, J.H. Ideker, Durability assessment of high-performance concrete with SRAs and FLWAs, Cem. Concr. Compos. 57 (2015) 94–101. https://doi.org/10.1016/j.cemconcomp.2014.12.004.

[86] S. Zhutovsky, K. Kovler, Influence of water to cement ratio on the efficiency of internal curing of high-performance concrete, Constr. Build. Mater. 144 (2017) 311–316. https://doi.org/10.1016/j.conbuildmat.2017.03.203.

[87] D. Jozwiak-Niedzwiedzka, Scaling resistance of high performance concretes containing a small portion of pre-wetted lightweight fine aggregate, Cem. Concr. Compos. 27 (2005) 709–715. https://doi.org/10.1016/j.cemconcomp.2004.11.001.

[88] I. De La Varga, J. Castro, D. Bentz, J. Weiss, Application of internal curing for mixtures containing high volumes of fly ash, Cem. Concr. Compos. 34 (2012) 1001–1008. https://doi.org/10.1016/j.cemconcomp.2012.06.008.

[89] S. Gupta, H.W. Kua, Effect of water entrainment by pre-soaked biochar particles on strength and permeability of cement mortar, Constr. Build. Mater. 159 (2018) 107–125. https://doi.org/10.1016/j.conbuildmat.2017.10.095.

[90] F. Liu, J. Wang, X. Qian, J. Hollingsworth, Internal curing of high performance concrete using cenospheres, Cem. Concr. Res. 95 (2017) 39–46. https://doi.org/10.1016/j.cemconres.2017.02.023.

[91] H.S. Wong, Concrete with superabsorbent polymer, Elsevier Ltd, 2018. https://doi.org/10.1016/B978-0-08-102181-1.00017-4.

[92] F.L. Buchholz, A.T. Graham, Modern superabsorbent polymer technology, Choice Rev. Online. 35 (1998) 35-5664-35–5664. https://doi.org/10.5860/choice.35-5664.

[93] E. Caló, V. V. Khutoryanskiy, Biomedical applications of hydrogels: A review of patents and commercial products, Eur. Polym. J. 65 (2015) 252–267. https://doi.org/10.1016/j.eurpolymj.2014.11.024.

[94] M.R. Guilherme, F.A. Aouada, A.R. Fajardo, A.F. Martins, A.T. Paulino, M.F.T. Davi, A.F. Rubira, E.C. Muniz, Superabsorbent hydrogels based on polysaccharides for application in agriculture as soil conditioner and nutrient carrier: A review, Eur. Polym. J. 72 (2015) 365–385. https://doi.org/10.1016/j.eurpolymj.2015.04.017.

[95] L.C. Davies, J.M. Novais, S. Martins-Dias, Detoxification of olive mill wastewater using superabsorbent polymers, Environ. Technol. (United Kingdom). 25 (2004) 89–100. https://doi.org/10.1080/09593330409355441.

[96] O.M. Jensen, P.F. Hansen, Water-entrained cement-based materials: II. Experimental observations, Cem. Concr. Res. 32 (2002) 973–978. https://doi.org/10.1016/S0008-

8846(02)00737-8.

[97] L.P. Esteves, Superabsorbent polymers: On their interaction with water and pore fluid, Cem. Concr. Compos. 33 (2011) 717–724. https://doi.org/10.1016/j.cemconcomp.2011.04.006.

[98] V. Mechtcherine, D. Snoeck, C. Schröfl, N. De Belie, A.J. Klemm, K. Ichimiya, J. Moon, M. Wyrzykowski, P. Lura, N. Toropovs, A. Assmann, S. ichi Igarashi, I. De La Varga, F.C.R. Almeida, K. Erk, A.B. Ribeiro, J. Custódio, H.W. Reinhardt, V. Falikman, Testing superabsorbent polymer (SAP) sorption properties prior to implementation in concrete: results of a RILEM Round-Robin Test, Mater. Struct. Constr. 51 (2018) 1–16. https://doi.org/10.1617/s11527-018-1149-4.

[99] K. Huber, Calcium-induced shrinking of polyacrylate chains in aqueous solution, J. Phys. Chem. 97 (1993) 9825–9830. https://doi.org/10.1021/j100140a046.

[100] R. Schweins, K. Huber, Collapse of sodium polyacrylate chains in calcium salt solutions, Eur. Phys. J. E. 5 (2001) 117–126. https://doi.org/10.1007/s101890170093.

[101] F. Fantinel, J. Rieger, F. Molnar, P. Hübler, Complexation of polyacrylates by Ca2+ ions. Time-resolved studies using attenuated total reflectance Fourier transform infrared dialysis spectroscopy, Langmuir. 20 (2004) 2539–2542. https://doi.org/10.1021/la030354e.

[102] H.X.D. Lee, H.S. Wong, N.R. Buenfeld, Self-sealing of cracks in concrete using superabsorbent polymers, Cem. Concr. Res. 79 (2016) 194–208. https://doi.org/10.1016/j.cemconres.2015.09.008.

[103] H.X.D. Lee, H.S. Wong, N.R. Buenfeld, Potential of superabsorbent polymer for self-sealing cracks in concrete, Adv. Appl. Ceram. 109 (2010) 296–302. https://doi.org/10.1179/174367609X459559.

[104] L.P. Esteves, P. Cachim, V.M. Ferreira, Mechanical properties of cement mortars with superabsorbent polymers, in: C.U. Grosse (Ed.), Adv. Constr. Mater. 2007, Springer Berlin Heidelberg, Berlin, Heidelberg, 2007: pp. 451–462. https://doi.org/10.1007/978-3-540-72448-3_45.

[105] P. Lura, K. Friedemann, F. Stallmach, S. Mönnig, M. Wyrzykowski, L.P. Esteves, Kinetics of water migration in cement-based systems containing superabsobent polymers, in: Appl. Super Absorbent Polym. Concr. Constr. State-of-the-Art Rep. Prep. by Tech. Comm. 225-SAP, Springer, 2012: pp. 21–37. https://doi.org/10.1007/978-94-007-2733-5_4.

[106] N. Nestle, A. Kühn, K. Friedemann, C. Horch, F. Stallmach, G. Herth, Water balance and

pore structure development in cementitious materials in internal curing with modified superabsorbent polymer studied by NMR, Microporous Mesoporous Mater. 125 (2009) 51–57. https://doi.org/10.1016/j.micromeso.2009.02.024.

[107] C. Schroefl, V. Mechtcherine, P. Vontobel, J. Hovind, E. Lehmann, Sorption kinetics of superabsorbent polymers (SAPs) in fresh Portland cement-based pastes visualized and quantified by neutron radiography and correlated to the progress of cement hydration, Cem. Concr. Res. 75 (2015) 1–13. https://doi.org/10.1016/j.cemconres.2015.05.001.

[108] F.L. Buchholz, Superabsorbent polymers: An idea whose time has come, J. Chem. Educ. 73 (1996) 512–515. https://doi.org/10.1021/ed073p512.

[109] L.P. Esteves, Recommended method for measurement of absorbency of superabsorbent polymers in cement-based materials, Mater. Struct. Constr. 48 (2015) 2397–2401. https://doi.org/10.1617/s11527-014-0324-5.

[110] S. Mönnig, Results of a comparative study of the shrinkage behaviour of concrete and mortar mixtures with different internal water sources, in: Proc. Int. RILEM Conf. Vol. Chang. Hardening Concr. Test. Mitig., 2006: pp. 67–75. https://doi.org/10.1617/2351580052.008.

[111] L. Dudziak, V. Mechtcherine, Reducing the cracking potential of ultra-high performance concrete by using Super Absorbent Polymers (SAP), in: Adv. Cem. Mater., 2009: pp. 11–19. https://doi.org/10.1201/b10162-7.

[112] N.A. Johansen, M.J. Millard, A. Mezencevova, V.Y. Garas, K.E. Kurtis, New method for determination of absorption capacity of internal curing agents, Cem. Concr. Res. 39 (2009) 65–68. https://doi.org/10.1016/j.cemconres.2008.10.004.

[113] H. Paiva, L.P. Esteves, P.B. Cachim, V.M. Ferreira, Rheology and hardened properties of single-coat render mortars with different types of water retaining agents, Constr. Build. Mater. 23 (2009) 1141–1146. https://doi.org/10.1016/j.conbuildmat.2008.06.001.

[114] O.M. Jensen, Use of Superabsorbent Polymers in Concrete, in: Concr. Int., Rilem publications, 2013: pp. 48--52.

[115] V. Mechtcherine, E. Secrieru, C. Schröfl, Effect of superabsorbent polymers (SAPs) on rheological properties of fresh cement-based mortars - Development of yield stress and plastic viscosity over time, Cem. Concr. Res. 67 (2015) 52–65. https://doi.org/10.1016/j.cemconres.2014.07.003.

[116] M.T. Hasholt, O.M. Jensen, S. Laustsen, Superabsorbent polymers as a means of improving frost resistance of concrete, Adv. Civ. Eng. Mater. 4 (2015) 237–256. https://doi.org/10.1520/ACEM20150012.

[117] S. Igarashi, Experimental study on prevention of autogenous deformation by internal curing using super-absorbent polymer particles, in: Int. RILEM Conf. Vol. Chang. Hardening Concr. Test. Mitig., RILEM Publications SARL, 2006: pp. 77–86. https://doi.org/10.1617/2351580052.009.

[118] P. Lura, Compressive strength of cement pastes and mortars with superabsorbent polymers, in: Proc. Int. RILEM Conf. Vol. Chang. Hardening Concr. Test. Mitig., Rilem Publications SARL Lyngby, 2006: pp. 117–125. https://doi.org/10.1617/2351580052.013.

[119] P. Lura, G. Ye, V. Cnudde, P. Jacobs, Preliminary results about 3D distribution of SAP in mortars, in: 1st Int. Conf. Microstruct. Relat. Durab. Cem. Compos. 13-15 Oct., 2008: pp. 1341–1348.

[120] H. Lam, Effects of Internal Curing Methods on Restrained Shrinkage and Permeability, Civ. Eng. (2005) 416–473.

[121] H.X.D. Lee, H.S. Wong, N. Buenfeld, Estimating the swelling ratio of superabsorbent polymers in cement-based materials, in: Int. RILEM Conf. Use Superabsorbent Polym. Other New Addit. Concr., RILEM Publications SARL, 2010: pp. 163–170.

[122] A. Assmann, H.W. Reinhardt, Tensile creep and shrinkage of SAP modified concrete, Cem. Concr. Res. 58 (2014) 179–185. https://doi.org/10.1016/j.cemconres.2014.01.014.

[123] D. Shen, C. Liu, J. Jiang, J. Kang, M. Li, Influence of super absorbent polymers on early-age behavior and tensile creep of internal curing high strength concrete, Constr. Build. Mater. 258 (2020) 120068. https://doi.org/10.1016/j.conbuildmat.2020.120068.

[124] L. Li, A.G.P. Dabarera, V. Dao, Time-zero and deformational characteristics of high performance concrete with and without superabsorbent polymers at early ages, Constr. Build. Mater. 264 (2020) 120262.

[125] H. Beushausen, M. Gillmer, The use of superabsorbent polymers to reduce cracking of bonded mortar overlays, Cem. Concr. Compos. 52 (2014) 1–8. https://doi.org/10.1016/j.cemconcomp.2014.03.009.

[126] F. Wang, Y. Zhou, B. Peng, Z. Liu, S. Hu, Autogenous shrinkage of concrete with super-absorbent polymer, ACI Mater. J. 106 (2009) 123–127. https://doi.org/10.14359/56458.

[127] J. Piérard, Mitigating autogenous shrinkage in HPC by internal curing using superabsorbent polymers, in: Int. RILEM Conf. Vol. Chang. Hardening Concr. Test. Mitig., RILEM Publications SARL, 2006: pp. 97–106. https://doi.org/10.1617/2351580052.011.

[128] M.R. Geiker, D.P. Bentz, O.M. Jensen, Mitigating autogenous shrinkage by internal curing, Am. Concr. Institute, ACI Spec. Publ. SP-218 (2004) 143–154. https://doi.org/10.14359/13060.

[129] J.O. Hasholt MT, Jespersen MHS, Mechanical properties of concrete with SAP. Part I: Development of compressive strength. In: Jensen OM, Hasholt MT, Laustsen S, editors, in: RILEM Proc. PRO 74 ‘‘Use Superabsorbent Polym. Other New Addit. Concr., Rilem publications, 2010: p. Lyngby, Denmark. Bagneux (France): RILEM Publicati.

[130] L. Dudziak, V. Mechtcherine, Mitigation of volume changes of ultra-high performance concrete (UHPC) by using super absorbent polymers, in: Proc. 2nd Int. Symp. Ultra High Perform. Concr. Kassel Univ. Press. Kassel, 2008: pp. 425–432.

[131] L. Dudziak, V. Mechtcherine, Enhancing early-age resistance to cracking in high-strength cement based materials by means of internal curing using super absorbent polymers, in: RILEM Proc. PRO, 2010: pp. 129–139.

[132] L.P. Esteves, Internal curing in cement-based materials\n, (2009).

[133] V. Mechtcherine, L. Dudziak, S. Hempel, Mitigating early age shrinkage of ultra-high performance concrete by using super absorbent polymers (SAP), Proc. Creep, Shrinkage, Durab. Mech. Concr. Concr. Struct. (2009) 847–853.

[134] H. Beushausen, M. Gillmer, M. Alexander, The influence of superabsorbent polymers on strength and durability properties of blended cement mortars, Cem. Concr. Compos. 52 (2014) 73–80. https://doi.org/10.1016/j.cemconcomp.2014.03.008.

[135] K. Gerasimova, Our common future, Our Common Futur. 8 (2017) 1–89. https://doi.org/10.4324/9781912281220.

[136] R.J. Andres, T.A. Boden, F.M. Bréon, P. Ciais, S. Davis, D. Erickson, J.S. Gregg, A. Jacobson, G. Marland, J. Miller, T. Oda, J.G.J. Olivier, M.R. Raupach, P. Rayner, K. Treanton, A synthesis of carbon dioxide emissions from fossil-fuel combustion, Biogeosciences. 9 (2012) 1845–1871. https://doi.org/10.5194/bg-9-1845-2012.

[137] Y. Yu, Q. Wang, P. Wang, Bioprocessing of bast fibers, in: Adv. Text. Biotechnol., Elsevier, 2019: pp. 1–19. https://doi.org/10.1016/B978-0-08-102632-8.00001-3.

[138] J. Summerscales, N.P.J. Dissanayake, A.S. Virk, W. Hall, A review of bast fibres and their composites. Part 1 - Fibres as reinforcements, Compos. Part A Appl. Sci. Manuf. 41 (2010) 1329–1335. https://doi.org/10.1016/j.compositesa.2010.06.001.

[139] J. Summerscales, N. Dissanayake, A. Virk, W. Hall, A review of bast fibres and their composites. Part 2 - Composites, Compos. Part A Appl. Sci. Manuf. 41 (2010) 1336–1344. https://doi.org/10.1016/j.compositesa.2010.05.020.

[140] D. Jones, G.O. Ormondroyd, S.F. Curling, C.M. Popescu, M.C. Popescu, Chemical compositions of natural fibres, in: Cereal Straw as a Resour. Sustain. Biomater. Biofuels Chem. Extr. Lignins, Hemicellul. Cellul., Elsevier, 2010: pp. 23–58. https://doi.org/10.1016/B978-0-08-100411-1.00002-9.

[141] A. Pietak, S. Korte, E. Tan, A. Downard, M.P. Staiger, Atomic force microscopy characterization of the surface wettability of natural fibres, Appl. Surf. Sci. 253 (2007) 3627–3635. https://doi.org/10.1016/j.apsusc.2006.07.082.

[142] P.H.F. Pereira, M. de F. Rosa, M.O.H. Cioffi, K.C.C. de C. Benini, A.C. Milanese, H.J.C. Voorwald, D.R. Mulinari, Vegetal fibers in polymeric composites: a review, Polímeros. 25 (2015) 9–22.

[143] A. Bourmaud, C. Morvan, A. Bouali, V. Placet, P. Perré, C. Baley, Relationships between micro-fibrillar angle, mechanical properties and biochemical composition of flax fibers, Ind. Crops Prod. 44 (2013) 343–351. https://doi.org/10.1016/j.indcrop.2012.11.031.

[144] A. Keller, M. Leupin, V. Mediavilla, E. Wintermantel, Influence of the growth stage of industrial hemp on chemical and physical properties of the fibres, Ind. Crops Prod. 13 (2001) 35–48. https://doi.org/10.1016/S0926-6690(00)00051-0.

[145] G. Coroller, A. Lefeuvre, A. Le Duigou, A. Bourmaud, G. Ausias, T. Gaudry, C. Baley, Effect of flax fibres individualisation on tensile failure of flax/epoxy unidirectional composite, Compos. Part A Appl. Sci. Manuf. 51 (2013) 62–70. https://doi.org/10.1016/j.compositesa.2013.03.018.

[146] N. Martin, N. Mouret, P. Davies, C. Baley, Influence of the degree of retting of flax fibers on the tensile properties of single fibers and short fiber/polypropylene composites, Ind. Crops Prod. 49 (2013) 755–767. https://doi.org/10.1016/j.indcrop.2013.06.012.

[147] Z. Li, X. Wang, L. Wang, Properties of hemp fibre reinforced concrete composites, Compos. Part A Appl. Sci. Manuf. 37 (2006) 497–505.

https://doi.org/10.1016/j.compositesa.2005.01.032.

[148] Swamy R.N, Vegetable Fiber Reinfored Cement Composites - A False Dream or A Potential Reality, in: Second Int. RILEM Symp. Veg. Plants Their Fibres as Build. Proceedi Mater. Proceeding 7, Routledge, London, UK. DOI, 1990: pp. 3–8.

[149] K. Arsène, M-A Savastano Jr, H. Allameh, S. M. Ghavami, W.O. Soboyejo, Cementitious composites reinforced with vegetable fibers, in: Proc. 1st Interam. Conf. Non-Conventional Mater. Technol. Eco-Construction Infrastruct., 2003: pp. 13–16. http://www.nku.edu/~allamehs1/Arsene-Natural Fibers fianl IAC NOCMAT.pdf.

[150] L.M. Srivastava, Cell wall, cell division, and cell growth, Plant Growth Dev. Horm. Environ. Ed. LM Srivastava. Acad. Press. San Diego. (2001) 23–74.

[151] A. Célino, S. Fréour, F. Jacquemin, P. Casari, The hygroscopic behavior of plant fibers: A review, Front. Chem. 1 (2014) 43. https://doi.org/10.3389/fchem.2013.00043.

[152] I.D. Cave, Theory of X-ray measurement of microfibril angle in wood, Wood Sci. Technol. 31 (1997) 143–152. https://doi.org/10.1007/bf00705881.

[153] L. Taiz, E. Zeiger, Plant physiology. 2nd edSinauer Associates, Inc., Publ. Saunderland, Massachusetts. 792p. (1998).

[154] T. Li, C. Chen, A.H. Brozena, J.Y. Zhu, L. Xu, C. Driemeier, J. Dai, O.J. Rojas, A. Isogai, L. Wågberg, L. Hu, Developing fibrillated cellulose as a sustainable technological material, Nature. 590 (2021) 47–56. https://doi.org/10.1038/s41586-020-03167-7.

[155] I. Sakurada, Y. Nukushina, T. Ito, Experimental determination of the elastic modulus of crystalline regions in oriented polymers, J. Polym. Sci. 57 (1962) 651–660. https://doi.org/10.1002/pol.1962.1205716551.

[156] Y. Li, Y.W. Mai, L. Ye, Sisal fibre and its composites: A review of recent developments, Compos. Sci. Technol. 60 (2000) 2037–2055. https://doi.org/10.1016/S0266-3538(00)00101-9.

[157] V. Placet, F. Trivaudey, O. Cisse, V. Gucheret-Retel, M.L. Boubakar, Diameter dependence of the apparent tensile modulus of hemp fibres: A morphological, structural or ultrastructural effect?, Compos. Part A Appl. Sci. Manuf. 43 (2012) 275–287. https://doi.org/10.1016/j.compositesa.2011.10.019.

[158] A. Kicińska-Jakubowska, E. Bogacz, M. Zimniewska, Review of Natural Fibers. Part I-Vegetable Fibers, J. Nat. Fibers. 9 (2012) 150–167.

https://doi.org/10.1080/15440478.2012.703370.

[159] J. Berthold, R.J.O. Olsson, L. Salmén, Water sorption to hydroxyl and carboxylic acid groups in Carboxymethylcellulose (CMC) studied with NIR-spectroscopy, Cellulose. 5 (1998) 281–298. https://doi.org/10.1023/A:1009298907734.

[160] A. Célino, O. Gonçalves, F. Jacquemin, S. Fréour, Qualitative and quantitative assessment of water sorption in natural fibres using ATR-FTIR spectroscopy, Carbohydr. Polym. 101 (2014) 163–170. https://doi.org/10.1016/j.carbpol.2013.09.023.

[161] W.E. Morton, J.W.S. Hearle, Physical Properties of Textile Fibres: Fourth Edition, Elsevier, 2008. https://doi.org/10.1533/9781845694425.

[162] P. Jongvisuttisun, K.E. Kurtis, The role of hardwood pulp fibers in mitigation of early-age cracking, Cem. Concr. Compos. 57 (2015) 84–93. https://doi.org/https://doi.org/10.1016/j.cemconcomp.2014.12.008.

[163] S. Kawashima, S.P. Shah, Early-age autogenous and drying shrinkage behavior of cellulose fiber-reinforced cementitious materials, Cem. Concr. Compos. 33 (2011) 201–208. https://doi.org/10.1016/j.cemconcomp.2010.10.018.

[164] B.J. Smith, A. Rawal, G.P. Funkhouser, L.R. Roberts, V. Gupta, J.N. Israelachvili, B.F. Chmelka, Origins of saccharide-dependent hydration at aluminate, silicate, and aluminosilicate surfaces, Proc. Natl. Acad. Sci. U. S. A. 108 (2011) 8949–8954. https://doi.org/10.1073/pnas.1104526108.

[165] K. Kochova, K. Schollbach, F. Gauvin, H.J.H. Brouwers, Effect of saccharides on the hydration of ordinary Portland cement, Constr. Build. Mater. 150 (2017) 268–275. https://doi.org/10.1016/j.conbuildmat.2017.05.149.

[166] S. Chakraborty, S.P. Kundu, A. Roy, B. Adhikari, S.B. Majumder, Effect of jute as fiber reinforcement controlling the hydration characteristics of cement matrix, Ind. Eng. Chem. Res. 52 (2013) 1252–1260. https://doi.org/10.1021/ie300607r.

[167] M.A. Mansur, M.A. Aziz, A study of jute fibre reinforced cement composites, Int. J. Cem. Compos. Light. Concr. 4 (1982) 75–82. https://doi.org/10.1016/0262-5075(82)90011-2.

[168] E. Boghossian, L.D. Wegner, Use of flax fibres to reduce plastic shrinkage cracking in concrete, Cem. Concr. Compos. 30 (2008) 929–937. https://doi.org/10.1016/j.cemconcomp.2008.09.003.

[169] T. Soleimani, A.A. Merati, M. Latifi, A.A. Ramezanianpor, Inhibition of cracks on the

surface of cement mortar using estabragh fibers, Adv. Mater. Sci. Eng. 2013 (2013). https://doi.org/10.1155/2013/656109.

[170] R.D. Toledo Filho, K. Ghavami, M.A. Sanjuán, G.L. England, Free, restrained and drying shrinkage of cement mortar composites reinforced with vegetable fibres, Cem. Concr. Compos. 27 (2005) 537–546. https://doi.org/10.1016/j.cemconcomp.2004.09.005.

[171] R.D.T. Filho, M.A. Sanjuán, Effect of low modulus sisal and polypropylene fibre on the free and restrained shrinkage of mortars at early age, Cem. Concr. Res. 29 (1999) 1597–1604. https://doi.org/10.1016/S0008-8846(99)00136-2.

[172] D. Sedan, C. Pagnoux, A. Smith, T. Chotard, Mechanical properties of hemp fibre reinforced cement: Influence of the fibre/matrix interaction, J. Eur. Ceram. Soc. 28 (2008) 183–192. https://doi.org/10.1016/j.jeurceramsoc.2007.05.019.

[173] K. Bilba, M.A. Arsene, A. Ouensanga, Sugar cane bagasse fibre reinforced cement composites. Part I. Influence of the botanical components of bagasse on the setting of bagasse/cement composite, Cem. Concr. Compos. 25 (2003) 91–96. https://doi.org/10.1016/S0958-9465(02)00003-3.

[174] R. Sudin, N. Swamy, Bamboo and wood fibre cement composites for sustainable infrastructure regeneration, J. Mater. Sci. 41 (2006) 6917–6924. https://doi.org/10.1007/s10853-006-0224-3.

[175] N.L. Thomas, J.D. Birchall, The retarding action of sugars on cement hydration, Cem. Concr. Res. 13 (1983) 830–842. https://doi.org/10.1016/0008-8846(83)90084-4.

[176] B. Na, Z. Wang, H. Wang, X. Lu, WOOD-cement compatibility review, Wood Res. 59 (2014) 813–825.

[177] S. Willför, A. Pranovich, T. Tamminen, J. Puls, C. Laine, A. Suurnäkki, B. Saake, K. Uotila, H. Simolin, J. Hemming, B. Holmbom, Carbohydrate analysis of plant materials with uronic acid-containing polysaccharides-A comparison between different hydrolysis and subsequent chromatographic analytical techniques, Ind. Crops Prod. 29 (2009) 571–580. https://doi.org/10.1016/j.indcrop.2008.11.003.

[178] Z. Li, L. Wang, X. Wang, Compressive and flexural properties of hemp fiber reinforced concrete, Fibers Polym. 5 (2004) 187–197. https://doi.org/10.1007/BF02902998.

[179] G. Ramakrishna, T. Sundararajan, Impact strength of a few natural fibre reinforced cement mortar slabs: A comparative study, Cem. Concr. Compos. 27 (2005) 547–553.

https://doi.org/10.1016/j.cemconcomp.2004.09.006.

[180] N.H. El-Ashkar, H. Nanko, K.E. Kurtis, Effect of Moisture State on Mechanical Behavior and Microstructure of Pulp Fiber-Cement Mortars, J. Mater. Civ. Eng. 19 (2007) 691–699. https://doi.org/10.1061/(asce)0899-1561(2007)19:8(691).

[181] M. Kalaivani, G. Shyamala, S. Ramesh, I. Rajasri Reddy, Experimental Investigation on Jute Fibre Reinforced Concrete with Partial Replacement of Fine Aggregate by Plastic Waste, in: IOP Conf. Ser. Mater. Sci. Eng., IOP Publishing, 2020: p. 32066. https://doi.org/10.1088/1757-899X/981/3/032066.

[182] Y. Ji, L. Pel, Z. Sun, The microstructure development during bleeding of cement paste: An NMR study, Cem. Concr. Res. 125 (2019) 105866.

[183] M. Tziotziou, E. Karakosta, I. Karatasios, G. Diamantopoulos, A. Sapalidis, M. Fardis, P. Maravelaki-Kalaitzaki, G. Papavassiliou, V. Kilikoglou, Application of 1H NMR to hydration and porosity studies of lime–pozzolan mixtures, Microporous Mesoporous Mater. 139 (2011) 16–24.

[184] X. Zhang, Y. Ji, L. Pel, Z. Sun, D. Smeulders, Early-age hydration and shrinkage of cement paste with coir fibers as studied by Nuclear Magnetic Resonance, Constr. Build. Mater. 336 (2022) 127460.

[185] P.J.M. Monteiro, G. Geng, D. Marchon, J. Li, P. Alapati, K.E. Kurtis, M.J.A. Qomi, Advances in characterizing and understanding the microstructure of cementitious materials, Cem. Concr. Res. 124 (2019) 105806. https://doi.org/https://doi.org/10.1016/j.cemconres.2019.105806.

[186] P.J. McDonald, V. Rodin, A. Valori, Characterisation of intra-and inter-C–S–H gel pore water in white cement based on an analysis of NMR signal amplitudes as a function of water content, Cem. Concr. Res. 40 (2010) 1656–1663.

[187] R.M.E. Valckenborg, L. Pel, K. Hazrati, K. Kopinga, J. Marchand, Pore water distribution in mortar during drying as determined by NMR, Mater. Struct. 34 (2001) 599–604.

[188] D. Snoeck, L. Pel, N. De Belie, The water kinetics of superabsorbent polymers during cement hydration and internal curing visualized and studied by NMR, Sci. Rep. 7 (2017) 1–14. https://doi.org/10.1038/s41598-017-10306-0.

[189] M.W. Bligh, M.N. D'Eurydice, R.R. Lloyd, C.H. Arns, T.D. Waite, Investigation of early hydration dynamics and microstructural development in ordinary Portland cement using 1H

NMR relaxometry and isothermal calorimetry, Cem. Concr. Res. 83 (2016) 131–139. https://doi.org/10.1016/j.cemconres.2016.01.007.

[190] A. Valori, P.J. McDonald, K.L. Scrivener, The morphology of C–S–H: Lessons from 1H nuclear magnetic resonance relaxometry, Cem. Concr. Res. 49 (2013) 65–81. https://doi.org/https://doi.org/10.1016/j.cemconres.2013.03.011.

[191] J. Liu, M. Wang, N. Liu, L. Teng, Y. Wang, Z. Chen, C. Shi, Development of ultra-fine SAP powder for lower-shrinkage and higher-strength cement pastes made with ultra-low water-to-binder ratio, Compos. Part B Eng. 262 (2023) 110810.

[192] D. Snoeck, L. Pel, N. De Belie, Superabsorbent polymers to mitigate plastic drying shrinkage in a cement paste as studied by NMR, Cem. Concr. Compos. 93 (2018) 54–62.

[193] D. Snoeck, L. Pel, N. De Belie, The water kinetics of superabsorbent polymers during cement hydration and internal curing visualized and studied by NMR, Sci. Rep. 7 (2017) 9514.

[194] S.E. Chidiac, S.N. Mihaljevic, S.A. Krachkovskiy, G.R. Goward, Efficiency measure of SAP as internal curing for cement using NMR & MRI, Constr. Build. Mater. 278 (2021) 122365.

[195] K. Friedemann, W. Schönfelder, F. Stallmach, J. Kärger, NMR relaxometry during internal curing of Portland cements by lightweight aggregates, Mater. Struct. 41 (2008) 1647–1655.

[196] L. Yang, X. Ma, J. Liu, X. Hu, Z. Wu, C. Shi, Improving the effectiveness of internal curing through engineering the pore structure of lightweight aggregates, Cem. Concr. Compos. 134 (2022) 104773. https://doi.org/https://doi.org/10.1016/j.cemconcomp.2022.104773.

[197] A. Paul, S. Murgadas, J. Delpiano, P.A. Moreno-Casas, M. Walczak, M. Lopez, The role of moisture transport mechanisms on the performance of lightweight aggregates in internal curing, Constr. Build. Mater. 268 (2021) 121191. https://doi.org/https://doi.org/10.1016/j.conbuildmat.2020.121191.

[198] P. Del Tredici, S.T.A. Pickett, Wild Urban Plants of the Northeast, Cornell University Press, 2020. https://doi.org/10.7591/9781501740459.

[199] M. Robert, P. Ovlaque, M.R. Foruzanmehr, Hollow floss fibers characterization and potential industrial applications, in: Chem. Lignocellul. Curr. Trends, CRC Press, 2018: pp. 22–41.

[200] S. Panahi, M.K. Moghaddam, M. Moezzi, Assessment of milkweed floss as a natural hollow

oleophilic fibrous sorbent for oil spill cleanup, J. Environ. Manage. 268 (2020) 110688. https://doi.org/10.1016/j.jenvman.2020.110688.

[201] C. Hyung-Mln, R.M. Cloud, Natural Sorbents in Oil Spill Cleanup, Environ. Sci. Technol. 26 (1992) 772–776. https://doi.org/10.1021/es00028a016.

[202] G.L. Louis, B.A.K. Andrews, Cotton/Milkweed Blends: A Novel Textile Product, Text. Res. J. 57 (1987) 339–345. https://doi.org/10.1177/004051758705700604.

[203] M. Bakhtiari, H. Hasani, M. Zarrebini, S. Hassanzadeh, Investigation of the thermal comfort properties of knitted fabric produced from Estabragh (Milkweed)/cotton-blended yarns, J. Text. Inst. 106 (2015) 47–56. https://doi.org/10.1080/00405000.2014.902167.

[204] A. Zarehshi, M. Ghane, Study of the water vapor permeability of multiple layer fabrics containing the milkweed fibers as the middle layer, J. Text. Inst. 113 (2022) 1531–1537. https://doi.org/10.1080/00405000.2021.1936387.

[205] C. Rajesh Kumar, D. Raja, S.K.S. Kumar, C. Prakash, Study on Moisture Behavior Properties of Milkweed and Milkweed/Cotton Blended Sanitary Napkins, J. Nat. Fibers. 19 (2022) 2849–2860. https://doi.org/10.1080/15440478.2020.1826384.

[206] P. Ghasaei, Z. Masumi, S.M. Hejazi, M. Sheikhzadeh, Using equal cross-section theory to investigate bending properties of cellulosic fiber reinforced cement panels, J. Ind. Text. 45 (2015) 118–132.

[207] P. Gu, R.K. Hessley, W.P. Pan, Thermal characterization analysis of milkweed flos, J. Anal. Appl. Pyrolysis. 24 (1992) 147–161. https://doi.org/10.1016/0165-2370(92)85026-H.

[208] I. Spiridon, Modifications of Asclepias syriaca fibers for paper production, Ind. Crops Prod. 26 (2007) 265–269.

[209] N. Reddy, Y. Yang, Non-traditional lightweight polypropylene composites reinforced withmilkweed floss, Polym. Int. 59 (2010) 884–890. https://doi.org/10.1002/pi.2798.

[210] X. Ma, G. Wen, Development history and synthesis of super-absorbent polymers: a review, J. Polym. Res. 27 (2020) 136. https://doi.org/10.1007/s10965-020-02097-2.

[211] T.L. Staples, P.K. Chatterjee, Absorbent Technology, Elsevier, 2002. http://www.sciencedirect.com/science/article/pii/S0920408302800111.

[212] M. Sayanjali Jasbi, H. Hasani, A. Zadhoush, S. Safi, Effect of alkali treatment on mechanical properties of the green composites reinforced with milkweed fibers, J. Text. Inst. 109 (2018) 24–31. https://doi.org/10.1080/00405000.2017.1320816.

[213] D. Ray, B.K. Sarkar, A.K. Rana, N.R. Bose, Effect of alkali treated jute fibres on composite properties, Bull. Mater. Sci. 24 (2001) 129–135. https://doi.org/10.1007/BF02710089.

[214] P. Ovlaque, M. Foruzanmehr, S. Elkoun, M. Robert, Milkweed floss fiber/PLA composites: effect of alkaline and epoxy-silanol surface modifications on their mechanical properties, Compos. Interfaces. 27 (2020) 495–513. https://doi.org/10.1080/09276440.2019.1655316.

[215] C. Wong, T. McGowan, S.G. Bajwa, D.S. Bajwa, Impact of fiber treatment on the oil absorption characteristics of plant fibers, BioResources. 11 (2016) 6452–6463. https://doi.org/10.15376/biores.11.3.6452-6463.

[216] M.N. Zakaria, Effect of hot water fibre treatment on the properties of kenaf / polyester composites, PhD, Univ. New South Wales. (2014) 1–196. http://hdl.handle.net/1959.4/53216 in https:// unsworks.unsw.edu.au.

[217] A. Jauneau, C. Morvan, F. Lefebvre, M. Demarty, C. Ripoll, M. Thellier, Differential extractability of calcium and pectic substances in different wall regions of epicotyl cells in young flax plants, J. Histochem. Cytochem. 40 (1992) 1183–1189. https://doi.org/10.1177/40.8.1377735.

[218] Y. Tan, H. Chen, R. He, Z. Yang, Effect of type and particle size of superabsorbent polymers on the hydration mechanism of pavement concrete, Int. J. Pavement Eng. (2021) 1–18. https://doi.org/10.1080/10298436.2021.2011280.

[219] Y. Bao, J. Ma, N. Li, Synthesis and swelling behaviors of sodium carboxymethyl cellulose-g-poly(AA-co-AM-co-AMPS)/MMT superabsorbent hydrogel, Carbohydr. Polym. 84 (2011) 76–82. https://doi.org/10.1016/j.carbpol.2010.10.061.

[220] T. Zheng, Y. Liang, S. Ye, Z. He, Superabsorbent hydrogels as carriers for the controlled-release of urea: Experiments and a mathematical model describing the release rate, Biosyst. Eng. 102 (2009) 44–50. https://doi.org/10.1016/j.biosystemseng.2008.09.027.

[221] C. Schröfl, D. Snoeck, V. Mechtcherine, A review of characterisation methods for superabsorbent polymer (SAP) samples to be used in cement-based construction materials: report of the RILEM TC 260-RSC, Mater. Struct. Constr. 50 (2017) 197. https://doi.org/10.1617/s11527-017-1060-4.

[222] L. Segal, J.J. Creely, A.E. Martin, C.M. Conrad, An Empirical Method for Estimating the Degree of Crystallinity of Native Cellulose Using the X-Ray Diffractometer, Text. Res. J. 29 (1959) 786–794. https://doi.org/10.1177/004051755902901003.

[223] N. Terinte, R. Ibbett, K.C. Schuster, Overview on native cellulose and microcrystalline cellulose I structure studied by X-ray diffraction (WAXD): Comparison between measurement techniques OVERVIEW ON NATIVE CELLULOSE AND MICROCRYSTALLINE CELLULOSE I STRUCTURE STUDIED BY X-RAY DIFFRACTION (, Lenzinger Berichte. 89 (2017) 118–131.

[224] S. Park, J.O. Baker, M.E. Himmel, P.A. Parilla, D.K. Johnson, Cellulose crystallinity index: Measurement techniques and their impact on interpreting cellulase performance, Biotechnol. Biofuels. 3 (2010) 10. https://doi.org/10.1186/1754-6834-3-10.

[225] A. Jillavenkatesa, S.J. Dapkunas, L.-S.H. Lum, Particle Size Characterization (SP 960-1), National Institute of Standards and Technology, 2001.

[226] M.A. Mosiewicki, N.E. Marcovich, M.I. Aranguren, Characterization of fiber surface treatments in natural fiber composites by infrared and Raman spectroscopy, in: N.E.B.T.-I.E. of N.F.C. for M.P. Zafeiropoulos (Ed.), Interface Eng. Nat. Fibre Compos. Maximum Perform., Woodhead Publishing, 2011: pp. 117–145. https://doi.org/10.1533/9780857092281.1.117.

[227] H. Yang, R. Yan, H. Chen, D.H. Lee, C. Zheng, Characteristics of hemicellulose, cellulose and lignin pyrolysis, Fuel. 86 (2007) 1781–1788. https://doi.org/10.1016/j.fuel.2006.12.013.

[228] X. Yang, L. Huang, L. Cheng, Study on the structure and the properties of akund fiber, Appl. Mech. Mater. 217–219 (2012) 617–621. https://doi.org/10.4028/www.scientific.net/AMM.217-219.617.

[229] S.K. Wiśniewska, J. Nalaskowski, E. Witka-Jezewska, J. Hupka, J.D. Miller, Surface properties of barley straw, Colloids Surfaces B Biointerfaces. 29 (2003) 131–142. https://doi.org/10.1016/S0927-7765(02)00178-9.

[230] T. Dong, G. Xu, F. Wang, Oil spill cleanup by structured natural sorbents made from cattail fibers, Ind. Crops Prod. 76 (2015) 25–33. https://doi.org/10.1016/j.indcrop.2015.06.034.

[231] C. Sawsen, K. Fouzia, B. Mohamed, G. Moussa, Effect of flax fibers treatments on the rheological and the mechanical behavior of a cement composite, Constr. Build. Mater. 79 (2015) 229–235. https://doi.org/10.1016/j.conbuildmat.2014.12.091.

[232] A.D. French, M. Santiago Cintrón, Cellulose polymorphy, crystallite size, and the Segal Crystallinity Index, Cellulose. 20 (2013) 583–588. https://doi.org/10.1007/s10570-012-

9833-y.

[233] M. Poletto, A.J. Zattera, R.M.C. Santana, Thermal decomposition of wood: Kinetics and degradation mechanisms, Bioresour. Technol. 126 (2012) 7–12. https://doi.org/10.1016/j.biortech.2012.08.133.

[234] V. Tserki, C. Panayiotou, N.E. Zafeiropoulos, A study of the effect of acetylation and propionylation on the interface of natural fibre biodegradable composites, Adv. Compos. Lett. 14 (2005) 65–71. https://doi.org/10.1177/096369350501400202.

[235] S. Ouajai, R.A. Shanks, Composition, structure and thermal degradation of hemp cellulose after chemical treatments, Polym. Degrad. Stab. 89 (2005) 327–335. https://doi.org/10.1016/j.polymdegradstab.2005.01.016.

[236] N. Karim, F. Sarker, S. Afroj, M. Zhang, P. Potluri, K.S. Novoselov, Sustainable and Multifunctional Composites of Graphene-Based Natural Jute Fibers, Adv. Sustain. Syst. 5 (2021) 2000228. https://doi.org/10.1002/adsu.202000228.

[237] H. Jiang, Y. Zhang, X. Wang, Effect of lipases on the surface properties of wheat straw, Ind. Crops Prod. 30 (2009) 304–310. https://doi.org/10.1016/j.indcrop.2009.05.009.

[238] S. Ajouguim, K. Abdelouahdi, M. Waqif, M. Stefanidou, L. Saâdi, Modifications of Alfa fibers by alkali and hydrothermal treatment, Cellulose. 26 (2019) 1503–1516. https://doi.org/10.1007/s10570-018-2181-9.

[239] A. Gholampour, T. Ozbakkaloglu, A review of natural fiber composites: properties, modification and processing techniques, characterization, applications, J. Mater. Sci. 55 (2020) 829–892. https://doi.org/10.1007/s10853-019-03990-y.

[240] D. Ray, B.K. Sarkar, A.K. Rana, N.R. Bose, Mechanical properties of vinylester resin matrix composites reinforced with alkali-treated jute fibres, Compos. Part A Appl. Sci. Manuf. 32 (2001) 119–127. https://doi.org/10.1016/S1359-835X(00)00101-9.

[241] S.M. Luz, J. Del Tio, G.J.M. Rocha, A.R. Gonçalves, A.P. Del'Arco, Cellulose and cellulignin from sugarcane bagasse reinforced polypropylene composites: Effect of acetylation on mechanical and thermal properties, Compos. Part A Appl. Sci. Manuf. 39 (2008) 1362–1369. https://doi.org/10.1016/j.compositesa.2008.04.014.

[242] M. Idicula, A. Boudenne, L. Umadevi, L. Ibos, Y. Candau, S. Thomas, Thermophysical properties of natural fibre reinforced polyester composites, Compos. Sci. Technol. 66 (2006) 2719–2725. https://doi.org/10.1016/j.compscitech.2006.03.007.

[243] X. Wang, L. Chang, X. Shi, L. Wang, Effect of hot-alkali treatment on the structure composition of jute fabrics and mechanical properties of laminated composites, Materials (Basel). 12 (2019) 1386. https://doi.org/10.3390/ma12091386.

[244] M. Teli, A. Jadhav, Effect of Mercerization on the Properties of Pandanus Odorifer Lignocellulosic Fibre, IOSR J. Polym. Text. Eng. 04 (2017) 07–15. https://doi.org/10.9790/019x-0401010715.

[245] S.A. Hosseini Ravandi, M. Valizadeh, Properties of fibers and fabrics that contribute to human comfort, in: G.B.T.-I.C. in C. Song (Ed.), Improv. Comf. Cloth., Woodhead Publishing, 2011: pp. 61–78. https://doi.org/10.1533/9780857090645.1.61.

[246] D.P. Bentz, K.A. Snyder, Protected paste volume in concrete: Extension to internal curing using saturated lightweight fine aggregate, Cem. Concr. Res. 29 (1999) 1863–1867. https://doi.org/10.1016/S0008-8846(99)00178-7.

[247] S. Kane, S.A. Miller, K.E. Kurtis, J.P. Youngblood, E.N. Landis, W.J. Weiss, Harmonized Life-Cycle Inventories of Nanocellulose and Its Application in Composites, Environ. Sci. Technol. 57 (2023) 19137–19147.

[248] A. Sabziparvar, L. Boulos, M.R. Foruzanmehr, Effect of fiber length and treatments on the hygroscopic properties of milkweed fibers for superabsorbent applications, Environ. Technol. Innov. 28 (2022) 102930. https://doi.org/10.1016/j.eti.2022.102930.

[249] M.S. Islam, S.J. Ahmed, Influence of jute fiber on concrete properties, Constr. Build. Mater. 189 (2018) 768–776. https://doi.org/10.1016/j.conbuildmat.2018.09.048.

[250] A.C. Stancato, A.K. Burke, A.L. Beraldo, Mechanism of a vegetable waste composite with polymer-modified cement (VWCPMC), Cem. Concr. Compos. 27 (2005) 599–603. https://doi.org/10.1016/j.cemconcomp.2004.09.011.

[251] J.W. Bentz, D.P.; Lura, P.; Roberts, Mixture proportioning for internal curing. Concr. Int. 2005, 27, 35–40, Concr. Int. 27 (2005) 35–40.

[252] T.C. Powers, T.L. Brownyard, Studies of the physical properties of hardened portland cement paste, in: Am. Concr. Institute, ACI Spec. Publ., 2008: pp. 265–617. https://doi.org/10.14359/8745.

[253] ASTM C305, Standard Practice for Mechanical Mixing of Hydraulic Cement Pastes and Mortars of Plastic Consistency, ASTM Lnternational. (2011) 1–3.

[254] S. Bai, X. Guan, G. Li, Early-age hydration heat evolution and kinetics of Portland cement

containing nano-silica at different temperatures, Constr. Build. Mater. 334 (2022) 127363. https://doi.org/10.1016/j.conbuildmat.2022.127363.

[255] P. Li, W. Li, K. Wang, J.L. Zhou, A. Castel, S. Zhang, S.P. Shah, Hydration of Portland cement with seawater toward concrete sustainability: Phase evolution and thermodynamic modelling, Cem. Concr. Compos. 138 (2023) 105007. https://doi.org/10.1016/j.cemconcomp.2023.105007.

[256] C.J. Adams, B. Bose, E. Mann, K.A. Erk, A. Behnood, A. Castillo, F.B. Rodriguez, Y. Wang, J. Olek, Superabsorbent Polymers for Internally Cured Concrete, (2022).

[257] C. Schröfl, K.A. Erk, W. Siriwatwechakul, M. Wyrzykowski, D. Snoeck, Recent progress in superabsorbent polymers for concrete, Cem. Concr. Res. 151 (2022) 106648. https://doi.org/https://doi.org/10.1016/j.cemconres.2021.106648.

[258] D. Snoeck, L.F. Velasco, A. Mignon, S. Van Vlierberghe, P. Dubruel, P. Lodewyckx, N. De Belie, The effects of superabsorbent polymers on the microstructure of cementitious materials studied by means of sorption experiments, Cem. Concr. Res. 77 (2015) 26–35.

[259] S.-H. Kang, S.-G. Hong, J. Moon, Importance of drying to control internal curing effects on field casting ultra-high performance concrete, Cem. Concr. Res. 108 (2018) 20–30. https://doi.org/https://doi.org/10.1016/j.cemconres.2018.03.008.

[260] L.E. Brower, C.F. Ferraris, Comparison of concrete rheometers, Am. Concr. Institute, ACI Spec. Publ. SP-233 (2006) 117–135. https://doi.org/10.14359/15838.

[261] S.E. Chidiac, F. Mahmoodzadeh, Plastic viscosity of fresh concrete - A critical review of predictions methods, Cem. Concr. Compos. 31 (2009) 535–544. https://doi.org/10.1016/j.cemconcomp.2009.02.004.

[262] P.F.G. Banfill, Rheology of Fresh Cement and Concrete: Proceedings of an International Conference, Liverpool, 1990, CRC Press, 1990.

[263] B. Felekoğlu, Rheological behaviour of self-compacting micro-concrete, Sadhana - Acad. Proc. Eng. Sci. 39 (2014) 1471–1495. https://doi.org/10.1007/s12046-014-0281-2.

[264] P.C. Aïtcin, R.J. Flatt, Science and technology of concrete admixtures, Woodhead publishing, 2015. https://doi.org/10.1016/C2015-0-00150-2.

[265] D. Jiao, R. De Schryver, C. Shi, G. De Schutter, Thixotropic structural build-up of cement-based materials: A state-of-the-art review, Cem. Concr. Compos. 122 (2021) 104152. https://doi.org/https://doi.org/10.1016/j.cemconcomp.2021.104152.

[266] D. Shen, X. Wang, D. Cheng, J. Zhang, G. Jiang, Effect of internal curing with super absorbent polymers on autogenous shrinkage of concrete at early age, Constr. Build. Mater. 106 (2016) 512–522.

[267] K. Scrivener, A. Ouzia, P. Juilland, A. Kunhi Mohamed, Advances in understanding cement hydration mechanisms, Cem. Concr. Res. 124 (2019) 105823. https://doi.org/10.1016/j.cemconres.2019.105823.

[268] H. Minard, S. Garrault, L. Regnaud, A. Nonat, Mechanisms and parameters controlling the tricalcium aluminate reactivity in the presence of gypsum, Cem. Concr. Res. 37 (2007) 1418–1426. https://doi.org/10.1016/j.cemconres.2007.06.001.

[269] R.F. Feldman, V.S. Ramachandran, The influence of CaS04.2H2O upon the hydration character of 3CaO.Al2O3, Mag. Concr. Res. 18 (1966) 185–196. https://doi.org/10.1680/macr.1966.18.57.185.

[270] M.C. Garci Juenger, H.M. Jennings, New insights into the effects of sugar on the hydration and microstructure of cement pastes, Cem. Concr. Res. 32 (2002) 393–399. https://doi.org/10.1016/S0008-8846(01)00689-5.

[271] A.T.W.M. Hendriks, G. Zeeman, Pretreatments to enhance the digestibility of lignocellulosic biomass, Bioresour. Technol. 100 (2009) 10–18. https://doi.org/10.1016/j.biortech.2008.05.027.

[272] S. Garrault, E. Finot, E. Lesniewska, A. Nonat, Study of C-S-H growth on C3S surface during its early hydration, Mater. Struct. Constr. 38 (2005) 435–442. https://doi.org/10.1617/14343.

[273] S. Garrault-Gauffinet, A. Nonat, Experimental investigation of calcium silicate hydrate (C-S-H) nucleation, J. Cryst. Growth. 200 (1999) 565–574. https://doi.org/10.1016/S0022-0248(99)00051-2.

[274] Y. Pu, L. Li, Q. Wang, X. Shi, L. Fu, G. Zhang, C. Luan, A.E.-F. Abomohra, Accelerated carbonation treatment of recycled concrete aggregates using flue gas: A comparative study towards performance improvement, J. CO2 Util. 43 (2021) 101362.

[275] F. Kaddah, E. Roziere, H. Ranaivomanana, O. Amiri, Complementary use of thermogravimetric analysis and oven to assess the composition and bound CO2 content of recycled concrete aggregates, Dev. Built Environ. 15 (2023) 100184. https://doi.org/https://doi.org/10.1016/j.dibe.2023.100184.

[276] R.B.B. Kammoe, R. Brice, Synthèse de nanoparticules de carbonate de calcium, (2010).

[277] J. Liu, N. Farzadnia, C. Shi, X. Ma, Shrinkage and strength development of UHSC incorporating a hybrid system of SAP and SRA, Cem. Concr. Compos. 97 (2019) 175–189. https://doi.org/10.1016/j.cemconcomp.2018.12.029.

[278] X. Pang, L. Sun, M. Chen, M. Xian, G. Cheng, Y. Liu, J. Qin, Influence of curing temperature on the hydration and strength development of Class G Portland cement, Cem. Concr. Res. 156 (2022) 106776. https://doi.org/https://doi.org/10.1016/j.cemconres.2022.106776.

[279] A.R. Jayapalan, B.Y. Lee, K.E. Kurtis, Can nanotechnology be 'green'? Comparing efficacy of nano and microparticles in cementitious materials, Cem. Concr. Compos. 36 (2013) 16–24.

[280] S. Weber, B. Der Deutschen, Curing of high strength concrete using light- weight aggregates, (1999) 377–391.

[281] G. Ren, B. Yao, M. Ren, X. Gao, Utilization of natural sisal fibers to manufacture eco-friendly ultra-high performance concrete with low autogenous shrinkage, J. Clean. Prod. 332 (2022) 130105. https://doi.org/https://doi.org/10.1016/j.jclepro.2021.130105.

[282] A. Sabziparvar, D. Taleponga, M.R. Foruzanmehr, Enhancing hydration and internal curing in cementitious mixes: The impact of pre-treated milkweed fibres, Case Stud. Constr. Mater. 20 (2024) e03079. https://doi.org/https://doi.org/10.1016/j.cscm.2024.e03079.

[283] E.T. Engelund, L.G. Thygesen, S. Svensson, C.A.S. Hill, A critical discussion of the physics of wood–water interactions, Wood Sci. Technol. 47 (2013) 141–161.

[284] R. Henkensiefken, J. Castro, D. Bentz, T. Nantung, J. Weiss, Water absorption in internally cured mortar made with water-filled lightweight aggregate, Cem. Concr. Res. 39 (2009) 883–892.

[285] X. Kong, Z. Zhang, Z. Lu, Effect of pre-soaked superabsorbent polymer on shrinkage of high-strength concrete, Mater. Struct. 48 (2015) 2741–2758.

[286] S. Meiboom, D. Gill, Modified spin-echo method for measuring nuclear relaxation times, Rev. Sci. Instrum. 29 (1958) 688–691.

[287] A. Damasceni, L. Dei, E. Fratini, F. Ridi, S.H. Chen, P. Baglioni, A novel approach based on differential scanning calorimetry applied to the study of tricalcium silicate hydration kinetics, J. Phys. Chem. B. 106 (2002) 11572–11578. https://doi.org/10.1021/jp020211l.

[288] A. Alzaza, K. Ohenoja, V. Isteri, T. Hanein, D. Geddes, M. Poikelispää, M. Illikainen, Blending eco-efficient calcium sulfoaluminate belite ferrite cement to enhance the physico–mechanical properties of Portland cement paste cured in refrigerated and natural winter conditions, Cem. Concr. Compos. 129 (2022) 104469. https://doi.org/10.1016/j.cemconcomp.2022.104469.

[289] E. Xanthakis, A. Le-Bail, H. Ramaswamy, Development of an innovative microwave assisted food freezing process, Innov. Food Sci. Emerg. Technol. 26 (2014) 176–181. https://doi.org/10.1016/j.ifset.2014.04.003.

[290] S. Zhang, Y. Zhao, H. Ding, J. Qiu, C. Hou, Effect of sodium chloride concentration and pre-curing time on the properties of cemented paste backfill in a sub-zero environment, J. Clean. Prod. 283 (2021) 125310. https://doi.org/10.1016/j.jclepro.2020.125310.

[291] S. Mindess, J.F. Young, D. Darwin, Concrete 2nd Edition, Am. Concr. Inst. 657 (2023) 644.

[292] Y.A.M. Cheumani, M. Ndikontar, B. De Jéso, G. Sèbe, Probing of wood–cement interactions during hydration of wood–cement composites by proton low-field NMR relaxometry, J. Mater. Sci. 46 (2011) 1167–1175.

[293] R.S. Menon, A.L. MacKay, J.R.T. Hailey, M. Bloom, A.E. Burgess, J.S. Swanson, An NMR determination of the physiological water distribution in wood during drying, J. Appl. Polym. Sci. 33 (1987) 1141–1155.

[294] W. Wang, K. Zhao, P. Zhang, J. Bao, S. Xue, Application of three self-developed ECT sensors for monitoring the moisture content in sand and mortar, Constr. Build. Mater. 267 (2021) 121008.

[295] Z. Wu, C. Shi, K.H. Khayat, Investigation of mechanical properties and shrinkage of ultra-high performance concrete: Influence of steel fiber content and shape, Compos. Part B Eng. 174 (2019) 107021.

[296] L. Yang, C. Shi, Z. Wu, Mitigation techniques for autogenous shrinkage of ultra-high-performance concrete–A review, Compos. Part B Eng. 178 (2019) 107456.

[297] J. Weiss, D. Bentz, A. Schindler, P. Lura, Internal Curing, Structure. (2012) 10–14. http://scholar.google.com/scholar?hl=en&btnG=Search&q=intitle:No+Title#0.

[298] Y. Liu, Y. Wei, Effect of calcined bauxite powder or aggregate on the shrinkage properties of UHPC, Cem. Concr. Compos. 118 (2021) 103967. https://doi.org/https://doi.org/10.1016/j.cemconcomp.2021.103967.

[299] M. Rahimi, O.A. Hisseine, A. Tagnit-Hamou, Effectiveness of treated flax fibers in improving the early age behavior of high-performance concrete, J. Build. Eng. 45 (2022) 103448. https://doi.org/https://doi.org/10.1016/j.jobe.2021.103448.

[300] X. Zhang, L. Pel, F. Gauvin, D. Smeulders, Reinforcing mechanisms of coir fibers in light-weight aggregate concrete, Materials (Basel). 14 (2021) 1–20. https://doi.org/10.3390/ma14030699.

[301] G. Ren, X. Gao, A. Su, Application of sisal fiber powder in ultra-high performance concrete: A renewable material for mitigating autogenous shrinkage, Constr. Build. Mater. 428 (2024) 136304. https://doi.org/https://doi.org/10.1016/j.conbuildmat.2024.136304.

[302] R.D. Tolêdo Filho, K. Scrivener, G.L. England, K. Ghavami, Durability of alkali-sensitive sisal and coconut fibres in cement mortar composites, Cem. Concr. Compos. 22 (2000) 127–143. https://doi.org/10.1016/S0958-9465(99)00039-6.

[303] J. Wei, C. Meyer, Degradation mechanisms of natural fiber in the matrix of cement composites, Cem. Concr. Res. 73 (2015) 1–16. https://doi.org/https://doi.org/10.1016/j.cemconres.2015.02.019.

[304] G. Vaickelionis, R. Vaickelioniene, Cement hydration in the presence of wood extractives and pozzolan mineral additives, Ceram. - Silikaty. 50 (2006) 115–122.

[305] D. Sirtoli, M. Wyrzykowski, P. Riva, P. Lura, Autogenous and drying shrinkage of mortars based on Portland and calcium sulfoaluminate cements, Mater. Struct. 53 (2020) 126. https://doi.org/10.1617/s11527-020-01561-1.

[306] X. Qin, A. Shen, Z. Lyu, L. Shi, J. Yang, H. Liu, Research on water transport behaviors and hydration characteristics of internal curing pavement concrete, Constr. Build. Mater. 248 (2020) 118714. https://doi.org/10.1016/j.conbuildmat.2020.118714.

[307] D. Tale Ponga, A. Sabziparvar, P. Cousin, L. Boulos, M. Robert, M.R. Foruzanmehr, Retarding Effect of Hemp Hurd Lixiviates on the Hydration of Hydraulic and CSA Cements, Materials (Basel). 16 (2023). https://doi.org/10.3390/ma16165561.

[308] C. Hua, P. Acker, A. Ehrlacher, Analyses and models of the autogenous shrinkage of hardening cement paste: I. Modelling at macroscopic scale, Cem. Concr. Res. 25 (1995) 1457–1468.

[309] C.C. Huang, L. Chen, G. Xiaohong, M. Zhao, T. Nguyen, S. Lee, The effects of humidity and surface free energy on adhesion force between atomic force microscopy tip and a silane

self-assembled monolayer film, J. Mater. Res. 25 (2010) 556–562. https://doi.org/10.1557/jmr.2010.0060.

[310] R. Henkensiefken, D. Bentz, T. Nantung, J. Weiss, Volume change and cracking in internally cured mixtures made with saturated lightweight aggregate under sealed and unsealed conditions, Cem. Concr. Compos. 31 (2009) 427–437.

[311] A.A. Melo Neto, M.A. Cincotto, W. Repette, Drying and autogenous shrinkage of pastes and mortars with activated slag cement, Cem. Concr. Res. 38 (2008) 565–574. https://doi.org/https://doi.org/10.1016/j.cemconres.2007.11.002.

[312] S. Lin, Early Age Deformation Characteristics of High Performance Concrete, (2003).

[313] B.F. Dela, L.F. Nielsen, H. Stang, Determination of Eigenstresses in Hardening Concrete., in: 16th Symp. Nord. Concr. Res., Norsk Betongforening, 1996: pp. 25-26 BT-Nordic Concrete Research.

[314] O.A. Hisseine, N.A. Soliman, B. Tolnai, A. Tagnit-Hamou, Nano-engineered ultra-high performance concrete for controlled autogenous shrinkage using nanocellulose, Cem. Concr. Res. 137 (2020) 106217. https://doi.org/https://doi.org/10.1016/j.cemconres.2020.106217.

[315] P.-C. Aitcin, A. Neville, P. Acker, Integrated view of shrinkage deformation, Concr. Int. 19 (1997) 35–41.

[316] D.P. Bentz, P.E. Stutzman, Curing, hydration, and microstructure of cement paste, ACI Mater. J. 103 (2006) 348.

[317] N. Bahari, H. Hasani, M. Zarrebini, S. Hassanzadeh, Investigating the effects of material and process variables on the mechanical properties of low-density thermally bonded nonwovens produced from Estabragh (milkweed) natural fibers, J. Ind. Text. 46 (2016) 719–736.

[318] G. Cicala, G. Cristaldi, G. Recca, A. Latteri, Composites Based on Natural Fibre Fabrics, Woven Fabr. Eng. 17 (2010) 317–342. https://doi.org/10.5772/10465.

[319] D. Lilargem Rocha, L.U.D. Tambara Júnior, M.T. Marvila, E.C. Pereira, D. Souza, A.R.G. de Azevedo, A review of the use of natural fibers in cement composites: concepts, applications and Brazilian history, Polymers (Basel). 14 (2022) 2043.

[320] K. Ghavami, Bamboo as reinforcement in structural concrete elements, Cem. Concr. Compos. 27 (2005) 637–649.

https://doi.org/https://doi.org/10.1016/j.cemconcomp.2004.06.002.

[321] L. Boulos, M.R. Foruzanmehr, M. Robert, Evolution of the interfacial transition zone and the degradation mechanism of zirconia treated flax fabric reinforced cementitious composites, Constr. Build. Mater. 190 (2018) 120–130. https://doi.org/https://doi.org/10.1016/j.conbuildmat.2018.09.104.

[322] S. Fadhil, M. Yaseen, The effect of adding different types of natural fibers on mechanical properties and impact resistance of concrete, Res. J. Appl. Sci. Eng. Technol. 9 (2015) 1091–1096. https://doi.org/10.19026/rjaset.9.2602.

[323] K. Farzanian, K. Pimenta Teixeira, I. Perdigão Rocha, L. De Sa Carneiro, A. Ghahremaninezhad, The mechanical strength, degree of hydration, and electrical resistivity of cement pastes modified with superabsorbent polymers, Constr. Build. Mater. 109 (2016) 156–165. https://doi.org/https://doi.org/10.1016/j.conbuildmat.2015.12.082.

[324] G. Zhang, H. Xia, Y. Niu, L. Song, Y. Zhao, X. Lv, H. Chen, D. Cao, Microstructure refinement and affected zone reinforcement for internal curing cement paste by composite microgel with nano silica, Cem. Concr. Compos. 138 (2023) 105013. https://doi.org/https://doi.org/10.1016/j.cemconcomp.2023.105013.

[325] B.J. Mohr, J.J. Biernacki, K.E. Kurtis, Microstructural and chemical effects of wet/dry cycling on pulp fiber–cement composites, Cem. Concr. Res. 36 (2006) 1240–1251.

[326] G.H.D. Tonoli, M.N. Belgacem, J. Bras, M.A. Pereira-da-Silva, F.A. Rocco Lahr, H. Savastano, Impact of bleaching pine fibre on the fibre/cement interface, J. Mater. Sci. 47 (2012) 4167–4177.

[327] G.H. Denzin Tonoli, A.E.F. de Souza Almeida, M.A. Pereira-da-Silva, A. Bassa, D. Oyakawa, H. Savastano Jr, Surface properties of eucalyptus pulp fibres as reinforcement of cement-based composites, (2010).

[328] M.M. Camargo, E. Adefrs Taye, J.A. Roether, D. Tilahun Redda, A.R. Boccaccini, A review on natural fiber-reinforced geopolymer and cement-based composites, Materials (Basel). 13 (2020) 4603.

[329] E. Jayamani, T.G. Loong, M.K. Bin Bakri, Comparative study of Fourier transform infrared spectroscopy (FTIR) analysis of natural fibres treated with chemical, physical and biological methods, Polym. Bull. 77 (2020) 1605–1629. https://doi.org/10.1007/s00289-019-02824-w.

[330] P. Harmsen, W. Huijgen, L. López, R. Bakker, Literature Review of Physical and Chemical Pretreatment Processes for Lignocellulosic Biomass, Wageningen UR-Food & Biobased Research, 2010. http://www.ecn.nl/docs/library/report/2010/e10013.pdf.

[331] J.A. Heredia-Guerrero, J.J. Benítez, E. Domínguez, I.S. Bayer, R. Cingolani, A. Athanassiou, A. Heredia, Infrared and Raman spectroscopic features of plant cuticles: A review, Front. Plant Sci. 5 (2014) 305. https://doi.org/10.3389/fpls.2014.00305.

[332] N.E. El Mansouri, J. Salvadó, Analytical methods for determining functional groups in various technical lignins, Ind. Crops Prod. 26 (2007) 116–124. https://doi.org/10.1016/j.indcrop.2007.02.006.

[333] M.S. Islam, M. Hasan, M.B. Ahmad, Chemical Modification and Properties of Cellulose-Based Polymer Composites, Lignocellul. Polym. Compos. Process. Charact. Prop. 9781118773 (2014) 301–324. https://doi.org/10.1002/9781118773949.ch14.

[334] F. Peng, J. Bian, P. Peng, Y. Guan, F. Xu, R.C. Sun, Fractional separation and structural features of hemicelluloses from sweet sorghum leaves, BioResources. 7 (2012) 4744–4759. https://doi.org/10.15376/biores.7.4.4744-4759.

[335] P.E. Kolattukudy, Cutin from Plants, Biopolym. Online. 3 (2002). https://doi.org/10.1002/3527600035.bpol3a01.

[336] I. Bykov, Characterization of Natural and Technical Lignins using FTIR Spectroscopy, Construction. (2008) 43.

[337] J.I. Morán, V.A. Alvarez, V.P. Cyras, A. Vázquez, Extraction of cellulose and preparation of nanocellulose from sisal fibers, Cellulose. 15 (2008) 149–159. https://doi.org/10.1007/s10570-007-9145-9.

[338] J.I. Santos, R. Martín-Sampedro, Ú. Fillat, J.M. Oliva, M.J. Negro, M. Ballesteros, M.E. Eugenio, D. Ibarra, Evaluating lignin-rich residues from biochemical ethanol production of wheat straw and olive tree pruning by FTIR and 2d-nmr, Int. J. Polym. Sci. 2015 (2015). https://doi.org/10.1155/2015/314891.

[339] M. Szymanska-Chargot, A. Zdunek, Use of FT-IR Spectra and PCA to the Bulk Characterization of Cell Wall Residues of Fruits and Vegetables Along a Fraction Process, Food Biophys. 8 (2013) 29–42. https://doi.org/10.1007/s11483-012-9279-7.